

**Studies towards oligodeoxynucleotide conjugates as  
potential photoactive antisense agents in chronic myeloid  
leukaemia.**

By

Conor Crean.

A thesis submitted to the University of Dublin for the degree of Doctor of  
Philosophy.

University of Dublin,  
Trinity College,  
Dublin 2.

June 2001

## **DECLARATION.**

This thesis has not been submitted as an exercise for a degree at any other university. Unless otherwise indicated the work described herein was carried out by the author alone. The author agrees that the college library may lend or copy this thesis upon request.

---

Conor Crean.

June 2001

*I would like to dedicate this thesis for my parents and family.*

## Summary.

The research presented in this thesis concerns the synthesis of oligodeoxynucleotide (ODN) conjugates and their use in the photochemical induction of oxidative damage to specific nucleic acid bases in a complementary ODN target strand as shown below:



The target strand used is an ODN model of the bcr/abl oncogenic mRNA present in chronic myeloid leukaemia (CML). As such, the aim of this research is the development of potential photoactive antisense agents, which could be used in future experiments to hinder expression of the oncogenic mRNA and be used in the development of therapeutic agents to treat CML. ODN conjugates were synthesised with photosensitising molecules, which were derivatives of a ruthenium polypyridyl complex and pteridinone derivatives. Thus, molecules were synthesised with functional groups that could be activated towards coupling with the 17-base ODN shown above. Phosphoramidite and succinimide ester coupling strategies were used to synthesise the conjugates, which were purified by electrophoresis and characterised by spectroscopic and mass spectrometric methods. The ability of the ODN conjugates to photoinduce specific damage to the target strand was assayed by gel electrophoresis experiments using  $^{32}\text{P}$  labeled target strands. Base sensitive modifications were induced specifically at the guanine 21 bases from the 5' end of the target using a ruthenium-ODN. A pteridinone-ODN produced such modifications at the guanines 18 and 21 bases from the 5' end of the target. The extent of base damage was visualised by autoradiography and phosphorimagery and quantified by densitometry. Investigations were also carried out using variant targets to study the effect of moving guanine 21 further away from the supposed location of the photosensitising molecules. In order to understand the mechanism of photooxidative damage, experiments were carried out using additives to investigate the role of molecular and singlet oxygen in the damage produced. A HPLC assay of the photooxidation products of 2'-deoxyguanosine in the presence of  $\text{Ru}(\text{phen})_3\text{Cl}_2$  or a pteridinone derivative was also carried out. This was used as a model to predict the photochemical behaviour of the ODN conjugates. The photooxidation products produced showed the relative contribution of competing oxidation mechanisms and thus helped to explain the photocleavage results with the ODN conjugates.

## **Acknowledgements.**

I would like to express my gratitude to Professor Kelly and Professor Corish in their respective roles as head of department for use of the equipment and facilities of the chemistry department during the course of my research. I would also like to thank Professor Mc Connell for the use of the equipment in the department of Genetics.

I would like to thank my supervisors Professor J.M. Kelly, Doctor P.H. Boyle and Doctor M. Lawler for all their encouragement and help throughout my research. For financial support I would like to acknowledge contributions from the Health Research Board, Enterprise Ireland, Trinity College, the Trinity Trust and BOC gases.

Thanks go to Doctor J O Brien for the running of NMR spectra and I would like to thank all the technical staff in the departments of Chemistry and Genetics too many to mention, for all their assistance in making life easier.

I would like to thank all the members past and present of the Kelly and Boyle research groups for help and friendship. In lab 0.17, those deserving special mention include Moss, Celine, Damien and Moh, (all doctors, if you can believe it). The present members Yvonne (who also suffers from gel fatigue), Tom (always time for a smoke) and the French invaders Fabian, Cedric and Alexandria. Within the Kelly research group special mention goes to Clare for teaching me all the gel techniques, Dr. Martin Feeney, for the good advice on all things chemical and Carlos for making the most stressed of us look relaxed. Thanks to the current Kelly group members Aoife, Karen, Michael, Michelle, Sarah and Suresh for staying awake during all the group meetings.

Thanks also to all my other post-grad friends in Trinity with whom I have shared a pint or two over the last 3 years and special thanks to all my friends outside college for still recognising me despite not seeing me very often.

Lastly I would like to thank elise for all her love and understanding, for helping me stay (in)sane and simply for being in my life.

## TABLE OF CONTENTS

<b>Declaration.....</b>	<b>2</b>
Summary.....	4
Acknowledgements.....	5
List of Abbreviations.....	11
<b>1.1. Introduction.....</b>	<b>13</b>
1.1. Nucleic acids.....	14
1.1.1. Primary structure of nucleic acids.....	17
1.1.2. Secondary structure of nucleic acids.....	18
1.1.3. Tertiary structure of nucleic acids.....	20
1.2. Antigene and antisense strategies.....	21
1.2.1. DNA as genetic material.....	21
1.2.2. Antigene strategy.....	23
1.2.3. Targeting of antisense oligonucleotides.....	24
1.2.4. Development of antisense strategy.....	25
1.3. The synthesis of nucleic acids.....	25
1.3.1. The synthesis of nucleic acid analogues.....	30
1.3.1.1. <i>Phosphorothioates (PS)</i> .....	31
1.3.1.2. <i>Methylphosphonates (MP)</i> .....	33
1.3.1.4. <i>Miscellaneous oligonucleotide analogues</i> .....	36
1.4. Antisense properties of modified oligonucleotides.....	36
1.4.1. Stability of duplex formation.....	37
1.4.2. Penetration of oligonucleotides into cells.....	38
1.4.3. Stability to nucleases.....	38
1.4.4. Mechanisms of antisense action.....	39
1.4.5. Non-antisense effects of antisense oligonucleotides.....	40
1.4.6. Design of antisense oligonucleotides.....	42
1.4.7. Chronic Myeloid Leukaemia (CML).....	42
1.4.7.1. <i>BCR-ABL as a target for antisense oligonucleotides</i> .....	44
1.5. Oligonucleotide Conjugates.....	44
1.5.1. Synthesis of oligonucleotide conjugates.....	45
1.5.2. Uses of Oligonucleotide conjugates.....	50
1.5.2.1. <i>Oligonucleotide intercalator conjugates</i> .....	50

1.5.2.2.	<i>Oligonucleotide conjugates with chemically reactive groups.</i>	51
1.5.2.3.	<i>Oligonucleotide conjugates with photoactive groups.</i>	53
1.6.	Oxidative damage to nucleoside and DNA bases.	62
1.6.1.	Hole transport mechanisms in DNA.	63
1.6.2.	Photodamage to guanine in DNA.	64
1.6.3.	Photodamage to nucleosides.	67
1.6.3.1.	<i>Type I photoproducts of nucleosides.</i>	67
1.6.3.2.	<i>Type II photoproducts from nucleosides.</i>	69
1.6.4.	Photooxidation of 8-oxo-2'-deoxyguanosine.	70
1.6.5.	Detecting DNA and nucleoside damage.	73
1.6.5.1.	<i>Detection of Type I photoproducts.</i>	73
1.6.5.2.	<i>Detection of Type II photoproducts.</i>	74
1.6.6.	Recent advances in detection methods.	74
1.6.7.	Alternative methods for measurement of oxidative DNA damage.	75
1.6.8.	Summary of photooxidative products.	75
<b>2.0</b>	<b>Molecules used for photoactive oligodeoxynucleotide conjugates.</b>	<b>77</b>
2.1.	Ruthenium polypyridyl complexes.	78
2.2.	Synthesis of Ruthenium polypyridyl oligonucleotide conjugates.	81
2.2.1.	<i>Synthesis of an activated ruthenium polypyridyl complex using a phosphoramidite derivative.</i>	82
2.2.2.	<i>Synthesis of an activated ruthenium polypyridyl complex using succinimide ester coupling.</i>	83
2.3.	The Chemistry of Pteridines.	85
2.3.1.	Synthesis of pteridine oligonucleotide conjugates.	87
2.3.1.	<i>Activation of a pteridinone by phosphoramidite methodology.</i>	88
2.3.2.	<i>Activation of a pteridinone by succinimide ester methodology.</i>	91
2.4.	Aims and objectives.	92
<b>3.0.</b>	<b>Synthesis and characterisation of oligodeoxynucleotide conjugates.</b>	<b>93</b>
3.1.	Synthesis of a pteridinone–phosphoramidite.	93
3.2.	Synthesis of a pteridinone succinimide ester.	98
3.3.	Synthesis of an activated ruthenium polypyridyl complex.	102
3.3.1.	<i>Synthesis of a ruthenium polypyridyl complex phosphoramidite.</i>	102
3.3.2.	<i>Synthesis of a ruthenium polypyridyl complex succinimide ester.</i>	104

3.4.	Synthesis and characterisation of ODN conjugates.....	110
3.4.1.	Synthesis of pteridinone-ODN (1) using phosphoramidite methodology. ....	111
3.4.2.	Syntheses of ODN conjugates using succinimide ester methodology.....	113
3.4.3.	Characterisation of ODN conjugates by electrospray mass spectrometry.....	116
<b>4.0.</b>	<b>Photooxidation of 2`-deoxyguanosine by free photosensitisers. ....</b>	<b>120</b>
4.1.	Photooxidation products of 2`-deoxyguanosine. ....	120
4.1.1.	Irradiation of 2`-deoxyguanosine in the presence of photosensitisers.....	121
4.2.	Effects of NaN <sub>3</sub> and D <sub>2</sub> O on the yields of photooxidation products. ....	123
4.2.1.	<i>Effects of additives on reaction of 2`-deoxyguanosine with methylene blue.</i>	<i>123</i>
4.2.2.	<i>Effects of additives on reaction of 2`-deoxyguanosine with Ru(phen)<sub>3</sub>Cl<sub>2</sub>.</i>	<i>126</i>
4.2.3.	<i>Effects of additives on reaction of 2`-deoxyguanosine with pteridinone (105).</i>	<i>129</i>
4.3.	Characterisation of photooxidation products by mass spectrometry.....	131
4.4.	Photooxidation of oligodeoxynucleotides with free photosensitisers.....	133
4.4.1.	Discussion of photocleavage results with free photosensitisers. ....	134
<b>5.0.</b>	<b>Photooxidative damage using oligodeoxynucleotide conjugates. ....</b>	<b>135</b>
5.1.	Photocleavage experiments with oligonucleotide conjugates.....	135
5.2.	Results using ruthenium ODN complex conjugate.....	136
5.2.1.	Discussion of photocleavage results with the ruthenium-ODN.....	140
5.3.	Effects of additives on photocleavage by ruthenium ODN. ....	142
5.3.1.	Discussion of Ru-ODN photocleavage results in the presence of additives.	143
5.4.	Photocleavage results for variant target strands using ruthenium-ODN. ....	145
5.4.1.	Discussion of photocleavage of variant target strands with ruthenium-ODN.	149
5.5.	Results with pteridinone-ODN conjugates. ....	153
5.5.1.	Discussion of photocleavage results with pteridinone-ODN conjugates.....	158
5.6.	Effects of additives on photocleavage by pteridinone-ODN 1. ....	160
5.6.1.	Discussion of the effects of additives using pteridinone-ODN 1. ....	161
5.7.	Results for variant target strands using pteridinone-ODN 1.....	162
5.7.1.	Discussion of photocleavage results of variant target strands with Pteridinone-ODN 1.	165



5.8. Conclusions and future work.....	166
<b>6.0. Materials and Methods.....</b>	<b>168</b>
6.1. Apparatus and Instruments.....	168
6.2. Syntheses.....	169
2,4-Diamino-6-pyrimidinethiol (126).....	169
2,4-Diamino-6-methylthiopyrimidine (127).....	170
2,4-Diamino-6-methylthio-5-nitrosopyrimidine (128).....	170
5-Amino-7-(methylthio)furazano[3,4-d]pyrimidine (129).....	170
5-Amino-7-propoxyfurazano[3,4-d]pyrimidine (130).....	171
2-Amino-3-(3-hydroxypropyl)-6,7-diphenyl-4(3H)-pteridinone (104).....	171
2-(N,N-Dimethylaminomethyleneamino)-3-(3-hydroxypropyl)-6,7-diphenyl-4(3H)- pteridinone (134).....	172
(3-(2-N,N-Dimethylaminomethyleneamino-3,4-dihydro-4-oxo-6,7diphenyl-3- pteridinyl)-propoxy) (2-cyanoethoxy) (N,N-diisopropylamino)phosphoramidite (134). .....	172
6-Amino-2-methylthio-4-(3H) pyrimidinone (143).....	174
6-Amino-2-methylthio-5-nitroso-4-(3H) pyrimidinone (138).....	174
2-(6-Carboxyhexylamino)-6-amino-5-nitroso-4-(3H) pyrimidinone (140).....	174
2-(6-Carboxyhexylamino)-6,7-diphenyl-4(-3H) pteridinone (105).....	175
2-(6-Succinimido-carboxyhexylamino)-6,7-diphenyl-4(-3H) pteridinone (141).....	175
4'-Methyl-2,2'-bipyridine-4-carboxaldehyde (119).....	176
4'-Methyl-2, 2'-bipyridine-4-carboxylic acid (46).....	177
Ru [(1,10-phenanthroline) <sub>2</sub> (4'-methyl-2, 2'-bipyridine-4-carboxylic acid)] <sup>2+</sup> (PF <sub>6</sub> ) <sub>2</sub> (114).....	177
Ru[(1,10-phenanthroline) <sub>2</sub> (4'-methyl-2, 2'-bipyridine-4-carboxysuccinimide)] <sup>2+</sup> - (PF <sub>6</sub> ) <sub>2</sub> (145).....	178
4-(6-bromohexyl-4'-methyl-2,2'-bipyridine (113) <sup>199</sup> .....	178
4-(6-hydroxyhexyl-4'-methyl-2,2'-bipyridine (114) <sup>199</sup> .....	178
Ru[(1,10-phenanthroline) <sub>2</sub> 4-(6-hydroxyhexyl-4'-methyl-2,2'-bipyridine)] (PF <sub>6</sub> ) <sub>2</sub> (114).....	178
Ru[(1,10-phenanthroline) <sub>2</sub> 4-(6-(2-cyanoethoxy) (N,N-diisopropylamino) phosphoramidite) hexyl-4'-methyl-2,2'-bipyridine] (PF <sub>6</sub> ) <sub>2</sub> (116).....	179
Pteridinone-ODN (1).....	179
Pteridinone-ODN (2).....	180

<i>Ruthenium-ODN</i> .....	180
<i>Radiolabelling experiment</i> .....	180
<i>General procedure for Irradiation experiments</i> .....	181
<i>Experiments with NaN<sub>3</sub></i> .....	181
<i>Experiments with D<sub>2</sub>O</i> .....	182
<i>Electrophoresis experiments</i> .....	182
<i>Procedure for 19% polyacrylamide electrophoresis gel</i> .....	182
<i>HPLC assay for oxidative damage to 2`deoxyguanosine</i> .....	182
<i>HPLC experiments with D<sub>2</sub>O</i> .....	183
<i>HPLC experiments with NaN<sub>3</sub></i> .....	183
References.....	184

## List of Abbreviations.

DNA.	Deoxyribonucleic acid
mRNA.	Messenger ribonucleic acid
ODN.	Oligodeoxynucleotide.
Bcr.	Breakpoint cluster region
Abl.	Abelson leukaemia virus
A.	Adenine
G.	Guanine
T.	Thymine
C.	Cytosine
U.	Uracil
tRNA.	Transfer ribonucleic acid
rRNA.	Ribosomal ribonucleic acid
HPLC.	High performance liquid chromatography
DCC.	Dicyclohexyl carbodiimide
Ms-Cl.	Mesitylene sulphonyl chloride
PS.	Phosphorothioates
MP.	Methylphosphonates.
Tr.	Trityl
T <sub>m</sub> .	Melting temperature
UV.	Ultra-violet
SVP.	Snake venom phosphodiesterase
SP.	Spleen phosphodiesterase
HART.	Hybrid arrest of translation
CMV.	Cytomegalovirus
CML.	Chronic myeloid leukaemia
Ph.	Philadelphia
EDTA.	Ethylene diamine tetraacetic acid
ATP.	Adenosine triphosphate
Por.	Porphyrin
TAP.	1,4,5,8-tetraazaphenanthrene
8-oxoG.	7,8-dihydro-8-oxoguanine
HOMO.	Highest occupied molecular orbital
FAPyG.	Formamidopyrimidine

dIz.	2,2-Diamino-[(2'-deoxy-β- <i>D</i> -erythro-pentofuranosyl)-4-amino]-5-imidazol-4-one
dz.	2,2-Diamino-[(2'-deoxy-β- <i>D</i> -erythro-pentofuranosyl)amino]-5(2 <i>H</i> )oxazolone
dGuo.	2'-Deoxyguanosine
8-oxodGuo.	7,8-Dihydro-8-oxo-2'-deoxyguanosine
GC-MS.	Gas chromatography-mass spectrometry
4-OH-8-oxodguo.	7,8-Dihydro-4-hydroxy-8-oxo-2'-deoxyguanosine
HPLC-EC.	High performance liquid chromatography-electrochemical detection
FGG.	Formamidopyrimidine glycosylase
Ru.	Ruthenium
Bipy.	2,2'-bipyridyl
Phen.	1,10-phenanthroline
Dppz.	Dipyrido[3,2- <i>a</i> :2',3'- <i>c</i> ]phenazine
MLCT.	Metal toligand charge transfer
TSU.	N,N,N',N'-Tetramethyl(succinimido)uronium tetrafluoroborate
dGMP.	2'-Deoxyguanosine mono phosphate
PAGE.	Polyacrylamide gel electrophoresis
ODU.	Optical density unit
Mw.	Molecular weight
Z.	Charge
AMU.	Atomic mass units
M <sup>+</sup> .	Molecular ion
IR.	Infra-red
λ.	Wavelength
TOCSY.	Total correlation spectroscopy
φ <sub>F</sub> .	Quantum yield
E°.	Electrochemical potential

## 1.1. INTRODUCTION.

The elucidation of the structure of nucleic acids almost 50 years ago has enabled much research into the role of nucleic acids in biological functions. Collaborations between chemists, biochemists, geneticists and molecular biologists have uncovered the processes involved in the causes of many diseases. In particular, much is now known about the expression of genes and the role that gene expression has in the development of cancerous cells. This knowledge has led to the development of antigene and antisense strategies as methods to arrest gene expression at the transcriptional or translational levels respectively. These approaches involve using synthetic nucleic acids (or their derivatives), which bind to their complementary strands and prevent mRNA synthesis (antigene) or protein synthesis (antisense). If these strategies are targeted to gene sequences known to have a role in genetic diseases, then it might be possible to arrest expression of disease causing genes and prevent genetic diseases.

The research presented in this thesis is concerned with studies to improve the antisense capabilities of normal oligonucleotides. This involved the synthesis of oligodeoxynucleotides (ODN) with photosensitising ruthenium polypyridyl complexes or pteridinone derivatives attached to their 5' end. These conjugates were designed so that, upon hybridisation to their complementary strands and irradiation, the photosensitisers would induce irreversible damage to specific sites in their target strand. It was hoped that this damage could then result in an antisense effect greater than that achievable with normal oligonucleotides in cell studies.

The target sequence used is a 34 base oligodeoxynucleotide (ODN) model of the junction region of the bcr/abl oncogenic mRNA present in chronic myeloid leukaemia (CML). It is shown below, hybridised to a complementary ODN to which a photosensitising molecule has been attached



In order to appreciate the different aspects of the research presented in this thesis, it is necessary to have an overview of the differing topics of nucleic acid structure, the synthesis of nucleic acids, their analogues and conjugates, successful antisense approaches,

chemical and photochemical damage to nucleic acids, the photochemistry of the photosensitising molecules, the disease chronic myeloid leukaemia and antisense approaches to target its characteristic bcr/abl mRNA. Accordingly, these topics are reviewed in the following sections.

### 1.1. Nucleic acids.

Nucleic acids are long threadlike polymers whose constituent monomers are termed nucleotides<sup>1</sup>. These monomers are composed of a heterocyclic base, a pentose sugar and a phosphate residue. The bases are either purines (adenine (A) and guanine (G)) or pyrimidines (cytosine (C), thymine (T) and uracil (U)) (see fig. 1.1.a).

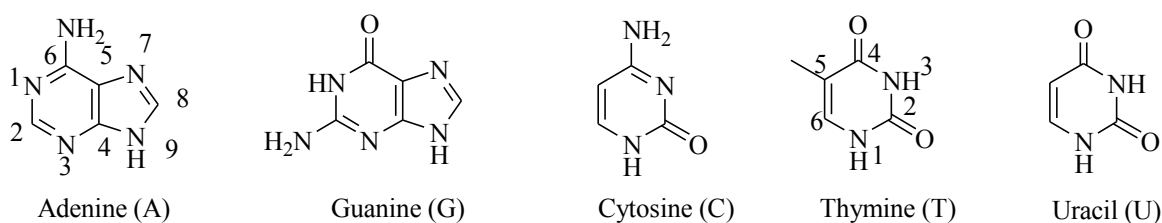
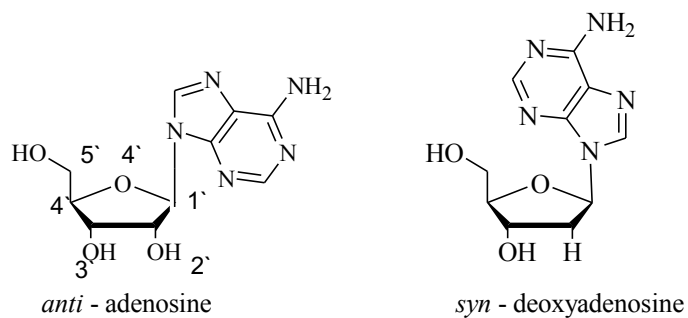


Figure 1.1.a. Heterocyclic bases in nucleic acids.

In nucleosides, the purine or pyrimidine base is bonded from a ring nitrogen to C1' of a pentose sugar. In ribonucleic acid (RNA), D-ribose is connected from the C1' of the sugar to N1 of C or U or to N9 of A or G. This  $\beta$ -glycosidic linkage is on the same side of the sugar ring as the C-5' hydroxyl group and the base can be in either a *syn* or *anti* conformation relative to the sugar ring (see fig.1.1.b.). In deoxyribonucleic acid (DNA) the sugar is 2'-deoxy-D-ribose and the four nucleosides are deoxyadenosine (dA), deoxyguanosine (dG), deoxycytidine (dC) and deoxythymidine (dT). In RNA, uracil replaces the deoxyribonucleobase thymine.



*Figure 1.1.b. Examples of a nucleoside and a deoxynucleoside in the syn and anti conformations.*

The phosphate esters of nucleosides are called nucleotides. Both the 3'- and 5'-hydroxyl groups are phosphorylated when the mononucleotides are linked to form a polynucleotide, where the 5'-phosphate of one nucleotide is attached to the 3'-hydroxyl of the next nucleotide to give the basic structure of a nucleic acid (see fig. 1.1.c.).

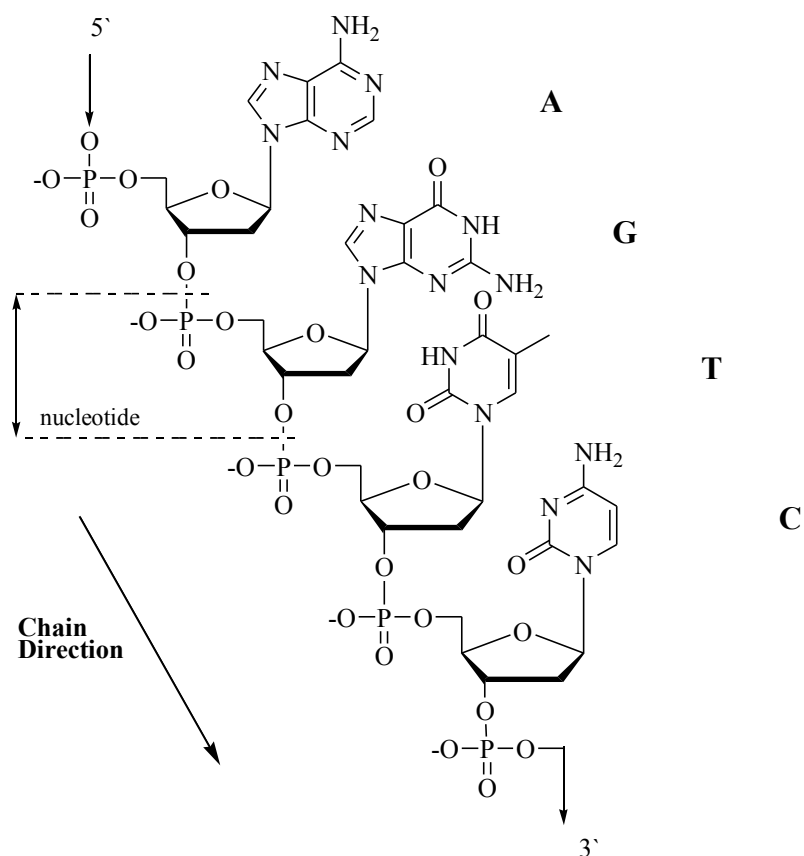


Figure 1.1.c. Structure of a 4 base oligodeoxynucleotide showing the 5' to 3' chain direction.

In order to minimise non-bonded interactions between atoms, the ribose rings are twisted to give a sugar pucker which is described by looking along the C1' - O4' - C4' plane indicated by the arrow in figure 1.1.d. If the endo displacement of C2' is greater than the exo displacement of C3' then the conformation is termed C2' endo. If the endo displacement of C3' is greater than the exo displacement of C2' then the conformation is termed C3' endo.

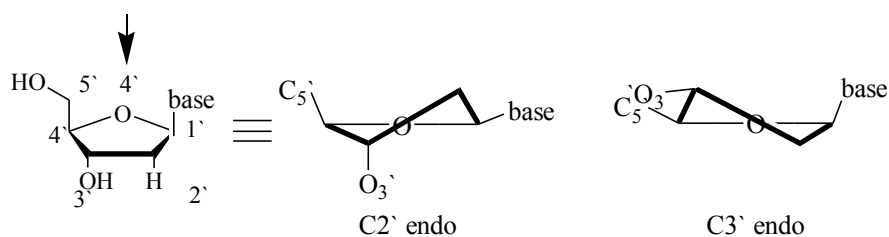


Figure 1.1.d. Conformation of the ribose sugars in nucleic acids.



### 1.1.1. Primary structure of nucleic acids.

Molecular studies on nucleic acids started in the early 20<sup>th</sup> century when nucleotides isolated from the nucleoprotein in pancreas glands were cleaved by alkaline hydrolysis to give phosphate residues and nucleosides<sup>1</sup>. A number of researchers contributed information, which later allowed the elucidation of the structure of nucleic acids. Using enzymatic hydrolysis, four crystalline deoxyribonucleosides were isolated from calf thymus DNA. Brown and Todd<sup>2</sup> synthesised nucleotide 5' phosphates and suggested the linkage between nucleotides was a phosphodiester with a  $\beta$  – glycosidic link<sup>3</sup>. Early x-ray diffraction studies by Astbury<sup>4</sup> showed that DNA possessed an ordered secondary structure and work by Gulland<sup>5</sup> using viscosity measurements postulated the presence of some type of hydrogen bonding between the nucleobase hydroxyl and amino groups. Linus Pauling<sup>6</sup> suggested a helical model for DNA with the sugar phosphate backbone at the centre with the bases pointing outwards. Chargaff *et al.*<sup>7</sup> made an important contribution when they discovered that the proportion of purines (G + A) was always equal to the proportion of pyrimidines (A + T) even though the ratio (G + A) / (A + T) varied from species to species.

Contributions to solving the structure were made by Franklin and Wilkins, when independently, their x-ray data showed two forms of DNA which were helical and were dependent on humidity<sup>1</sup>. The change of structure with humidity led Franklin to propose that the polar phosphate groups were exposed to water on the outside of the helix with the bases on the inside. Watson and Crick drew on all this information and they deduced the type of hydrogen bonding that was involved (see fig. 1.1.e.). They suggested that there was complementary base pairing between A and T and between G and C which was in accordance with the earlier works of Gulland<sup>5</sup> and Chargaff<sup>7</sup>.

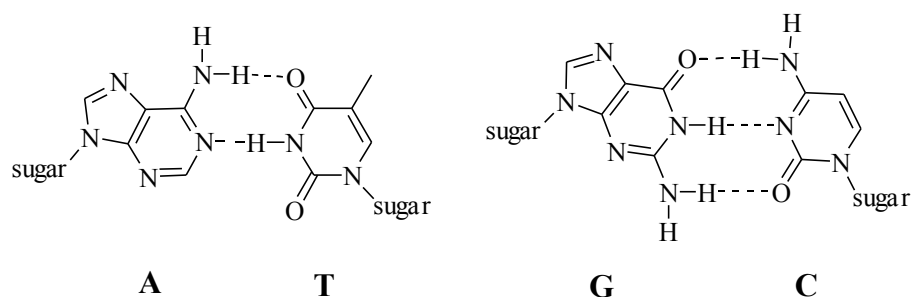


Figure 1.1.e. Watson - Crick hydrogen bonding base pairs.

Watson and Crick<sup>8</sup> then proposed that DNA consists of two antiparallel polynucleotide chains wound about a common axis to form a right handed spiral staircase like double helical structure (see fig.1.1.f.). The sugar phosphate links act as the backbone and the bases are towards the centre and are hydrogen bonded to appropriate bases on the opposite strand. This winding of the structure generates two grooves, the major groove and the minor groove.

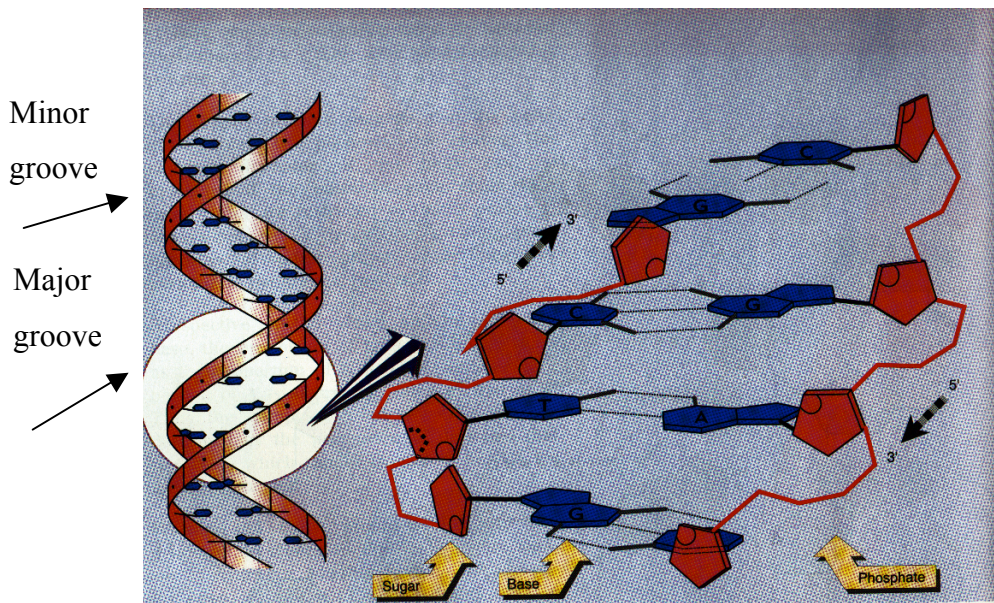


Figure 1.1.f. General structure of double stranded DNA<sup>9</sup>.

### 1.1.2. Secondary structure of nucleic acids.

As has been mentioned previously, initial investigations revealed two distinct conformations of DNA. At low humidity and high salt concentrations A-DNA is the favoured form while at high humidity and low salt concentrations the dominant structure is called B-DNA. There are in actuality a wide variety of right handed double helical conformations, which can be generally divided into the families of A-DNA (where the sugar pucker is C3'-endo) and B-DNA (where the sugar pucker is C2'-endo).

The general properties of A-form DNA follow the Watson - Crick model with antiparallel right handed double helices. The sugar rings are parallel to the helix axis and the phosphate backbone is on the outside of a cylinder of 24 Å in diameter. The bases are displaced 4.5 Å away from the centre of the helix creating a 3 Å wide hollow core. There

are 11 base pairs in a complete helical turn of 28 Å, the stacked bases are tilted sideways by an angle of 20° with respect to the helix axis and the furanose ring has a C3'-endo pucker with the nucleobase in an anti conformation. These properties give A-DNA a deep major groove and a shallow minor groove.

In B-DNA the base pairs are not tilted but lie directly on the helix axis resulting in major and minor grooves of approximately equal depth. The bases on each strand are stacked directly above each other and are perpendicular to a line drawn down the centre of the helix. The sugar pucker is C2'-endo and the base is in the anti conformation. There are 10 base pairs per helical turn and they are displaced 3.6 Å from the centre of the helix axis giving a narrower core than A-DNA. As B-DNA is associated with high humidity, both the major and minor grooves have highly ordered substructures of water molecules.

An unusual form of DNA is Z-DNA (see fig. 1.1.g.), a left-handed helix (stabilised by high concentrations of MgCl<sub>2</sub> or NaCl) where cytosines have an *anti* conformation and guanines have a *syn* conformation. This generates a zig-zag backbone with a sugar pucker that is C2'-endo at dC and C3'-endo at dG.

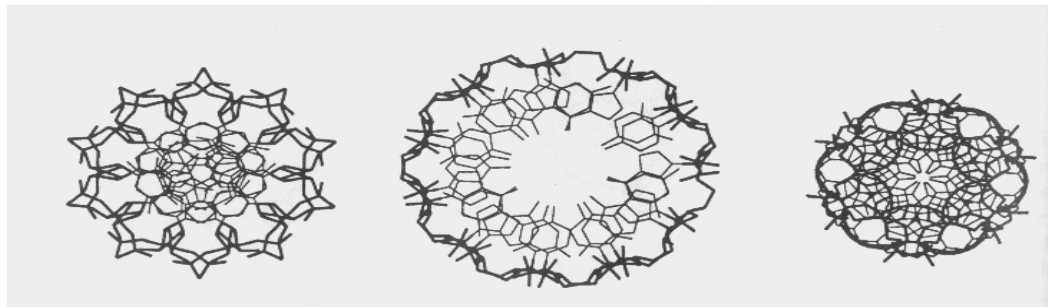
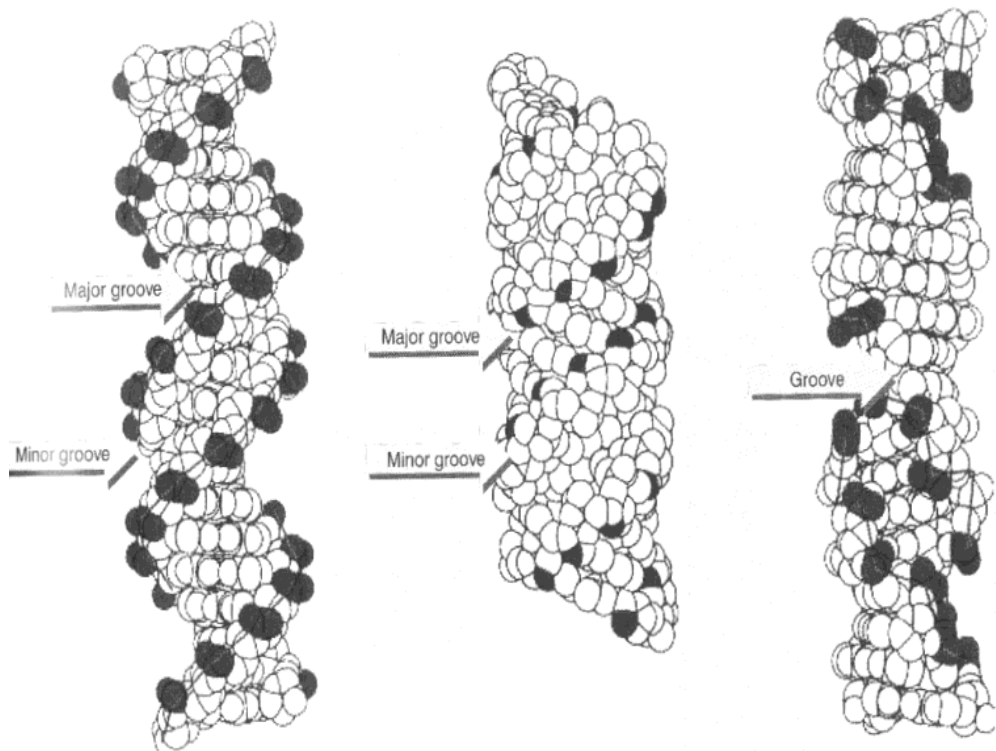
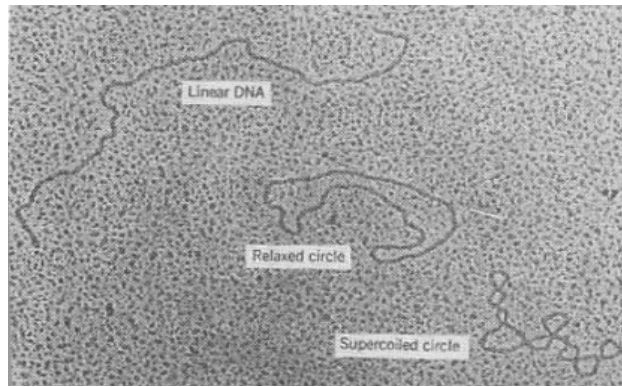


Figure 1.1.g. Structures of B, A and Z – DNA<sup>9,10</sup>

### 1.1.3. Tertiary structure of nucleic acids.

The double helical structure of DNA does not in actuality exist as a long straight rod but is coiled in space to fit into the dimensions of the cell it occupies. *In vivo* DNA generally has a closed structure and in eukaryotic genomes it exists as large loops which can be twisted around the helix axis to give so called supercoiled DNA (see fig. 1.1.h.).



*Figure 1.1.h. Supercoiled DNA<sup>9</sup>.*

## **1.2. Antigene and antisense strategies.**

An antisense oligonucleotide is a synthetic nucleotide whose base sequence is complementary to a specific region within a target mRNA. The antisense oligonucleotide is designed to hybridise with its target and disrupt mRNA function and so inhibit gene expression at the translational level. In order to understand the mechanisms and potential of antisense therapy it is first necessary to introduce the cellular processes involved in gene expression.

### **1.2.1. DNA as genetic material.**

When information is passed from one generation to another (on a cellular level), it occurs by the passing on of a set of genes needed for the manufacture of the cellular components necessary for the development of the next generation. The vehicle of this genetic information was shown to be DNA in the 1920's<sup>1</sup>. It became known that genes function by expressing proteins and that it is the specific sequence of nucleotides in DNA that generate specific proteins.

The expression of genes as information is a two-stage process, which starts with the unwinding of the double helix to allow transcription of a single stranded RNA identical to one of the strands of the DNA. This is then followed by translation of the nucleotide sequence of the RNA into a sequence of amino acids. The DNA strand which directs the

RNA synthesis is called the template or antisense strand and the second DNA strand which has the same sequence as the RNA to be synthesised is called the coding or sense strand.

The transcription process generates three types of RNA, which are known as messenger RNA (mRNA), transfer RNA (tRNA) and ribosomal RNA (rRNA). In translation it is the mRNA that is translated into the protein sequence while tRNA and rRNA provide the other components of the apparatus where protein assembly occurs. Each mRNA contains a coding region that is related to a particular protein sequence and each trinucleotide or codon of this coding region represents one amino acid. Before the mRNA is translated it is called precursor mRNA and contains coding sequences called exons and non-coding regions called introns. Splicing then occurs whereby the introns are excised from the mRNA and the exons are joined together to form mature mRNA which is then transported to the cytoplasm where translation occurs. It is the tRNA that provides the amino acid, which is covalently attached to one end of the tRNA (see fig.1.2.a.). The tRNA also contains a trinucleotide sequence called the anticodon, which is complementary to the codon for that amino acid on the mRNA strand.

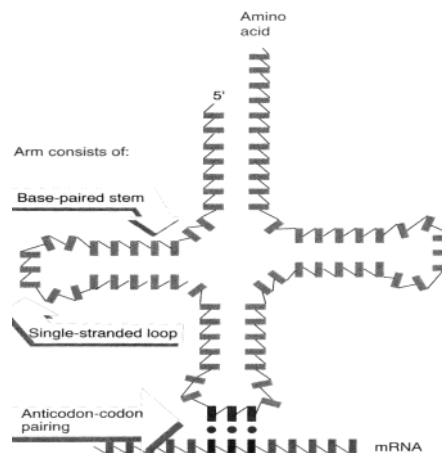


*Figure 1.2.a. Structure of codon : anticodon region of an mRNA : tRNA complex<sup>9</sup>.*

The molecular factory where the protein assembly occurs is a ribonucleoprotein particle with two sub units called a ribosome. These particles provide the environment that controls the recognition between the codon and the anti-codon. A ribosome attaches to the mRNA at or near the 5' end of its coding region and the initiating tRNA then associates with the mRNA-ribosomal unit (see fig.1.2.b.). The synthesis of all proteins starts with the amino acid methionine. Its tRNA has a special initiation codon the triplet of which is AUG. At any given moment during polypeptide synthesis, the ribosome contains two

tRNA molecules corresponding to successive codons. The proximity of their two amino acid residues allows the enzyme mediated peptide bond to form. Thus, the peptide elongates as one tRNA leaves the ribosome and the next one arrives as the ribosome moves along the coding region of the mRNA. At the end of the coding region there is one of three special termination codons, which halt elongation and facilitate the release of the polypeptide from the ribosome.

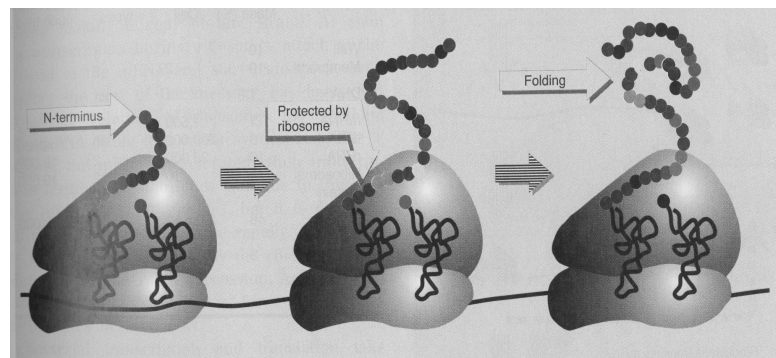


Figure 1.2.b. The molecular assembly of a protein by ribosomes along an mRNA strand<sup>9</sup>.

### 1.2.2. Antigene strategy.

DNA is transcribed into mRNA, which is translated into proteins. The antigene approach targets the arrest of gene expression at the transcriptional level. This involves using a synthetic oligonucleotide, which is targeted to the double stranded DNA with the aim of preventing binding of transcription factors and thus inhibiting the action of an enzyme called RNA polymerase. This would prevent the DNA from unwinding, replicating and synthesising the precursor mRNA.

This approach is possible because some double stranded sequences in DNA can form a triple helix upon addition of a third oligonucleotide strand. The base pairs in double stranded DNA also have hydrogen bonding capabilities in the major and minor grooves and it was shown that double helices containing only purines in one strand could bind a third strand containing only pyrimidines in the major groove. The hydrogen bonding involved is called Hoogsteen bonding and is shown in the following diagrams along with an example of a triple helix.

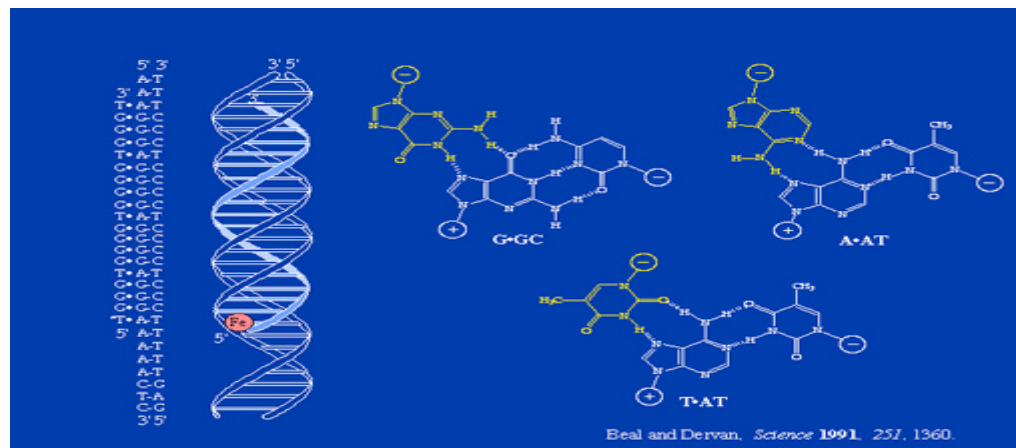


Figure 1.2.c. Hoogsteen hydrogen bonding and DNA triple helix<sup>11</sup>.

### 1.2.3. Targeting of antisense oligonucleotides.

This research is mainly concerned with antisense strategy and therefore a more in depth introduction to this area is necessary. There are a number of steps involved in the expression of genes, therefore in principle it is possible to use an antisense molecule at a number of different stages to disrupt the expression process. Antisense oligonucleotides have been used to target tRNA<sup>12</sup> and also to precursor mRNA where the intron / exon junction region was targeted to block access of a spliceosome to the splice junction in the hope that RNA that is not properly spliced is degraded and therefore not translated properly<sup>13</sup>. Ribosomal RNA has also been targeted<sup>14</sup>, but the main target for antisense oligonucleotides has been the mature mRNA itself with the primary aim being the inhibition of the translation process<sup>15</sup>. Mature mRNA contains a number of defined targets including a 5' cap region and an untranslated leader sequence, which are upstream of the AUG initiation codon. Oligonucleotides that bind to the 5' cap region are expected to



physically block the initial binding of part of the ribosome while those complementary to the initiation codon are expected to prevent the assembly of the entire ribosomal unit<sup>16</sup>. Most examples of successful antisense therapy involve targeting the coding region of the mRNA with the aim being to block the elongation of the assembling polypeptide. Such an antisense strategy was at first thought to work by physically blocking interactions between the ribosome and the mRNA<sup>17</sup> but it became known that ribosomes can unwind RNA secondary structure and thus could remove any potential blocking oligonucleotide. Further examination<sup>18</sup> revealed that an enzyme known as RNase-H was responsible for any inhibitory antisense effect seen by molecules targeting the coding region of the mRNA. This enzyme which is ubiquitous in eukaryotic cells cleaves the RNA portion of DNA:RNA hybrids thus preventing the RNA from being translated. The antisense strand is not affected and should be able to target other RNA strands producing what is, in effect, a catalytic reaction.

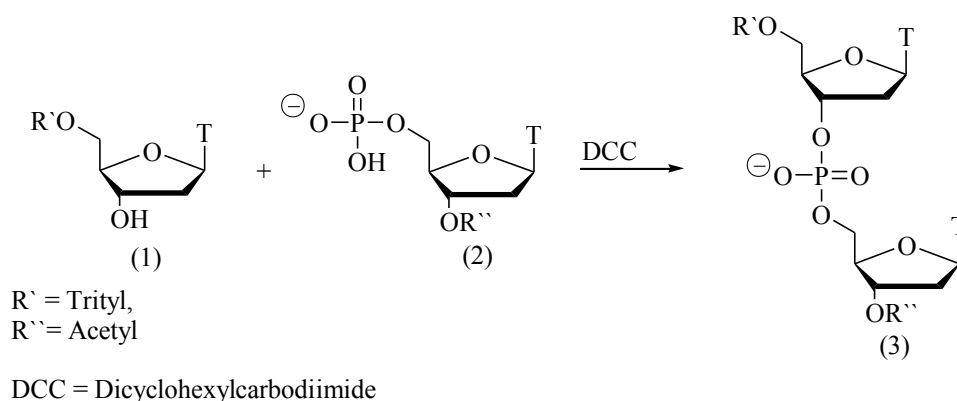
#### **1.2.4. Development of antisense strategy.**

There are a number of criteria that have to be met by an antisense oligonucleotide in order for an appreciable antisense effect to be measured. The hybrid formed between the oligonucleotide and its target must be stable under physiological conditions. The interaction must be specific for the target strand. The oligonucleotide must have a lifetime long enough *in vivo* to display its desired action and therefore must be stable to endo and exo-nucleases. The oligonucleotide must be capable of passing through the cell membrane to reach its site of action. Normal phosphodiester oligonucleotides can satisfy some but not all of these criteria and for this reason it was necessary to develop modified oligonucleotides so that significant antisense effects could be achieved. In order to introduce the chemistry involved in the modification of oligonucleotides it is necessary to mention the evolution of the solid phase synthesis of nucleic acids which in itself is one of the main reasons behind the development of antigen and antisense technology.

#### **1.3. The synthesis of nucleic acids.**

The first synthesis of a dinucleotide with a 3' → 5' phosphodiester linkage was reported in 1955 by Michelson and Todd<sup>19</sup>. They activated a nucleoside hydrogen

phosphonate with N-chlorosuccinimide to give a phosphorochloridate, which, upon reaction with another nucleoside gave a dinucleotide phosphodiester. The behaviour of this dinucleotide towards snake venom phosphodiesterase was the same as that of degraded DNA and for this reason the authors postulated similar internucleotide linkages. After this initial work many researchers successfully developed a number of methods for the synthesis of nucleotides<sup>20</sup> including the phosphodiester approach. This involved the condensation of a 5'-O-trityl-2'-deoxynucleoside (1) with a 3'-O-acetylnucleoside-5'-phosphate (2) mediated by a condensing agent such as dicyclohexylcarbodiimide<sup>21,22</sup> (DCC) forming a dinucleotide phosphodiester (3), see scheme 1.3.a.



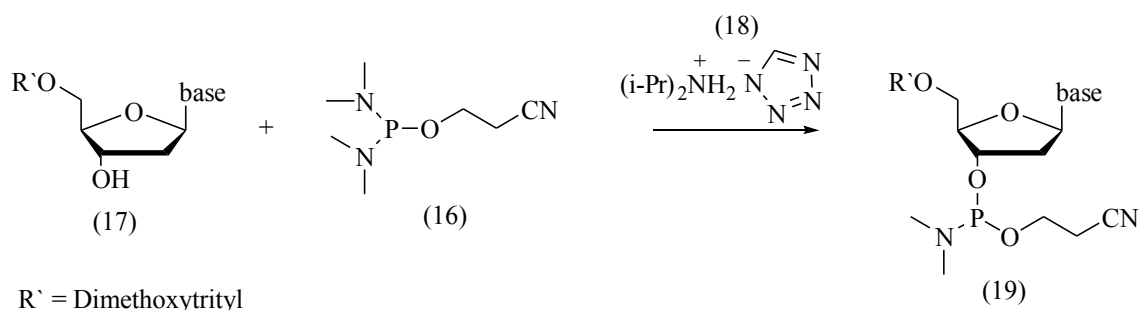
*Scheme 1.3.a. Nucleotide synthesis by phosphodiester methodology.*

This approach was routinely used for 20 years to synthesise short chain oligonucleotides. The protocol was time consuming, however, due to the necessary purification of intermediates by ion exchange chromatography. Letsinger and Ogilvie<sup>23,24</sup> overcame this problem by masking the phosphodiester as a  $\beta$ -cyanoethyl phosphotriester thus giving a non-ionic intermediate which could be purified by conventional chromatography.





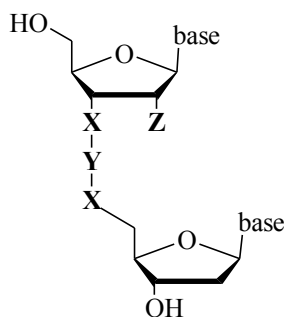
to the efficiency of the synthetic cycle when they replaced the phosphate protecting methyl group with a  $\beta$  - cyanoethyl group. This group did not require removal by thiophenol treatment (which also contaminates the final ODN) but could be removed by the same  $\text{NH}_4\text{OH}$  treatment used to cleave the oligonucleotide from the silica support. Hamamoto and Takaku<sup>31</sup> improved the stability of the synthesis of the phosphoramidites themselves when they used bis-diisopropylamino cyanoethoxy phosphoramidites (16) as phosphitylating agents (see scheme 1.3.d.), which were more stable than the chlorophosphines used previously. Compound (16) could be activated towards coupling with a 5'-O-protected 2'-deoxynucleoside (17) by diisopropylammonium tetrazolide (18) to give the phosphoramidite (19).



*Scheme 1.3.d Synthesis of 2'-deoxynucleoside phosphoramidites.*

Due to these improvements to the route for the synthesis of oligonucleotides it is now possible to buy the phosphoramidite of any 2'-deoxynucleoside and the synthesis of oligodeoxynucleotides up to 80 bases in length has become completely automated and highly efficient. The following diagram represents the synthetic cycle in an automated nucleic acid synthesiser.





<b>X</b>	<b>Y</b>	<b>Z</b>	<b>NAME</b>
O	P(O)S	H	phosphorothioate
O	P(O)CH <sub>3</sub>	H	methylphosphonate
O	P(O)NHR	H	phosphoramidate
NH (either)	P(O)O	H	Bridged phosphoramidate
O	P(O)O	OCH <sub>3</sub>	2'-O-methyl ribonucleotide

Figure 1.3.f. Structure of the main modified oligonucleotides.

#### 1.3.1.1. Phosphorothioates (PS).

In PS oligonucleotides, one of the phosphodiester oxygen atoms not linked to the sugar is replaced by a sulphur atom giving an anion with the negative charge located primarily on sulphur<sup>33</sup>. This introduction of sulphur creates a chiral centre and thus a non-stereoselective synthesis of a 17 base oligonucleotide would generate a mixture of ~ 130000 diastereomers. Thus, there would be an obvious need for a stereoselective synthesis if stereopure compounds were necessary for antisense applications. PS oligonucleotides can be synthesised by modifications of previously mentioned phosphonate, phosphotriester and phosphoramidite methodologies.<sup>34</sup> Burgers and Eckstein<sup>35</sup> synthesised diribonucleoside phosphorothioates using elemental sulphur in pyridine to oxidise an intermediate phosphotriester and achieved quantitative conversion to phosphorothioate after 16 hours at 20°C. The R(p) and S(p) diastereomers were then purified by size exclusion chromatography. The analogous diastereomers of deoxyphosphorothioate were synthesised by Uznanski *et al*<sup>36</sup>. In order to use PS oligonucleotides as antisense agents it was necessary to apply solid phase technology to their synthesis. Such a method was developed based on phosphoramidite coupling using elemental sulphur instead of I<sub>2</sub> / H<sub>2</sub>O in the oxidation step<sup>37</sup>. Oligonucleotides of various lengths and number of thioate links in specific sites were synthesised and separation of diastereomers by HPLC was possible, its ease dependent on the number of thioate linkages present and the number of bases in total.

The main problem with this approach was the relatively slow (7.5 mins.) sulphur transfer rate and the insolubility of S<sub>8</sub> in a range of organic solvents. This problem was

overcome by the development of a number of reagents such as 3H-1,2,benzodithiol-3-one (Beaucage reagent) (20), tetraethylthiuramdisulphide (21) and dibenzoyltetrasulphide (22), which were very efficient at oxidising phosphite triesters to phosphorothioates<sup>38,39,40</sup> as shown in fig. 1.3.g. The development of such efficient sulphurizing agents has allowed scale up of the synthesis and purification of these modified oligonucleotides to reach the multigram level<sup>41</sup>.

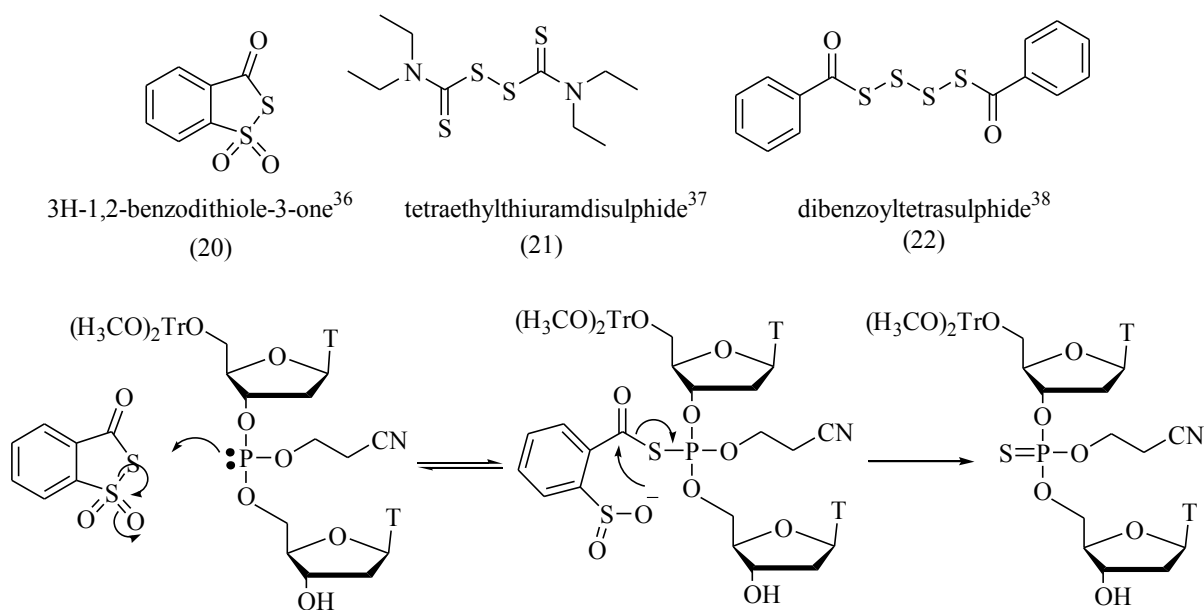


Figure 1.3.g. Examples of sulphurizing agents and the mechanism of phosphorothioate formation by "Beaucage's reagent".

With regard to the chirality of the phosphorothioate linkage there have been a number of successes in stereospecific synthesis using phosphoramidite coupling. Chirally pure oligonucleotides were first made through dimer coupling of pure dinucleoside derivatives or by tedious HPLC separation of diastereomeric mixtures. Hayakawa et. al.<sup>42</sup> achieved 65% diastereoselectivity in dimer synthesis through attaching the activating agent tetrazole to a bulky chiral auxiliary (23) (see fig. 1.3.h.). Another approach used a stereohindered nucleoside phosphoramidite (24) with which diastereoselectivity greater than 98% was achieved in dimer synthesis<sup>43</sup>, although this has not yet been applied to solid phase synthesis of stereopure long chain phosphorothioates.



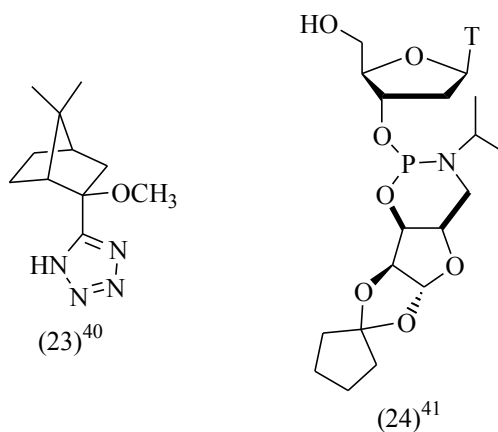


Figure 1.3.h. Reagents used in stereospecific phosphorothioate synthesis.

### 1.3.1.2. Methylphosphonates (MP).

The replacement of the  $O^-$  group in phosphodiester by  $CH_3$  generates a methylphosphonate internucleotide linkage. MP oligonucleotides can be synthesised in an analogous way to phosphoramidite coupling using methylphosphonamidites. Jaeger and Engels<sup>44</sup> reacted 5'-*O*-tritylthymidine (25) with the phosphorylating agent dimethylaminomethylphosphine (26) to form the methylphosphonamidite (27), which was coupled with 3'-*O*-benzylthymidine (28) using benzotriazole (29) to give the dinucleoside methylphosphonamidite (30) as depicted in figure 1.3.i.

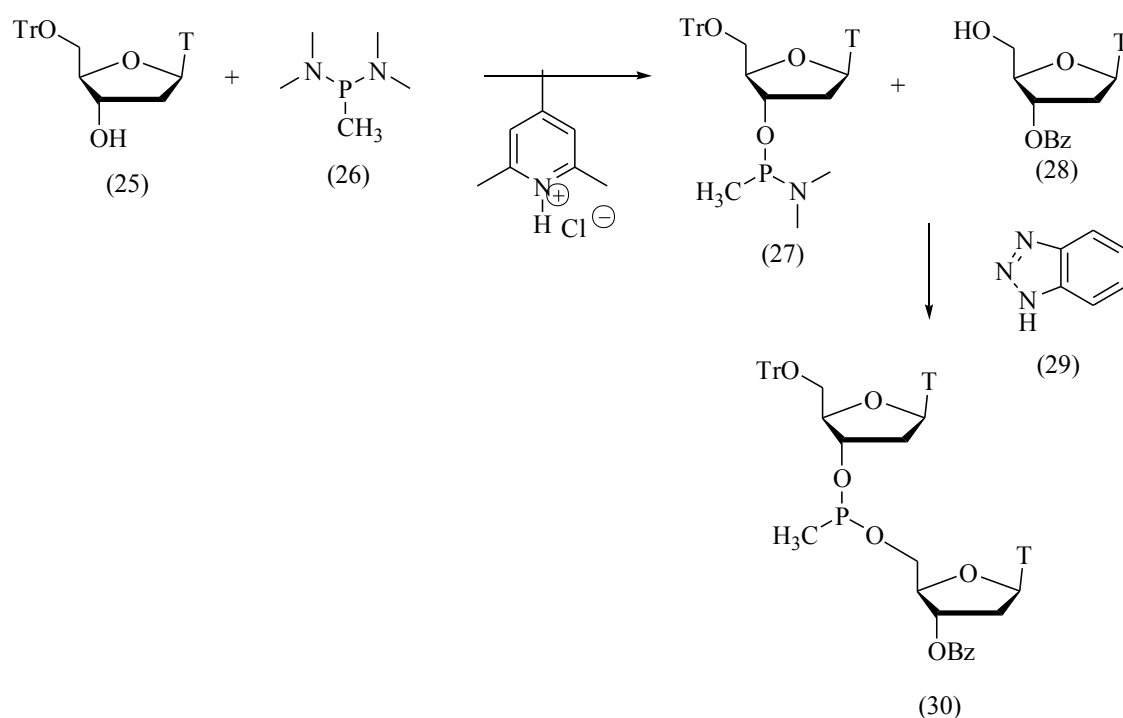


Figure 1.3.i. Synthesis of dinucleoside methylphosphonamidites.

Dorman et. al.<sup>45</sup> used a slightly different method to generate methylphosphonamidites using the reaction of 5'-*O*-dimethoxytrityl-2'-deoxynucleosides with chloromethylamino-phosphine. These reagents are now commercially available and the coupling chemistry is applicable to solid phase technology with only a slight modification from phosphodiester synthesis. The exocyclic amino groups in the nucleic acid bases are benzyl protected and in phosphodiester synthesis the deprotection is effected by  $\text{NH}_4\text{OH}$  treatment for 8 hours at  $60^\circ\text{C}$ . These conditions will cleave the methylphosphonate linkage and milder treatment involving  $\text{NH}_4\text{OH}$  treatment for 2 hours at room temperature followed by ethylenediamine / ethanol (1:1) treatment for 7 hours at room temperature removes the protecting groups without damaging the methylphosphonate group.

As with phosphorothioates, MP oligonucleotides have a chiral centre in the internucleotide linkage. Phosphorus(III) species in methylphosphonamidites have low configurational stability and can undergo epimerisation at the phosphorus atom and it is because of this that phosphorus(V) species have been targeted in attempts to carry out stereospecific syntheses<sup>46,47,48</sup>. This approach involved the reaction of 5'-monomethoxytrityl-2'-deoxythymidine (31) with methane phosphonate dichloride (32) followed by reaction with 4-nitrophenol (33) to give the separable diastereomers (34) as shown in fig. 1.3.j. The Grignard reagent *t*-butyl magnesium chloride was used to activate

the 5'OH of 3'-*O*-acetylthymidine (35) towards coupling with either diastereomer of (34) in a stereospecific manner.

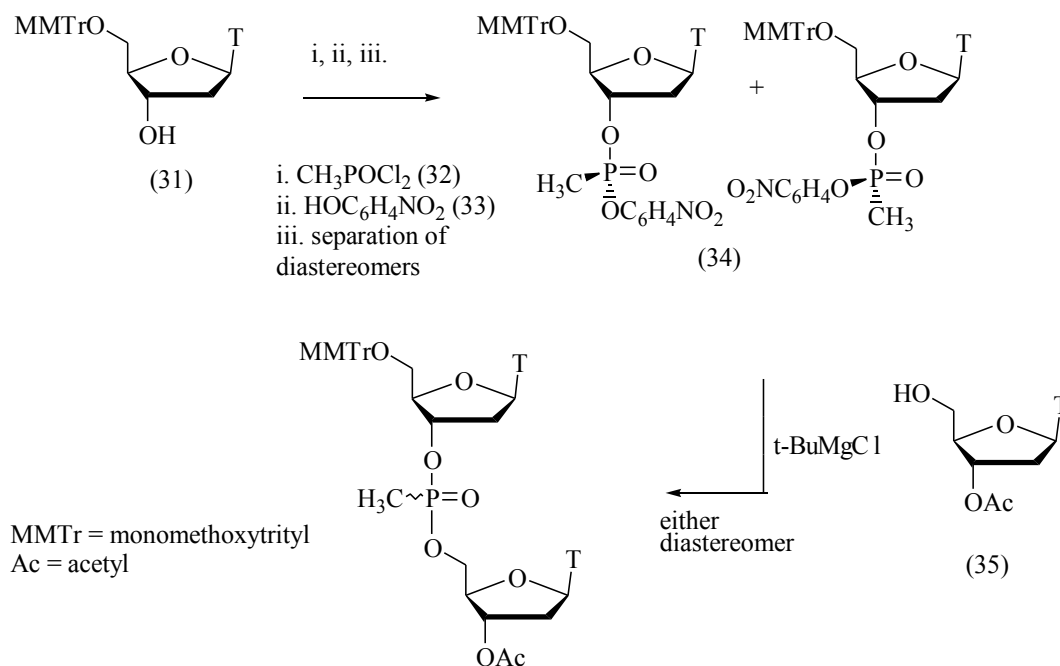


Figure 1.3.j. Stereospecific synthesis of dinucleoside methylphosphonamidites.

Diastereomeric purities of up to 95% were achieved in the synthesis of tetramers using this approach. The method was initially thought not to be applicable to solid phase technology, due to the viscous suspension usually generated from magnesium alkoxides. Le Bec and Wickstrom<sup>49</sup> overcame this by using a solid support to synthesise stereopure dinucleotide methylphosphonates via this Grignard approach. Again this approach, if extendable to longer chains, could be important if stereopure antisense oligonucleotides are needed for therapeutic applications.

#### 1.3.1.4. Miscellaneous oligonucleotide analogues.

Among the many other modified oligonucleotides those, which have proven to be most applicable to antisense applications, include:

##### 1.3.1.4.a. Phosphoramidates.

These are an easily obtained analogue using phosphoramidite methodology. The oxidation of phosphite triesters by  $I_2$  in the presence of an alkylamine generates the phosphoramidate internucleotide linkage<sup>50</sup>. Bridged phosphoramidates can be similarly synthesised using 3' or 5' amino functionalised nucleoside phosphoramidites<sup>51,52</sup>.

##### 1.3.1.4.b. $\alpha$ - anomeric Nucleotides.

In virtually all naturally occurring nucleosides and nucleotides the glycosidic linkage is in its  $\beta$  - anomeric form (see fig. 1.3.k). Morvan *et. al.*<sup>53</sup> successfully synthesised the unnatural  $\alpha$  - anomers by using  $\alpha$  - anomeric nucleoside phosphoramidites.

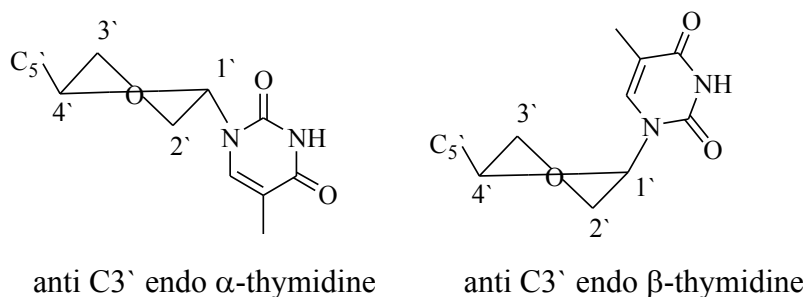


Figure 1.3.k. Structure of  $\alpha$  and  $\beta$  nucleosides.

Other nucleotide analogues of varying importance in antisense applications are 2'-modified oligoribonucleotides, phosphorodithioates, oligonucleotides with modified bases and those with non-phosphorus internucleotide linkages of which peptide nucleic acids are of particular interest. Of major importance to this research are oligonucleotides with functional molecules attached in specific sites and this will be dealt with in detail in a later section.

## 1.4. Antisense properties of modified oligonucleotides.

As was mentioned previously, there was a necessity to develop modified oligonucleotides because of the instability of natural phosphodiester towards certain enzymes, which are ubiquitous *in vivo*. They include both exo and endonucleases and it has been shown that unmodified oligonucleotides can be completely degraded after 15 minutes exposure to them<sup>34</sup>. The site of nucleolytic attack is the phosphate centre and this was the target for modifications when oligonucleotide analogues were developed to improve nuclease stability. With regard to the analogues mentioned in the previous section and any other prospective antisense agents there are a number of factors which must be taken into account individually and in combination when designing an antisense molecule and when interpreting the results of antisense experiments.

#### **1.4.1. Stability of duplex formation.**

The strength of the duplex formed between an oligonucleotide and its target sequence is characterised by the melting temperature ( $T_m$ ) of the double strand that is formed. In the double strand due to the stacking of the bases there are considerable  $\pi - \pi$  interactions which reduce the UV absorption of the bases. As the double strand is heated the two strands unpair and become single-stranded with a resulting increase in the absorption of the bases. Measurement of the absorbance at 260 nm versus temperature for a duplex gives an S shaped curve and it is the temperature at the midpoint of this curve which is denoted the melting temperature. Thus, comparisons between the  $T_m$ 's of unmodified oligonucleotides and modified oligonucleotides gives a measure of the relative binding affinities of the various duplexes. Factors which affect the  $T_m$  for modified oligonucleotides include the electronic nature of the modification, its steric bulk and absolute stereochemistry. The importance of binding affinity is shown by antisense experiments at increased temperatures where lower biological activity is seen due to the denaturing of the duplex. Phosphorothioate oligonucleotides can lower the  $T_m$  by an average of 0.5° C per phosphorothioate linkage present.<sup>54</sup> This can be rationalised in terms of the increased bulk of the sulphur atom relative to oxygen and if the negative charge is localised on sulphur and pointing in towards the helical centre it may cause increased repulsion between negative charges on opposite strands.<sup>55</sup> The  $T_m$  would also be decreased due to diastereomeric mixtures of phosphorothioates, which would have unequal affinity for their target strand.

Those oligonucleotides with non-ionic modifications such as methylphosphonates will have increased binding affinity as the charge repulsion between opposite strands in phosphodiester is removed. The steric bulk and diastereomeric mixture will however have a destabilising effect. A remarkable increase in  $T_m$ , was achieved using  $\alpha$ -anomeric oligonucleotides.<sup>56</sup> The  $T_m$  of a normal 14-mer  $\beta$ -anomeric phosphodiester with its RNA target was 27° C but the  $T_m$  of the  $\alpha$ -anomer with the RNA target was 53° C. This dramatic rise was explained by the extra stability of the duplex due to the fact that  $\alpha$ -anomer - RNA duplexes bind in a parallel manner (i.e. both strands run from 3' to 5') rather than the anti parallel binding of normal DNA - RNA hybrids (see fig. 1.1.f.). Increases in  $T_m$  have also been seen with 2' - *O* -methyloligoribonucleotides<sup>57</sup> and methylphosphonates with a 2' - *O* -methyl group<sup>58</sup>.

#### **1.4.2. Penetration of oligonucleotides into cells.**

Oligonucleotides can enter cells by a mechanism thought to be receptor-mediated endocytosis and non-ionic modified oligonucleotides are known to enter faster than their ionic counterparts. Various attempts have been made to improve cellular penetration including incorporation into liposomes and the conjugation of molecules to one end of the oligonucleotide to aid transport through the cell membrane<sup>34</sup>. However, the cellular uptake of oligonucleotides, which are highly charged polyanions, is of crucial importance in determining their antisense capabilities. The mechanism is not completely understood and many factors can influence cell uptake and thus biological activity. These include cell type, chemical modification and the sequence and length of the oligonucleotide itself. Therefore each potential antisense molecule should be treated individually for generalisations cannot always be applied.

#### **1.4.3. Stability to nucleases.**

Phosphorothioates are stable to the exonucleases snake venom phosphodiesterase (svp) and spleen phosphodiesterase (sp) and one diastereomer is cleaved by the

endonuclease EcoRI while the other is completely resistant. Under HIV assay conditions the half life of a phosphodiester oligonucleotide was 17 hours while the analogous phosphorothioate was undamaged after 1 week. Methylphosphonates are stable to most nucleases as are phosphoramidates,  $\alpha$ -anomeric oligonucleotides, phosphorodithioates and 2'-O-methylribonucleotides. An approach to achieving the antisense potential of phosphodiesters with nuclease resistance is to include some modified linkages in a phosphodiester. Stec *et. al.*<sup>59</sup> used phosphorothioates to protect the 3' and 5' ends of a 15 mer phosphodiester and found a half life of 1 month in human serum as opposed to 2 - 3 days for the unprotected oligonucleotide. Similarly terminal modification by two adjacent methylphosphonates leads to increased nuclease stability. These end modified molecules are not however protected from endonucleases and internal modifications have to be incorporated. The combination of some modifications can increase nuclease stability but they might also decrease the actual antisense effect. It is therefore necessary to know the cellular response for different types of modified oligonucleotides before using them to increase stability.

#### **1.4.4. Mechanisms of antisense action.**

With the knowledge of the specificity of oligonucleotides towards binding with their target RNA and knowledge of the transcription and translation processes, it was originally envisaged that antisense effects would be as a result of physically blocking the ribosomal machinery, which synthesises proteins. This hybrid arrest of translation (HART) was used to explain early apparent antisense action.

It is now known that ribosomes can destabilise secondary structures within the mRNA as they move along the coding region and thus would be expected to disrupt potential DNA - RNA antisense - sense duplexes during translation. Minshull and Hunt<sup>18</sup> showed that the RNA of DNA-RNA hybrids was degraded by an enzyme called ribonuclease H (RNaseH), which catalyses the hydrolysis of RNA in such duplexes. It is the action of this enzyme, which is thought to be responsible for the most effective antisense results published to date. Therefore in the design of oligonucleotide analogues it is hoped to achieve or surpass the RNaseH induction capabilities of normal phosphodiester oligonucleotides while improving on their nuclease instability.

Of the main modified oligonucleotides mentioned so far only phosphorothioates<sup>60</sup> and phosphorodithioates<sup>61</sup> can elicit an antisense response attributable to RNaseH.  $\alpha$ -anomeric oligonucleotides, methylphosphonates, phosphoramidates and 2'-O-methyloligoribonucleotides did not induce RNaseH cleavage and any antisense effects seen have probably been as a result of HART due to the stronger binding of these oligonucleotides for their target RNA.  $\alpha$ -anomeric oligonucleotides have been shown to physically arrest translation when targeted to the region 5' to the initiation codon and the initiation codon itself, presumably by preventing the formation of the ribosomal initiation complex<sup>62</sup>. 2'-O-methyloligoribonucleotides were also used to successfully target splice sites in pre-mRNA by a similar blocking mechanism<sup>63</sup>.

Agrawal *et.al.*<sup>60</sup> showed that RNaseH cleavage of a target mRNA by phosphorothioates was not as efficient as normal phosphodiester but that it did occur at low concentrations. They also showed that phosphodiester oligonucleotides containing sequences which were phosphorothioate or methylphosphonate could also induce RNaseH cleavage to some extent. This result in combination with the extra nuclease stability of such chimeric oligonucleotides has led to the design of a number of 2<sup>nd</sup> generation antisense agents. The design of these agents takes favourable properties from different types of oligonucleotides to try and improve the overall antisense effect. This approach was developed in 1987 by Inoue *et al.*<sup>64</sup> where they used a 2'-O-methyloligoribonucleotide mixed with a phosphodiester to induce RNaseH cleavage of a target mRNA. Many chimeric oligonucleotides have been developed recently<sup>65</sup>, however, there is a problem with the design and use of these chimera, the use of pure oligonucleotides and the interpretation of experimental results with them. This is because there are a number of non-antisense effects both sequence specific and sequence non-specific which have been reported incorrectly as antisense effects.

#### **1.4.5. Non-antisense effects of antisense oligonucleotides.**

The underlying principle of antisense therapy, that of specific binding of the antisense molecule to the target RNA does not take into account the complexity of the cellular environment, i.e. the interactions between the antisense molecule and other



molecules in the cell. For this reason oligonucleotides have been found to induce a variety of biological effects other than or in addition to antisense effects. Therefore, interpretation of experimental results must take into account other potential interactions of the antisense oligonucleotide. Control experiments normally used include a sense strand, a scrambled antisense strand and mismatch strands. If these controls show no response and the antisense strand gives a response it may still not be sufficient to say the response is an actual antisense response.

An early non-antisense effect with phosphodiester oligonucleotides was caused by their susceptibility to nucleases. The nucleases break down the oligonucleotide to nucleosides, which can be then rephosphorylated producing an imbalance in cellular pools of nucleoside triphosphates. This can prevent the cells ability to replicate properly and produce an effect, which may seem to be via an antisense mechanism but is in fact not<sup>66</sup>.

Phosphorothioates were shown to have antisense effects at sub-micromolar concentrations<sup>67</sup> but at 1-10  $\mu\text{M}$  concentrations the oligonucleotides bind non-specifically to enzymes involved in protein synthesis so called “poly anionic effects”, giving downregulation of translation but not by an antisense mechanism. It has been shown that phosphorothioates bind to a number of proteins important in cellular processes<sup>68</sup> in a manner which, is non-sequence specific. Other binding of phosphorothioates to proteins is sequence specific and this can be an advantage. This so called “aptameric” effect has been used by Bergan *et al.*<sup>69</sup> to specifically bind and inhibit an oncogenic protein present in chronic myeloid leukaemia. Other non-antisense effects are seen in phosphorothioates with CpG and G<sub>4</sub> motifs. Some CpG sequences have been shown to stimulate the immune system producing non-antisense responses<sup>70</sup>. Oligonucleotides with G tetrads can form tetramers with Watson-Crick and Hoogsteen base pairing. Such tetramers can have an undesirable non-antisense interaction with proteins<sup>71</sup>.

These examples show the complexity of the interactions that can occur and the difficulty in assigning a cellular response to be specifically antisense. Presumably a lot of early publications proclaiming antisense effects were in fact due to non-antisense effects but as technology has advanced and become more specialised it has become possible to design oligonucleotides with reduced side effects so that results only due to an antisense mechanism can be identified.

#### **1.4.6. Design of antisense oligonucleotides.**

With the combined knowledge of the factors mentioned in the previous sections, it is now possible to design a protocol for selecting a potential antisense molecule for a well understood target. The secondary structure of the target mRNA might mean a specific sequence within the target is inaccessible and therefore use of a number of oligonucleotides in a screening process is necessary to see which oligonucleotides can hybridise with the target and produce an antisense response. It is also important if using a phosphorothioate to choose one without CpG or G<sub>4</sub> motifs or other sequences, which might form self-complementary hairpins that compete with binding to the target. If a CpG motif is necessary then its immunostimulatory properties can be reduced by replacing the nucleosides with 2'-*O*-methylribonucleosides or by having a methylphosphonate internucleotide linkage. The effect of G<sub>4</sub> motifs can be minimised by using 7 - deazaguanine instead of guanine. The choice of chemical modification can reduce side effects. Inclusion of 2'-*O*-methylribonucleotides or methylphosphonates can reduce the polyanionic effects of phosphorothioates. Mixed backbone oligonucleotides either end-modified or centrally modified are currently the most popular agents currently under investigation<sup>70</sup>. Together with careful design of control experiments these oligonucleotides have great potential as therapeutic agents acknowledged by the fact that a lot of the contributors to the current literature are from pharmaceutical companies who have a number of antisense agents in various stages of clinical trials. The federal drug administration in the USA recently approved a phosphorothioate antisense agent called vitravene™ for treatment of human cytomegalovirus (CMV).

#### **1.4.7. Chronic Myeloid Leukaemia (CML).**

Chronic myeloid leukaemia is a genetic disorder of hemopoietic stem cells and presents itself in chronic phase for a period of time up to 4 years before progressing to a blast crisis, which is resistant to treatment and almost always fatal. The only known treatment for the disease is allogenic bone marrow transplantation, which is limited as it requires a suitable donor. 95% of CML patients have the so called philadelphia (Ph) chromosome, which is

generated by a reciprocal translocation between the Abelson (ABL) gene on chromosome 9 and the breakpoint cluster region (BCR) on chromosome 22. The BCR gene has two exons termed b2 and b3. If neither exon is removed in splicing, the chimeric mRNA is called b2a2 and if the b2 exon is removed by splicing, the mRNA is called b3a2. The gene sequences of these two mRNA are shown below in figure 1.4.a.

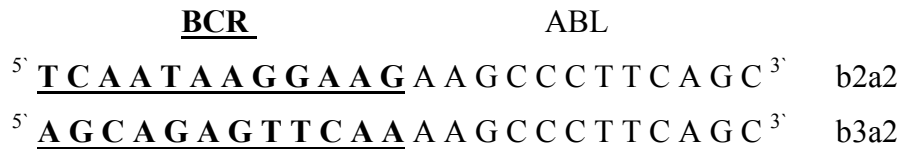
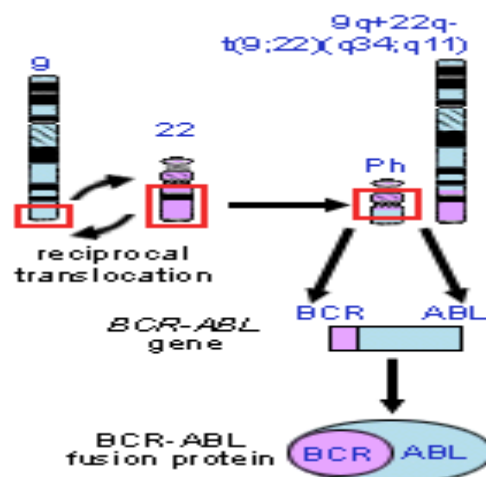


Figure 1.4.a. Gene sequence of the b2a2 and b3a2 mRNA in CML.

The BCR-ABL mRNA codes for a p210<sup>BCR-ABL</sup> protein (figure 1.4.b.) with tyrosine kinase activity. It seems likely that activation of this kinase is the first step in the oncogenesis of CML as the expression of this protein blocks CML from programmed cell death (apoptosis) leading to an excessive accumulation of myeloid cells<sup>72</sup>.



*Figure 1.4.b. Formation of BCR-ABL fusion protein.*

*1.4.7.1. BCR-ABL as a target for antisense oligonucleotides.*

In order to apply antisense approaches uniquely to the BCR-ABL gene amongst mutated and non-mutated cells it is necessary to target the junction region between the BCR and ABL gene sequences. As this part of the gene sequence is down stream of the initiation codon, it is not thought to be in a region of the mRNA that is most open for access of the antisense molecule. Despite this there have been successes in inhibiting p210 expression using antisense phosphodiester<sup>73</sup>, phosphorothioates<sup>74</sup> and chimeric oligonucleotides<sup>75</sup>. Szczylik *et al.*<sup>73</sup> reported specific inhibition of leukaemic cell lines from CML blast crisis patients when targeting both the b2a2 and b3a2 chimera. Currently there are a number of antisense oligonucleotides targeted to the BCR-ABL gene that are in various stages of clinical trials<sup>70</sup> showing the success of antisense approaches to target CML. The central aim of the research presented in this thesis is the use of antisense oligonucleotide conjugates activatable by light to specifically damage bases in a 34 base ODN model of the junction region of th BCR-ABL mRNA. It is hoped to improve upon the antisense capabilities of normal oligonucleotides by the conjugation of photosensitisers (either ruthenium polypyridyl complexes or pteridine molecules) to the 5` end of a 17 base ODN complementary to part of the 34-mer target as shown below.



## **1.5. Oligonucleotide Conjugates.**

As was mentioned in section 1.2.3., there are a number of problems with the use of phosphodiester oligonucleotides in antisense therapy. One of the approaches to overcome these obstacles was dealt with in section 1.3. and involved the synthesis of oligonucleotide

analogues. Another approach is to synthesise oligonucleotide conjugates using molecules specifically designed to augment the antisense capabilities of phosphodiester oligonucleotides.

This section deals with the covalent attachment of such molecules to oligonucleotides and encompasses the coupling chemistries used and the applications of the conjugate molecules. Oligonucleotide conjugates have been synthesised for a number of reasons related to antisense or antigene strategy such as increasing the stability of duplexes or triplexes, improving cellular uptake and inducing irreversible damage to target oligonucleotide strands. More generally, such conjugates have been designed for use as probes for reactions in double stranded nucleic acids and as alternatives to radioactive labelling of oligonucleotides.

### 1.5.1. Synthesis of oligonucleotide conjugates.

The main methods used to synthesise oligonucleotide conjugates have included:

- (i) Preparation of synthons for conjugation using standard coupling reactions.
- (ii) Functionalising oligonucleotides during automated synthesis for subsequent coupling.
- (iii) Activation of oligonucleotides post-synthesis followed by coupling reactions.

The most common method used to synthesise oligonucleotides employs phosphoramidite coupling. In an extensive review, Beaucage and Iyer<sup>76</sup> detailed a wide range of conjugates that can be synthesised using phosphoramidite derivatives with fluorescent, lipophilic, intercalating and DNA cleaving molecules.

A general procedure for direct ligand incorporation by phosphoramidite coupling is outlined below in figure 1.5.a. and involves conjugation of a molecule X (36), which contains an alcohol functional group. After reaction of (36) with a phosphitylating agent such as ( $\beta$ -cyanoethoxy)*bis*-diisopropylaminophosphine (37), the resulting phosphoramidite (38) can be coupled with the terminal 5'-OH of the oligonucleotide (39) in the DNA synthesiser and the conjugate (40) is then released following oxidation, cleavage from the solid support and deprotection.

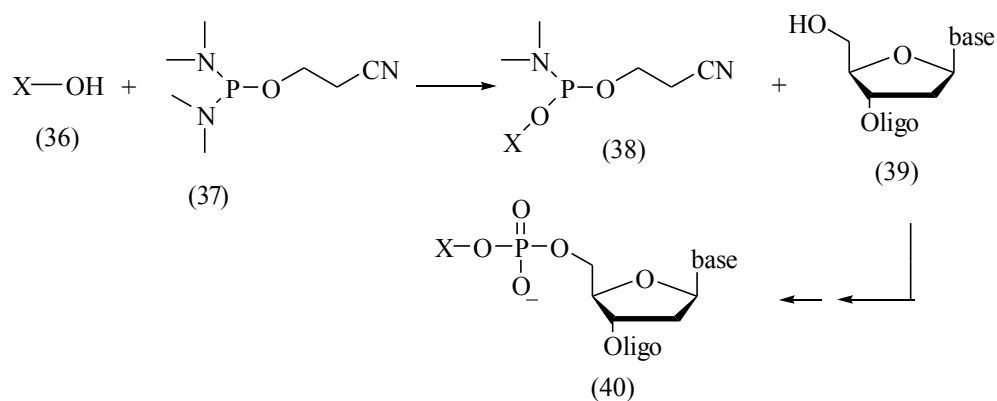
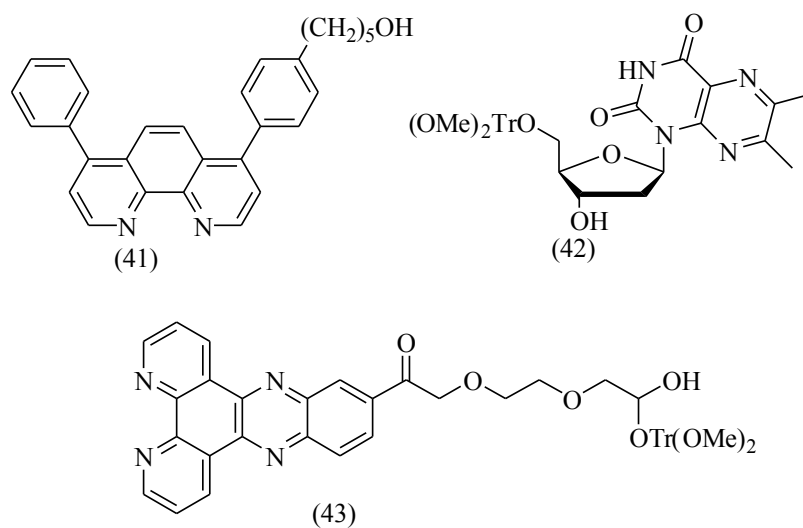


Figure 1.5.a. Conjugate synthesis via phosphoramidite coupling.

Many conjugates have been synthesised by this route including a number of pteridine nucleosides and ruthenium complexes<sup>77,78,79,80,81</sup>, some with functionalised ligands (41), (42) and (43) as shown in Figure 1.5.b.



Tr = trityl

Figure 1.5.b. Examples of derivatives conjugated by phosphoramidite coupling.

It is possible to modify the protocols for automated oligonucleotide synthesis and functionalise the oligonucleotide during its synthesis towards coupling after cleavage from

the solid support. The oxidation of phosphite triester intermediates is usually effected by an aqueous I<sub>2</sub> solution; however, if the water is replaced by an amine such as ethylene diamine, then a phosphoramidate is produced. The free amino group of this intermediate can be reacted with conjugating molecules directly or via various reactive intermediates<sup>82</sup> such as a succinimide ester. It is also possible to introduce an amino group by reacting the 5'-OH with an aminoalkyl phosphoramidite. This generates an oligonucleotide derivative with a free amino group at its 5'-terminus. Varying the length of the alkyl chain allows the synthesis of conjugates with differing distances between the conjugate molecule and the oligonucleotide strand. Amino functionalised oligonucleotides have been used to synthesise conjugates with porphyrin groups<sup>83,84</sup> (44), chlorin derivatives<sup>85</sup> (45) and a number of ruthenium complex derivatives<sup>86,87,88</sup> with ligands (46, 47 and 48) as shown in figure 1.5.c.

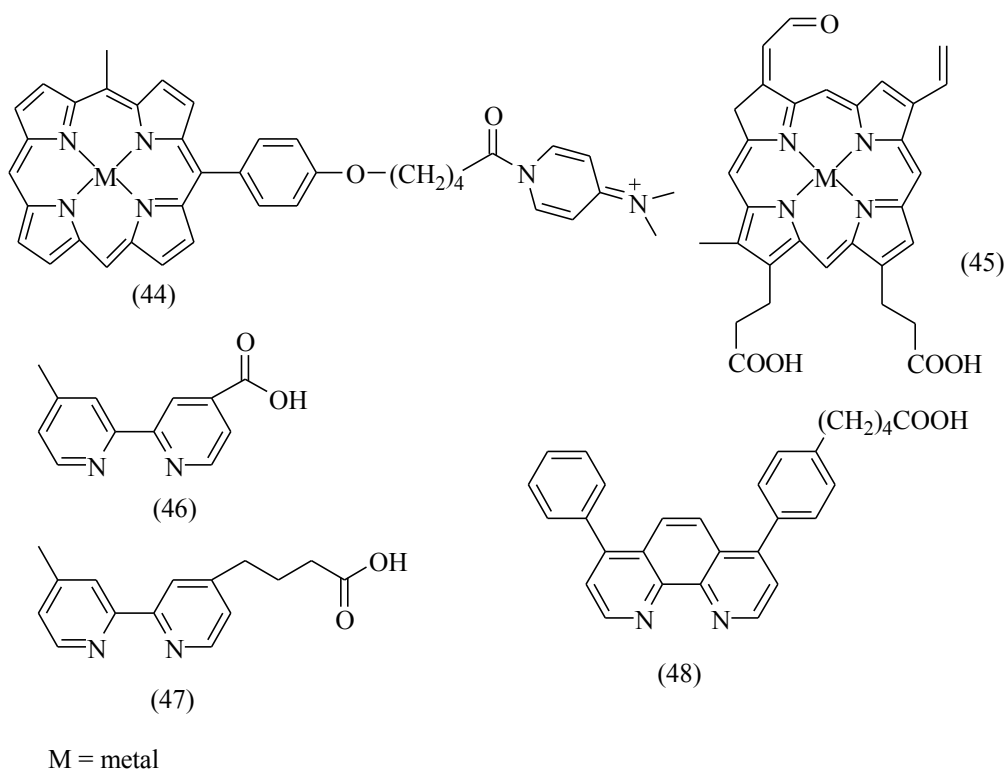


Figure 1.5.c. Molecules conjugated to amino functionalised oligonucleotides.

One of the most widely used methods for the synthesis of oligonucleotide conjugates with antisense or antigene properties involves direct reaction of the molecule to be conjugated with an oligonucleotide containing a terminal phosphate or thiophosphate residue. It is necessary to activate the phosphate residue towards such coupling and several methods have been employed.

1. Activation of the phosphate (49) with molecules such as dicyclohexylcarbodiimide (50) (DCC) followed by reaction with a primary amine giving the phosphoramidate (51) and dicyclohexyl urea (52) as shown below in figure 1.5.d.

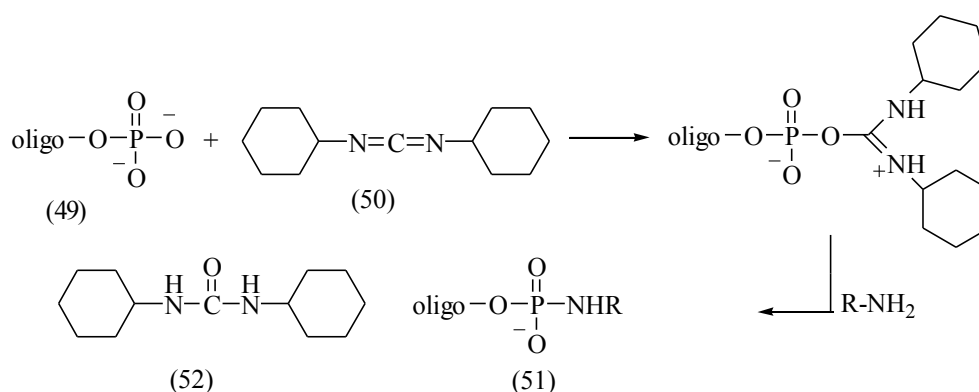


Figure 1.5.d. Phosphate activation with DCC.

2. The phosphate can also be conveniently activated by a mixture of triphenyl phosphine (53), dipyridylsulphide (54) and an amine (55) as shown in figure 1.5.e. If the amine used is a nucleophilic catalyst such as N-methyl imidazole or N,N-dimethylaminopyridine then, zwitterionic intermediates such as (56) and (57) are produced.

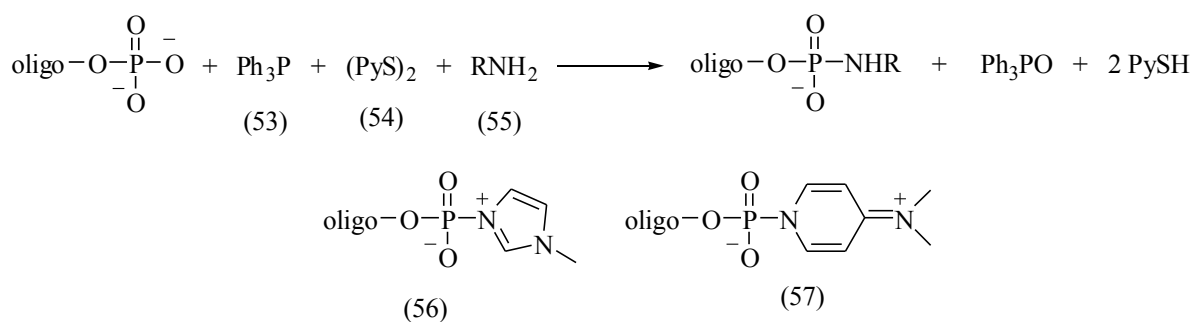


Figure 1.5.e. Activation of 5'-phosphorylated oligonucleotide.

These derivatives are easily purified, stable in aqueous media and can then be reacted with the amino group of the molecule to be conjugated. Derivatives like this have been used to synthesise conjugates with derivatives of 1,10-phenanthroline<sup>89</sup>, (58) ethylenediamine-



tetraacetic acid<sup>90</sup> (59), psoralen<sup>91,92</sup> (60), benzopyridoindoles<sup>93</sup> (61) and benzo-pyridoquinoxalines<sup>94</sup> (see fig. 1.5.f).

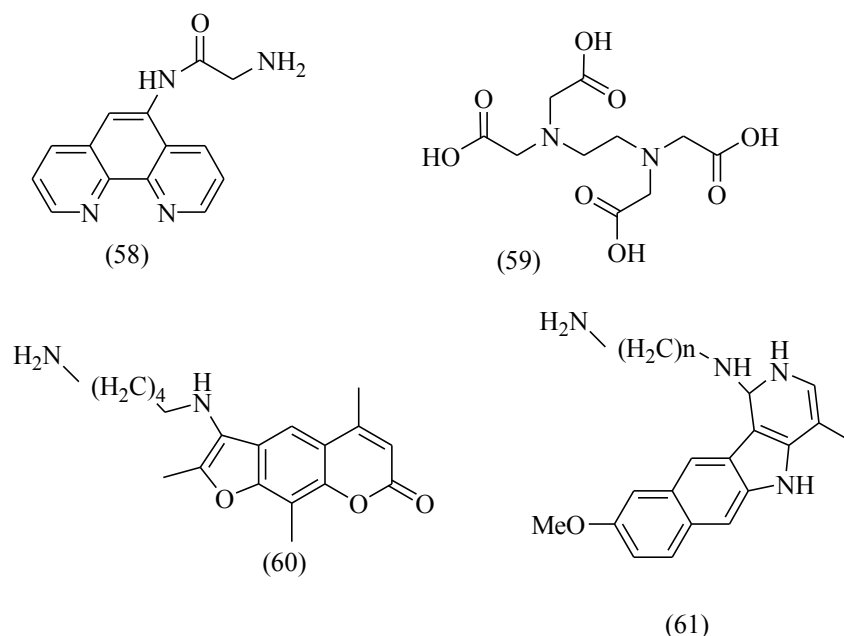


Figure 1.5.f. Some molecules that have been conjugated to activated phosphates.

An alternative to activated phosphates is to introduce the more nucleophilic thiophosphate group. Thiophosphorylation can be achieved enzymatically using  $\gamma$ -thio-ATP in the presence of polynucleotide kinase enzyme<sup>82</sup> or by reaction of the terminal 5'-OH group of the oligonucleotide with bis (cyanoethyl) N, N-diisopropylamino phosphoramidite (16) followed by oxidation with sulphur in pyridine<sup>95</sup>. Again a wide variety of conjugates have been synthesised using this approach including proflavine<sup>96,97</sup> and psoralen derivatives<sup>98</sup>.

Thus, using the various methodologies described above, it is possible to synthesise a wide variety of oligonucleotide conjugates. Grimm *et al.*<sup>99</sup> recently described methods for the terminal functionalisation of oligonucleotides with amino, sulfhydryl, thiophosphate or carboxyl groups, thus allowing for the conjugation of molecules with either nucleophilic or electrophilic functional groups.

## 1.5.2. Uses of Oligonucleotide conjugates.

The previous section has detailed the ease with which a large number of molecules can be conjugated to different functional groups on oligonucleotides or their derivatives. The main reasons for introducing such modifications is the improvement of antisense or antigene properties including increased binding strength, resistance to nucleases, enhanced cellular uptake and induction of chemical or photochemical damage. The design of conjugates with photoactive molecules attached was the main aim of this research along with the photoinduction of oxidative damage to specific bases in a target oligonucleotide strand. It was hoped that these modifications could permanently damage the target strand and arrest gene expression at the translational or transcriptional level. A number of reviews and books have covered some of the advances made<sup>34,100,101</sup>.

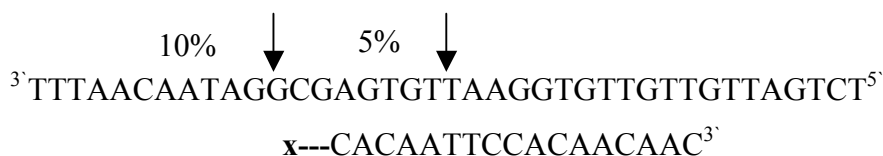
### 1.5.2.1. Oligonucleotide intercalator conjugates.

The stability of the double helix formed between the antisense and sense strands can be increased by the covalent attachment of an intercalating molecule to the antisense strand. Intercalating molecules have planar polycyclic aromatic rings, which slide between adjacent heterocyclic bases in double stranded DNA and increase stability as a result of  $\pi$ - $\pi$  interactions between the intercalator and the nucleobases. Toulme *et al.*<sup>102</sup> conjugated 2-methoxy-6-chloro-9-aminoacridine to the 3'-end of various short (5-15 bases) oligonucleotides. They showed an increase in duplex stability relative to unmodified oligonucleotides by virtue of increases in melting temperature with the oligonucleotide intercalator conjugates. These conjugates were then used to inhibit mRNA translation in an *E.coli* system where a region close to a ribosomal binding site was targeted but they could not rule out contributions from non-specific effects. Other acridine conjugates have been shown to increase duplex stability and inhibit protein synthesis<sup>103</sup> and such conjugates have also been shown to increase triplex stability<sup>93,94,104,105</sup>. Another advantageous property of intercalator conjugates is their higher penetration through cell membranes due to the contribution from the hydrophobic intercalator molecule. Also, these conjugates have improved stability to exonucleases if the site of conjugation is the 3' or 5' end of the oligonucleotide.

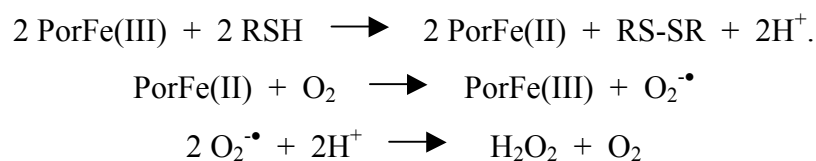
1.5.2.2. *Oligonucleotide conjugates with chemically reactive groups.*

Oligonucleotides bearing chemically reactive groups can be used for sequence specific modification and/or cleavage of targeted nucleic acids. Alkylating groups such as *p*-(*N*-2-chloroethyl-*N*-methylamino)benzaldehyde have been conjugated with this aim in mind and it is the ethylammonium cations produced that alkylate guanine, adenine and cytosine residues<sup>106</sup>. Sequence specific oxidative damage of nucleic acids has been achieved with a number of oligonucleotide conjugates. The most widely studied are those complexes of Fe(II) with ethylenediaminetetraacetic acid (EDTA)<sup>90,107,108,109</sup> with porphyrins<sup>110,111,112</sup>, complexes of copper with 1,10-phenanthroline<sup>89,113</sup> and other complexes of porphyrin derivatives with various metals<sup>114,115,116</sup>.

Chu and Orgel<sup>90</sup> studied the following system (X = molecule producing reactive species):



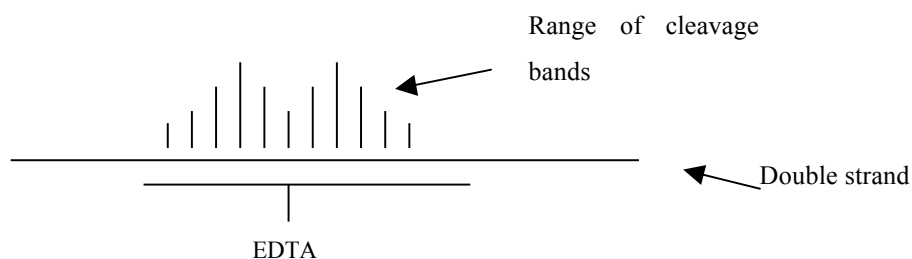
They found that upon hybridisation, cleavage occurred after addition of Fe<sup>2+</sup> ions and the reducing agent dithiothreitol. The main cleavage points were as indicated by the arrows above at positions 4 bases either side of the phosphate residue containing the conjugated molecule (other bases in between were damaged to a lesser extent). The cleavage pattern was accounted for by two different orientations of the EDTA group relative to the target strand. The cleavage was caused by hydroxyl radicals that were formed by the following reactions. Por = porphyrin, RSH = dithiothreitol.



Thus, the complex is reduced in the presence of dithiothreitol and then reacts with oxygen to form the superoxide radical anion. The anion then reacts to form hydrogen peroxide and the hydroxyl radicals are produced from the following Fenton reaction.



The hydroxyl radicals produced react indiscriminately with various regions of DNA including the sugar residues and the bases producing both direct cleavage of the strand (frank breaks) and piperidine sensitive cleavage sites. The nucleic acid bases have very high reactivity<sup>117</sup> with respect to electrons and hydroxyl radicals ( $10^9$ - $10^{10} \text{ M}^{-1}\text{s}^{-1}$ ), whereas the ribose moiety is less reactive to hydroxyl radicals  $\sim 10^9 \text{ M}^{-1}\text{s}^{-1}$  and much less to electrons  $\sim 10^7 \text{ M}^{-1}\text{s}^{-1}$ . The range of cleavage bands produced by Chu and Orgel<sup>90</sup> reflect the fact that hydroxyl radicals can diffuse from their site of generation and react at a number of base sites. Dreyer and Dervan<sup>108</sup> used a similar conjugate but with the EDTA conjugated to a modified thymine base in the centre of the oligonucleotide. They induced cleavage in the target strand that was spread out in both directions from the site of the conjugate as shown below.



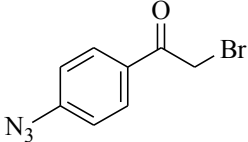
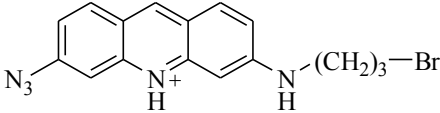
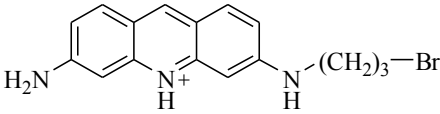
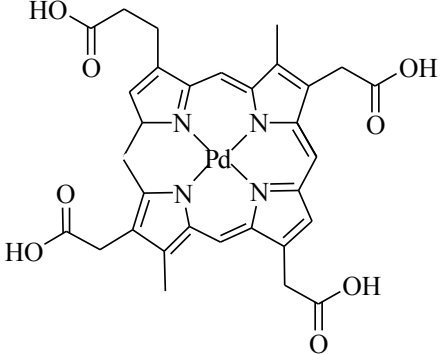
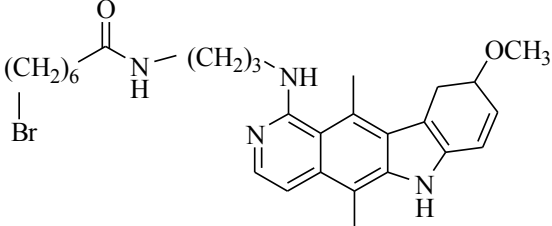
The cleavage pattern was more attributed to the orientation of the chelate in both directions rather than the diffusion of the reacting species. It was also shown that the extent of cleavage was dependent on the length of the linking group between the EDTA residue and the oligonucleotide<sup>110</sup>. Demonstration that the bases were attacked by hydroxyl radicals resulting in piperidine sensitive residues was shown by Boidot-Forget *et al.*<sup>109</sup> who used an EDTA conjugate that was additionally stabilised by conjugation of an intercalating acridine molecule. They also successfully targeted triple stranded regions as did Strobel *et al.*<sup>112</sup>.

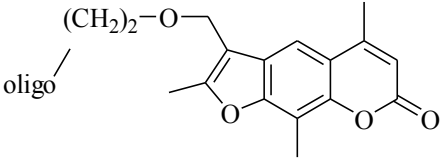
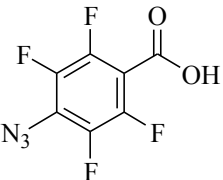
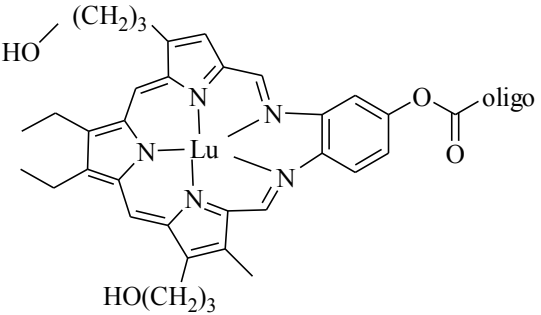
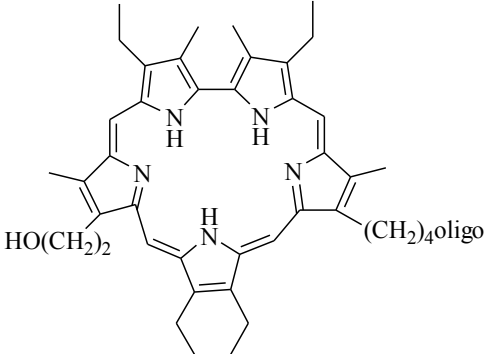
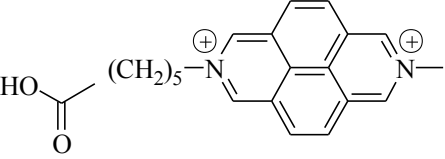
Similar radical induced cleavage was achieved with copper *bis*-1,10-phenanthroline complex conjugates<sup>113</sup> in the presence of  $\text{H}_2\text{O}_2$ , where the radicals were proposed to abstract a hydrogen atom from the C1' of the sugar leading to 3' and 5' dephosphorylation reactions. In contrast to the porphyrin cleavage pattern the phenanthroline complex produced less spread out cleavage bands suggesting the radicals produced in this case did not diffuse far before reaction<sup>89</sup> (possibly due to the partial intercalation of the copper

complex). Meunier *et al.*<sup>115,116,118</sup> used manganese porphyrin complex conjugates and successfully cleaved single stranded and double stranded targets. They found considerable dependence of type and length of linker on the amount of cleavage produced. For example, in the double stranded target, if the linker was an alkyl chain then, hydrophobic repulsions between the chain and the major groove resulted in low cleavage. If however, the linker was an alkyl polyamine with protonatable groups, the binding of the linker was stronger in the major groove and the porphyrin moiety was held closer to the target bases resulting in higher yields of damage. These examples have shown that it is possible to chemically induce site specific damage to target oligonucleotides but that the exact system used determines the specificity and amount of cleavage produced.

#### 1.5.2.3. *Oligonucleotide conjugates with photoactive groups.*

Oligonucleotide conjugates have also been used to induce specific damage to target nucleic acids either by photocrosslinking reactions or photooxidative damage. This latter process can occur by two competing photosensitisation mechanisms. Direct electron transfer (type I reaction) from guanine residues to excited state molecules followed by further reactions of the guanine radical cation produced. Alternatively, excited state molecules with a sufficiently high energy can transfer energy to ground state molecular oxygen (type II reaction) generating the highly reactive species singlet oxygen ( $^1\text{O}_2$ ), which also reacts preferentially with guanine residues. Potential advantages of photoactive oligonucleotide conjugates include the fact that no damage occurs in the dark, so if the conjugates could enter cells and hybridise to their target with high efficiency then side reactions could be minimised. Limitations include the fact that the penetration of radiation into desired cells might not be sufficient to achieve a significant antisense effect. However, if fibre optic systems could be employed to directly irradiate target organs (as is carried out extensively in photodynamic therapy) then the potential of these conjugates could be realised, otherwise photoactive antisense conjugates would be limited to eye or skin treatment and for extracorporeal irradiation of blood. The following table shows the main photoactive molecules that have been conjugated to oligonucleotides, their site of conjugation and their function upon irradiation.

Linker molecule:	Structure:	Conjugation Site and function:	Ref.
<i>p</i> -azidophenacylbromide (62)		5'-thiophosphate, crosslinker.	119
3-azido-6-(3-bromopropylamino)acridine (63)		5'-thiophosphate, crosslinker.	96
Alkylbromoproflavin (64)		3' and / or 5'-thiophosphate crosslinker, oxidative damage	97
Palladium (II) Coproporphyrin (65)		5'-activated phosphate, crosslinker	120
Ellipticine derivative (66)		3'-thiophosphate, direct photocleavage and crosslinker.	121

Linker molecule:	Structure:	Conjugation Site and function:	Ref.
Psoralen derivative (67)		5'-phosphate, crosslinker	122
<i>p</i> -Azidotetrafluorobenzoic acid (68)		5' amino modified phosphate, crosslinker	123
Texaphyrin derivative (69)		5'-amino modified phosphate, oxidative damage	124
Sapphyrin derivative (70)		5'-phosphate, oxidative damage and crosslinker	125
Diazapyrene derivative (71)		5'-amino modified phosphate, crosslinker	126

Linker molecule:	Structure:	Conjugation Site and function:	Ref.
Chlorin derivative (46)		5'-activated phosphate, crosslinker and oxidative damage	85
Fullerene derivative (72)		5'-thiophosphate, oxidative damage	133
Rhodium complex derivative (73)		5'-amino modified phosphate, oxidative damage	136
Anthraquinone derivative (24)		Amino peptide nucleic acid, oxidative damage.	127
Dibenzoyl-diazomethane derivative (25)		5'-amino modified phosphate crosslinker	128



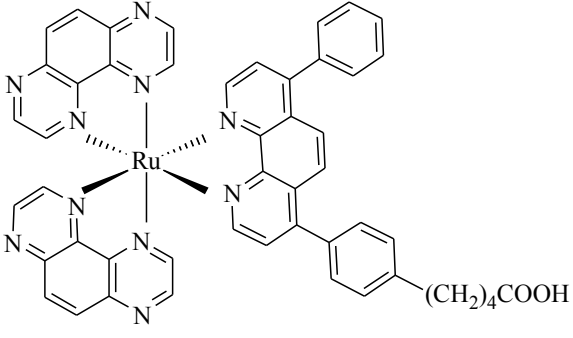
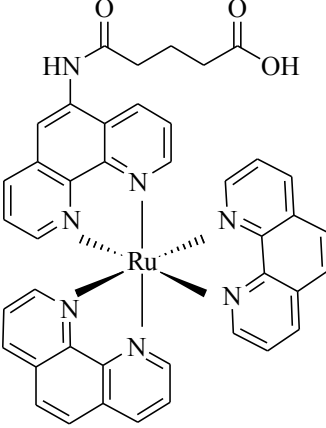
Linker molecule:	Structure:	Conjugation Site and function:	Ref.
Ruthenium complex derivative (76)		Amino functionalised base, crosslinker.	88
Ruthenium Complex derivative (77)		Amino functionalised base, oxidative damage.	137, 138

Figure 1.5.g. Molecules used in photoactive oligonucleotide conjugates.

Le Doan *et al.*<sup>96</sup> conjugated a 3-azidoproflavine (63) derivative to the 5`end of octathymidylate and targeted the following 5`-radiolabelled 27 base complementary sequence (lines indicate sites of photodamage).



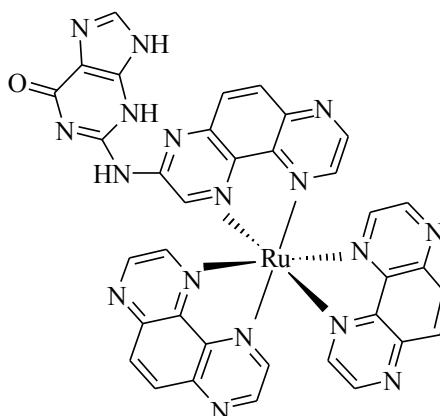
Upon irradiation ( $\lambda > 300\text{nm}$ ) of the hybridised strands and electrophoresis it was observed that there were bands which migrated slower than the 27-mer. These were attributed to a crosslinked species where the proflavin was covalently attached to the target strand. Excision of the slower migrating bands from the gel followed by piperidine treatment and re-electrophoresis revealed the sites of crosslinking as shown above. The most intense site for crosslinking corresponded to a parallel binding of the conjugate with respect to the 27-mer. Some cleavage was seen at the other end of the target and this was explained by the

formation of a triple helix between the target strand and two conjugate strands, as shown below.



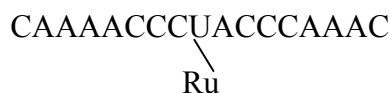
These results show that a single stranded and a double stranded region can be targeted for photocrosslinking suggesting potential in antisense and antigene applications. Further investigations<sup>97</sup> showed that photodamage other than crosslinking occurred with proflavin conjugates. The damage was mainly at guanine residues and was attributed to photooxidation reactions involving  $^1\text{O}_2$  or radicals, since proflavin is known to generate  $^1\text{O}_2$ <sup>129</sup> and induce radical reactions in DNA<sup>130</sup>. Psoralen conjugates were also used to photoinduce crosslinks to a single stranded DNA target<sup>91</sup>. The psoralen molecule intercalates in the DNA and irradiation induces a cycloaddition reaction between the 5,6 bond of pyrimidine residues and either the 4'-5'- double bond of the psoralen furan ring or the 3,4 double bond of the psoralen pyrone ring. Psoralen conjugated to a methyl phosphonate oligonucleotide<sup>92</sup> was shown to inhibit translation of rabbit globin mRNA when targeted to the coding region, due to the blocking of elongation of the ribosomal complex as a result of adduct formation.

It has been shown that ruthenium *tris*-1,4,5,8 tetraazaphenanthrene forms an adduct with guanosine monophosphate upon irradiation and upon acidic hydrolysis the following molecule was isolated and characterised<sup>131</sup>.



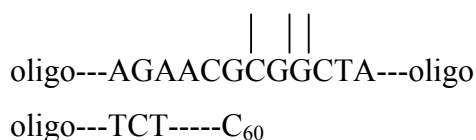
Adduct formation was attributed to electron transfer from guanine to the photoexcited ruthenium complex. This was then followed by deprotonation of the guanine radical cation and protonation of the ruthenium complex. The adduct could then be formed from the reaction of the guanine neutral radical and the protonated ruthenium complex. In a recent

paper<sup>88</sup> Ortman *et al.* synthesised a conjugate with ruthenium *bis*-(1,4,5,8 tetra-azaphenanthrene) 4,7-diphenylphenanthroline attached to a modified uracil base as shown below.



Upon hybridisation with its radiolabelled complementary strand and irradiation, gel electrophoresis revealed formation of a photoadduct. This shows that the photophysical properties of the free complex were retained upon formation of the oligonucleotide conjugate.

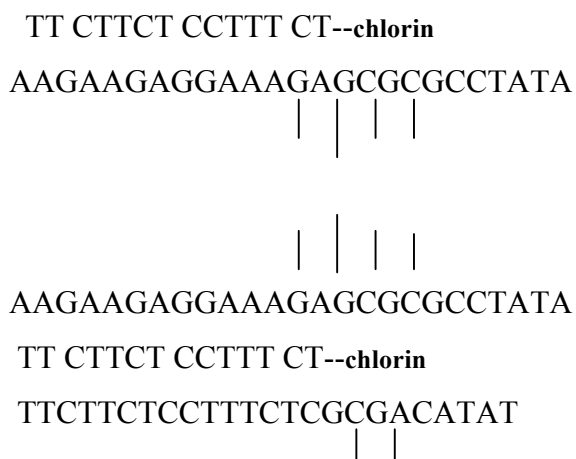
A number of oligonucleotide conjugates and free molecules<sup>132</sup> have been used to induce damage at guanine bases in nucleic acids upon irradiation by mechanisms known as photodynamic action. The mechanisms involved are dealt with in detail in section 1.6. Those conjugates which have been found to photoinduce oxidative damage to complementary nucleic acids include derivatives of fullerene<sup>133</sup>, chlorin<sup>85,134</sup>, rhodium complexes<sup>87,135,136</sup> and ruthenium complexes<sup>137,138</sup>. Fullerene functionalised with a bromoacetate group was conjugated to the 5' end of a 45-mer<sup>133</sup>. Irradiation of the conjugate with its complementary sequence induced damage at guanine bases as shown below.



The piperidine-sensitive lesions were only generated in the single stranded region adjacent to the fullerene molecule. Fullerene efficiently generates <sup>1</sup>O<sub>2</sub> by energy transfer from its excited state to ground state molecular oxygen but singlet oxygen was found not to be involved in the damage produced above. An eosin conjugate was also synthesised (eosin is also known to produce <sup>1</sup>O<sub>2</sub>) and comparisons were made using both conjugates. D<sub>2</sub>O is known to enhance the lifetime of <sup>1</sup>O<sub>2</sub> 10 fold and when the eosin conjugate duplex was irradiated in D<sub>2</sub>O, increased cleavage at the target guanines was observed. This however was not the case for the fullerene conjugate where no increase in cleavage was observed. The authors concluded that the proximity of the electron rich guanine bases to the fullerene

might inhibit the production of  $^1\text{O}_2$  and instead the guanines transfer an electron to the excited fullerene and damage occurs by a type I mechanism.

Chlorin oligonucleotide conjugates<sup>85</sup> have also been used to photoinduce piperidine sensitive lesions at guanine bases in single stranded and double stranded DNA as well as form photoadducts and induce frank breaks in target strands.



As shown above, guanines were damaged in the single stranded as well as the double stranded region in contrast to the results obtained with the fullerene and eosin conjugates. Cleavage was found to be oxygen dependent and was also diminished upon addition of  $\text{NaN}_3$  (a known quencher of  $^1\text{O}_2$ ) but not enhanced in  $\text{D}_2\text{O}$ . These conflicting results were explained by saying that  $\text{D}_2\text{O}$  enhances the lifetime of  $^1\text{O}_2$  in bulk solution but that any  $^1\text{O}_2$  produced in the solvent cage around the photosensitiser would not be affected. Thus, the damage mechanism was thought to involve singlet oxygen but with a contribution from electron transfer processes also.

Rhodium polypyridyl complexes have also been conjugated to oligonucleotides<sup>135,136</sup> with the aim of investigating electron transfer reactions in DNA.

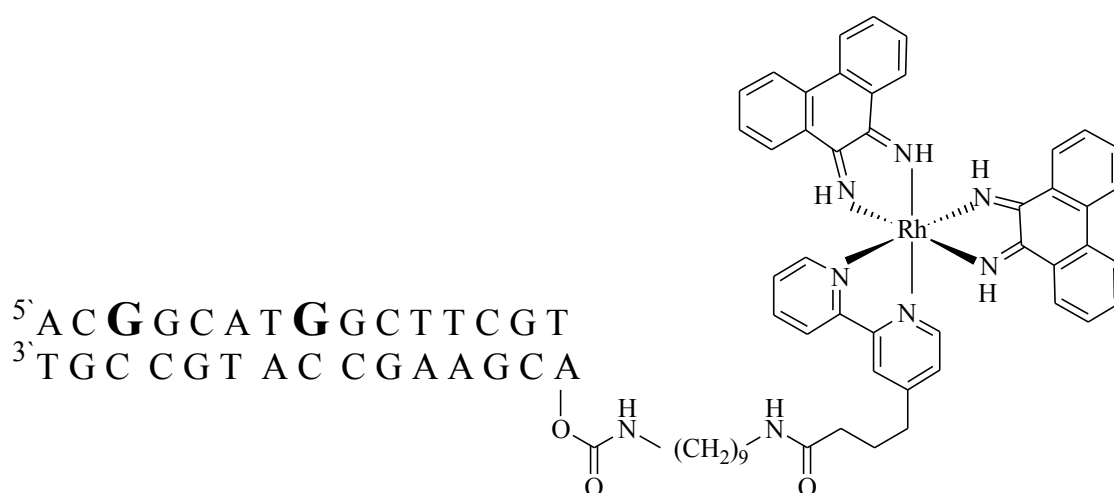


*Figure 1.5.h. Rhodium complex linked to oligonucleotide to study electron transfer through a double helix*

The complex linker in the above diagram was designed as such to allow one of the 9,10-phenanthroline ligands to intercalate in the double stranded region. Upon irradiation, piperidine sensitive guanine residues were produced to a greater extent at the 5' guanines of the two GG doublets than at the other guanine bases (attributed to electron transfer through the double helix, which stops at the 5'G of GG doublets).

The results shown above indicate that oligonucleotide conjugates can be used successfully to photoinduce oxidative damage to specific sites in nucleic acid targets. It is clear that the mechanisms of damage are important and can involve  $^1\text{O}_2$ , electron transfer and electron transfer through the double helix. As the main aim of this research is the design and use of photoactive oligonucleotide conjugates it is clear that it is important to investigate the mechanisms, the intermediate reactive species and the final damaged products at guanine. These details should allow us to develop protocols for the optimal design of oligonucleotide conjugates.

## 1.6. Oxidative damage to nucleoside and DNA bases.

The heterocyclic bases in DNA, when subjected to UV radiation can give rise to photoproducts whose biological effects have been implicated in cell death, mutagenesis and carcinogenesis<sup>139</sup>. UV-B and UV-C radiation can react directly with the pyrimidine bases to form dimers<sup>140</sup>. UV-A and indeed visible radiation can also induce oxidative damage to DNA bases and in particular guanine by photochemical mechanisms involving photosensitising molecules and oxygen. This section deals with the consequences of irradiation of DNA and/or nucleosides in the presence of photosensitising molecules and the mechanisms by which photodamage can occur.

It is possible to determine the species most likely to react with excited state molecules or  $^1\text{O}_2$  by looking at the one electron reduction potentials for the various nucleosides or nucleobases in DNA<sup>141</sup>.

Species	$E^\circ$ ( vs NHE)	Species	$E^\circ$ ( vs NHE)
rG	1.29	<u>G</u> GG	0.64
rA	1.42	<u>G</u> G	0.82
dC	1.6	<u>G</u> A	1
dT	1.7	<u>G</u> C	1.15
8-oxoG	0.53	<u>G</u> T	1.16
( <u>8-oxoG</u> )G	0.08		
<u>G</u> (8-oxoG)	0.18		

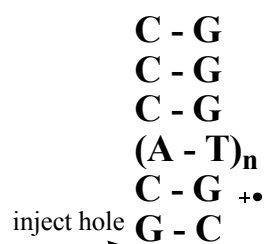
(r = ribonucleoside, d = 2'-deoxynucleoside, NHE = Normal Hydrogen Electrode)

Table 1.6.a. One electron redox potentials for nucleosides and nucleobases<sup>141</sup>.

From the first four values in Table 1.6.a., it can be seen that guanine is the most easily oxidised base and thus the guanine radical cation is the initial product of DNA oxidation induced by a variety of species including ruthenium complexes<sup>142</sup> and ionising radiation<sup>143</sup>. Thus it is the chemistry of the guanine radical cation that determines the final type I products of oxidative damage to DNA.

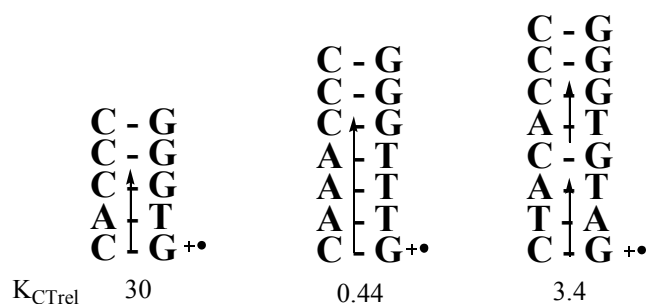
### 1.6.1. Hole transport mechanisms in DNA.

It was observed that the reactivity of guanines in nucleic acids was sensitive to the sequence of surrounding bases. Specifically, Gs located 5' to other purines (particularly another G) were much more reactive than those with 3' pyrimidines. This is verified by the redox potentials in table 1.6.a. This result has been seen with a number of photosensitisers including anthraquinones<sup>144</sup>, flavins<sup>145</sup> and pteridine derivatives<sup>146</sup>. This effect was explained by Saito *et al.*<sup>147,148</sup> who calculated that the HOMO (highest occupied molecular orbital) of a stacked GG dinucleotide was localized on the 5'-G and thus this was the site most likely to lose an electron. Because of differences in ionization potential a guanine radical cation generated can undergo migration to a more stable G<sup>•+</sup> site<sup>141</sup>. This hole migration is thought to be more efficient in duplex DNA (particularly B-form) but can also occur in single stranded DNA to certain neighbouring bases<sup>149</sup>. This process was seen previously (Figure 1.5h.) in investigations carried out by Hall *et al.*<sup>136</sup>. In their case the rhodium complex was intercalated a distance from the sites of damage suggesting the hole transfer could occur over a distance. Both 5' guanines in the sequence in figure 1.5h. were damaged equally but when the intervening bases were altered to contain bulges, the damage at the distant G decreased suggesting this charge transfer process was sensitive to base stacking<sup>150</sup>. There has been a lot of research recently into charge transport process in DNA<sup>151,152,153,154</sup>. These studies involved generating a guanine radical cation in a double stranded region and examining the rate of the charge transfer through a series of 1-4 A-T pairs to a GGG site which acted as a sink from which the hole could not escape.



The transport process competes with the hydration of the guanine radical cation leading to oxidised species, which cause strand cleavage upon piperidine treatment. Thus, the amount of cleavage produced at the initial G<sup>•+</sup> site relative to the GGG sites gives a measure of the efficiency of the hole transport process. It was found that the efficiency of hole transport decreased as the number of A – T pairs was increased up to 3. This suggested the “super exchange” hopping mechanism was distance dependent. However, if

a C–G step is inserted between the A–T pairs, then the efficiency of charge transport improves.



$K_{\text{CTrel}}$  = relative rate constant for charge transfer reaction.

It was suggested that this hopping mechanism could explain transport processes over distances greater than 50 Å if G – C pairs are not separated by too many A – T pairs. In summary, the guanine bases become oxidised and behave like relay stations for charge transport. Each individual jump is distance dependent but the overall jump over a long distance is not distance dependent if the hopping steps are not significant. These processes could be important in diseases related to oxidative damage of nucleic acids. For example, the P53 tumour suppressor gene has CGG and AGG mutational hotspots. If guanine damage occurred it could migrate to these sites and explain the high mutatability of these regions.

### 1.6.2. Photodamage to guanine in DNA.

By examining the reaction of guanine with radicals it is possible to understand how the type I products are formed, as some of the intermediates are the same as those formed from electron transfer from guanine to an excited photosensitiser. The guanine system has been studied by O'Neill<sup>155,156</sup> and summarised in reviews by Steenken<sup>157</sup> and Breen and Murphy<sup>158</sup>. Results have indicated that hydroxyl radicals add to C-4, C-5 and C-8 of guanine residues (78) in DNA to form the corresponding radicals G4-OH (79), G5-OH (80) and G8-OH (81) as shown below in figure 1.6.a.



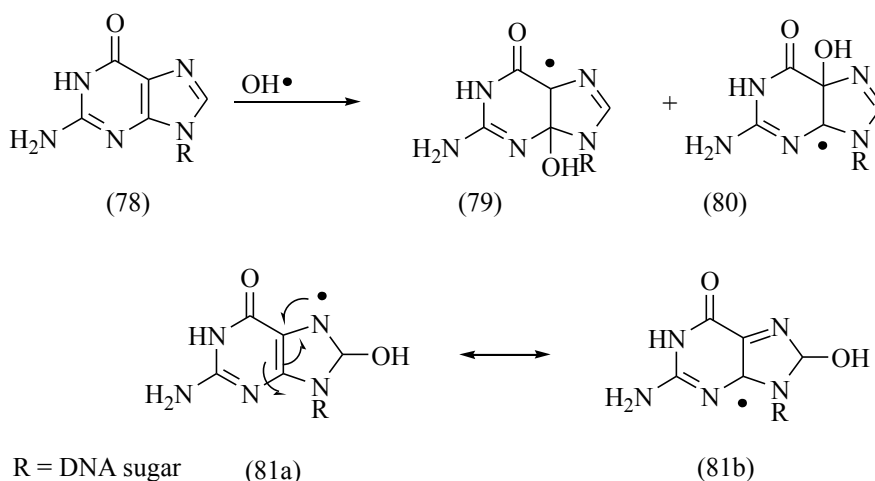


*Figure 1.6.a. Radicals produced from guanine in DNA.*

It is the radical produced by addition at C-8 that gives the most interesting chemistry as G8-OH radical (81) can undergo both oxidation and reduction to give different products. For example (81a) can ring open directly and then undergo reduction to form a formamidopyrimidine compound (FAPyG), (82) (as shown in figure 1.6.b.), which was isolated from irradiated DNA over 40 years ago<sup>157</sup>

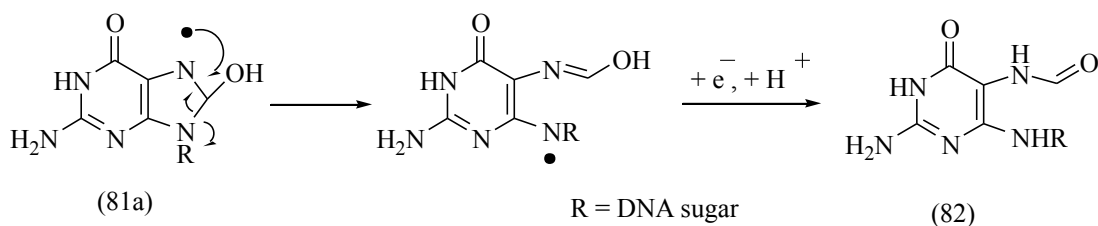


*Figure 1.6.b. Formation of FAPyG.*

Within DNA, it is (81b) that is most important. It can lose an electron and a proton to form 7,8-dihydro-8-oxoguanine (8-oxoG), which is the most abundant lesion formed and is found by many agents including ionising radiation<sup>159</sup> and photodynamic agents such as methylene blue<sup>160</sup> and riboflavin<sup>161</sup>. A suggested mechanism for its formation in this latter case<sup>161</sup> involves electron transfer from guanine in DNA to triplet excited riboflavin giving the guanine radical cation (82), which can be hydrated and then following loss of an electron and a proton forms 8-oxoG (83) as shown in figure 1.6.c.

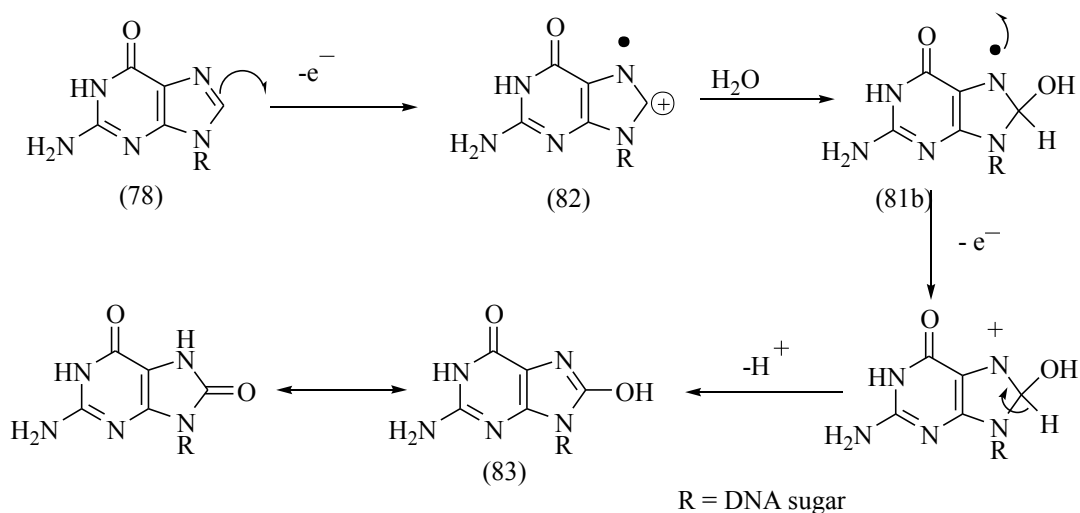


Figure 1.6.c. Mechanism of formation of 8-oxoG via type I mechanism.

8-OxoG can also be formed in DNA from a type II reaction<sup>162</sup> (figure 1.6.d.). The mechanism proposed involves a  $2\pi + 4\pi$  cycloaddition reaction between  $^1\text{O}_2$  and the C-4,C-5 and N-7,C-8 double bonds of guanine to form an endoperoxide (84) which can ring open to 8-hydroperoxyguanine (85), which in turn may be reduced to (83).

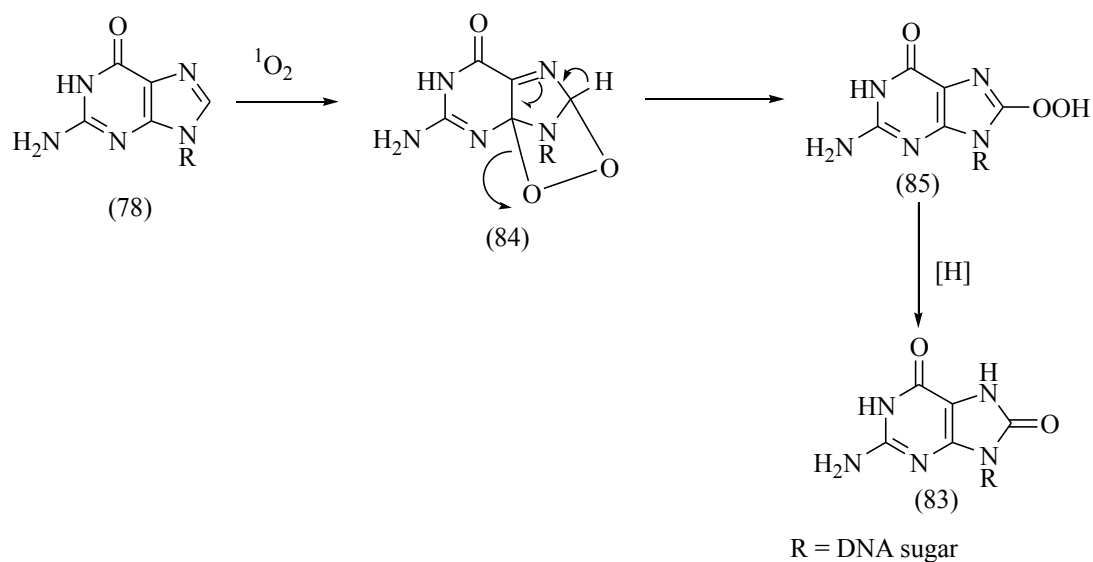


Figure 1.6.d. Mechanism of formation of 8-oxoG via type II mechanism.

### 1.6.3. Photodamage to nucleosides.

The heterocyclic bases in nucleosides and nucleotides might be expected to react in the same manner as the bases in DNA and RNA. This, however, is not the case for a number of reasons, which include the electronic effects of base stacking within the DNA helix and the polyanionic nature of the helix, which may be an electrostatic hindrance to potential reactions. Steric hindrances due to the nature of the double helix and the base pairing can be considered as protecting the bases from certain reactions (e.g. the guanine radical cation in double stranded DNA can transfer the positive charge to its hydrogen bonded cytosine in the opposite strand possibly making it more difficult to deprotonate than if the radical cation is free in solution). For these reasons an analysis of the oxidation products of nucleosides does not provide a good model for the products formed in double stranded DNA. Such an analysis could, however, provide a model for what can occur in single stranded DNA and if not, the use of a nucleoside model would in any case reveal important information about the mechanism of photodynamic action of photosensitisers. The relative contributions of type I and type II mechanisms would reveal what type of photosensitising mechanism gives the most specific DNA damage.

#### 1.6.3.1. *Type I photoproducts of nucleosides.*

It was suggested<sup>161</sup> that the hydration of the guanine radical cation (82), which occurs in DNA and leads to 8-oxoG formation does not occur in 2'-deoxyguanosine (dguo) where instead a rapid deprotonation of (82) occurs to give a neutral radical G(-H)• (86) as shown in figure 1.6.e. (a different cationic form of (82) is drawn for simplicity). This radical does not hydrate but instead reacts with dioxygen to initiate a series of reactions that lead ultimately to the formation of imidazolone and oxazolone products. A proposed mechanism involves deprotonation of (82) followed by reaction with dioxygen and water to give the peroxy radical (87).

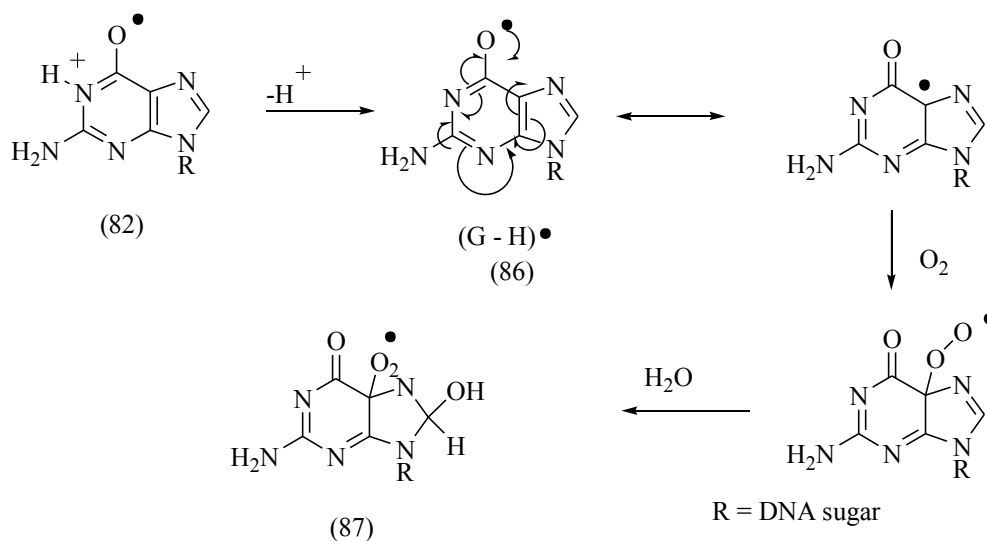


Figure 1.6.e. Reaction of the guanine radical cation (7) produced from 2'-deoxyguanosine.

The next steps involve conversion of (87) to its corresponding hydroperoxide (88). The pyrimidine ring can then open at the C-5, C-6 bond with decarboxylation occurring to give a carbinolamine (89) which ring opens to (90) (figure 1.6.f). Loss of formamide gives the compound 2,2-diamino-[(2'-deoxy- $\beta$ -D-erythro-pentofuranosyl)-4-amino]-5-imidazol-4-one (91), (dIz), which is then hydrolysed to give the final major type I oxidation product of dguo, the compound 2,2-diamino-[(2'-deoxy- $\beta$ -D-erythro-pentofuranosyl)amino]-5(2H)-oxazolone (92) (dz)<sup>163</sup>.

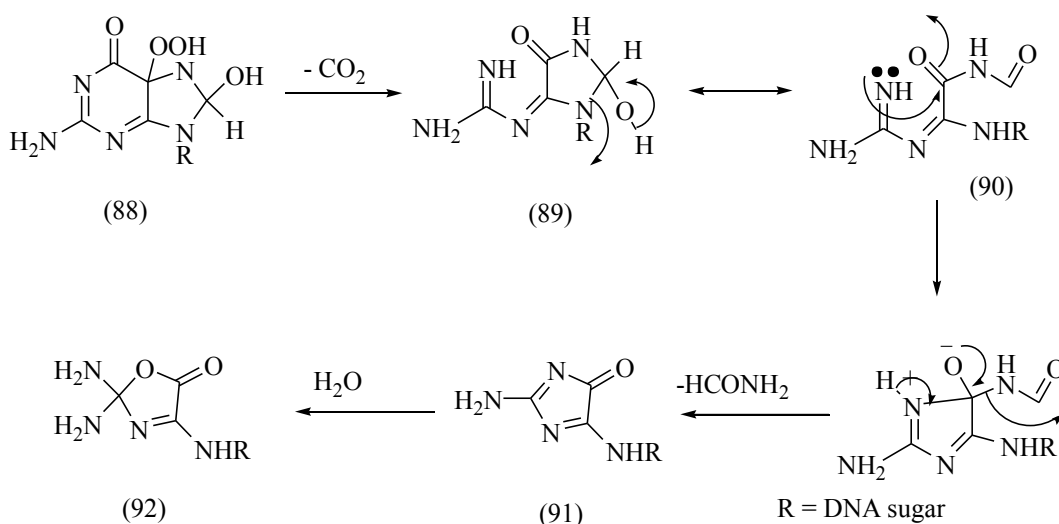


Figure 1.6.f. Formation of type I oxazolone product from 2'-deoxyguanosine.

Both (91) and (92) have been detected from the decomposition of dguo by a number of methods<sup>164,165,166</sup> and have been characterised extensively by NMR studies carried out by Raoul *et al.*<sup>167</sup>. They have also been detected in double stranded DNA exposed to high intensity UV (266nm) laser pulses<sup>168</sup>, where it is thought that certain local structures within the DNA can lead to some guanine radical cations being deprotonated to form oxazolone while others by reason of perhaps being more protected, are hydrated to form 8-oxoG.

#### 1.6.3.2. Type II photoproducts from nucleosides.

Photoexcited sensitisers can transfer excitation energy to molecular O<sub>2</sub> and generate <sup>1</sup>O<sub>2</sub>. From the data table in 1.6.a., <sup>1</sup>O<sub>2</sub> is most likely to react with a guanine residue and Ravanat *et al.*<sup>164</sup> identified distinct type I and type II products from the phthalocyanine and naphthalocyanine photosensitised oxidation of dguo. The major type II products were identified as the 4R\* and 4S\* diastereomers of 7,8-dihydro-4-hydroxy-8-oxo-2'-deoxyguanosine, (4-OH-8-oxodguo), (93). 7,8-Dihydro-8-oxo-2'-deoxyguanosine (8-oxodguo), the nucleoside analogue of 8-oxoG, was also detected as being produced from 2'-deoxyguanosine by a type II mechanism<sup>169</sup>. Its generation reached a plateau, then steadied off, suggesting that it is a substrate for further oxidative reactions. Indeed <sup>1</sup>O<sub>2</sub> can react with 8-oxodg to form 4-OH-8-oxo-dg<sup>166</sup>. The 4-hydroxy diastereomers were characterised using NMR and mass spectrometry where they were generated by methylene blue mediated oxidation of dguo and its 3', 5'-di-O-acetylated derivative.

A suggested mechanism involves initial formation of transient diastereomeric endoperoxides (94) through a Diels Alder cycloaddition of  $^1\text{O}_2$  to the C-4, C-5 and N-7, C-8 double bonds of the imidazole ring in dguo (78). Reduction of the endoperoxides then gives a mixture of two diastereomers as shown in figure 1.6.g.

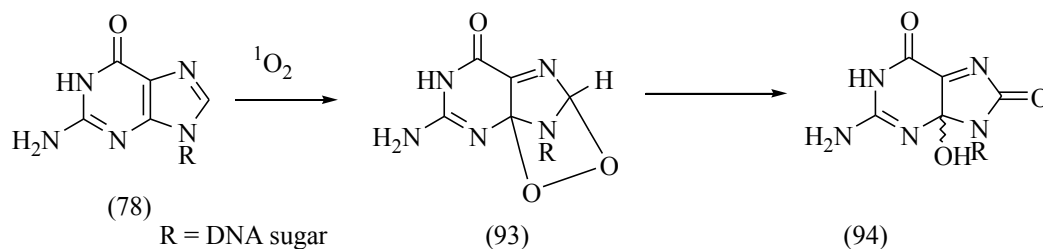


Figure 1.6.g. Formation of 4-hydroxy-8-oxo-2'-deoxyguanosine.

Sheu and Foote<sup>170</sup> reported that a methyl group at the C-8 position of guanine stabilises the primary endoperoxide formed from the cycloaddition and allows its characterisation by low temperature NMR studies, thus supporting the proposed mechanism. The diastereomers (94) were produced in relatively similar yields by Ravanat and Cadet<sup>169</sup> indicating that the addition of oxygen is non-stereospecific. They also detected 8-oxodG in small amounts. Other workers have also detected these now characteristic type II products, including Waldemar *et al.*<sup>166</sup> who studied the oxidation of dguo by thermally generated triplet excited ketones. They found equal amounts of type I and type II products, established by comparison of their results with those obtained using predominant type I (benzophenone and riboflavin) and type II (rose bengal and methylene blue) photosensitisers.

#### 1.6.4. Photooxidation of 8-oxo-2'-deoxyguanosine.

As was stated previously 8-oxoG is the main oxidative lesion generated in double stranded DNA. The lesion can be generated by at least 3 distinct mechanisms: Singlet oxygen, hydroxyl radicals and one electron oxidations. When introduced into defined DNA sequences, 8-oxoG has been shown to cause G > T transversions<sup>171</sup>. However, this was found not to be the case when single stranded DNA exposed to methylene blue was transfected into *E. coli*.<sup>172</sup> This suggested that 8-oxoG produced in single stranded DNA

underwent further reaction as was mentioned previously, where it was found that the production of 8-oxodg was not linear in time but steadied off quickly<sup>173</sup>. The authors suggested that this meant 8-oxodg was a better substrate for oxidation than dg and this can be supported by comparing the redox potentials for G and 8-oxoG given in table 1.6.a. To investigate this secondary oxidation, studies were carried out using synthetic 8-oxodg to identify its photooxidation products<sup>174</sup>.

Results showed that a number of decomposition products were formed. The identifiable products were 4-OH-8-oxodguo (10%) (93), oxazolone (35%) (92) and 1-((2-deoxy- $\beta$ -D-erythro)-pentofuranosyl) cyanuric acid (50%) (95) were identified. The formation of these products from 8-oxodguo is shown in figure 1.6.h.

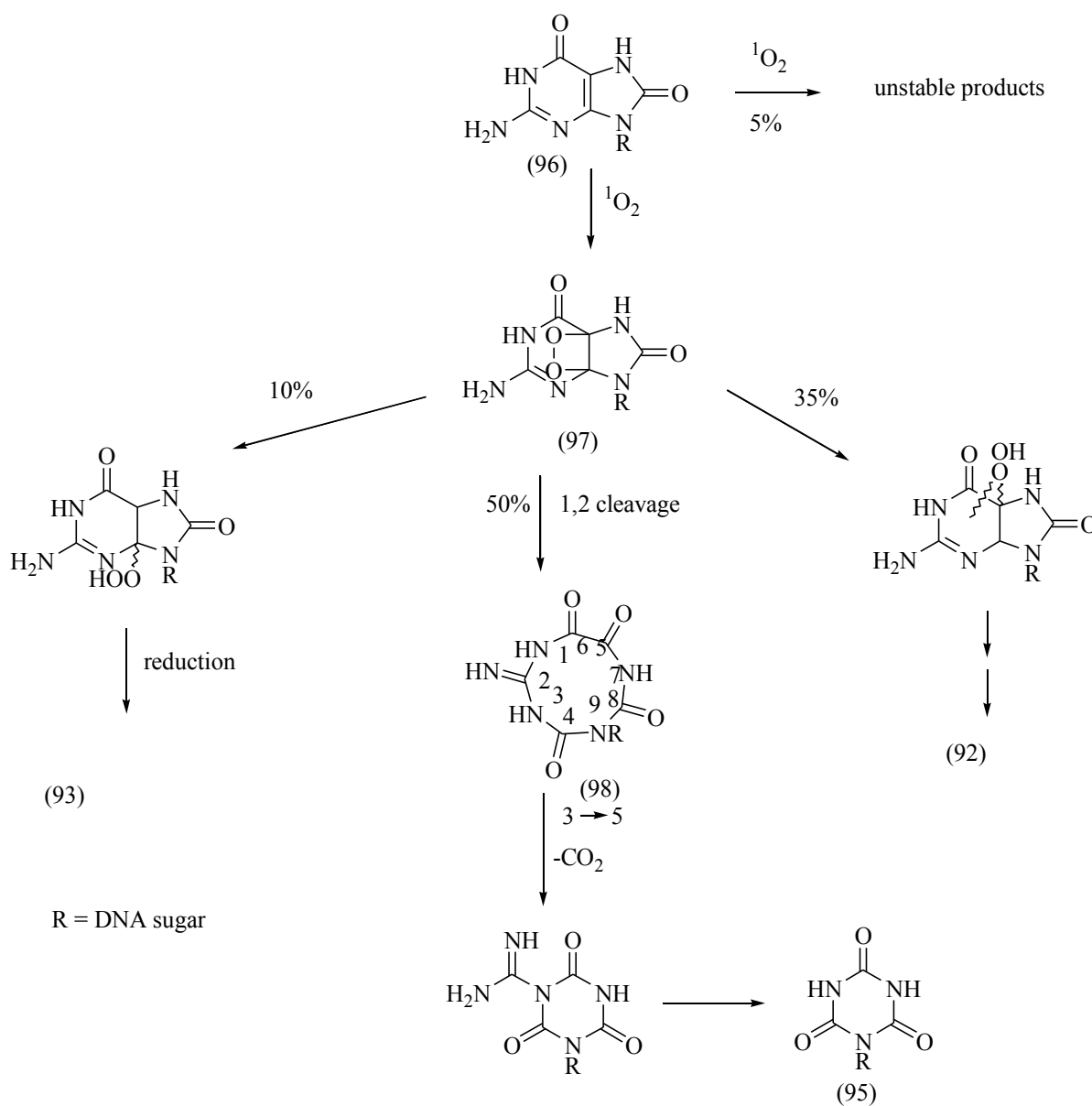
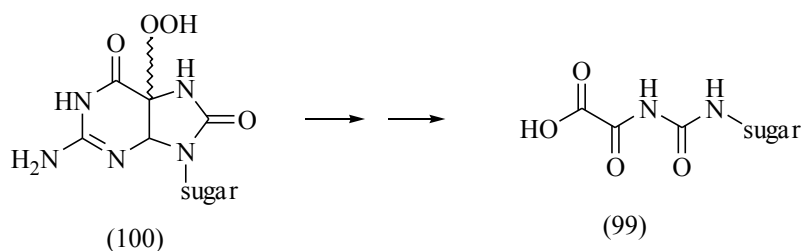


Figure 1.6.h. Oxidation products of 8-oxodG<sup>174</sup>.

The suggested mechanism involved  $2\pi + 2\pi$  cycloaddition of  $^1\text{O}_2$  with the 6,8-diketo tautomer of 8-oxo-dg (96) generating an intermediate oxetane (97) (a derivative of which was characterised by low temperature NMR studies<sup>170</sup>). The main breakdown of (97) leads to formation of a 9 membered ring compound (98) and reaction between N(3) and C(5) leads to formation of cyanuric acid (95).

It should be noted that oxazolone could also be formed from a type II mechanism and also that 8-oxodg seemed to react to a greater extent with type II rather than type I sensitisers. These results suggest that the reason 8-oxodg in single stranded DNA does not induce G  $\rightarrow$  T transversions is because it decomposes in the presence of  $^1\text{O}_2$  to the aforementioned products.

A recent publication<sup>175</sup> investigated the  $^1\text{O}_2$  mediated photooxidation of 8-oxo-7,8-dihydroguanine when synthetically inserted into single stranded DNA sequences. In contrast to the products produced from the  $^1\text{O}_2$  photooxidation of 8-oxodG (96) shown in fig. 1.6.h. the main product identified was oxaluric acid (99).



*Figure 1.6.i. Formation of oxaluric acid.*

Its formation was attributed (using labelling experiments and mass spectral data) to the breakdown of the 5'-endoperoxide (100) shown in fig. 1.6.j. Interestingly, neither 4-hydroxy-8-oxoguanine or cyanuric acid were produced in any detectable yield. This suggests a considerable difference in reactivity between the free nucleoside and the nucleoside inserted into single stranded DNA (and probably when in double stranded DNA as no 4-hydroxy-8-oxoguanine has been detected here either). Investigations into the mutagenic potential of oxaluric acid in double stranded DNA have shown<sup>176</sup> that it induces G to T and G to C transversions, suggesting it may have a role in mutagenesis and carcinogenesis.



### 1.6.5. Detecting DNA and nucleoside damage.

Because of the link between DNA lesions and cell death, the development of assays to detect these lesions is of critical importance. Such assays need to be highly sensitive to allow for detection of small amounts of a modified base in large amounts of DNA. For this reason two approaches have developed. Firstly, damaged bases are excised by hydrolysis or enzymatic digestion and separated from non-damaged DNA components by HPLC, GC and capillary electrophoresis followed by detection by various methods including mass spectrometry, fluorescence and amperometry. The second approach involves keeping the DNA intact and base modifications are measured by immunological methods or by repair enzyme activity.

#### 1.6.5.1. Detection of Type I photoproducts.

The low redox potential of 8-oxoG compared to the other bases has been used in the development of a sensitive HPLC – electrochemical assay for its detection<sup>177</sup>. This assay was used by Berger *et al.*<sup>178</sup> where they coupled reverse phase HPLC with electrochemical detection to monitor formation of 8-oxoG and 8-oxoA as well as their corresponding nucleoside analogues. With this assay it was necessary to use at least 50µg of DNA and the detection limit was estimated at the ability to detect 10 modifications per 10<sup>6</sup> DNA bases. Ravanat *et al.*<sup>164</sup> developed a method to detect the type I products of dguo based on the alkaline lability of imidazolone (91) and oxazolone (92). 10 mins at 65°C in 1M NaOH was sufficient time to release guanidine from both products. The guanidine can then be reacted quantitatively with 1, 2-naphthoquinone-4-sulfonic acid, (NQS) (101) to yield the highly fluorescent derivative (102) as shown in figure 1.6.j.

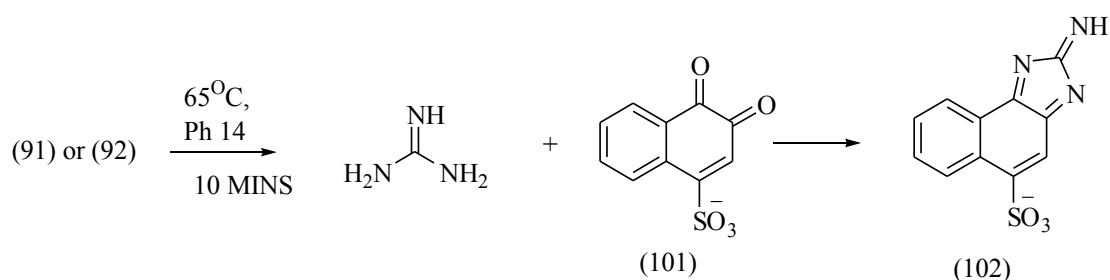


Figure 1.6.k. Fluorescence detection of type I photoproducts.

Because of the sensitivity of fluorescence detection, this accurate method was used for a number of years to detect type I photooxidation products until recently with advances made in HPLC tandem mass spectrometry.

#### 1.6.5.2. *Detection of Type II photoproducts.*

The previously described analytical methods use reverse phase chromatography to initially separate modified from non-modified bases. This chromatography is not ideal for the detection of the more polar type II oxidation products 4-OH-8oxodGuo (93), which can be eluted in the void volume of C-18 columns. Ravanat *et al.*<sup>179</sup> used normal phase chromatography with an amino modified silica column to separate the methylene blue mediated photooxidation products of dGuo. They were able to detect oxazolone and also resolve the two diastereomers of 4-OH-8-oxodGuo. This assay is also useful, as there is no need to remove the sensitiser by pre-treatment as methylene blue elutes in the void volume of the column. By a combination of both these methods and by comparison with sensitisers whose mechanisms are known, more oxidation products were uncovered and their mechanistic details elucidated for a number of photosensitising molecules.

#### 1.6.6. **Recent advances in detection methods.**

More advanced detection methods have developed recently and thermospray mass spectrometry was used as a detection method in 1992<sup>180</sup> to characterise the radiation induced decomposition products of thymine and thymidine. Gas chromatography coupled to mass spectrometry (GC-MS) has also been used to detect modifications and has the ability to detect one lesion per  $10^6$  DNA bases. However a number of papers reported that GC-MS greatly overestimates the amount of damage that occurs<sup>181,182</sup>. Comparisons were made between HPLC-EC and GC-MS assays for 8-oxoG formation in calf thymus DNA. Over 380 more 8-oxoG lesions per  $10^6$  bases were found by the GC-MS assay than for the HPLC-EC method. These results suggested artefactual oxidation of normal DNA bases during the silylation derivitisation reaction necessary to increase volatility for GC analysis. It was found that this background could be removed by HPLC pre-purification of

the reaction mixture prior to GC-MS analysis. An accurate GC-MS assay was developed<sup>183</sup> for the identification of the DNA lesion FAPyG (82), generated from hydroxyl radicals as shown previously. Previously used hydrolysis methods to digest modified nucleobases involved formic acid and it was shown that this decomposed FAPyG. Using HF in pyridine allowed for quantitative release of the lesion, which was then derivatised and characterised by GC-MS. A very sensitive assay was developed by Ravanat *et al.*<sup>184</sup> where they coupled HPLC to two mass spectrometers to detect 8-oxodGuo in cellular liver DNA and in urine samples. Normal HPLC-MS has a detection limit for 8-oxodGuo of 5 pmol but this tandem MS / MS assay has a detection limit of 20 fmol.

#### **1.6.7. Alternative methods for measurement of oxidative DNA damage.**

Instead of using chemical means for hydrolysis, DNA can also be digested to nucleotides by the enzyme alkaline phosphatase prior to HPLC analysis. Repair endonucleases specific for certain types of lesion can also be used<sup>181</sup>. Formamidopyrimidine glycosylase (FPG) recognises 8-oxoG as well as FAPy derivatives and creates breaks at the sites of these alterations in DNA. Damage can be assessed by elution through membrane filters. Oxazolone has also been shown to be a substrate for FPG also<sup>185</sup>. Work is being carried out by Pflaum and co-workers<sup>186</sup> using various repair agents such as FPG protein, OGG1 enzyme, endonuclease III and exonuclease III to quantify various types of DNA modifications produced by several type I photosensitisers and an exclusive <sup>1</sup>O<sub>2</sub> producer termed NDPO<sub>2</sub>.

It is clear that research in this area is advancing dramatically with the combination of chemical and biological methods of analysis. This combinatorial approach is helping to uncover enzyme repair pathways in cells which will give more information regarding the importance of oxidative DNA lesions in the cellular processes that can lead to mutagenesis, carcinogenesis and cell death.

#### **1.6.8. Summary of photooxidative products.**

##### *I. DNA.*

The predominant photoproduct of guanine by a type I mechanism is 8-oxoguanine (83). Oxazolone (92) can also be formed in double stranded DNA and its formation is suggested to be due to localised structures, which allow deprotonation of the guanine radical cation. 8-oxoguanine is also the main photoproduct in DNA by a type II mechanism although 4-hydroxy-8-oxoguanine can also be produced but at low concentrations.

## 2. *Nucleosides.*

The predominant type I products are imidazolone and oxazolone formed by a series of reactions initiated by deprotonation of the guanine radical cation. The predominant type II products are the diastereomers of 4-hydroxy-8-oxo-2'-deoxyguanosine (93). 8-oxo-2'-deoxyguanosine (96) can be produced but not to any great extent as it reacts further with  $^1\text{O}_2$  to give cyanuric acid (95), oxazolone (92) and 4-hydroxy-8-oxo-2'-deoxyguanosine (93).

## 2.0 MOLECULES USED FOR PHOTOACTIVE OLIGODEOXY-NUCLEOTIDE CONJUGATES.

One of the aims of the research presented in this thesis is the synthesis of oligonucleotide conjugates using photosensitising molecules attached to the 5'-end of the following 17 base oligodeoxynucleotide.



The molecules chosen for conjugation are the ruthenium polypyridyl complexes (102), (103) and the pteridine derivatives (104) and (105) shown below.

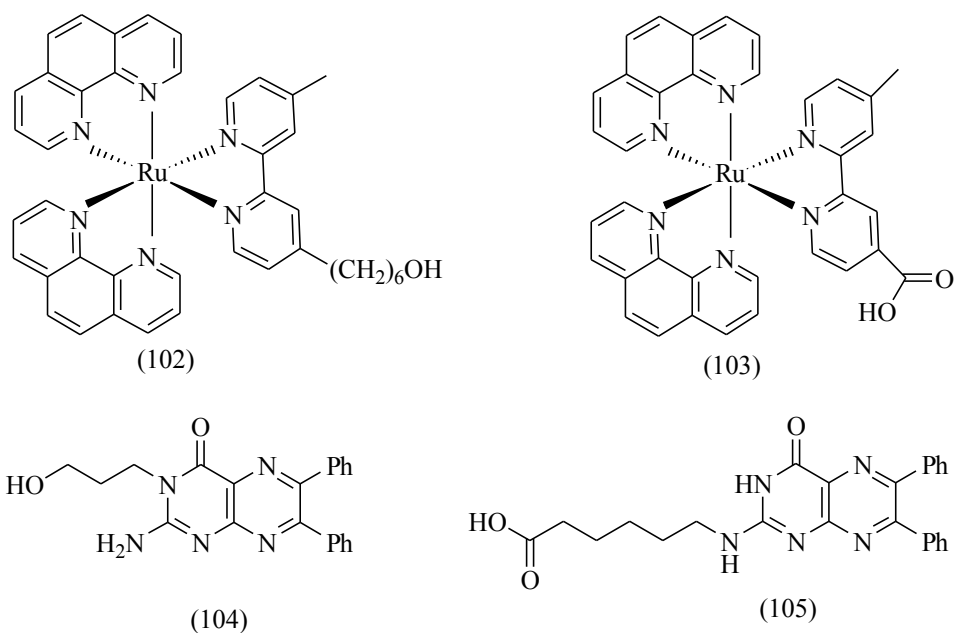


Figure 2.0.a. Structure of photosensitisers used.

This section outlines the properties of these molecules that make them suitable for the aims of this research. This involves describing their photochemistry in the presence of nucleic acids and the syntheses of the molecules shown above.

## 2.1. Ruthenium polypyridyl complexes.

Complexes of Ru (II) with bidentate polypyridyl ligands have been studied extensively in the past 10 years<sup>187</sup>. In particular, there has been considerable research in the interaction of ruthenium polypyridyl complexes with nucleic acids and their ability upon irradiation to form adducts and induce oxidative damage to guanine residues. The most commonly used polypyridyl ligands are 2,2'-bipyridyl (106) (bipy), 1,10-phenanthroline (107) (phen), 1,4,5,8-tetraazaphenanthrene (108) (tap) and dipyrido[3,2-a:2',3]-c phenazine (109) (dppz) (shown in fig. 2.1.a.) and one of the most widely studied complexes is  $\text{Ru}(\text{bipy})_3^{2+}$ . This complex provides a model with which to explain the electronic configuration and hence photoreactivity of most ruthenium polypyridyl complexes.

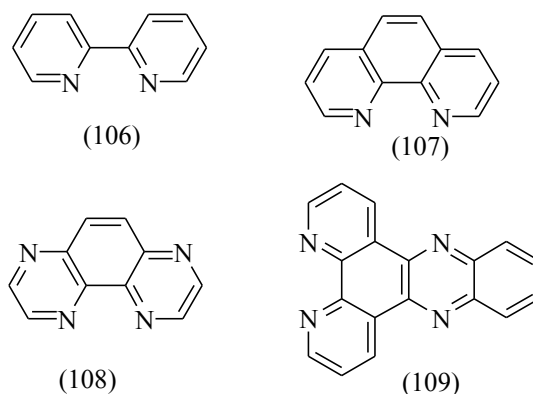


Figure 2.1.a. Commonly used polypyridyl ligands.

$\text{Ru}^{2+}$  ions form low spin octahedral complexes with ligands such as bipy or phen and the stability of these complexes is due to the symmetrical  $t_{2g}^6$  electronic configuration. The absorption and emission spectra of  $\text{Ru}(\text{bipy})_3^{2+}$  and a generalised Jablonski diagram are shown below in figure. 2.1.b.

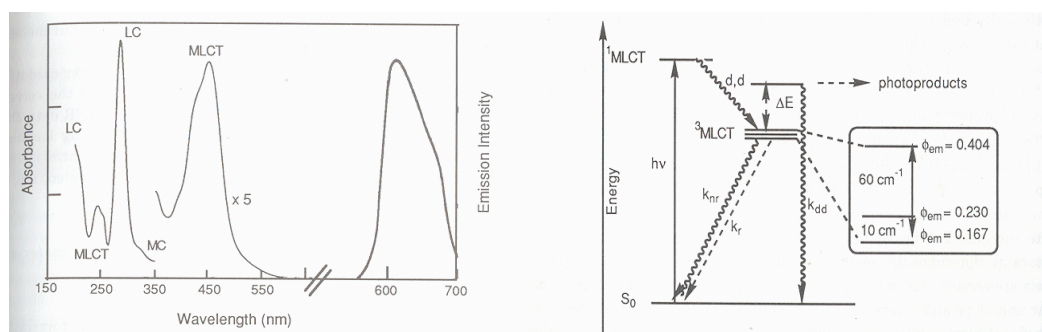


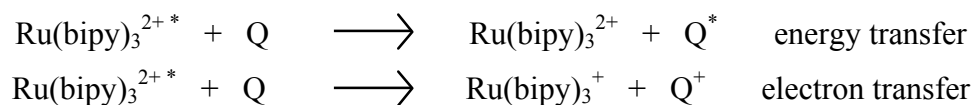
Figure 2.1.b. Absorption/emission spectra and Jablonski diagram of MLCT excited state manifold of  $\text{Ru}(\text{bipy})_3^{2+}$  in aqueous solution<sup>187</sup>.

The bands for the absorption spectrum have been assigned as:

- 185nm and 285nm = ligand centred  $\pi\text{-}\pi^*$  transitions.
- 238nm, 250nm and 452nm = metal to ligand charge transfer (MLCT)  $d\text{-}\pi^*$  transitions.

Thus, excitation of an electron into the singlet MLCT absorption manifold leads rapidly (300fs)<sup>188</sup> to intersystem crossing with unit efficiency to a triplet MLCT state from which the emission centred at 602nm (77K,  $\tau = 5.1\mu\text{s}$ ) occurs. This emissive state is said to be a composite of a number of low lying states close in energy to each other.

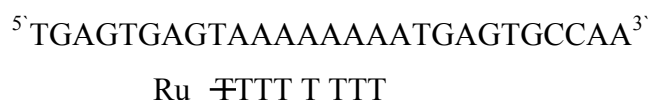
The charge transfer excited states in  $\text{Ru}(\text{bipy})_3^{2+}$  and  $\text{Ru}(\text{phen})_3^{2+}$  are sufficiently long lived to undergo quenching reactions by electron transfer or energy transfer with suitable donor molecules Q.



An important molecule that undergoes electron transfer to some excited state ruthenium complexes is guanine in nucleosides, nucleotides and nucleic acids. Kelly *et al.*<sup>189</sup> showed that the excited state of  $\text{Ru}(\text{tap})_3^{2+}$  is much more strongly quenched by poly [d(G-C)] than the excited state of  $\text{Ru}(\text{phen})_3^{2+}$ . This was attributed to the fact that the  $^3\text{MLCT}$  state of  $\text{Ru}(\text{tap})_3^{2+}$  is more strongly oxidising than that of  $\text{Ru}(\text{phen})_3^{2+}$  and that an electron transfer occurred from guanine to the excited state complexes much more efficiently with the tap complex. This was verified by flash photolysis studies, which identified  $\text{Ru}^+$  reduced species and an oxidised nucleotide intermediate<sup>190</sup>. More recently other ruthenium complexes with tap ligands have been shown to undergo reductive

electron transfer reactions with guanosine monophosphate and guanine residues in DNA<sup>191</sup>.

Another important quencher molecule that can undergo energy transfer reactions with excited state ruthenium complexes is molecular oxygen. Demas *et al.*<sup>192</sup> showed that O<sub>2</sub> quenches the charge transfer excited state of a number of complexes including Ru(bipy)<sub>3</sub><sup>2+</sup> and Ru(phen)<sub>3</sub><sup>2+</sup>. An energy transfer reaction was proposed and the product was the reactive molecule <sup>1</sup>O<sub>2</sub>. The efficiencies of singlet oxygen formation for Ru(bipy)<sub>3</sub><sup>2+</sup> and Ru(phen)<sub>3</sub><sup>2+</sup> were shown to be 0.855 and 0.744 respectively per quenching encounter. These values compare favourably with well known <sup>1</sup>O<sub>2</sub> producers methylene blue (0.5) and rose bengal (0.8). Both Ru(bipy)<sub>3</sub><sup>2+</sup> and Ru(phen)<sub>3</sub><sup>2+</sup> were then shown to photoinduce cleavage of covalently closed circular DNA<sup>193</sup> and the extent of photodamage produced was later shown to be enhanced on use of a D<sub>2</sub>O buffer (extends the lifetime of <sup>1</sup>O<sub>2</sub>) and decreased on addition of the <sup>1</sup>O<sub>2</sub> quencher histidine<sup>194</sup>. These results provided evidence that ruthenium polypyridyl complexes could photoinduce damage to nucleic acids by a mechanism involving <sup>1</sup>O<sub>2</sub>. Subsequently, the base specificity of the photodamage was investigated when Ru(bipy)<sub>3</sub><sup>2+</sup> and Ru(phen)<sub>3</sub><sup>2+</sup> were irradiated in the presence of a 5'-radiolabelled 27 base nucleic acid strand<sup>195</sup>. After irradiation no significant cleavage was observed, however, piperidine treatment at 90<sup>0</sup>C revealed damage occurred at each of the guanine residues. It was then attempted to photoinduce damage at specific guanine residues by linking a ruthenium complex to the 3'-end of a thiophosphate modified octathymidylate and target specific guanine residues in the following 27 base target.



Irradiation of the above system resulted in some adduct formation which, upon piperidine treatment revealed cleavage bands predominantly at the guanine bases located in close proximity to the photosensitiser. Results also showed that the ODN conjugate itself was damaged upon irradiation and this was attributed to <sup>1</sup>O<sub>2</sub> attack at the thiophosphate linker group. These preliminary studies in this research group led to the development of alternative methods for the synthesis of such photoactive ODN conjugates.

Initial studies in the use of ruthenium-ODN conjugates as photoactive antisense agents in chronic myeloid leukaemia were carried out in this research group by O'Keeffe<sup>137</sup>. These studies concerned the conjugation of a ruthenium *tris*-1,10-phenanthroline complex where one of the phenanthroline ligands was 5-amido-glutaric



acid-1,10-phenanthroline. The complex was conjugated to the 5'-end of an amino modified 9-mer and targeted to the following 24-mer target.



The target represents a model of the junction region of the bcr/abl oncogenic mRNA present in chronic myeloid leukaemia with the ruthenium complex located in close proximity to G15. Irradiation of the system with a sensitiser:target ratio of 10:1 produced piperidine sensitive modifications predominantly at G23 (8.5%) and G15 (5.5%). The damage at the distant guanine base was attributed to a hairpin formation, which brings G23 in close proximity to the sensitiser molecule. Experiments in D<sub>2</sub>O revealed increased cleavage suggesting an involvement of <sup>1</sup>O<sub>2</sub> in the damage mechanism. The research presented in this thesis and that carried out by Y Kavanagh<sup>138</sup> in this research group is a continuation of the aforementioned work by O'Keeffe<sup>137</sup>. The target strand has been extended to 34 bases and the ODN conjugate has been extended to 17 bases in an attempt to increase the stability of the duplex formed. My research is based on using different photosensitising molecules to try and improve upon the specific cleavage achieved by O'Keeffe<sup>137</sup> and to gain a greater understanding of the mechanism of photodamage. Alternative coupling chemistries were also investigated to try and develop the best methods for the synthesis of photoactive oligonucleotide conjugates.

## 2.2. Synthesis of Ruthenium polypyridyl oligonucleotide conjugates.

Ruthenium polypyridyl complex derivatives have been conjugated to oligonucleotides for a number of different reasons including the study of transport processes in DNA<sup>196</sup> and as alternatives to radioactive labels in DNA probes<sup>197</sup>. A wide variety of coupling chemistries have been used for conjugations and the methods chosen for investigation in this research involve using phosphoramidite derivatives and succinimide ester derivatives.

### 2.2.1. Synthesis of an activated ruthenium polypyridyl complex using a phosphoramidite derivative.

There are a number of advantages in synthesising oligonucleotide conjugates using phosphoramidite methodology. These include the high reactivity of phosphoramidites, which usually leads to high coupling efficiencies (>90%). The conjugation is carried out while the oligonucleotide is still attached to the solid support on the automated synthesiser. Thus when the coupling reaction is complete, the conjugate can be easily washed free of unreacted molecules thus easing the subsequent purification of the conjugate.

As an alternative to radioactive labels, Bannwarth and Schmidt<sup>198</sup> conjugated a ruthenium polypyridyl complex to an oligonucleotide via its phosphoramidite. One of the ligands was 4,7-diphenyl-1,10-phenanthroline, which had been functionalised with a spacer group and an alcohol group. The phosphoramidite was successfully formed and the conjugation reaction was successful although attempts to purify the phosphoramidite were inefficient, so the coupling reaction was carried out with the crude reaction mixture.

The method used in this research was developed by S. Leturgie<sup>199</sup> and involved functionalising 4,4'-dimethyl 2,2'-bipyridyl with an alkyl chain and an alcohol group. The procedure used involved reacting 4,4'-dimethyl 2,2'-bipyridyl (110) with n-butyl lithium (111) followed by an equivalent of 1,5-dibromopentane (112) (as shown in fig. 2.2.a.) using the method of Ellison and Iwamoto<sup>200</sup>.

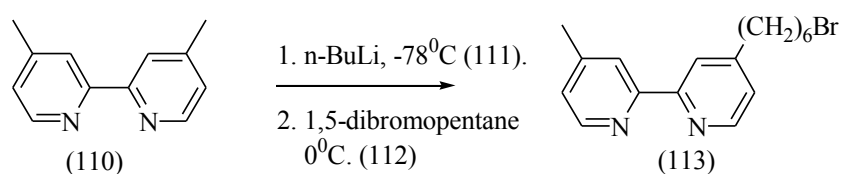
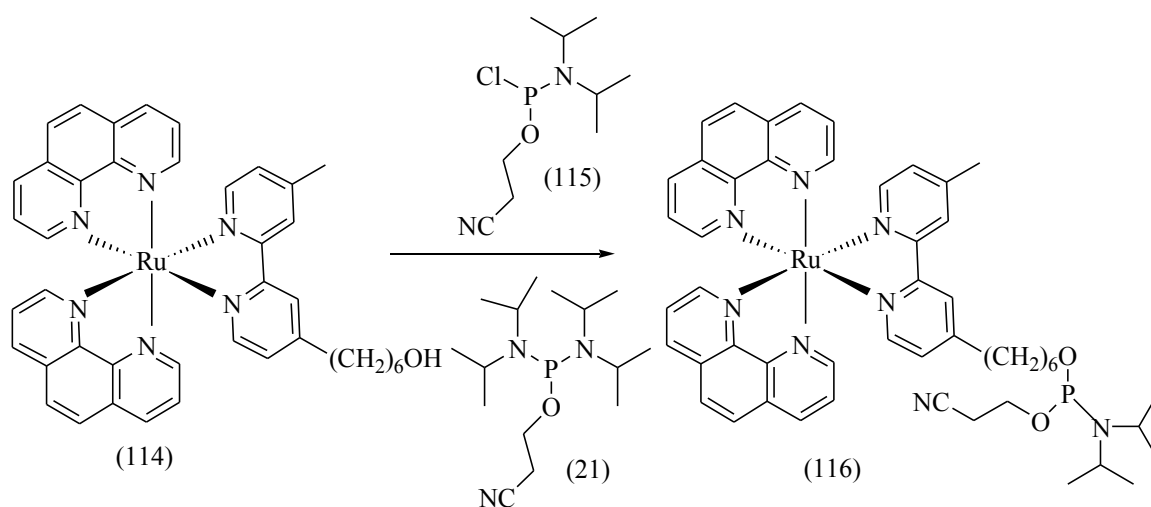


Figure 2.2.a. Synthesis of 4-methyl-4'-bromohexyl-2,2'-bipyridine.

The bromo derivative (113) could then be converted to its corresponding alcohol by hydrolysis with NaOH, although Leturgie<sup>199</sup> found it necessary to firstly form the methyl ester then form the alcohol derivative by basic hydrolysis. Once the functionalised bipyridine had been synthesised it could be used to form a complex on reaction with Ru(phen)<sub>2</sub>Cl<sub>2</sub> according to the method of Ellis *et al.*<sup>201</sup>. The *tris* ruthenium complex (114) could then be phosphitylated either by reaction with 2-cyanoethoxy(N,N-diisopropylamino)chlorophosphine (115) or 2-cyanoethoxy *bis* (N,N-

diisopropylamino)phosphoramidite (21) to form the activated phosphoramidite (116) prior to conjugation with the 5'-OH of the 17 base oligonucleotide as shown below in Fig. 2.2b. and as carried out previously for modified bipyridyl ligands<sup>202</sup>



*Figure 2.2.b. Synthesis of ruthenium polypyridyl oligonucleotide conjugate using phosphoramidite methodology.*

As one of the aims of my research is to develop better methods for the synthesis of oligonucleotide conjugates it was decided to develop a method for the purification of the ruthenium complex phosphoramidite with the aim being to improve the efficiency of the coupling reaction.

### *2.2.2. Synthesis of an activated ruthenium polypyridyl complex using succinimide ester coupling.*

This coupling method has been used for a number of carboxyl functionalised polypyridyl ligands<sup>86,87,88</sup> some of which are shown in fig. 1.5c. The procedure involved in the conjugation involves forming the succinimide ester (118) of the functionalised ligand (46) by reaction with for example, N-hydroxysuccinimide (116) in the presence of dicyclohexylcarbodiimide (50)<sup>86</sup> or N,N,N',N'-tetramethyl(succinimido)uronium tetrafluoroborate (TSU) (117)<sup>197,203</sup> as shown below in fig. 2.2.c.

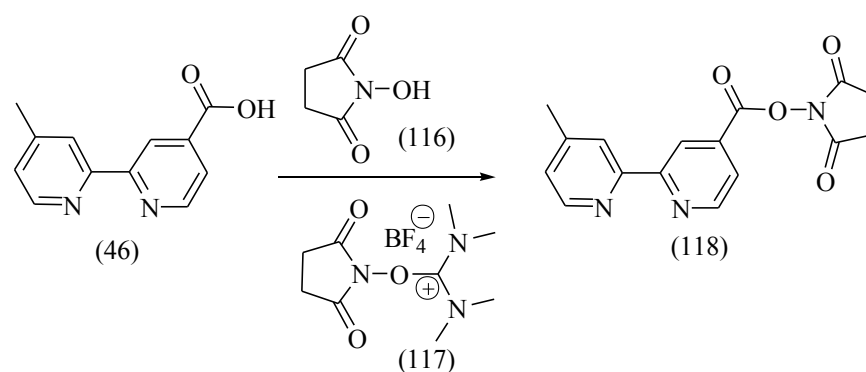


Figure 2.2.c. Synthesis of succinimide ester of 4-methyl-4'-carboxyl-2,2'-bipyridine.

This active ester (118) can then be used to form an amide bond with an appropriately amino functionalised oligonucleotide. Telser *et al.*<sup>86</sup> used oligonucleotides with cytidines and/or thymidines modified with amino linking groups but the amino group can be situated in a number of places on the oligonucleotide so that the conjugated molecule can be site specifically incorporated. Succinimide ester coupling techniques have been successfully used in this research group by O'Keeffe<sup>137</sup> and Kavanagh<sup>138</sup>. The approach taken in this research uses 4-methyl-4'-carboxyl-2,2'-bipyridine (46) as used by Telser *et al.*<sup>86</sup> however the ligand was synthesised using an improved method developed by Khan *et al.*<sup>204</sup>. Indeed, this research group have recently published a number of papers on the synthesis of oligonucleotides site specifically labelled with ruthenium polypyridyl complexes<sup>205,206,207,208</sup>.

The synthetic route followed is shown in fig. 2.2d. and involves the oxidation of 4,4'-dimethyl-2,2'-bipyridine (110) with SeO<sub>2</sub> in dioxane. The monoaldehyde product (119) is isolated from unreacted starting material by conversion to its water soluble bisulfite followed by aqueous extraction. The reformed aldehyde can then be oxidised with Ag<sub>2</sub>O to form the desired 4-methyl-4'-carboxyl-2,2'-bipyridine (46).

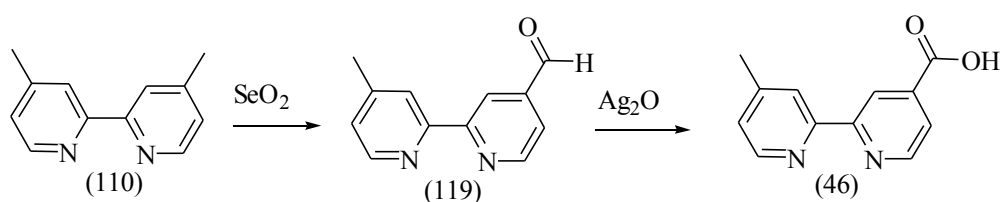


Figure 2.2.d. Synthesis of 4-methyl-4'-carboxyl-2,2'-bipyridine.

This route is much simpler than previous methods<sup>86</sup> which required soxhlet extraction for 2 days to isolate the product in less than 10% yield. This modified ligand could then be reacted with Ru(phen)<sub>2</sub>Cl<sub>2</sub> to form the *tris* polypyridyl complex as described previously<sup>201</sup>. The ruthenium complex can then be activated to form the corresponding succinimide ester derivative by reaction with TSU in anhydrous DMF, which is used as a crude product for conjugation with the 5'-aminohexyl modified 17 base oligodeoxynucleotide. The choice of this method should provide a relatively straightforward route to the synthesis of an ODN conjugate with a photoactive molecule site specifically incorporated at the 5' end. This should provide useful information as to whether succinimide coupling method gives an easier synthetic route in comparison to phosphoramidite coupling.

### 2.3. The Chemistry of Pteridines.

Pteridines are naturally occurring nitrogen containing heterocyclic molecules that are found throughout nature in plants and animals in small amounts<sup>209</sup>. The following figure shows the general pteridine ring system (120), the molecule pterin (121) (2-amino-4(3*H*)-pteridinone) and two important biological pteridines, biopterin (122) and folic acid (123).

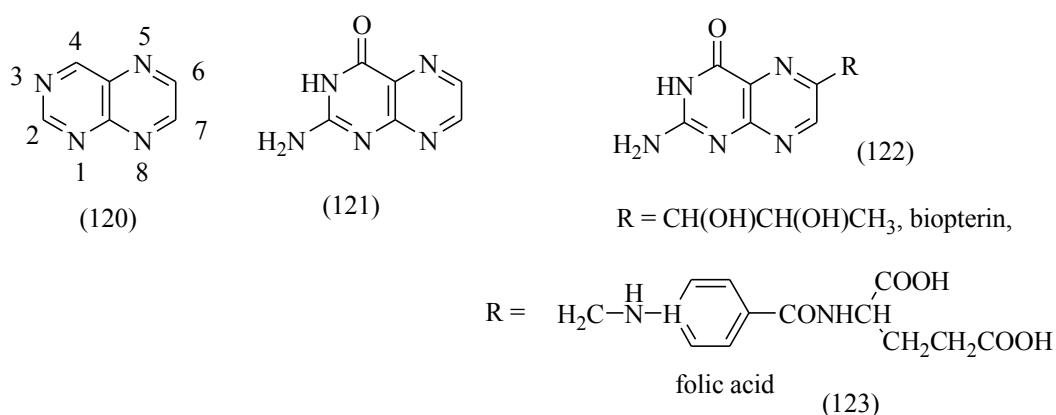


Figure 2.3.a. Structure of some pteridines.

Both (122) and (123) have important biological functions<sup>210</sup>, in that tetrahydrobiopterin is a coenzyme in metabolic reactions involving the hydroxylation of aromatic rings and tetrahydrofolic acid is a coenzyme involved in the biosynthesis of pyrimidine and purine bases. Certain pteridines are also important in photobiological processes. The enzyme DNA photolyase which catalyses the repair of pyrimidine dimers was shown to contain a pteridine co-factor as a light gathering chromophore<sup>211</sup>. Pteridines have also been identified in the eyes of vertebrates and invertebrates further suggesting their importance in photobiology<sup>212</sup>. These facts have led to a number of investigations into the photochemistry of pteridines<sup>210,212,213,214,215,216</sup>. The first main investigation on the photophysics of pterin (121) was carried out by Chahidi *et al.*<sup>212</sup> and a number of important results were revealed.

1. The fluorescence of pterin in aqueous solution is pH dependent with the neutral and anionic forms being weakly fluorescent with a quantum yield ( $\phi_F$ ) of 0.057 for the anion at pH 10, while the cationic form is practically non-fluorescent at room temperature.
2. In general, the fluorescence intensity is weaker at room temperature than at 77K and the low quantum yield shows that considerable non-radiative deactivation processes occur.
3. The neutral species gives rise to two phosphorescent emissions, which have been ascribed to two triplet  $\pi-\pi^*$  states resulting from the lactam – lactim tautomerisation of pterin.
4. The triplet energy level lies at  $22000\text{ cm}^{-1}$  ( $264\text{ kJ mol}^{-1}$ ) above the ground state. This is higher than the  $13800\text{ cm}^{-1}$  and  $7700\text{ cm}^{-1}$  corresponding to the  $^1\Sigma_g^+$  and  $^1\Delta_g$  energy levels of  $^1\text{O}_2$  suggesting the possibility of energy transfer from excited pterins to molecular oxygen. Indeed, the transient triplet absorption is quenched by  $\text{O}_2$  with a bimolecular rate constant of  $1.3 \times 10^9\text{ m}^{-1}\text{s}^{-1}$ .
5. A quenching rate constant for guanosine of  $3.5 \times 10^9\text{ M}^{-1}\text{s}^{-1}$  and that for azide of  $0.46 \times 10^9\text{ M}^{-1}\text{s}^{-1}$  suggest that the triplet state of pterin is effectively quenched by these species. In quenching experiments with guanosine it was possible to identify a semi-reduced pterin molecule spectroscopically.

These results show that pterin as a representative of photostable pteridines produces a triplet state (with an intersystem crossing quantum yield of 0.2) and that this state can react with both guanosine via a type I reaction and with molecular  $\text{O}_2$  via a type II process. Other studies on the photophysics of pteridines have mainly concentrated on the photodecomposition of certain derivatives, e.g. prolonged irradiation of folic acid at 350nm

in the presence of oxygen produces 6-formylpterin<sup>210</sup> and irradiation of 6-carboxypterin produces pterin<sup>216</sup>.

Ito and Kawanishi<sup>217</sup> investigated the photooxidation properties of a number of pteridine derivatives including pterin, 6-carboxypterin, biopterin and folic acid targeted to single stranded and double stranded DNA sequences. Their results showed that most of the pteridines were capable of photoinducing piperidine sensitive modifications to all guanine residues in single stranded DNA and to the 5`G of GG doublets and to a lesser extent, the 5`G of GA doublets in double stranded DNA. Mechanistically, they found no enhancing effect when irradiations were carried out in D<sub>2</sub>O, suggesting a <sup>1</sup>O<sub>2</sub> independent mechanism. To support this the authors studied the photoexcited pterins in the presence of 2`-deoxyguanosine monophosphate (dGMP). Using the combination of photoinduced radicals with stable nitroxide radicals, it was shown that the pteridines reacted by a type I reaction with dGMP and did not react with the other nucleotide monophosphates. Enzyme digests of irradiated DNA samples revealed that 8-oxo-7,8-dihydro 2`-deoxyguanosine (8-oxodg) was produced suggesting that pteridines can photoinduce electron transfer from guanine in DNA to the pterin triplet state resulting in guanine radical cation formation which goes on to form 8-oxodg. These results show that pteridines are excellent photosensitising molecules for the photooxidation of guanine in DNA by a type I mechanism, although it is possible that they can also produce <sup>1</sup>O<sub>2</sub>.

A number of pteridine molecules have been conjugated to oligonucleotides<sup>218,219,220</sup> including nucleosides with lumazine (6,7-dimethyl-2,4(1*H*, 3*H*)-dione) (42) instead of a normal nucleic acid base. These molecules were successfully conjugated using both phosphoramidite and active ester methodologies. Hawkins *et al.*<sup>220</sup> synthesised 18 highly fluorescent pteridine nucleoside analogues and incorporated them into nucleic acids for use as fluorescent probes and indeed some of these nucleoside phosphoramidites are available from Trilink biotechnology company.

### **2.3.1. Synthesis of pteridine oligonucleotide conjugates.**

The conjugation techniques of phosphoramidite coupling and succinimide ester coupling were chosen as the methods for coupling pteridine derivatives to the 5`-end of the 17 base oligodeoxynucleotide shown in the summary at the start of this thesis. This

required the synthesis of a pteridine derivative with an alcohol functional group and another with a carboxylic acid functional group as shown in figure 2.0.a.

### 2.3.1. Activation of a pteridinone by phosphoramidite methodology.

The route chosen for the synthesis of 3-hydroxypropyl-6,7-diphenyl-4-(3*H*)-pteridinone (104) was modified from that developed by Boyle and Lockhart for the synthesis of 3-hydroxyethyl-6,7-diphenyl-4-(3*H*)-pteridinone<sup>221</sup> and extended to the synthesis of (104) by Boyle and Camier<sup>222</sup>. The overall synthetic route is outlined below in figure 2.3.b.

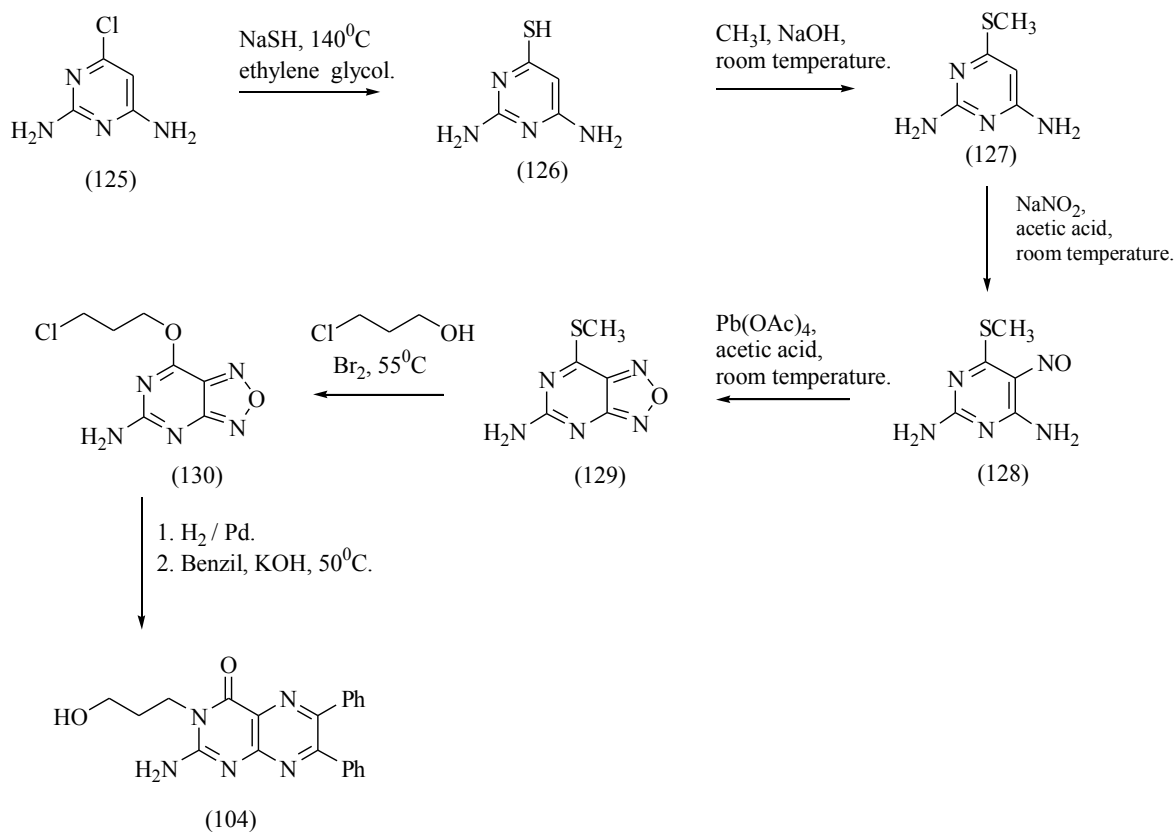


Figure 2.3.b. Synthesis of 3-hydroxypropyl-6,7-diphenyl-4-(3*H*)-pteridinone(104).

The synthesis firstly involves the thiolation of 2,6-diamino-4-chloropyrimidine (125) with sodium hydrosulfide in ethylene glycol<sup>223</sup>. The thiol hydrogen of (126) can then be substituted by a methyl group upon reaction with iodomethane. The purpose of this transformation is to facilitate the introduction of the alkyl spacer group at a later stage in the synthesis. The methylthiopyrimidine (127) is then nitrosated in position 5 of the ring



with  $\text{NaNO}_2$  in glacial acetic acid, which generates the electrophilic nitrosonium ion<sup>224</sup>. 2,6-diamino-4-methylthio-5-nitrosopyrimidine (128) can then be oxidatively cyclised with lead tetraacetate to form the furazanopyrimidine (129)<sup>225</sup>. This reaction proceeds through the oxime tautomer of the nitroso pyrimidine and evidence has been provided that the mechanism can occur by an ionic or a radical intermediate<sup>226,227</sup>. The furazanopyrimidine (129) can then undergo substitution of the methylthio group upon reaction with 3-chloropropanol in the presence of  $\text{Br}_2$ <sup>221</sup>. The reaction is thought to proceed via a bromonium intermediate, which facilitates the substitution by the 3-chloropropanol. Evidence of formation of the ionic intermediate akin to the reaction of bromine with alkenes is given by the disappearance of the characteristic bromine colour. If the alkoxyfurazano pyrimidine (130) produced is then hydrogenated in water, the following resonance stabilised cation (131) is produced.

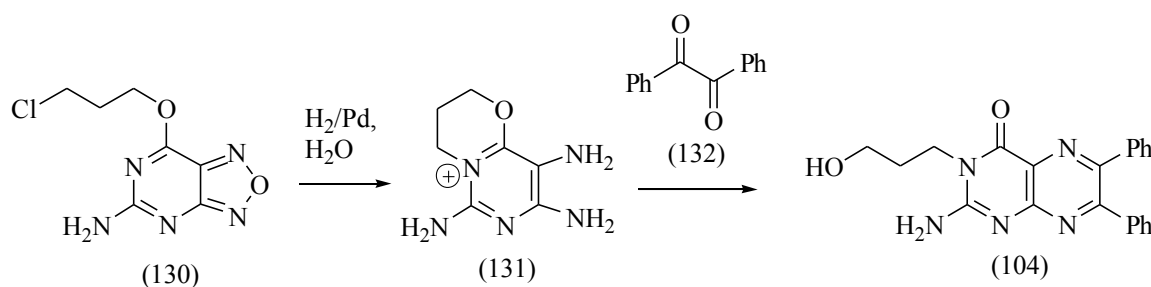


Figure 2.3.c. Formation of pyrimido[(6,1-*b*)1,3]oxazine and its reaction to form 3-hydroxypropyl-6,7-diphenyl-4-(3H)-pteridinone.

This cation can then be condensed *in situ* with benzil (132) in basic solution *via* an Isay condensation to generate the pteridinone derivative with the propanol side chain on position N-3.

This molecule is now ideally designed for incorporation into an oligonucleotide as it has a functional group that can be easily activated and a spacer group, which means that when conjugated the molecule will not be too close to adjacent bases and thus should not disrupt duplex formation. Indeed, this molecule has been activated to its corresponding phosphoramidite and conjugated to an oligonucleotide<sup>228,229</sup>, although the conjugation was carried out with the crude phosphoramidite and no real evidence of conjugate formation was provided.

The synthesis of the phosphoramidite of 3-hydroxypropyl-6,7-diphenyl-4-(3H)-pteridinone (104) could be then be carried out using either of the phosphitylating agents as shown in figure 2.3.d.

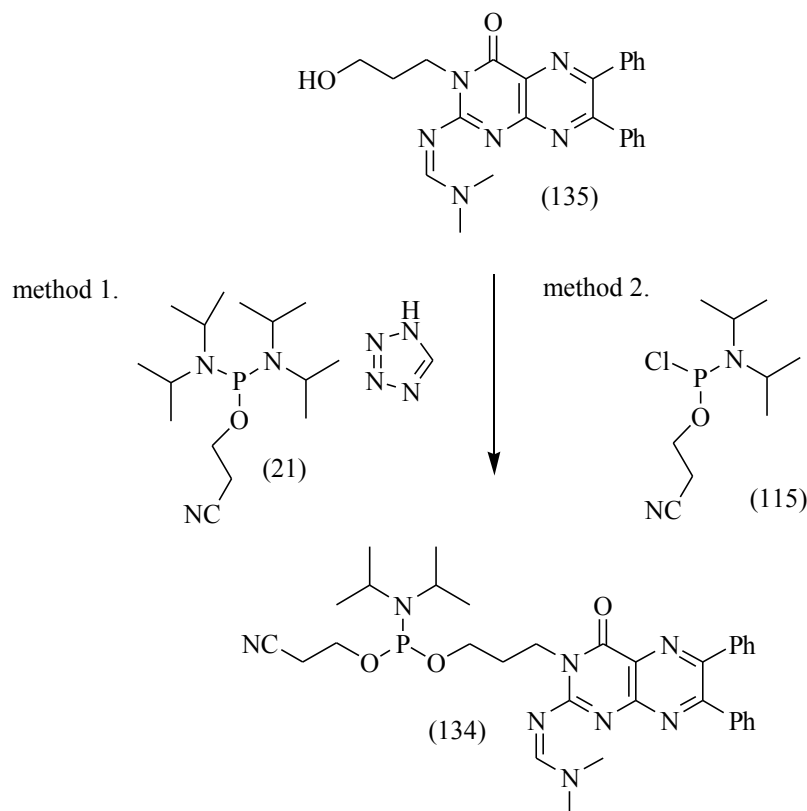


Figure 2.3.d. Synthesis of a pteridinone phosphoramidite.

As the above diagram shows, it is necessary to protect the 2-amino group of (104) in order to form the phosphoramidite (134). The formamidine derivative (135) used is compatible with the conditions of the automated DNA synthesiser and its removal is effected by the same treatment that deprotects the exocyclic amino groups on guanine and adenine<sup>230</sup>. It was found by Camier<sup>228</sup>, that attempted phosphitylation of the unprotected pteridine led mainly to formation of an oxidised phosphorus (V) species, but that masking of the amino group prevented this oxidation somehow and led to the desired phosphorus (III) product. Similar oxidation occurred for Frier *et al.*<sup>231</sup> in their attempts to form phosphoramidites of flavin derivatives. They attributed the oxidation to a photoelectron transfer from diisopropylethylamine solvent and the flavin leading to activation of molecular oxygen. This could perhaps explain why some oxidised phosphoramidite always appears in the reaction products. In any case, the phosphoramidites once made are very reactive although some can be purified by chromatography, many have been used crude in conjugation reactions. One of the aims of this research is to develop a method for the purification of pteridine phosphoramidites and thus improve upon the efficiency of the coupling reaction with the 5'-OH of the oligonucleotide.

### 2.3.2. Activation of a pteridinone by succinimide ester methodology.

As an alternative to phosphoramidite coupling for a pteridine derivative it was decided to use succinimide ester coupling and thus a method was developed to synthesise 2-(6-carboxyhexylamino)-6,7-diphenyl-4-(3*H*) pteridinone (105) adapting the approach used by Sugimoto *et al.*<sup>232</sup> and shown below in figure 2.3.e.

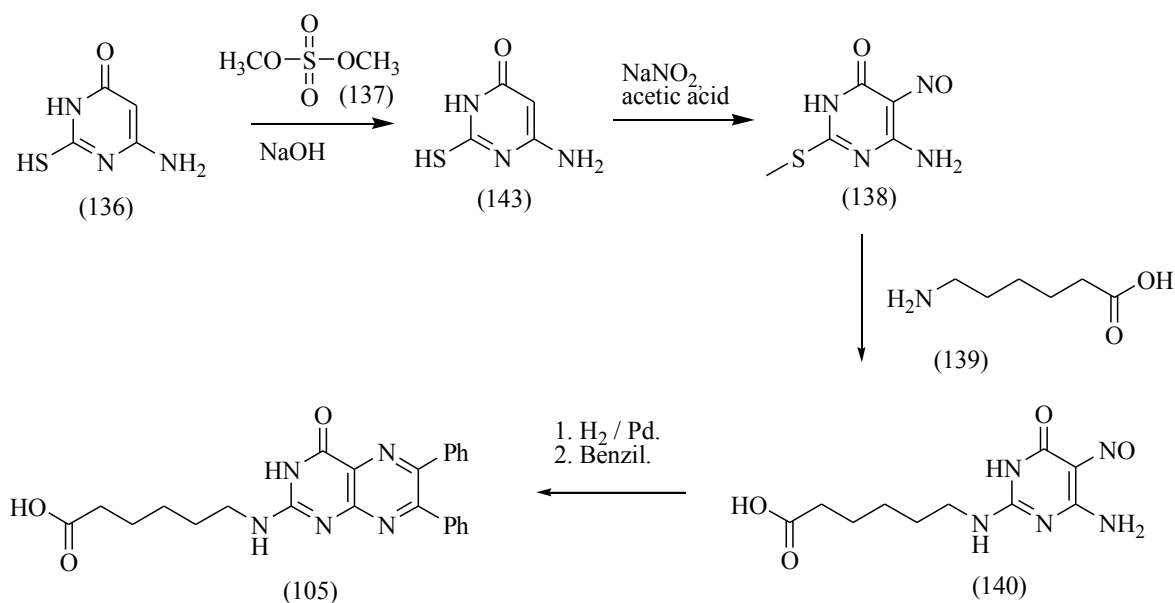


Figure 2.3.e. Synthesis of 2-(6-carboxyhexylamino)-6,7-diphenyl-4-(3*H*) pteridinone (105).

The starting pyrimidine thiol (136) is methylated with dimethyl sulfate (137) according to the method of Ward and Baker<sup>233</sup> and then nitrosated similarly to the method described in the previous section<sup>234</sup>. The carboxyl-functionalised spacer group can then be introduced by nucleophilic displacement of the methylthio group of (138) with the amino group of 6-aminohexanoic acid (139). At this stage the pteridine can be synthesised again by hydrogenation of (140) in 2M NaOH followed by an Isay condensation with benzil (132).

As was mentioned in previous sections, it is possible to activate carboxyl functionalised molecules towards coupling with an oligonucleotide by forming its succinimide ester. This can be easily done using *N,N,N',N'*-tetramethyl(succinimido)uronium tetrafluoroborate (TSU) (117) as was described in section 2.2.2. for a ruthenium complex derivative and is shown below in fig. 2.3.f. for 2-(6-carboxyhexylamino)-6,7-diphenyl-4-(3*H*) pteridinone. At this stage the activated

compound (141) is ready to be conjugated with the hexylamino modified 17 base oligodeoxynucleotide.

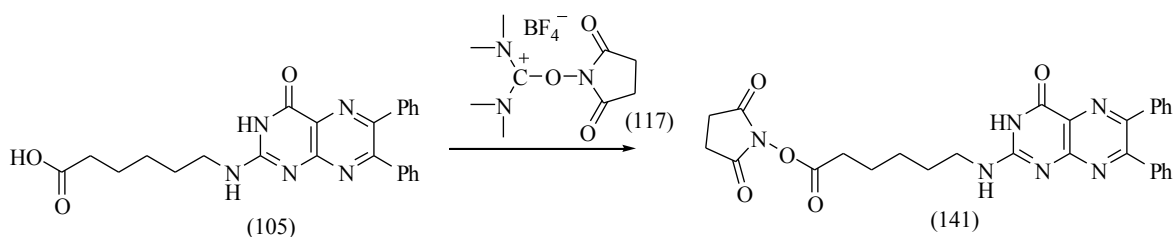


Figure 2.3.f. Synthesis of 2-(6-succinimido-carboxyhexylamino)-6,7-diphenyl-4H-pteridinone (141).

#### 2.4. Aims and objectives.

The aims of the research presented in this thesis fall into two areas.

Firstly, the aim is to synthesise ODN conjugates. Within this area, conjugates will be synthesised with ruthenium polypyridyl complex and pteridinone derivatives site specifically incorporated. Different coupling chemistries will be used and this will allow for determination of the better method in terms of ease of activation, success of conjugation and ease of purification of the ODN conjugates.

Secondly, the differences between the conjugates synthesised will allow for effective comparison of their abilities to photoinduce specific damage to guanines in the target 34-mer. It is hoped that the conjugates will improve upon the specific damage achieved by O' Keeffe<sup>137</sup> in previous work in this laboratory and lead to a greater understanding of the photochemical processes involved. Detailed investigations will be carried out with the conjugates synthesised to optimise cleavage of the target 34-mer and to gain a greater understanding of the mechanism of photooxidative damage. Additionally, a HPLC assay will be used to model the photochemical behaviour of the photosensitising molecules and this should help the interpretation of results using the ODN conjugates.

### 3.0. SYNTHESIS AND CHARACTERISATION OF OLIGODEOXY-NUCLEOTIDE CONJUGATES.

#### 3.1. Synthesis of a pteridinone–phosphoramidite.

One of the main aims of the present work was to conjugate pteridinone derivatives to the 5'-end of the following 17 base oligodeoxynucleotide (ODN).



To achieve this aim a pteridinone derivative was synthesised with a functional group that could be activated towards coupling with the 5'-OH of the above 17-mer. Phosphoramidite methodology was chosen as one of the coupling methods and to facilitate this a pteridinone was synthesised with a 3-hydroxypropyl side chain attached to N-(3). The overall synthetic route is shown in figure 3.1.a.

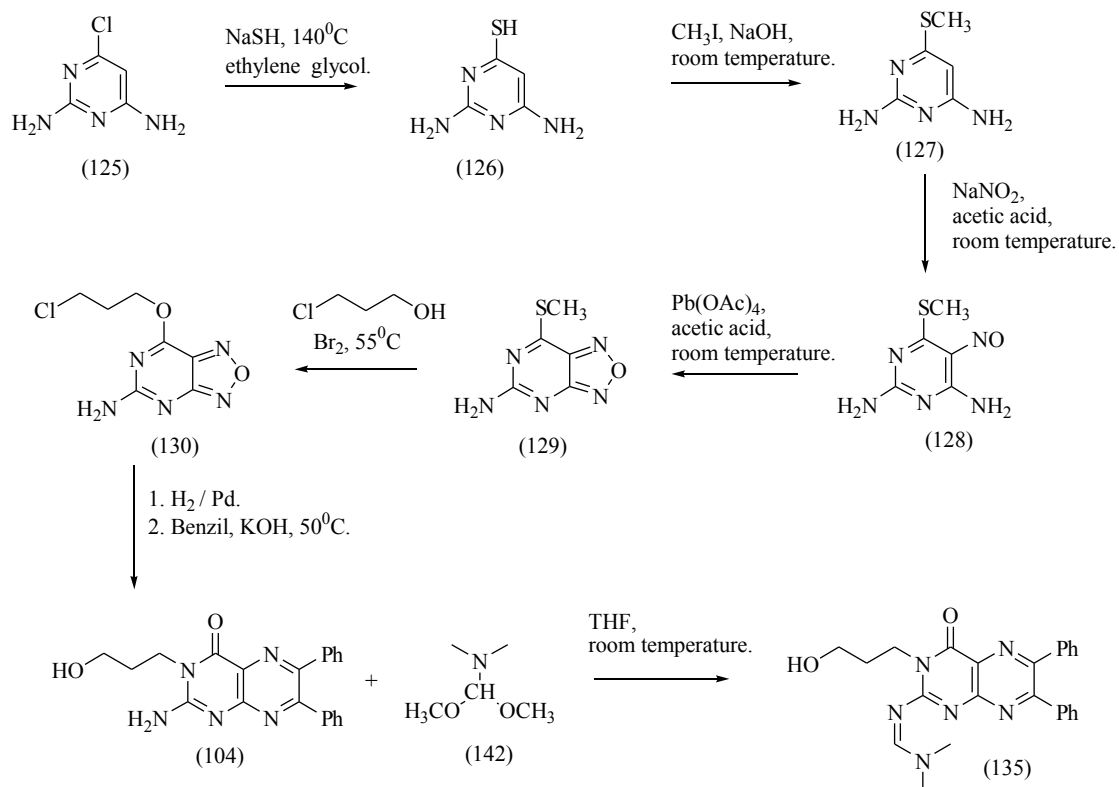


*Figure 3.1.a. Synthetic route to form 2-(N,N-dimethylaminomethyleneamino)-3-(3-hydroxypropyl)-6,7-diphenyl-4(3H)-pteridinone(135)*

The synthesis began with the formation of 2,4-diamino-6-pyrimidine thiol (126) from the reaction of 2,4-diamino-6-chloropyrimidine (125) with sodium hydrosulphide hydrate<sup>223</sup>. The product was isolated as its sulphate salt, although the yield was quite low (58%) due to a problematic work up involving pH adjustment with acid, which reacted with the excess hydrosulphide to produce H<sub>2</sub>S and colloidal sulphur. The pyrimidine thiol (126) thus obtained was then methylated using iodomethane in a basic aqueous solution at room temperature, generating the methylthiopyrimidine (127), distinguished by its CH<sub>3</sub> singlet in its <sup>1</sup>H NMR spectrum. The next step required nitrosation of the methylthio pyrimidine (127) in position 5. This was achieved by reacting (127) with sodium nitrite, which in the presence of glacial acetic acid generates the electrophilic nitrosonium ion<sup>224</sup>. Formation of 2,4-diamino-5-nitroso-6-methylthiopyrimidine (128) was evidenced by the colour change from a brown suspension to a bright pink suspension characteristic of nitroso pyrimidines. This nitroso compound was found to be insoluble in all deuterated solvents including trifluoroacetic acid and, as such characterisation by NMR was not possible.

Synthesis of 5-amino-7-(methylthio)furazano[3,4-*d*]pyrimidine (129) was achieved by lead tetraacetate oxidative cyclisation<sup>225</sup> as described in section 2.3.1. To prevent air / light oxidation of the lead tetraacetate to lead (II) species, the reaction flask was wrapped in tin foil and the oxidising agent was added in portions over a 60 minute period against a flow of N<sub>2</sub> gas. A colour change from purple to orange was observed and the <sup>1</sup>H NMR spectrum of the isolated product showed only the SCH<sub>3</sub> singlet and one NH<sub>2</sub> singlet. The conversion of this furazano pyrimidine (129) to 5-amino-7-propoxyfurazano[3,4-*d*]pyrimidine (130) was effected by treatment with 3-chloropropanol in the presence of Br<sub>2</sub><sup>226</sup>. The rigorously dried alcohol was used as the solvent as well as being the nucleophile in the reaction. Upon dropwise addition of Br<sub>2</sub>, the dark brown bromine colour disappeared after a short period of time indicating that the reaction was proceeding via a sulphonium intermediate, which facilitates the substitution reaction. Thus, further additions of Br<sub>2</sub> were made when the colour from the previous addition had disappeared and the additions were continued until the bromine colour remained permanently. The product, 5-amino-7-propoxyfurazano[3,4-*d*]pyrimidine (130) was isolated in 48% yield and its <sup>1</sup>H NMR is distinguishable from the starting material by the presence of the alkyl signals and the disappearance of the SCH<sub>3</sub> singlet.

The next step in the synthesis of 2-amino-3-(3-hydroxypropyl)-6,7-diphenyl-4-(3*H*)-pteridinone (104) was hydrogenation of (130) using a palladium catalyst, which generated the triamino pyrimidine intermediate (see fig 2.3.c.). This compound is very sensitive to air oxidation although it can be isolated as its hydrochloride salt<sup>221</sup>. In this case the salt was not isolated and the hydrogenation mixture after hydrogen uptake had ceased was filtered directly under vacuum into a basic ethanolic solution of benzil. Upon heating at 35-40<sup>0</sup>C for 1.5 hours the reaction proceeded *via* an Isay condensation reaction. The product 2-amino-3-(3-hydroxypropyl)-6,7-diphenyl-4(3*H*)-pteridinone (104) was then purified by flash chromatography, generating the desired target, a pteridinone derivative with an *n*-propanol group in position N-3 of the ring.

It is necessary to protect exocyclic amino groups in molecules that are to be incorporated in solid phase automated DNA synthesis. The amino group of the pteridinone (104) was protected by reaction with N,N-dimethylformamidedimethylacetal<sup>230</sup> (142) The product, 2-(N,N-dimethylaminomethyleneamino)-3-(3-hydroxypropyl)-6,7-diphenyl-4(3*H*)-pteridinone (134) was purified by chromatography in 62% yield. The amidine compound was distinguished by the characteristic <sup>1</sup>H NMR signals of the formamidine proton at 8.9 ppm as well as the two CH<sub>3</sub> singlets at 2.6 and 2.7 ppm.

Two methods were chosen to prepare the phosphoramidite of (135) as shown below in figure 3.1.b.

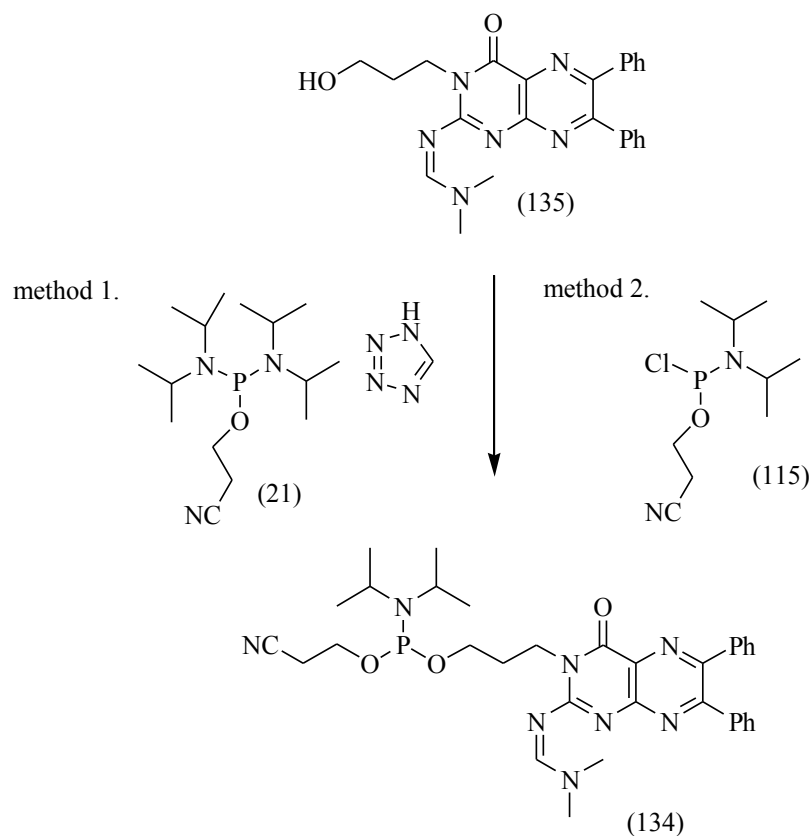


Figure 3.1.b. Synthesis of (3-(2-*N,N*-dimethylaminomethyleneamino-3,4-dihydro-4-oxo-6,7-diphenyl-3-pteridinyl)-propoxy) (2-cyanoethoxy) (*N,N*-diisopropylamino) phosphine(134).

The first method uses 2'-cyanoethyl *N,N,N',N'*-tetraisopropylaminophosphorodiamidite (21) as the phosphitylating agent. This compound requires activation by a weak acid and tetrazole is often used as it is a non-hygroscopic acid that can be easily dried. The acid protonates one of the diisopropylamino groups making it a better leaving group and thus, easing the substitution by the alkoxy group of (135). This is the method of choice for phosphoramidite formation (section 1.3.) due to the relative stability of the phosphitylating agent. The second method uses 2-cyanoethyl *N,N*-diisopropylaminochlorophosphine (115) as the phosphitylating agent, which is very reactive, requires no activation and thus is very sensitive to heat and moisture. Using both methods, special care was taken to ensure that all glassware and syringes were dried and cooled in a vacuum dessicator prior to use. The procedure using either method was straightforward and isolated crude products were analysed by  $^{31}\text{P}$  NMR to assess the extent of product formation.

The chemical shifts of pentavalent phosphorus atoms are shifted upfield compared to trivalent phosphorus. This is a general trend for phosphorus where, as coordination number increases, the chemical shift moves more upfield<sup>235</sup>. This trend cannot be



explained by electronegativities of substituents but rather, is due to the effects of  $\pi$ -bonding between phosphorus and oxygen and changes in bond angles. It is possible that the donating power of the extra electrons, due to more bonds in phosphorus(V), is more important than the withdrawing power (due to the electronegativities of the bonding atoms) in determining the magnetic field experienced by the phosphorus nucleus and thus the extent of shielding. Using the phosphorodiamidite (21), peaks were identified for the phosphorus (III) product (134) at 148 ppm and unreacted phosphorodiamidite at 124 ppm. There were also a number of peaks in the P(V) region representing decomposition products. In contrast, use of the more reactive chlorophosphine gave a cleaner reaction. Thus, in my hands the chlorophosphine (115) proved to be the better reagent for phosphoramidite formation most probably due to the ease of use of the reagent relative to that of using both tetrazole and the phosphorodiamidite (21) at the small scale at which the reactions were carried out (~30mg scale). There were also differences in the purity of some batches of both phosphitylating agents used and even the opening of the reagent bottle could cause some decomposition due to the unsuitable packaging of such a reactive compound.

Various unsuccessful attempts were undertaken to purify the pteridinone phosphoramidite (134) by precipitation into cold hexane and also by silica chromatography. Many phosphoramidites have been purified by chromatography<sup>20</sup>, although many others have been used without purification<sup>202</sup>. It is thought that decomposition on a column can be due to the acidic nature of the silica even if diisopropylethylamine is used in the mobile phase as an acid scavenger. Successful purification was eventually achieved by using neutral alumina as the stationary phase with the purification carried out in the dark to prevent any possible photodecomposition of the product. Evidence for purification can be seen by comparing the <sup>31</sup>P NMR spectra of unpurified and purified pteridinone phosphoramidites as shown in figure 3.1.c.

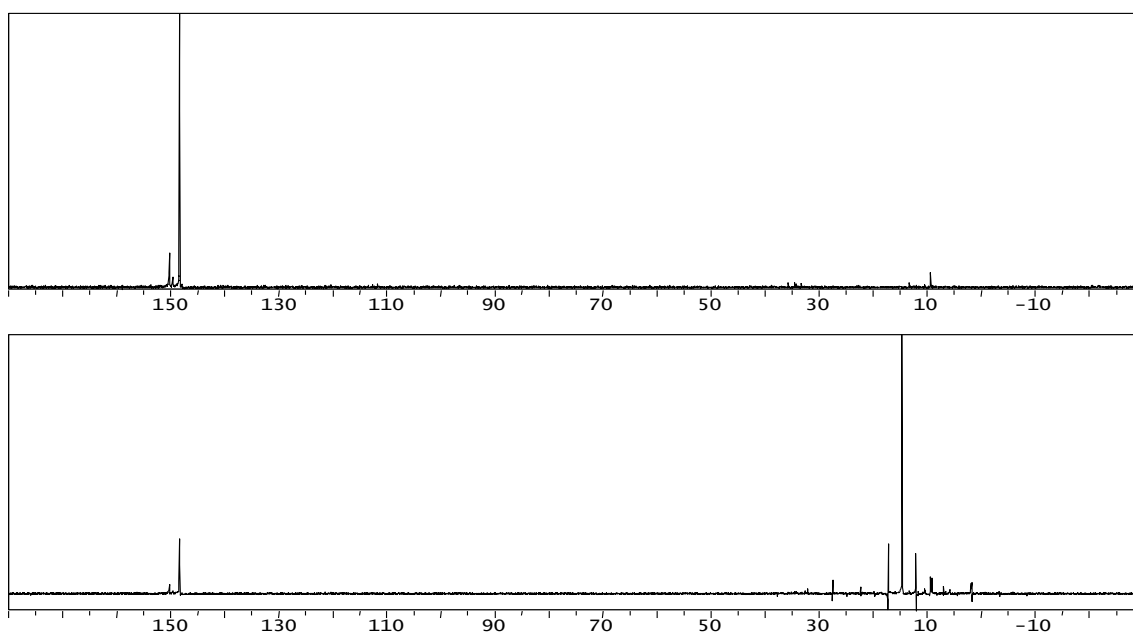


Figure 3.1.c.  $^{31}\text{P}$  NMR spectra of purified (top) and unpurified (bottom) pteridinone phosphoramidite (134).

Once purified, the pteridinone phosphoramidite was found to be stable after one week although no extensive decomposition studies were carried out due to the precious nature of the product and the desire to synthesise the oligonucleotide conjugate. It has thus been shown that pteridinone phosphoramidites can be synthesised with relative ease and that a protocol for their purification can be developed. A major problem was the presence of considerable amounts of decomposition products, which resulted in low yields. This was an expensive loss of product after a seven-step synthesis and it was hoped that no further decomposition of the phosphoramidite would occur, that might affect the yield of the coupling reaction to the oligonucleotide.

### 3.2. Synthesis of a pteridinone succinimide ester.

As was mentioned in section 3.1, there are considerable difficulties involved in the preparation and purification of some phosphoramidite derivatives. The ease with which decomposition occurred resulting in low yields of activated compound led to a search for an alternative coupling method for a pteridinone derivative. The method chosen uses

succinimide ester derivatives, which can be conjugated to amino modified oligonucleotides (see section 1.5.1.). To use succinimide ester coupling, it was necessary to synthesise a pteridinyl amino acid and the method used was a modification of that developed by Sugimoto *et al.*<sup>232</sup>. The reaction sequence is shown below in figure 3.2.a.

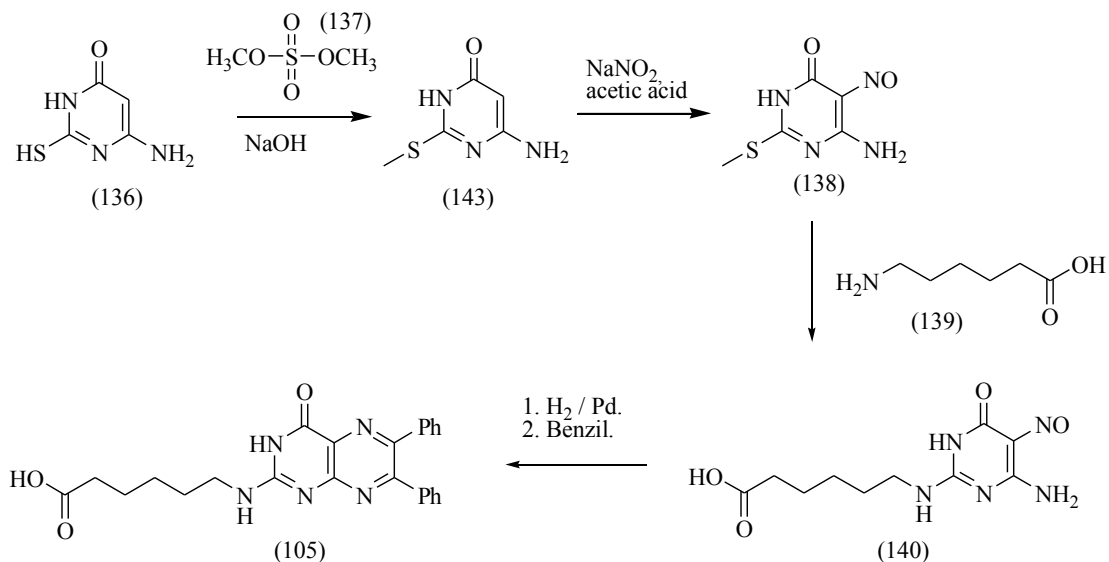


Figure 3.2.a. Synthesis of 2-(6-carboxyhexylamino)-6,7-diphenyl-4(3H)pteridinone (105).

This four step synthesis began with the S-methylation of 6-amino-2-mercapto-4(3H) pyrimidinone (136) achieved by refluxing its sodium salt with 1 equivalent of dimethyl sulphate<sup>233,234</sup> (137). Methylation was also attempted using iodomethane but dimethyl sulphate proved to be the more effective reagent, despite the evolution of toxic sulphur gases, which necessitated the use of a perchlorate scrubber. The product 6-amino-2-methylthio-4(3H) pyrimidinone (143) was obtained in 70% yield. It showed a singlet in the <sup>1</sup>H NMR spectrum arising from the methylthio group. Nitrosation of the pyrimidine (143) in position 5 was effected by treatment with 1.5 equivalents of sodium nitrite in glacial acetic acid at 0°C to give 6-amino-2-methylthio-5-nitroso-4(3H) pyrimidinone (138) in 86% yield as a blue/purple solid. The characterisation of this nitroso compound by NMR was not possible due to its insolubility in deuterated solvents including trifluoroacetic acid. Such nitrosation reactions are common in heterocyclic chemistry and the distinct colour change is usually indicative of product formation. The pyrimidinyl amino acid (140) was then generated by refluxing 6-amino-2-methylthio-5-nitroso-4(3H) pyrimidinone (138) in 6-aminohexanoic acid (139). This substitution is monitored by the colour change from the blue nitrosopyrimidine to the deep red pyrimidinyl amino acid

(140), indeed this colour change was used as the sole indicator of this type of reaction in an early study by Cresswell and Strauss<sup>236</sup>. The <sup>1</sup>H NMR spectrum of (140) in DMSO was difficult to interpret, as there only seemed to be proton signals for four CH<sub>2</sub> groups even though five CH<sub>2</sub> carbons were visible in the DEPT spectrum. To attempt to identify the missing proton signal some of the product was dissolved in NaOD and a proton spectrum revealed that the signal for the fifth CH<sub>2</sub> group was hidden underneath the NH signals at 3.31 ppm (which were removed in NaOD due to deuterium exchange).

The conversion of (140) into a pteridinone was achieved by a similar method used to synthesise (104) in section 3.1. The compound (140) was hydrogenated in 2M NaOH using a palladium catalyst to generate 2-(6-carboxyhexylamino)-5,6-diamino-4(3*H*) pyrimidinone, which, was not isolated due to its ease of hydrolysis. The reaction mixture, once hydrogen uptake had ceased, was filtered under vacuum directly into an ethanolic solution of one equivalent of benzil and refluxed until tlc showed that no benzil remained. The pteridinone (105) was then purified by flash chromatography. The presence of the 10-phenyl protons in the <sup>1</sup>H NMR spectrum provided evidence of pteridinone formation, also, the fluorescence of the product on tlc plates was also used as qualitative evidence. Electrospray mass spectrometry of (105) in positive mode was inconclusive, though, the compound was characterised in positive mode as its methyl ester (formed from refluxing the pteridinone in an acidic methanol solution) with a molecular ion [M<sup>+</sup>] of 444 amu. Due to the presence of a carboxyl functional group, it was preferable to monitor molecular ion formation in the negative mode, where deprotonation of the acid generated the [M<sup>-</sup>] ion at 428 amu and indeed, negative mode mass spec. analysis generated such a molecular ion and provided further evidence of pteridinyl amino acid formation.

The succinimide ester of 2-(6-carboxyhexylamino)-6,7-diphenyl-4(-3*H*) pteridinone (140) was then prepared using a method developed by Bannwarth *et al.*<sup>197,203</sup> and shown below in figure 3.2.b. The esterification reaction was firstly carried out using anhydrous DMF and was later shown to be possible using a DMF/dioxane/water solvent mixture.

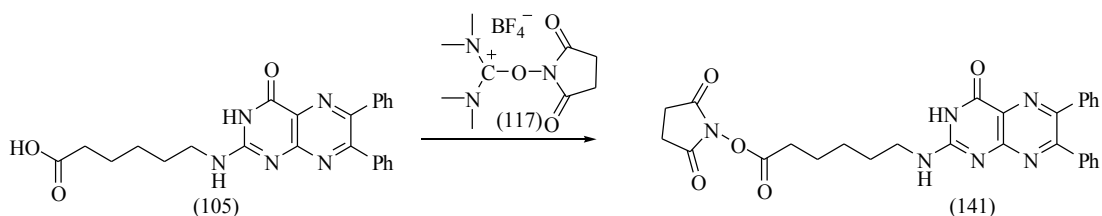


Figure 3.2.b. Synthesis of 2-(6-succinimido-carboxyhexylamino)-6,7-diphenyl-4(-3H) pteridinone (141).

It is notable though, that in contrast to phosphoramidite methodology, the active ester synthesis does not require anhydrous conditions and thus easier purification of the ester is envisaged and the likelihood of product decomposition is greatly reduced. The reaction between 2-(6-carboxyhexylamino)-6,7-diphenyl-4(3H)pteridinone (105) and *O*-(*N*-succinimidyl)-*N,N,N',N'*-tetramethyluronium tetrafluoro borate (TSU) (117) in anhydrous DMF was found to proceed smoothly at room temperature in the dark and was complete after two hours. The reaction was found to be cleaner and gave higher yields using anhydrous DMF than by using a DMF/dioxane/water solvent mixture. Flash chromatography of the crude product afforded 2-(6-succinimido-carboxyhexylamino)-6,7-diphenyl-4(-3H) pteridinone (141) in 55% yield. The positive mode electrospray mass spectrum of the product gave a clean spectrum with a molecular ion [ $M^+$ ] of 527.3 amu. The NMR spectra of the succinimide ester showed one signal for the succinimide carbonyl groups and one signal for the succinimide  $CH_2$  groups, due to the symmetry of the succinimide ring.

It can be concluded by comparison of the last two sections that, it is easier to synthesise the succinimide ester of a pteridinone derivative than to prepare its phosphoramidite, since the succinimide ester is much more stable than the phosphoramidite. However, the reason that phosphoramidite coupling to oligonucleotides is so effective is the efficiency of the coupling reaction. Thus, only after the ease of conjugation of the two pteridinone derivatives to the oligonucleotide is discussed will it be possible to decide the relative advantages and disadvantages of each approach.

### 3.3. Synthesis of an activated ruthenium polypyridyl complex.

Another of the main aims of the present work was to conjugate a ruthenium polypyridyl complex to the 17-mer oligodeoxynucleotide (ODN) shown in the summary. This was achieved by modifying one of the ligands so that it contained a functional group, which could be activated towards coupling with the 17 mer. Similar research had been carried out previously in this laboratory by O'Keeffe<sup>137</sup> and Leturgie<sup>199</sup> and currently by Kavanagh<sup>138</sup> and the present work was envisaged as a continuation and expansion of previous work with the aim of gaining more knowledge about the best methods to employ to synthesise ODN conjugates.

#### 3.3.1. *Synthesis of a ruthenium polypyridyl complex phosphoramidite.*

With this approach in mind, it was decided to functionalise 4,4'-methyl-2,2'-bipyridine (110) with an activatable group and form the complex with Ru(phen)<sub>2</sub>Cl<sub>2</sub>. 4,4'-Methyl-2,2'-bipyridine (110) had previously been converted to 4-(6-hydroxyhexyl)-4'-methyl-2,2'-bipyridine (144) and a complex formed with it and Ru(bpy)<sub>2</sub>Cl<sub>2</sub><sup>199</sup>. The complex had been successfully conjugated to a 9-mer ODN using phosphoramidite methodology, although the phosphoramidite had not been purified prior to use. With the success achieved in purifying a pteridinone phosphoramidite (section 3.1), it was decided to repeat the synthesis of the hydroxyhexyl modified ligand, form the complex with ruthenium bis 1,10-phenanthroline dichloride and then synthesise and purify the phosphoramidite prior to coupling with the 5'-OH of the 17-mer. The approach adopted in the current work is outlined in figure 3.3.a.

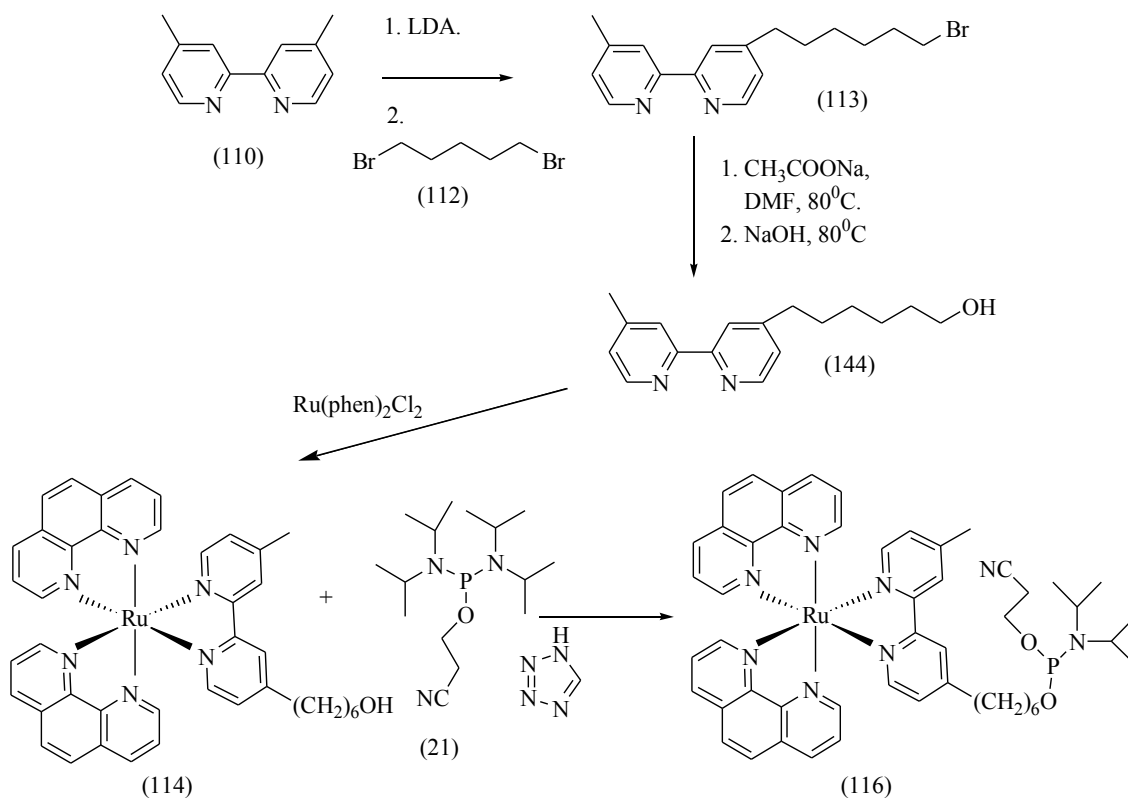


Figure 3.3.a. Synthesis of the phosphoramidite of  $\text{Ru}[(1,10\text{-phenanthroline})_2\ 4\text{-}(6\text{-hydroxyhexyl-4'-methyl-2,2'-bipyridine})] (\text{PF}_6)_2$  (114).

The procedure of Leturgie<sup>199</sup> was followed for the synthesis of the modified bipyridyl ligand. The first step was successful, although, separation of 4-(6-bromohexyl)-4'-methyl-2,2'-bipyridine (113) from unreacted starting material was difficult and required a number of chromatographic separations. This seemed to be due to the fact that, the bipyridine system dominated the chromatography and addition of the bromo alkyl group did not alter greatly the position of the product relative to the starting material on tlc. It was not possible to transform this compound to the corresponding alcohol (144) with NaOH directly, due to the incompatibility of the bromo compound (113) with the reaction conditions necessary. Therefore an indirect method involving formation of the methyl ester followed by hydrolysis led to the synthesis of 4-(6-hydroxyhexyl)-4'-methyl-2,2'-bipyridine (144). The ruthenium complex (114) was made using a method developed by Ellis *et al.*<sup>201</sup> which involved adding a 10% molar excess of the ligand in ethanol to an aqueous solution of  $\text{Ru}(\text{phen})_2\text{Cl}_2$ . Purification by cation exchange chromatography was necessary to obtain a pure sample of ruthenium bis 1,10-phenanthroline-4-(6-hydroxyhexyl)-4'-methyl-2,2'-bipyridine (114).

Attempts to synthesise the phosphoramidite (116) were not as successful as those achieved with the pteridinone derivative (135). The reaction was carried out using both phosphitylating agents (21 and 115 in figure 3.1.b.) but  $^{31}\text{P}$  NMR analysis of crude reactions revealed only small amounts of P(III) product in spectra dominated by P(V) hydrolysis products. Numerous unsuccessful attempts were made to try and isolate the phosphoramidite product by chromatography using both silica and alumina as stationary phases. The amount of P(III) species in the NMR after purification was increased relative to the P(V) species but unfortunately, insufficient amounts of the phosphoramidite were present in the reaction mixture and the coupling reaction with the 17 mer was not carried out.

### 3.3.2. *Synthesis of a ruthenium polypyridyl complex succinimide ester.*

An alternative approach was then taken to attempt conjugation of a ruthenium complex to the 17 mer, which involved using succinimide ester methodology. This methodology had been used previously to make such ODN conjugates (section 1.5.1.) and with the knowledge of the ease of synthesis and purification of the succinimido pteridinone (105), this seemed the most obvious approach to take. In order to generate a succinimide ester, it was first necessary to functionalise 4,4'-methyl-2, 2'-bipyridine (110) with a carboxylic acid group. This was achieved using the methods of Khan *et al.*<sup>204</sup>, which were adapted to synthesise the ruthenium complex (103) as shown in figure 3.3.b.



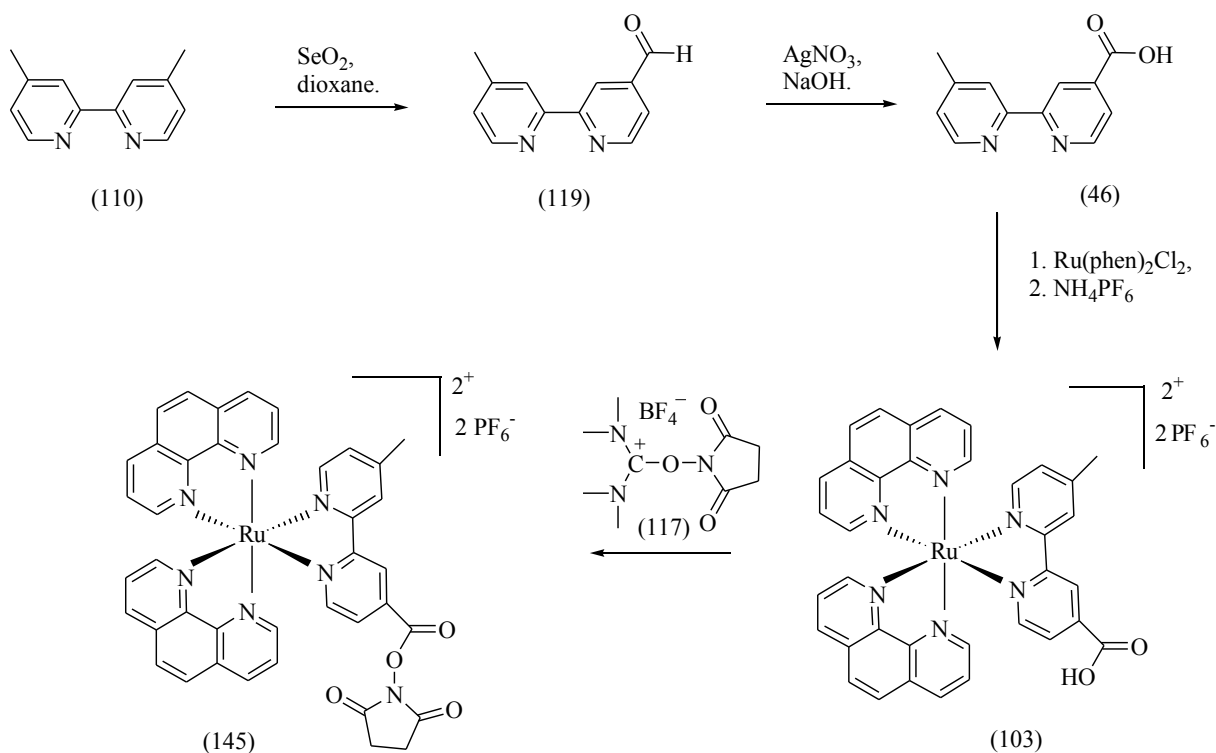


Figure 3.3.b. Synthesis of  $\text{Ru}[(1,10\text{-phenanthroline})_2(4'\text{-methyl-2,2'-bipyridine-4-carboxysuccinimide})]^{2+}(\text{PF}_6)^{-} \cdot 2$  (145).

As the previous reaction scheme shows, the first step involved selenium dioxide oxidation of 4,4'-methyl-2,2'-bipyridine (110) using dry dioxane as a solvent. This synthetic route had a number of advantages over the method described in figure 3.3.a, the first of which is, that chromatography was not necessary for purification in this case. This was because the aldehyde (119) was isolated as its water soluble bisulphite adduct, which was separated from unreacted starting material by simple extraction and then isolated by baseification followed by another extraction to give 4'-methyl-2,2'-bipyridine-4-carboxaldehyde (119) in 38% yield. The  $^1\text{H}$  NMR spectrum of this product gave the distinctive splitting pattern of the bipyridyl protons as well as the methyl singlet, the aldehyde singlet and the aldehyde carbon as shown in figure 3.3.c.

Signal(ppm)	multiplicity	proton
7.18-7.19	1H, doublet	H5
7.71-7.72	1H, doublet	H5'
8.28	1H, singlet	H3
8.57-8.58	1H, doublet	H6
8.83	1H, singlet	H3'
8.88-8.89	1H, doublet	H6'
2.47	3H, singlet	CH <sub>3</sub>
10.19	1H, singlet	CHO

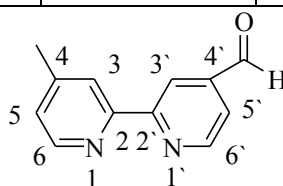
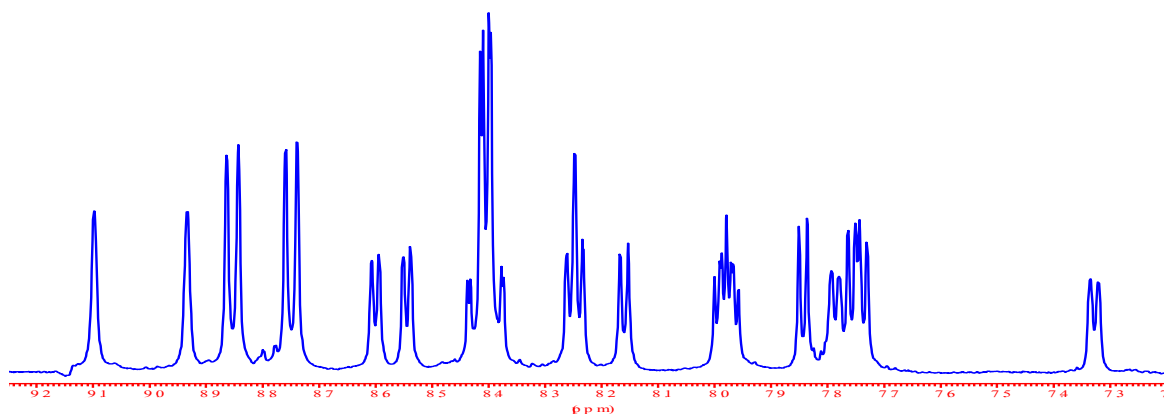


Figure 3.3.c. <sup>1</sup>H NMR data for 4'-methyl-2, 2'-bipyridine-4-carboxaldehyde (119).

The oxidation of (119) to the carboxylic acid (46) was effected using Ag<sub>2</sub>O, which was generated in situ from the reaction of AgNO<sub>3</sub> with NaOH. The product 4'-methyl-2, 2'-bipyridine-4-carboxylic acid (46) was isolated in 74% yield and distinguished from the starting material in NMR by the disappearance of the aldehyde proton signal and the shift of the carbonyl carbon peak from 191 to 167 ppm in the <sup>13</sup>C NMR spectrum.

The formation of the ruthenium complex (103) was then carried out as previously described<sup>201</sup>. In this case, after 3 hours reflux there appeared no residual Ru(phen)<sub>2</sub>Cl<sub>2</sub> on tlc and only one orange spot was visible. After removal of the ethanol by evaporation, the product was precipitated by addition of a 5 molar excess of ammonium hexafluorophosphate, which was left to stir for 30 minutes. The water insoluble ruthenium bis (1, 10-phenanthroline)-4'-methyl-2, 2'-bipyridine-4-carboxylic acid hexafluorophosphate (103) was isolated by filtration as a dark red solid in 77% yield and analysis by mass spectrometry gave a clean spectrum with a molecular ion (M/z +, where z = 2) at 338 amu corresponding to the desired complex.

From the structure of this complex it can be seen that the bipyridyl ligand is unsymmetric and thus the overall complex is not symmetric with the two phenanthroline ligands possibly in unequivalent chemical environments. This could explain the complexity of the aromatic region of the <sup>1</sup>H NMR spectrum as shown in figure 3.3.d.



*Figure. 3.3.d. Aromatic region of the  $^1\text{H}$  NMR spectrum of ruthenium bis (1, 10-phenanthroline)-4-methyl-2, 2'-bipyridine-4'-carboxylic acid (103).*

With regard to the bipyridyl ligand, it was possible to assign all its proton signals by comparison with the spectrum of the free ligand. It was necessary to use a H-H tocsy spectrum (shown in figure 3.3.e) to try and assign all the peaks representing the phenanthroline ligands.

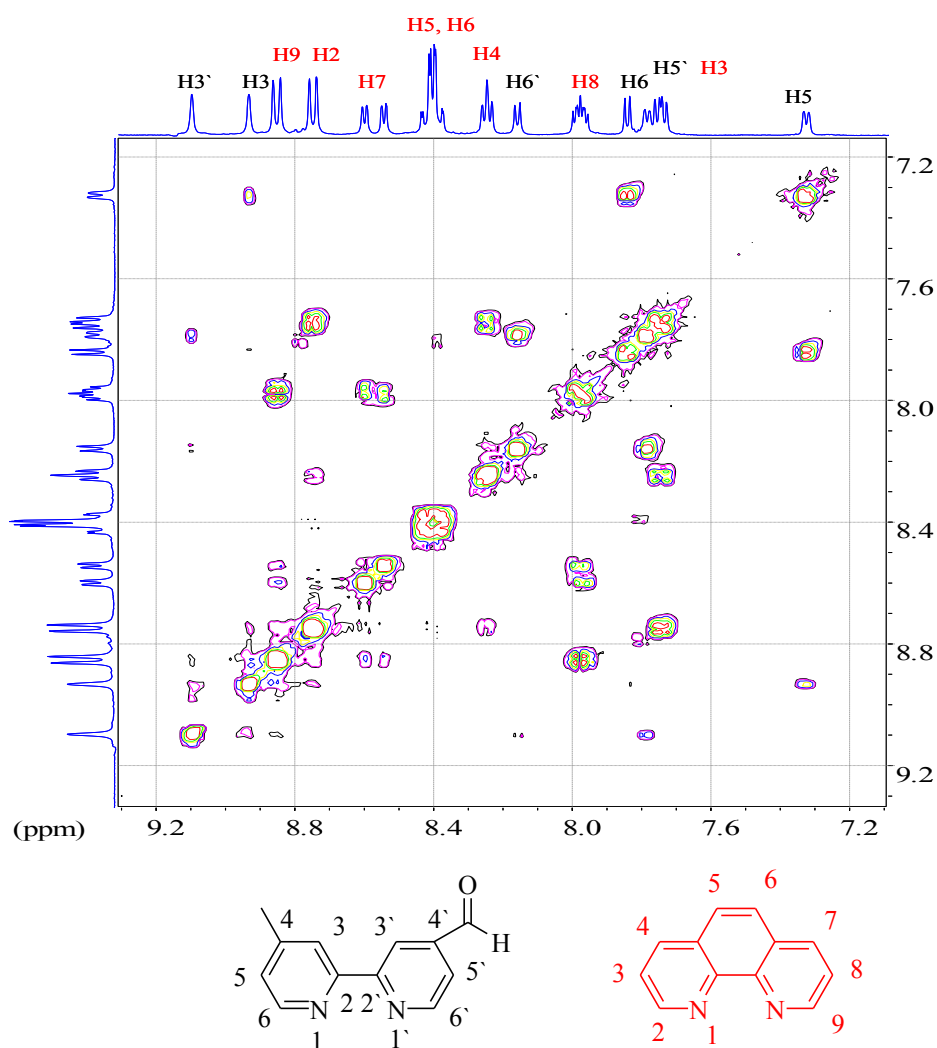


Figure 3.3.e. *H-H tocsy spectrum of aromatic region of the  $^1\text{H}$  NMR spectrum of ruthenium bis (1, 10-phenanthroline)-4-methyl-2, 2'-bipyridine-4'-carboxylic acid (103).*

By integration alone it was possible to assign the multiplet at 8.4 ppm (integrating to 4) as representing H5, H6 of two phenanthrolines and this was reinforced by the tocsy spectrum which shows that this multiplet interacts with no other signals in the spectrum, as would be expected for such isolated protons. The strength of the interactions between correlated proton signals could then be used to assign the remaining peaks in the spectrum. The two doublets at 8.7 and 8.85 ppm represent either of the set of H2 or H9 protons, rationalised by their downfield chemical shift due to the deshielding effect of the adjacent ring nitrogens. If one says for example that the doublet at 8.85 ppm represents the H9 protons then the spectrum shows that it interacts with the signals at 8.5 and 8.0 ppm. As it interacts more strongly with the 8.0 ppm signal it can be deduced that this represents H8 and the other signal at 8.5 ppm represents H7, with which H9 interacts less strongly as it is further away. Using this rationale, the signals for H2, H3 and H4 can be assigned as 8.7, 7.7, and

8.23 ppm respectively. The same results are obtained if one looks at the signals assigned to H4 and H7 and examines the strength of the interactions with their correlated protons.

It is not possible to support this explanation by looking at the observed splitting patterns, as the patterns are inconsistent with what would be expected. For example the signal assigned for H7 gives a double doublet while that assigned for H4 gives an apparent triplet. The splitting pattern should be the same for these two protons and the fact that it is not might be explained by the following. The triplet for H4 is actually a double doublet with different coupling constants to nearby protons than H7 has and that the difference in coupling constants is somehow due to the nearby unsymmetrical bipyridyl ligand. It is known that the chemical shifts of some protons in octahedral ruthenium polypyridyl complexes can be influenced by the induced magnetic field of the adjacent aromatic ligands<sup>237</sup>. So perhaps because of the octahedral nature of the complex, the position of the carboxylic acid group has some influence on the environment of the H4 or H7 of one phenanthroline, which affects the strength of coupling with nearby protons. Also, the expected splitting patterns for the H3 and H8 protons are not the same, which again speaks for some difference in the magnetic field experienced by part of one phenanthroline relative to the other in the NMR experiment. Fortunately the correlation spectrum and the mass spectrum give sufficient information to unambiguously identify the reaction product to be the desired complex.

The procedure for the formation of Ru[(1,10-phenanthroline)<sub>2</sub> (4'-methyl-2, 2'-bipyridine-4-carboxysuccinimide)]<sup>2+</sup>(PF<sub>6</sub>)<sub>2</sub> (145) was the same as the procedure used when synthesizing 2-(6-succinimido-carboxyhexylamino)-6,7-diphenyl-4-(-3H) pteridinone (141). Thus, 1.1 equivalents of TSU (117) were added to the complex (103) in anhydrous DMF (with acid scavenger DIPEA present) and the reaction was stirred in the dark and monitored by tlc. After 1 hour there was no appearance of product and an extra equivalent of TSU was added with stirring for a further hour. After this time no new spots had appeared but on closer examination of the tlc plate it appeared that the spot visible actually had regions of different colour intensities and could feasibly represent two products. The crude reaction mixture was analysed by mass spectrometry and this revealed that the mixture did indeed contain peaks for both the starting complex and the desired succinimide ester with M/z + values of 338 and 387 respectively. Numerous attempts were then made to try and influence the reaction and increase the amount of the ester that was being produced, but none were successful and it appeared by comparison of the intensities of the mass spectral peaks that there were approximately equal amounts of starting material and product. There should be no reason why the proximity of the carboxyl group to the

bipyridine ring should deactivate ester formation, hence the reason why the reaction does not go to completion (which it does in other cases in a matter of minutes<sup>197</sup> could be due to some decomposition of the TSU or even some solvent effects. Further investigation into this could probably increase the extent of the reaction, but it was decided to use the crude product mixture as it was to attempt coupling to the oligonucleotide. It was thought that the coalescence of the two spots on tlc would mean attempted purification by chromatography would be ineffective and that any unesterified complex would not react with the oligonucleotide in the coupling step in any case.

It can be concluded that, in contrast to the earlier time consuming attempts to synthesise the phosphoramidite of a ruthenium complex, this succinimide ester approach was much more straightforward. However, as was mentioned in the previous results sections the comparative merits of either methodology could not be determined until it was known how effective the conjugation reactions were and how unproblematic the final ODN conjugates could be purified.

#### **3.4. Synthesis and characterisation of ODN conjugates.**

The results described in this section concern the coupling of the previously described activated molecules to the 5' end of the following 17 base ODN.



The 5'-OH of this 17 mer was conjugated directly with the pteridinone phosphoramidite (134) while the 5'-OH was firstly reacted with a hexylamino phosphoramidite linker molecule prior to conjugation with the activated succinimide esters of the pteridinone (105) and the ruthenium complex (103). The syntheses of the ODN's, the conjugation reactions and purification of the products were carried out by Mr Clarke Stevenson in the laboratory of Professor Jeremy Davies in Queens University Belfast. The syntheses were carried out on an Applied Biosystems 380B automated DNA synthesiser and in each case purification was achieved by a combination of precipitation, electroelution and preparative PAGE. The success of the conjugations were assessed by PAGE and UV spectroscopy and the ODN conjugates were characterised by a method developed using electrospray time of flight mass spectrometry.

### 3.4.1. Synthesis of pteridinone-ODN (1) using phosphoramidite methodology.

This conjugation reaction was carried out with the 17 mer attached to the polymer support on the synthesiser. The pteridinone phosphoramidite was added in solution in 10 fold excess following removal of the dimethoxytrityl group on the 5'-OH of the terminal nucleotide thymidine. The normal coupling time of 60 secs. was doubled to increase the likelihood of successful coupling and following completion of the synthetic cycle, the completed oligonucleotide was cleaved from the support and the amino and cyanoethyl protecting groups were removed by treatment with conc.  $\text{NH}_3$  for 3 hours at  $55^\circ\text{C}$ . At this stage the reaction solution had a yellow colour and a spot on tlc was fluorescent possibly indicating a successful reaction because, if the pteridinone had not reacted it would have been removed by cleaning steps on the synthesiser and its fluorescence would not be seen.

The ODN conjugate was then precipitated from n-butanol, dried down and divided into 3 samples one of which was used in an attempt at purification by PAGE. Control lanes included in the gel included free 17 mer and two dyes which migrate at the same rate as oligonucleotides of specified length. A schematic of the gel is shown in figure 3.4.a.

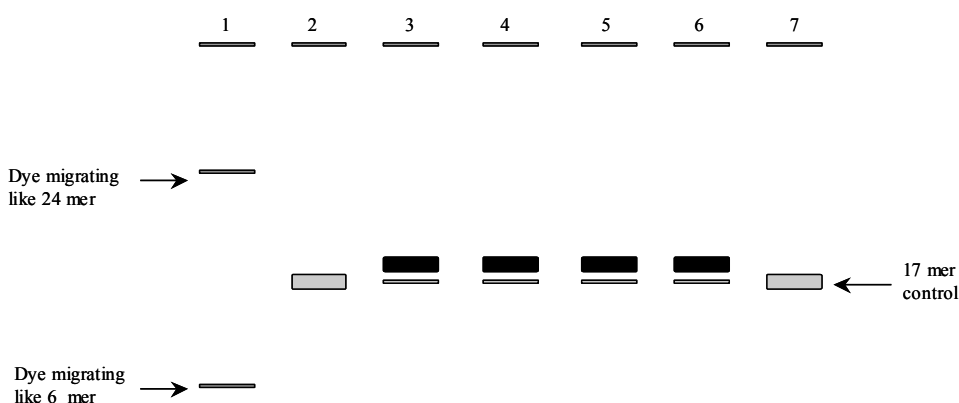
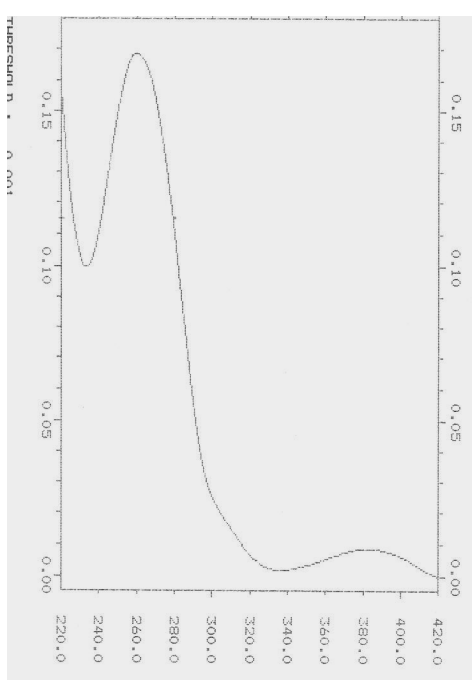
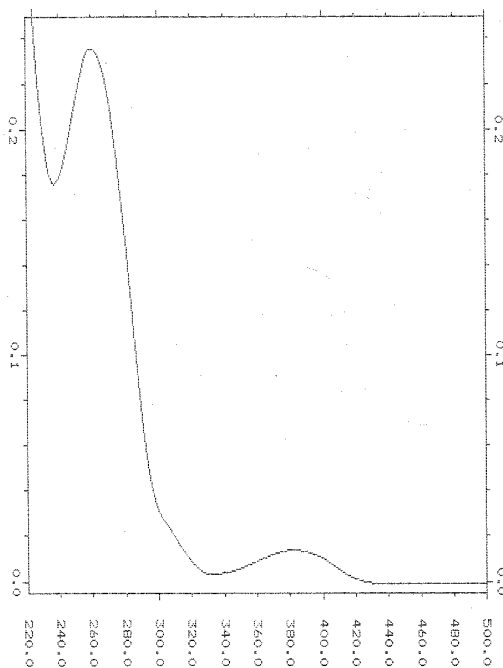


Figure 3.4.a. Schematic of preparative PAGE gel for pteridinone-ODN (1).

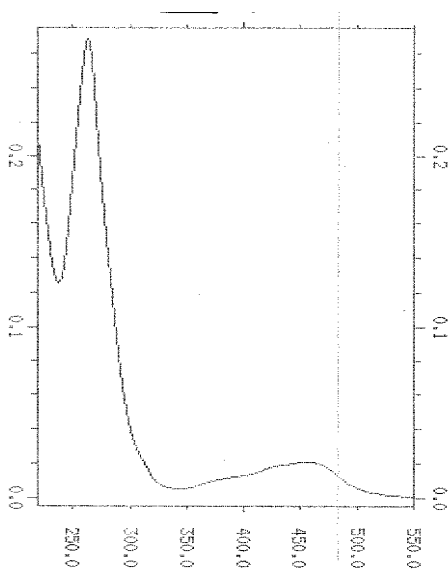
The lanes with the ODN conjugate (3 - 6) showed the presence of free 17 mer as well as a band representing an ODN that migrated approximately like an 18 mer. This was considered to be the band for the desired conjugate and was excised from the gel by scalpel and injected into an electroelution apparatus. After electroelution, the solution in the well containing pteridinone ODN (1) was removed and the conjugate was precipitated from cold 95% ethanol and analysed by UV spectroscopy. The UV spectrum (A in figure 3.4.b.) shows successful coupling with absorption bands for both the DNA bases (260nm) and the pteridinone moiety (380nm).



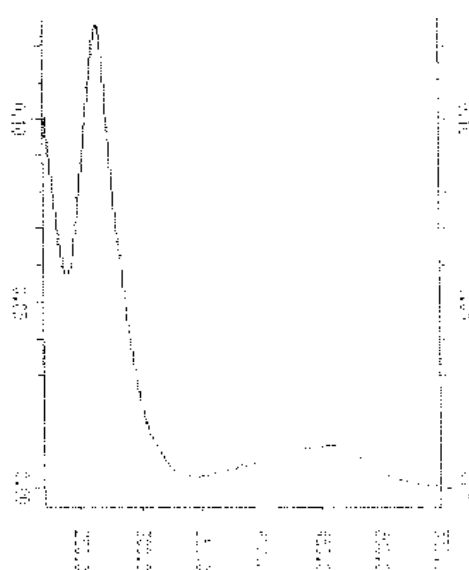
A. Pteridinone-ODN (1)



B. Pteridinone-ODN (2)



C. Ruthenium-ODN (major band)



D. Ruthenium-ODN (minor band)

Figure 3.4.b. UV spectra of ODN conjugates.

It can be said then, that the pteridinone phosphoramidite was sufficiently stable to undergo the coupling reaction, which occurred to such an extent that there was not a great amount of unreacted 17 mer present and this fact allowed for clear resolution of the bands in the gel and no contamination by free 17 mer occurred in the excision step.



### **3.4.2. Syntheses of ODN conjugates using succinimide ester methodology.**

These conjugation reactions were carried out after the amino modified 17-mer had been removed from the synthesiser and purified by PAGE. The coupling reactions were carried out using an approximate 25 fold excess of the activated compound with 16  $\mu$ l of the amino 17-mer in an eppendorf which was shaken for 1 hour at 40<sup>0</sup>C. For the pteridinone-ODN (2) after the coupling time, the solution was passed through a size exclusion resin, which retains small molecules and allows the passage through of large ODN molecules. The column fractions were pooled, dried down and purified by PAGE. The gel is shown as gel A in figure 3.4.c.

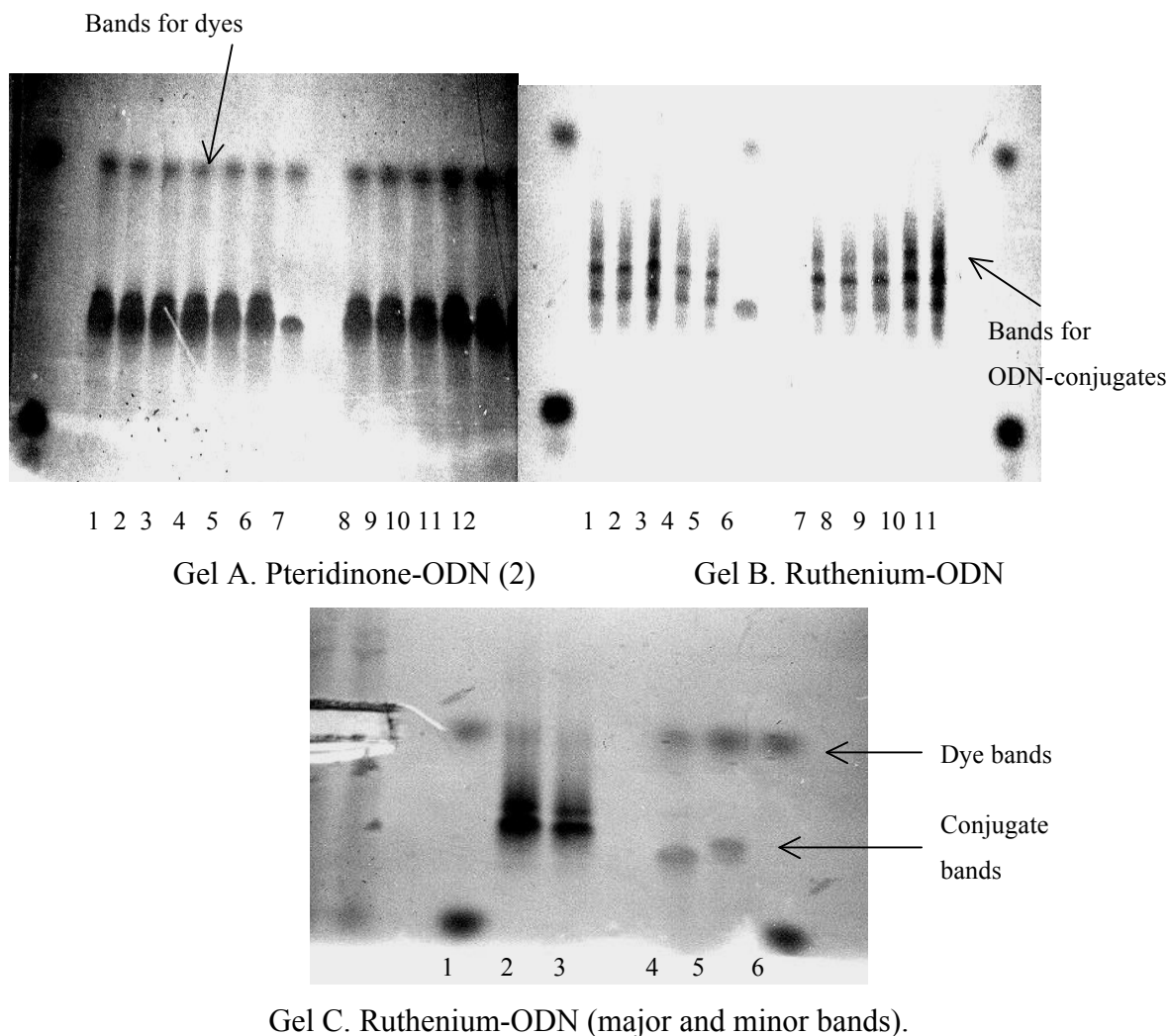


Figure 3.4.c. PAGE gels for the synthesis of ODN conjugates.

The lanes containing the ODN conjugate (lanes 1-7 and 8-12) show the presence of free 17 mer and another band which migrates slower, that was thought to be the desired pteridinone -ODN. Visual comparison of the intensities of fluorescence of the two bands led to an estimation of a coupling yield of ~30%. The bands were not very clearly resolved and this could have been due to the lower yield of coupling (relative to the phosphoramidite route) or just the fact that the gel was not run long enough to allow the two bands to become clearly resolved. The band thought to represent the desired ODN conjugate was excised from the gel, purified by electroelution and analysed by UV. The spectrum (B in figure 3.4.b.) again shows successful coupling with the presence of both the expected absorbance bands. The choice of using this coupling method was thus validated by successful coupling although the poor resolution on the gel could have resulted in contamination of the ODN conjugate with free 17 mer.

The conjugation reaction with the activated ester of the ruthenium complex was carried out similarly to that for the pteridinone described above (i.e with a larger excess of

the activated ester). The amount of activated compound used was based on an assumption that the ratio of succinimide ester to unreacted ruthenium complex was about 50:50. After the coupling time the crude reaction mixture was first purified by electroelution to remove excess free ruthenium complex, which migrated towards the negative electrode, while the ODN conjugate migrated towards the positive electrode. The orange solution removed from the well in the electroelution apparatus was precipitated from n-butanol and the orange supernatant was removed. This was thought to be residual free ruthenium species, which had bound to the conjugate by electrostatics. The precipitation process was repeated until the supernatant was clear and a dark orange pellet remained to which was added some loading dye and the soluble material was loaded on a PAGE gel. The photo of this gel (Gel B figure 3.4c.) shows three ODN bands (lanes 1-5 and 7-11), which migrate slower than the free 17 mer. These bands were excised, electroeluted and were shown by UV spectroscopy to contain both ruthenium and ODN absorbance bands at 450nm and 260 nm respectively.

If we assumed that only the DNA absorbs at 260nm we can by knowing the extinction coefficient of the 17 mer calculate the amount of ODN in odu's present in each of the three bands produced. The sum for the 3 bands was less than 1.5 odu's and since the reaction was carried out using 16 odu's of the amino 17 mer it was concluded that these bands were only minor side products of the reaction and not the desired product. It was found, that in the eppendorf in which the reaction was carried out there remained a dark orange pellet and this pellet after purification produced the gel shown as gel C in figure 3.4c. Lanes 2 and 3 show the bands produced from the orange pellet and show a major band (lower) and a minor band (upper), which migrate approximately like 20 mers. This is what might be expected after attaching a bulky positively charged group to a 17 mer. Lanes 4 and 5 in gel c show the free 17 mer and the purified pteridinone-ODN (2) respectively for comparison of migration rates.

It was notable that there was no free 17 mer in lanes 2 and 3 probably as a result of a high coupling yield due to underestimating the amount of activated ester used in the coupling reaction. The fact that there are two bands was unexpected and when they were subsequently analysed by UV they both showed the presence of ruthenium and ODN moieties (spectra C and D in figure 3.4c).

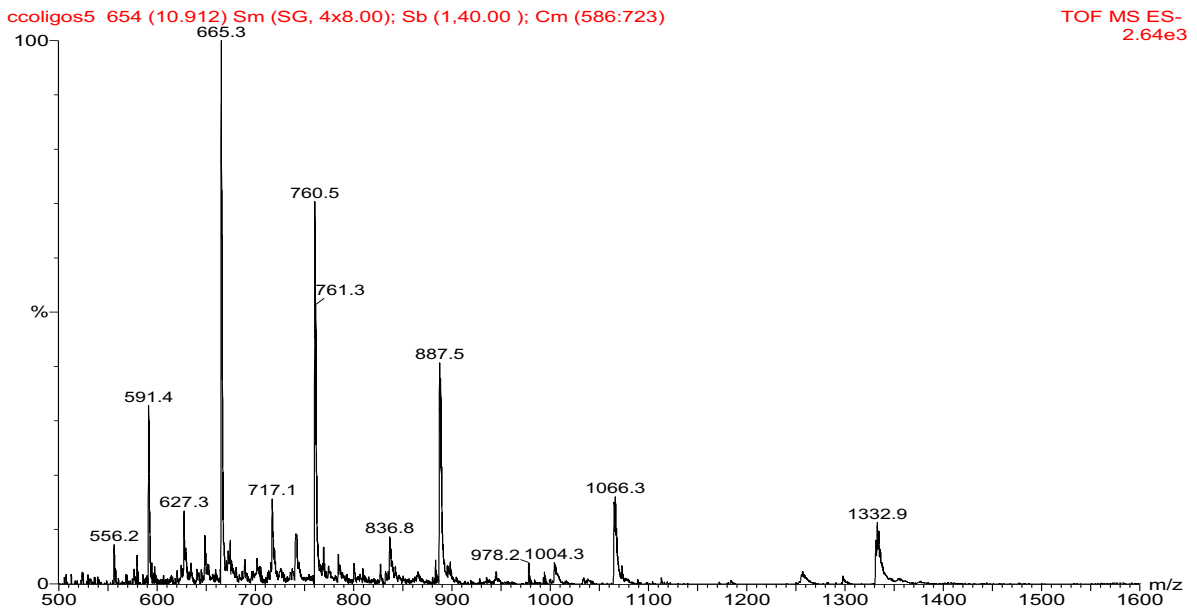
It can be concluded that the conjugation reactions were successful in each case and that purification by PAGE was successful for both the pteridinone-ODN conjugates. In the case of the ruthenium-ODN, the purification possibly produced two conjugates and before these conjugates could be used for photochemical experiments it was necessary to discover

the identity of the major and minor bands. It was decided to develop a method using electrospray mass spectrometry to characterise each ODN conjugate unambiguously.

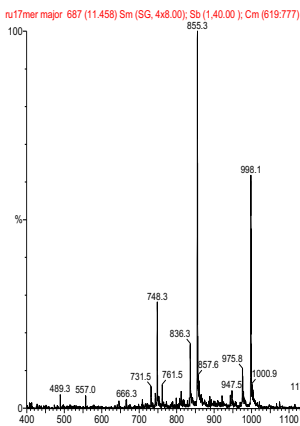
### **3.4.3. Characterisation of ODN conjugates by electrospray mass spectrometry.**

There was some doubt regarding use of the UV spectra alone as evidence of successful conjugation reactions. This is because the same UV spectra would be obtained if the free sensitiser were present in the same solution as the ODN. The purification steps should remove free sensitizer molecules and make this possibility remote but successful mass spectra would put the identification of the conjugates beyond any doubt. The free amino 17-mer was used as a standard to develop the experimental conditions of the mass spectrometer to suit analysis of the conjugates. This involved changing various experimental conditions including flow rate, solvent and desolvation temperatures until a set of conditions were obtained that resulted in clean spectra for the free 17-mer.

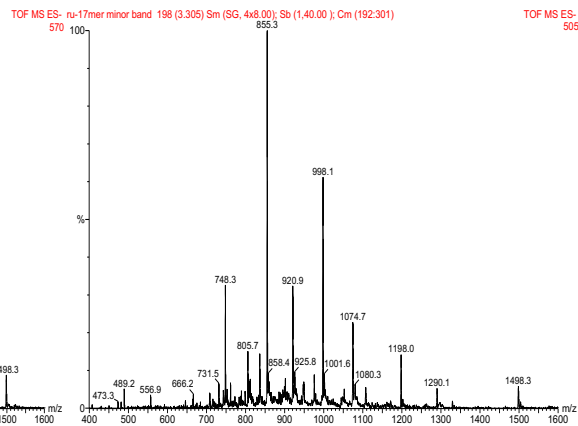
The spectrum for the amino 17-mer shown as A. in figure 3.4.d. shows a series of peaks representing multiply charged ions.



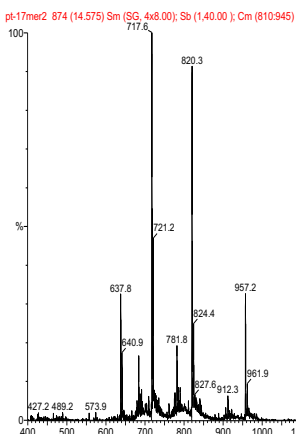
*A. Amino 17-mer.*



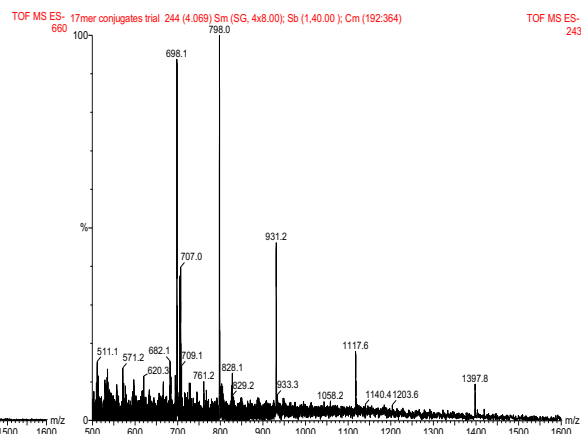
*B. Ruthenium-ODN (major band).*



*C. Ruthenium-ODN minor band.*



*D. Pteridinone-ODN 2.*



*Pteridinone-ODN 1.*

*Figure 3.4.d. Mass spectra of ODN conjugates.*

The 17 base ODN contains 16 phosphate OH groups and one 3' OH group and in negative mode ESMS analysis any number of these groups can be deprotonated to give a series of

multiply charged ions. If one OH was deprotonated the molecular ion peak would appear at  $M_w / Z(Z = 1) - 1$  proton. Two formulae can be used to determine firstly the charge ( $Z$ ) on a multiply charged peak and secondly, the molecular weight ( $M_w$ ) of the entire molecule that the peak represents.

For two adjacent peaks  $M_1$  and  $M_2$  where  $M_1 > M_2$  then,

$$Z_{M_1} = M_2 - 1.0079 / M_1 - M_2 \quad \text{and}$$

$$M_w = Z_{M_1}(M_1) + Z_{M_1}(1.0079)$$

The spectra obtained for all the ODN conjugates shown in figure 3.1.4d. were processed using the above formulae and the resulting molecular weights are shown in table 3.1.4e.

Molecule	Mw. (AMU)	Experimental Mw.
Free amino 17-mer	5336.6	5336.2
Pteridinone-ODN 1	5592.8	5592.7
Pteridinone-ODN 2	5748.1	5749.2
Ruthenium-ODN (minor band)	5994.1	5993.6
Ruthenium-ODN (major band)	5994.1	5993.4

*Figure 3.4.e. Mass spectrometry results for the ODN conjugates.*

The results showed that in each case the ODN conjugate was synthesised successfully. It was useful to note that none of the conjugates were contaminated by free 17-mer as no series of peaks representing the 17-mer was present in any of the other spectra. This indicates that the excision of the bands from the PAGE gels was accurately carried out and this is especially important for pteridinone-ODN 2 where the conjugate was not fully resolved from the unreacted 17-mer. The spectra for the minor and major bands of the ruthenium-ODN show that both bands are dominated by the desired conjugate and this makes it difficult to explain the differences in migration rates between the two bands in the gel. There is a mini series of peaks within both spectra, which give molecular weights of 5861.1 (major) and 6454 (minor). The differences in mass between these values and that of the conjugate cannot be related to any other conceivable conjugates that could have formed, however the mini series in the spectrum for the minor band is of significant intensity and could indicate some unknown ODN species that was bound somehow to the ruthenium-ODN and inhibited its migration rate.

Another possible explanation for the differing migration rates of conjugates of the same molecular weight could involve some secondary structure within the conjugate. If

the ODN strand was wrapped around the ruthenium complex and held by electrostatic attraction then, depending on the extent of wrapping there would be differences in rates of unwrapping when the electric field was applied in the gel. This could result in the appearance of two bands even if unwrapping by the electric field did not occur and just migrated differently to some conjugate without this secondary structure. Recently, It has been shown that some diastereomers of Ruthenium-ODN conjugates can be resolved using HPLC<sup>238</sup>. It is more reasonable to suggest that the bands produced for the Ru-ODN could be due to differing migration rates of diastereomers of the conjugates synthesized.

In conclusion, it can be said that both succinimide ester and phosphoramidite methodologies were used effectively in 5' conjugation reactions. Comparing the relative ease of the synthesis of the activated compounds it can be said that the succinimide ester approach was the easiest approach to take. Although, purification by this route could be particularly difficult because of the necessity to remove the excess unreacted coupling molecule and unreacted ODN and this could have been significant in the synthesis of the pteridinone-ODN (2). If the excision of the band from the gel had not been so accurate then contamination by free 17-mer could have easily occurred. The phosphoramidite route had the advantage that unreacted Pteridinone was removed by flushing solvent through the synthesiser and also the high reactivity of the phosphoramidite ensured a high coupling yield and therefore less free 17 mer was present to contaminate the excision of the bands from the gel. In the case of the ruthenium species it has been shown that the succinimide ester route is preferable due to difficulties in purifying ruthenium polypyridyl phosphoramidites although, if attempted the phosphoramidite route might ease the gel purification step. In fact both coupling methods have their advantages and disadvantages and there is no "method of choice" but rather the method to use depends on the ease of synthesis of the activated compounds to be conjugated in each particular case.

## **4.0. PHOTOOXIDATION OF 2`-DEOXYGUANOSINE BY FREE PHOTSENSITISERS.**

### **4.1. Photooxidation products of 2`-deoxyguanosine.**

It is possible to obtain information about the mechanism of photodynamic action of a photosensitising molecule by irradiation of 2`-deoxyguanosine in its presence and identification of the photooxidation products. The mechanisms that can operate are termed type I (where the initial event can involve electron transfer from the nucleoside to the excited state sensitiser) and type II (initially involving energy transfer from the excited sensitiser to molecular O<sub>2</sub> generating <sup>1</sup>O<sub>2</sub>, which can then react with regions of high electron density within the nucleoside). The products produced can indicate the relative contributions of the photomechanisms that operate for a particular photosensitiser and could model the photosensitisers behaviour in single stranded and double stranded DNA

This section details the photoproducts generated from irradiation of 2`-deoxyguanosine in the presence of Ru(phen)<sub>3</sub>Cl<sub>2</sub> (fig. 4.1.a)(as a model for the behaviour of ruthenium polypyridyl complexes) and in the presence of pteridinone (105) (as a model for the general behaviour of pteridine derivatives). The products produced were compared to those produced from the irradiation of 2`-deoxyguanosine in the presence of methylene blue. This photosensitiser acts by both type I and type II mechanisms and its photo-induced oxidation products of 2`-deoxyguanosine can be resolved by HPLC using an amino functionalised silica column. The effects of additives on the product yield were investigated to reinforce evidence for the operation of a particular photooxidation mechanism. The following figure shows the photosensitisers used and the main photooxidation products discussed in this chapter.



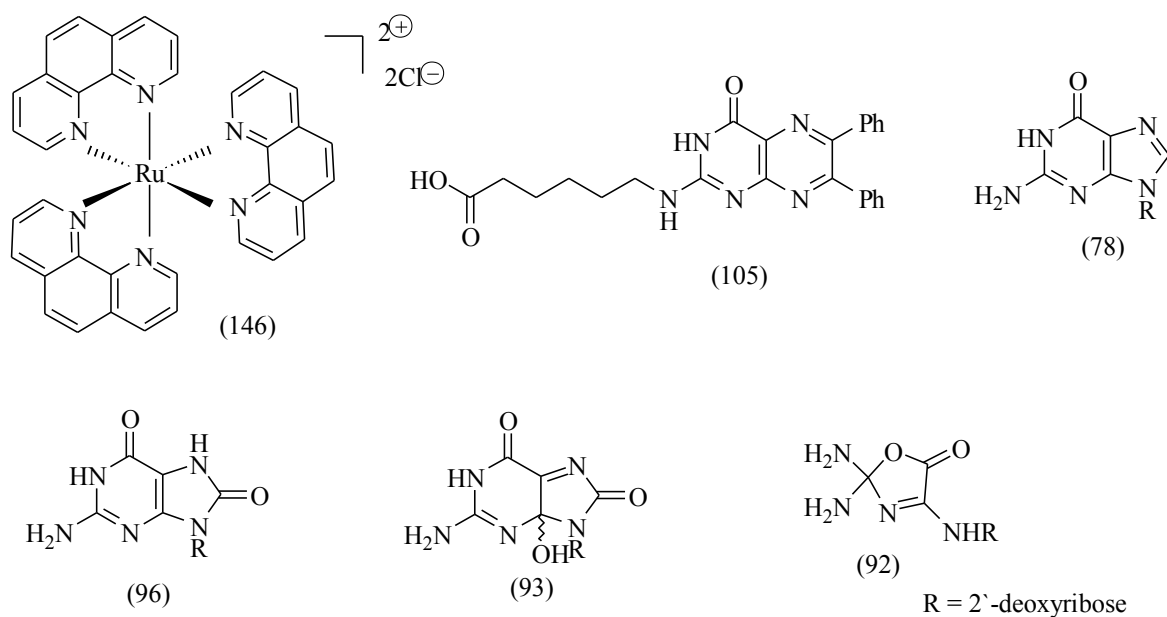


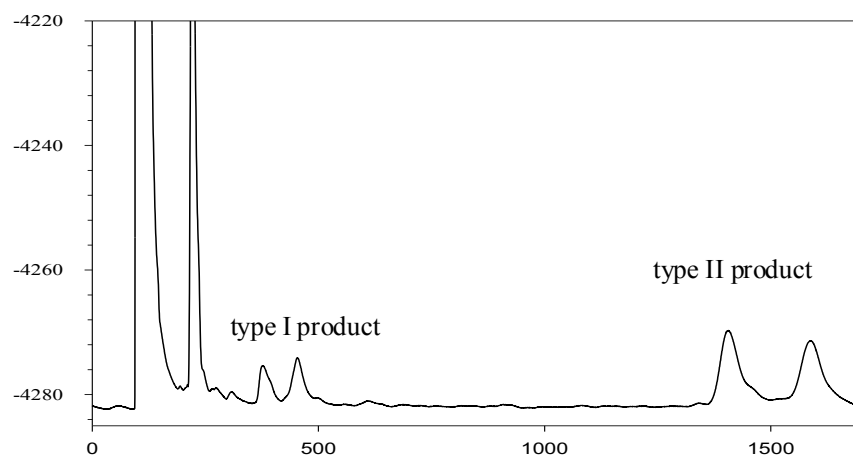
Figure 4.1.a. Photosensitisers used and the main photooxidation products of 2'-deoxyguanosine.

#### 4.1.1. Irradiation of 2'-deoxyguanosine in the presence of photosensitisers.

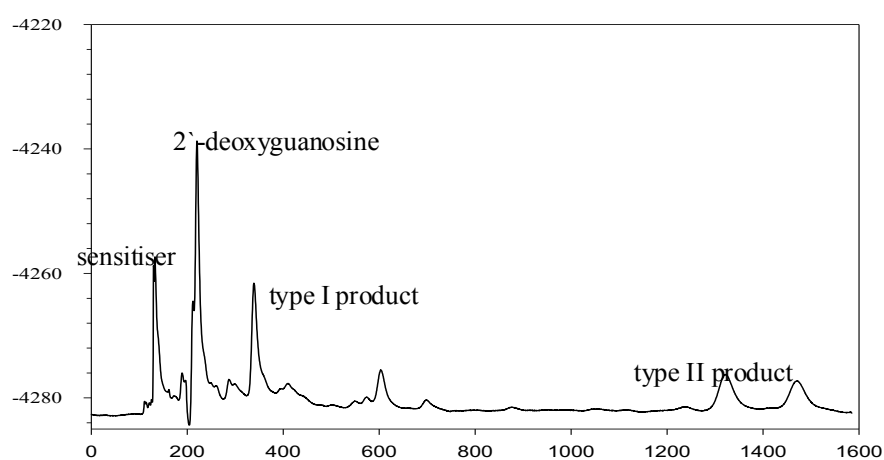
The following HPLC traces (fig. 4.1.b.) represent products from the irradiation for 60 mins. of a solution of 2mM 2'-deoxyguanosine and 1mM of:

- A. Methylene blue:
- B.  $Ru(phen)_3Cl_2$ .
- C. Pteridinone (105).





*Trace B. Ru(phen)<sub>3</sub>Cl<sub>2</sub>.*



*Trace C. Pteridinone (105).*

*Figure 4.1.b. HPLC traces of photooxidation products of 2'-deoxyguanosine produced from different photosensitisers.*

The methylene blue trace (A) shows the presence of 3 distinct products identified as the type I produced oxazolone (92) and the resolved type II diastereomers of 4-OH-8-oxodguo (93). Traces B and C also show that the type II products are produced from Ru(phen)<sub>3</sub>Cl<sub>2</sub> (146) and pteridinone (105) respectively. The trace for Ru(phen)<sub>3</sub>Cl<sub>2</sub> (B) has two small peaks in the region where the type I oxazolone elutes in the methylene blue trace and comparisons of retention times with trace A. indicate that the peak at ~350 secs. represents the oxazolone. Therefore Ru(phen)<sub>3</sub>Cl<sub>2</sub> photooxidises 2'-deoxyguanosine by both type I and type II mechanism with the suggestion that the type II mechanism predominates.

The trace for the pteridinone (C) shows a larger peak for the oxazolone and smaller amounts of the type II products. Thus, the pteridinone photooxidises 2'-deoxyguanosine

again by both type I and type II mechanism but in contrast to Ru(phen)<sub>3</sub>Cl<sub>2</sub> the type I mechanism seems to be more important.

#### 4.2. Effects of NaN<sub>3</sub> and D<sub>2</sub>O on the yields of photooxidation products.

Singlet oxygen (<sup>1</sup>O<sub>2</sub>) has a lifetime of approximately 4 μs in H<sub>2</sub>O, while its lifetime in D<sub>2</sub>O is enhanced 13 fold<sup>239</sup>. It is therefore possible to deduce the involvement of <sup>1</sup>O<sub>2</sub> in a photooxidation reaction mechanism by carrying out the irradiations having substituted D<sub>2</sub>O for H<sub>2</sub>O. Similarly, sodium azide<sup>240</sup> (NaN<sub>3</sub>) is a known quencher of <sup>1</sup>O<sub>2</sub> and so carrying out the irradiation in its presence could also verify or negate the involvement of <sup>1</sup>O<sub>2</sub> in the mechanism of photodynamic action of a particular photosensitiser by examining the yields of the oxidation products produced.

##### 4.2.1. Effects of additives on reaction of 2'-deoxyguanosine with methylene blue.

The following HPLC trace (fig. 4.2.a.) shows the superposition of HPLC traces for irradiations of 2'-deoxyguanosine and methylene blue in H<sub>2</sub>O and D<sub>2</sub>O. The effect of using D<sub>2</sub>O can be clearly seen in the increased levels of the type II products. There is also an increase in the level of the type I oxazolone peak indicating its possible formation by a type II mechanism. The most obvious difference between the H<sub>2</sub>O and D<sub>2</sub>O experiments is the decrease in the size of the 2'-deoxyguanosine peak in the D<sub>2</sub>O trace. Differences in the retention times of peaks can be attributed to changes in column back-pressure on different HPLC experiments.

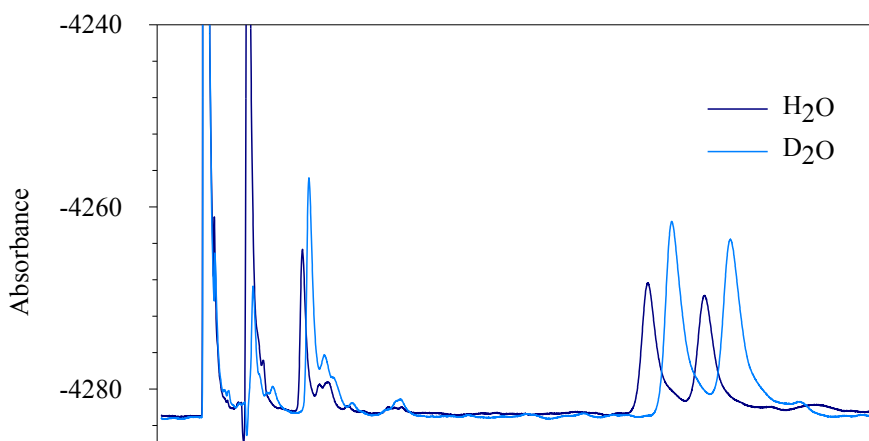
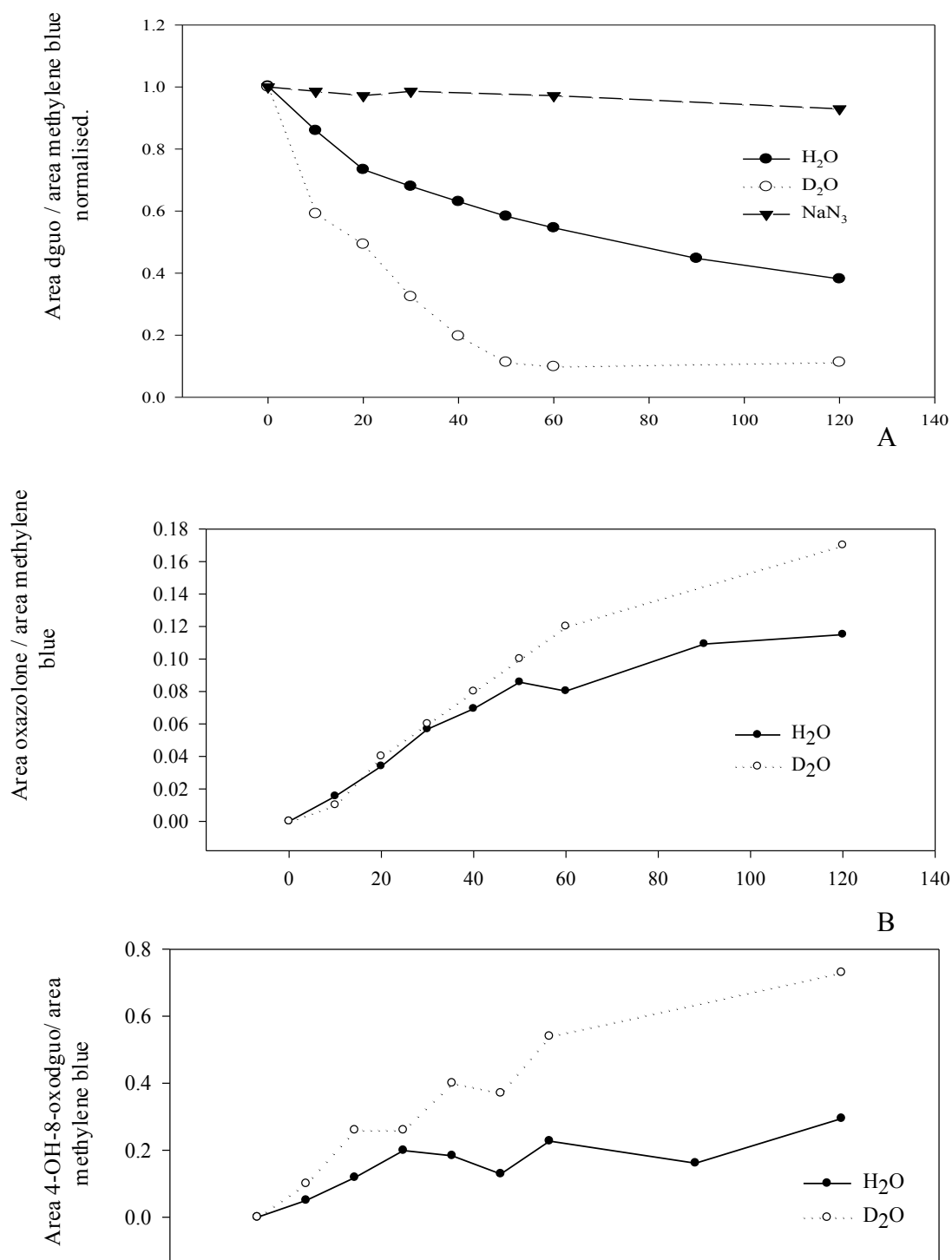


Figure 4.2.a. HPLC traces for 60 mins. irradiation of 2'-deoxyguanosine and methylene blue in H<sub>2</sub>O and D<sub>2</sub>O.

A more detailed view of the effects of using additives can be shown graphically as follows in fig. 4.2.b., where the graphs shown represent: A. the loss of 2'-deoxyguanosine, B. the formation of oxazolone and C. the formation of 4-OH-8-oxodguo for the photooxidation of 2'-deoxyguanosine by methylene blue in H<sub>2</sub>O, D<sub>2</sub>O and 10mmol NaN<sub>3</sub>.



*Figure 4.2.b. Graphs of levels of photooxidation products and effects of additives for reaction of 2'-deoxyguanosine with methylene blue. Normalisation in graph A means each value is expressed in terms of the value at 0 mins. irradiation. Graph A is the loss of 2'-deoxyguanosine, B is the formation of oxazolone and C is the formation of 4-OH-8-oxodguo.*

To account for fluctuations in the amounts of material injected each time onto the column, the area of the sensitiser peak was taken as an internal standard against which the areas of the other peaks were compared. This assumes the sensitiser itself undergoes no reaction with 2'-deoxyguanosine or any products and relies on clear resolution of the sensitiser peak from any other peak.

Graph A, shows a significant increase in the rate of 2'-deoxyguanosine destruction when the reaction medium is changed from H<sub>2</sub>O to D<sub>2</sub>O. The graph for the irradiations in NaN<sub>3</sub> shows very little loss of 2'-deoxyguanosine even after 120 mins. The HPLC trace for this experiment shows no formation of either the type I oxazolone or the type II products and this should not be the case if NaN<sub>3</sub> only quenches the <sup>1</sup>O<sub>2</sub> reaction. This suggests some interference of sodium azide in both mechanisms either by quenching the excited state of the sensitiser or affecting the interactions between the sensitiser and the substrate in solution. Thus, in this case, the use of NaN<sub>3</sub> as an indicator of the reaction mechanism cannot apply.

Graph B shows comparable rates of oxazolone formation in H<sub>2</sub>O and D<sub>2</sub>O up to 50 mins. irradiation. This supports the fact that oxazolone is formed by a singlet oxygen independent mechanism. The increase in oxazolone formation at longer irradiation times could be explained by the formation of 8-oxodguo (96), which can decompose into oxazolone by a type II mechanism. Raoul and Cadet<sup>174</sup> suggested that if 2'-

deoxyguanosine is irradiated for long periods of time with photosensitisers producing  $^1\text{O}_2$ , then the  $^1\text{O}_2$  oxidation of 8-oxodg (96) could become an important process.

Graph C shows an increase in 4-OH-8-oxodguo (93) formation in  $\text{D}_2\text{O}$  relative to  $\text{H}_2\text{O}$  and thus the evidence shows the significant involvement of  $^1\text{O}_2$  in the photooxidation of 2'-deoxyguanosine by methylene blue and that oxazolone formation occurs at short irradiation times by a type I  $^1\text{O}_2$  independent mechanism. These mechanisms of photodynamic action for methylene blue are well known, as outlined in section 1.6.2., but it was necessary to present these results in order to use methylene blue as a standard by which to compare the effects of additives on the photooxidation of 2'-deoxyguanosine with  $\text{Ru}(\text{phen})_3\text{Cl}_2$  and the pteridinone (105).

#### 4.2.2. Effects of additives on reaction of 2'-deoxyguanosine with $\text{Ru}(\text{phen})_3\text{Cl}_2$ .

The following HPLC trace (fig. 4.2.c.) shows the superposition of HPLC traces for irradiations of 2'-deoxyguanosine and  $\text{Ru}(\text{phen})_3\text{Cl}_2$  in  $\text{H}_2\text{O}$  and  $\text{D}_2\text{O}$ .

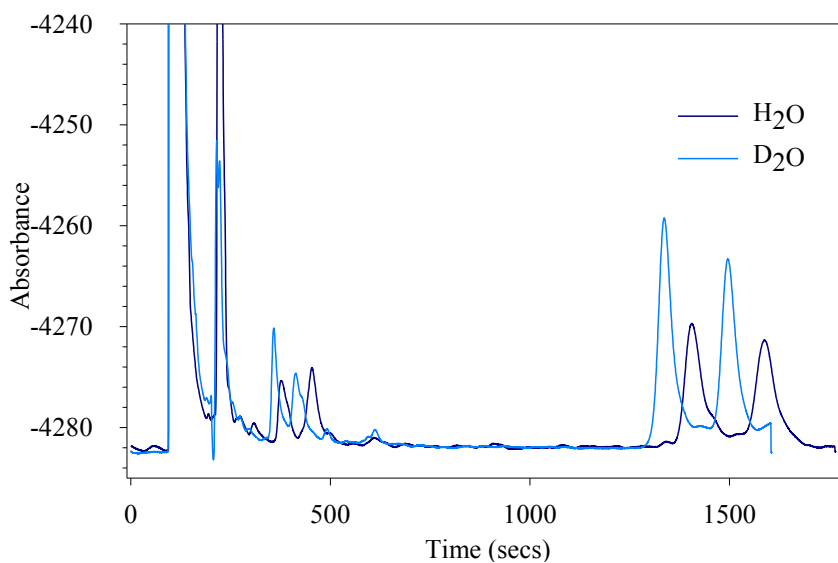
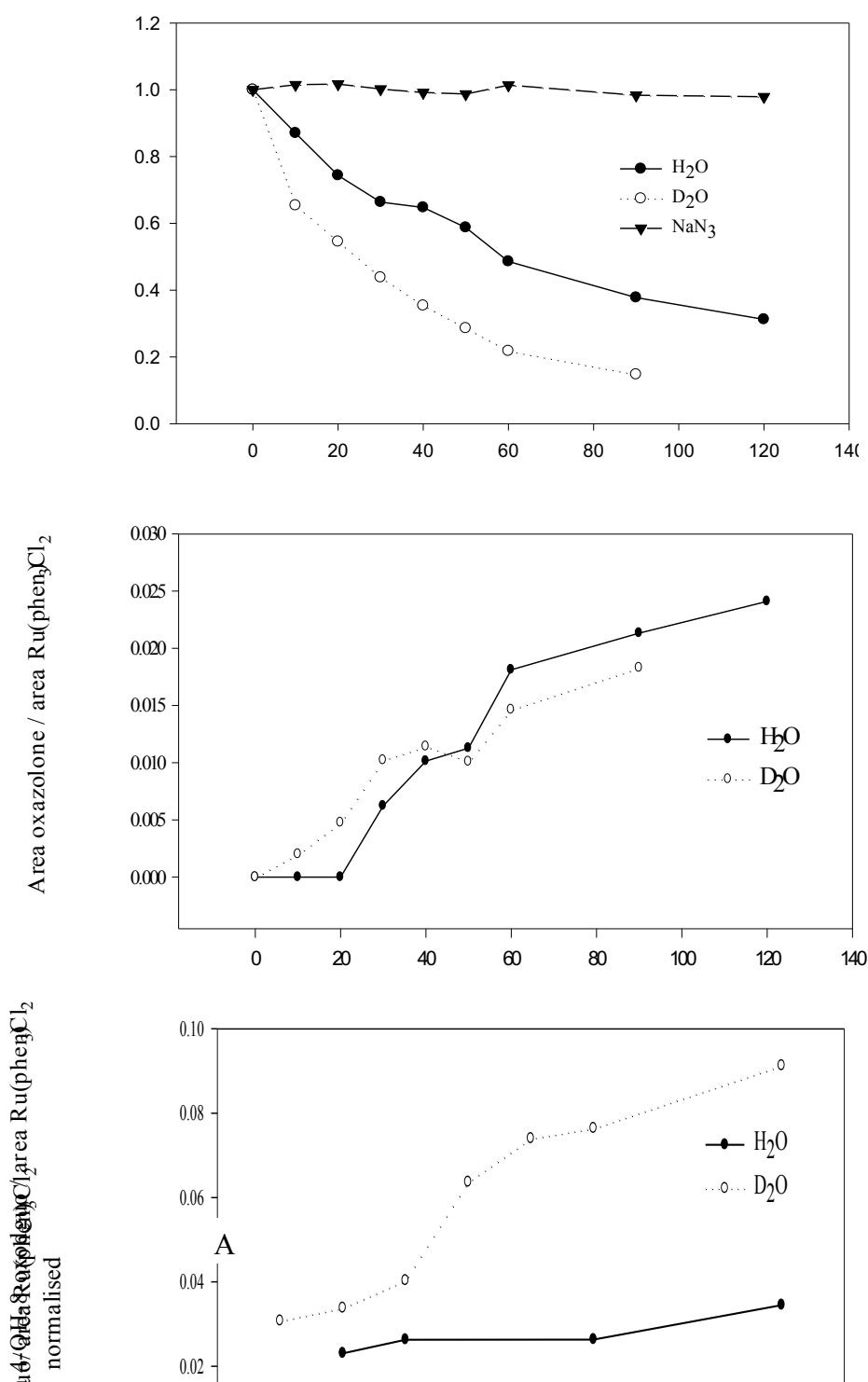


Figure 4.2.c. HPLC traces for 60 mins. irradiation of 2'-deoxyguanosine and  $Ru(phen)_3Cl_2$  in  $H_2O$  and  $D_2O$ .

As with methylene blue it can be clearly seen that the irradiation experiment in  $D_2O$  gives a much higher yield of the type II products than the  $H_2O$  experiment and that the yield of the type II products is much more affected by the change in solvents than the yield of the type I product. Graphically the effects of additives are shown below in fig. 4.2.d., where the graphs represent: A. the loss of 2'-deoxyguanosine, B. The formation of oxazolone and C. the

formation of 4-OH-8-oxodguo for the photooxidation of 2'-deoxyguanosine by  $Ru(phen)_3Cl_2$  in  $H_2O$ ,  $D_2O$  and 10mmol  $NaN_3$ .



B

C

*Figure 4.2.d. Graphs for reaction of 2'-deoxyguanosine with Ru(phen)<sub>3</sub>Cl<sub>2</sub>. Graph A is the loss of 2'-deoxyguanosine, B is the formation of oxazolone and C is the formation of 4-OH-8-oxodguo.*

As was the case with methylene blue, graph A for Ru(phen)<sub>3</sub>Cl<sub>2</sub> shows increased 2'-deoxyguanosine loss in D<sub>2</sub>O providing strong evidence for the participation of <sup>1</sup>O<sub>2</sub> in the photoreaction. Graph B shows little difference between the amounts of oxazolone produced in H<sub>2</sub>O and D<sub>2</sub>O. The larger relative amount of oxazolone produced in the H<sub>2</sub>O experiment could be accounted for by saying that D<sub>2</sub>O leads, in this case to such an



increased amount of 2'-deoxyguanosine loss by a type II mechanism that the amount that can react by a type I mechanism is lower. This is supported by graph C, which shows a much higher yield of 4-OH-8-oxodguo when the reaction medium is D<sub>2</sub>O rather than H<sub>2</sub>O. Consequently, it can be said that the photooxidation of 2'-deoxyguanosine by Ru(phen)<sub>3</sub>Cl<sub>2</sub> occurs by both type I and type II mechanisms with the type II mechanism predominating, as was the case with methylene blue.

#### 4.2.3. Effects of additives on reaction of 2'-deoxyguanosine with pteridinone (105).

The following HPLC trace shows the superposition of HPLC traces for irradiations of 2'-deoxyguanosine and the pteridinone (105) in H<sub>2</sub>O and D<sub>2</sub>O.

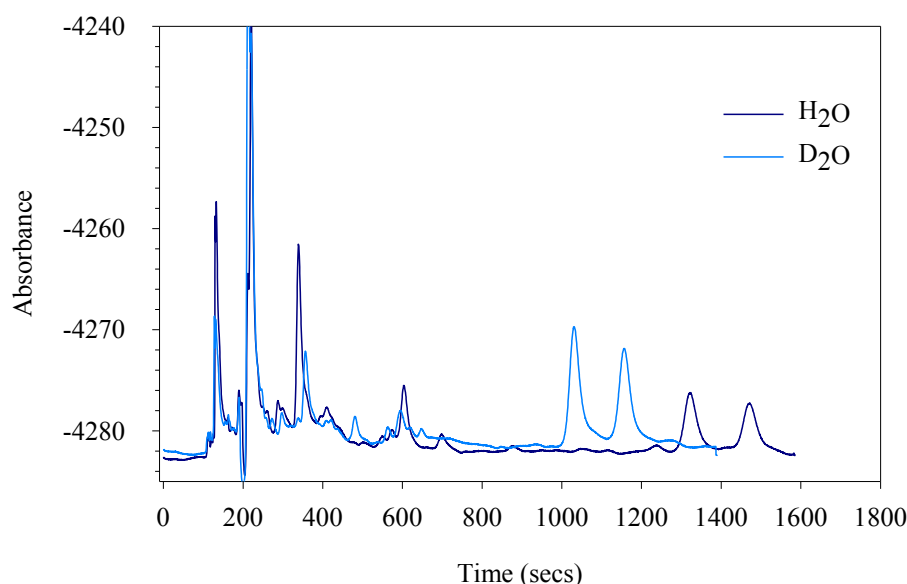


Figure 4.2.e. HPLC traces for 60 mins. irradiation of 2'-deoxyguanosine and pteridinone (105) in H<sub>2</sub>O and D<sub>2</sub>O.

Comparison of the two HPLC traces above shows increased levels of the type II products and decreased levels of the type I product. This latter observation can be explained by the fact that the increased loss of 2'-deoxyguanosine by a type II mechanism in D<sub>2</sub>O is such that less of the nucleoside is available to react by a type I reaction. The HPLC traces show that the peak for the pteridinone was not clearly resolved from other contaminant peaks and also a product peak appeared after longer irradiation times, which co-eluted with the 2'-deoxyguanosine peak. It was therefore not possible to use the sensitiser peak as an

internal standard in this case. It was however possible to plot formation of oxazolone and 4-OH-8-oxodg as a function of irradiation time in H<sub>2</sub>O and D<sub>2</sub>O and comment on the general trends observed (figure 4.2.f.).

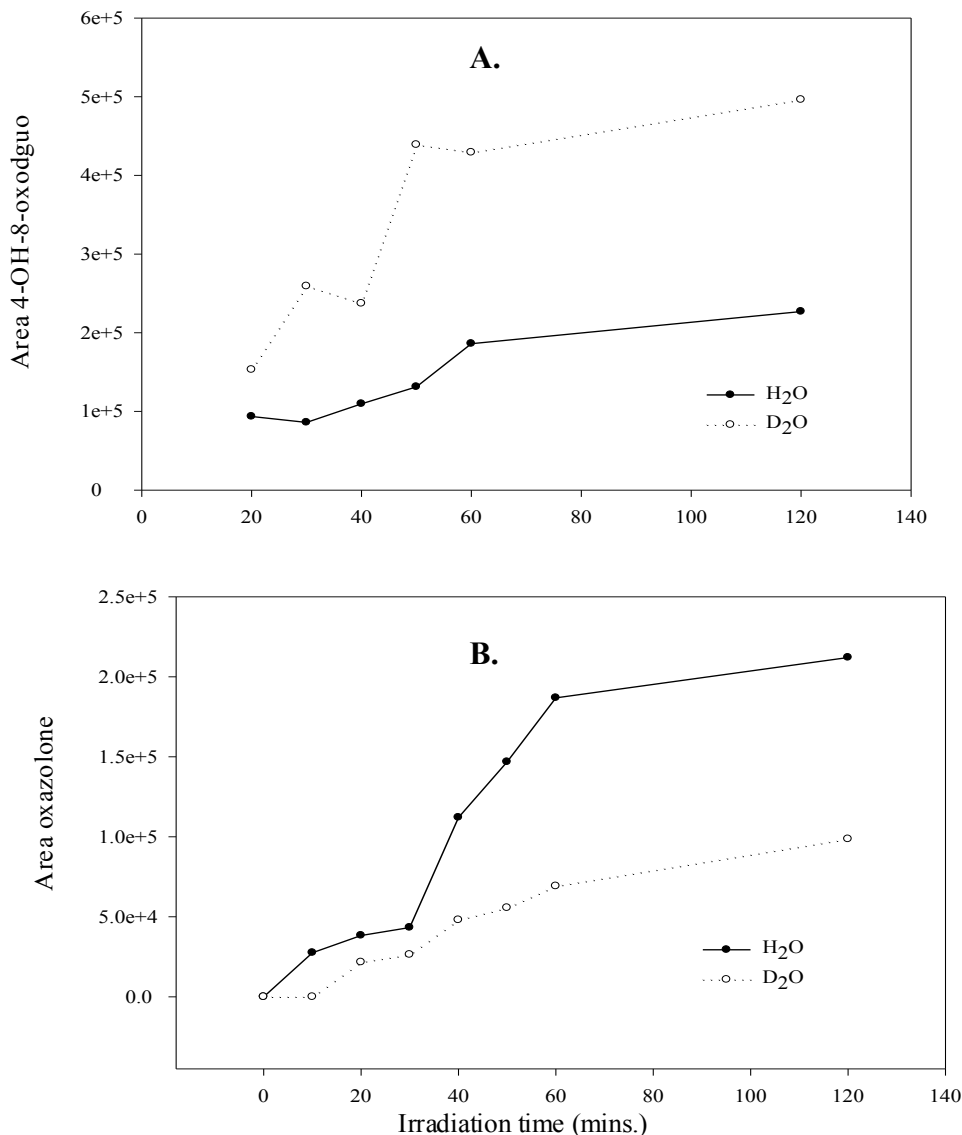


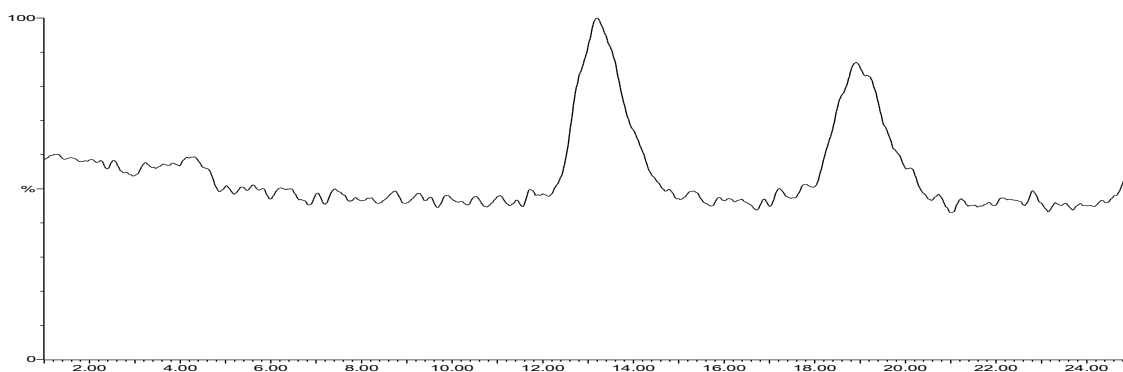
Figure 4.2.f. Graphs of levels of type II (A) and type I (B) photooxidation products for the reaction of 2'-deoxyguanosine with pteridinone (105) in H<sub>2</sub>O and D<sub>2</sub>O.

In this case the fluctuations between injections are not accounted for and so the errors are slightly more pronounced. The irradiation experiment in D<sub>2</sub>O shows (graph A) increased amounts of 4-OH-8-oxodguo relative to the H<sub>2</sub>O experiment. Graph B shows comparable levels of oxazolone at short irradiation times in H<sub>2</sub>O and D<sub>2</sub>O indicating

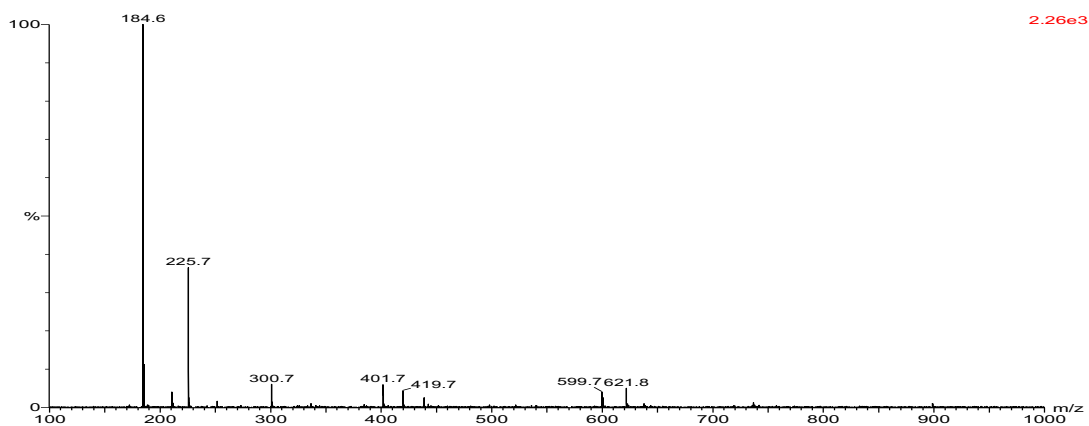
formation by a  $^1\text{O}_2$  independent mechanism with lower amounts of the type I product in  $\text{D}_2\text{O}$  again possibly reflecting lower amounts of 2'-deoxyguanosine available for reaction by a type I mechanism due to greater amounts reacting by a type II mechanism in  $\text{D}_2\text{O}$ .

#### 4.3. Characterisation of photooxidation products by mass spectrometry.

The identity of the oxidation products of 2'-deoxyguanosine described in the previous section were made by comparison with literature HPLC traces<sup>179</sup>. With the availability of an electrospray time of flight mass spectrometer it was possible to unambiguously identify the type II diastereomers of 4-OH-8-oxodguo. The products from an irradiation of 2'-deoxyguanosine and  $\text{Ru}(\text{phen})_3\text{Cl}_2$  were injected on the column and the outlet was run to waste for 20 minutes then connected to the mass spectrometer. This was necessary because the flow rate required to elute the diastereomeric peaks was not compatible with the flow rate of the mass spectrometer. The diastereomeric peaks eluted after several minutes and the following ion chromatogram was obtained (A in fig.4.3.a). The spectra obtained from either peak in the chromatogram were identical and are shown as B in fig.4.3.a.



A.



**B.**

*Figure 4.3.a. Ion chromatogram (A) and mass spectrum (B) of 4-OH-8-oxo-2`-deoxyguanosine diastereomers.*

The dominant peak in the spectrum at 184.6 amu corresponds to protonated 4-OH-8-oxoguanine and is accounted for by the loss of the ribose moiety from 4-OH-8-oxodguo. The peak at 300.7 amu corresponds to the molecular ion of 4-OH-8-oxo-2`-deoxyguanosine. The other peaks in the spectrum are possibly due to the buffer present in the mobile phase, which accounts for the high background in the ion chromatogram.

It was not possible to characterise the oxazolone peak produced from the irradiation of 2`-deoxyguanosine in the presence of the pteridinone by mass spectrometry. Clean spectra could not be obtained possibly due to the number of peaks that elute close together at the expected retention time of the oxazolone. However the products from a methylene blue photosensitisation reaction with 2`-deoxyguanosine were injected and the outlet connected to the spectrometer after 4 minutes. A peak was detected soon after whose spectrum gave a molecular ion peak,  $M^+$  at 131.6 amu. This corresponds to the loss of the nucleoside sugar from oxazolone generating the free oxazolone compound, a similar fragmentation as occurred for 4-OH-8-oxo-2`-deoxyguanosine. The fact that the sugar group was not present could be due to the irradiation itself but the fragmentation was more likely a result of the elevated operating temperatures of the electrospray ionisation chamber in the spectrometer. Similar results were obtained recently<sup>184</sup> using a different spectrometer where the dominant peak in the mass spectra for these products corresponded to the compounds after loss of the ribose sugar.

#### 4.4. Photooxidation of oligodeoxynucleotides with free photosensitisers.

The earlier results from this chapter showed that Ru(phen)<sub>3</sub>Cl<sub>2</sub> and pteridinone (105) were capable of efficiently photooxidising 2'-deoxyguanosine. This section examines if the photosensitisers are capable of photoinducing irreversible damage to guanine bases in oligodeoxynucleotide targets. Experiments were carried out using the two photosensitisers and the following <sup>32</sup>P-labeled targets.

**24-mer**                                    <sup>5'</sup> T C A A T A A G<sup>8</sup> G<sup>9</sup> A A G<sup>12</sup> A A G<sup>15</sup> C C C T T C A G<sup>23</sup> C <sup>3'</sup>

**34-mer**    <sup>5'</sup> T G A C C A T C A A T A A G<sup>14</sup> G<sup>15</sup> A A G<sup>18</sup> A A G<sup>21</sup> C C C T T C A G<sup>29</sup> C  
G<sup>31</sup> G<sup>32</sup> C C <sup>3'</sup>

The following gel scans represent such experiments using a 1:1 target:sensitiser ratio.

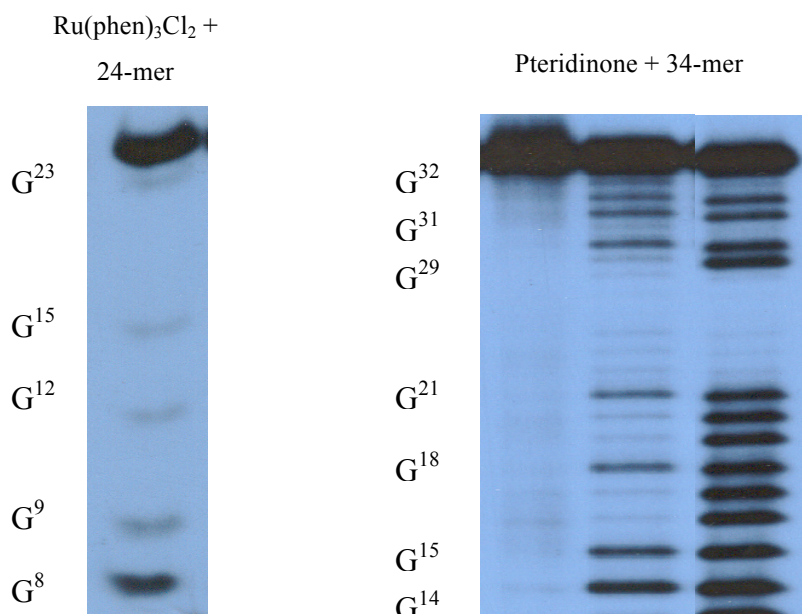


*Figure 4.4.a. Lane 1 represents Ru(phen)<sub>3</sub>Cl<sub>2</sub> targeted to the 24-mer. Lanes 2-4 represent the pteridinone targeted to the 34-mer. All experiments represent high ionic strengths(100mM NaCl) and are piperidine treated unless stated. Lane 1, 10 mins., Lane 2, 7.5 mins. no piperidine, Lane 3, 7.5 mins., Lane 4, G + A sequencing lane.*

The results from the above gel show that:

- With the sensitiser, no damage occurs in irradiated samples unless piperidine treated (lane 2).
- With both sensitiser, irradiation plus piperidine produces guanine specific cleavage (lanes 1 + 3).
- There is a slight preference for cleavage at the 5`G of the GG doublet for the pteridinone and a significant preference for the 5`G with Ru(phen)<sub>3</sub>Cl<sub>2</sub>.

#### **4.4.1. Discussion of photocleavage results with free photosensitisers.**

Firstly, the fact that the photosensitisers efficiently produced guanine specific damage in the oligonucleotide targets suggests that they are good candidates for use in ODN conjugates. The guanines are specifically oxidised due to their having the lowest oxidation potential of all the DNA bases (see table 1.6.a.). Irradiation plus piperidine treatment is required to reveal the sites of base damage and this can be attributed to oxidation of the guanine moieties. These modified bases, upon hot piperidine treatment, cause cleavage of the ODN strand. This will be discussed in greater detail in the next chapter but could be due to the induced formation of some of the modified guanines produced by the HPLC assay. The gel scan shows that there is a preference for cleavage of the 5`G of the GG doublets in the targets. This result is known for double stranded DNA (see section 1.6.1.) and is related to the fact that the HOMO for GG doublets is localised on the 5` G and thus this base is the most easily oxidised site. The fact that this pattern occurs for the single stranded targets is possibly due to the formation of a hairpin, which places the GG doublet in a mini-double stranded region as shown below



This preference for the 5' G is expected with the pteridinone and its predominant type I mechanism as the double strand would facilitate electron transfer to the GG site. This however would not be expected for Ru(phen)<sub>3</sub>Cl<sub>2</sub>, which mainly operates by a type II mechanism. Any singlet oxygen produced should not really have a preference for the 5' G but the effect is seen to be most dramatic with the ruthenium complex.

Summarising the results from this chapter, it can be said that the evidence shows both Ru(phen)<sub>3</sub>Cl<sub>2</sub> and pteridinone (105) photooxidise 2'-deoxyguanosine by a combination of type I and type II mechanisms. The difference between the two photosensitisers lies in the relative contribution of each mechanism to the particular photosensitiser. The HPLC traces suggest that a type I mechanism occurs to a greater extent with the pteridinone than with Ru(phen)<sub>3</sub>Cl<sub>2</sub>. The consequences of the different relative contributions of each mechanism will become apparent when analysing the experimental results for the irradiation of the 34-mer ODN in the presence of the complementary ODN conjugates. Important factors may include the different products produced by the different ODN conjugates, the behaviour of the lesions generated in the single stranded and double stranded regions of the experimental model (i.e. further reaction of the lesion or its possible migration through the double strand) and the comparative piperidine susceptibility of the different lesions produced.

## **5.0. PHOTOOXIDATIVE DAMAGE USING OLIGODEOXY-NUCLEOTIDE CONJUGATES.**

### **5.1. Photocleavage experiments with oligonucleotide conjugates.**

The experimental results described hereafter represent studies using the oligodeoxynucleotide (ODN) conjugates, whose syntheses were described in chapter 3. These pteridinone-ODN conjugates and the ruthenium polypyridyl complex conjugate were designed to be complementary to part of a 34 base ODN model of the junction region of the bcr/abl mRNA present in chronic myeloid leukaemia (as shown below).

5' TGACCATCAATAAGGAAGAA G<sup>21</sup> CCCTTCAGCGGCC 3'  
 3' GGTAGTTATTCCTTCTT –sensitiser

With the aim being to specifically damage the target strand at G<sup>21</sup>, the general experimental procedure involved the following:

The 5'-<sup>32</sup>P labelled target and the ODN conjugate were mixed together in a buffered solution at high salt concentration (100mM) and heated to 85°C then cooled slowly to encourage hybridisation of the two strands. The samples were then irradiated using a medium pressure Hg lamp (at a temperature less than 10°C) with water (removes IR radiation) and pyrex glass (removes  $\lambda < 330\text{nm}$ ) filters. After irradiation the samples were treated with piperidine to induce cleavage of the target strand at any photo-modified bases. The cleavage products generated were separated by polyacrylamide electrophoresis, visualised by autoradiography and/or phosphorimager and quantified by densitometry. The sites of cleavage were identified by comparison to Maxam and Gilbert<sup>241</sup> sequencing experiments in which treatment of the target oligonucleotide with formic acid followed by hot piperidine cleaves the target at every purine base. This produces a ladder like sequence in the gel against which cleavage bands in the experiments can be compared for sites of damage.

## 5.2. Results using ruthenium ODN complex conjugate.

The 34-mer was firstly irradiated in the presence of a 10-fold excess of the ruthenium ODN. This was carried out to ensure that a sufficient amount of the target would be damaged so that visualisation of the cleavage bands would be possible. The following image represents a scan of the autoradiography film produced. The intensity of the bands relative to each other does not entirely reflect the percentage of products. This is because the films are easily overexposed and thus the films are mainly used for visual effect, however if not overexposed the films can be quantitative.

TCAGCGGCC



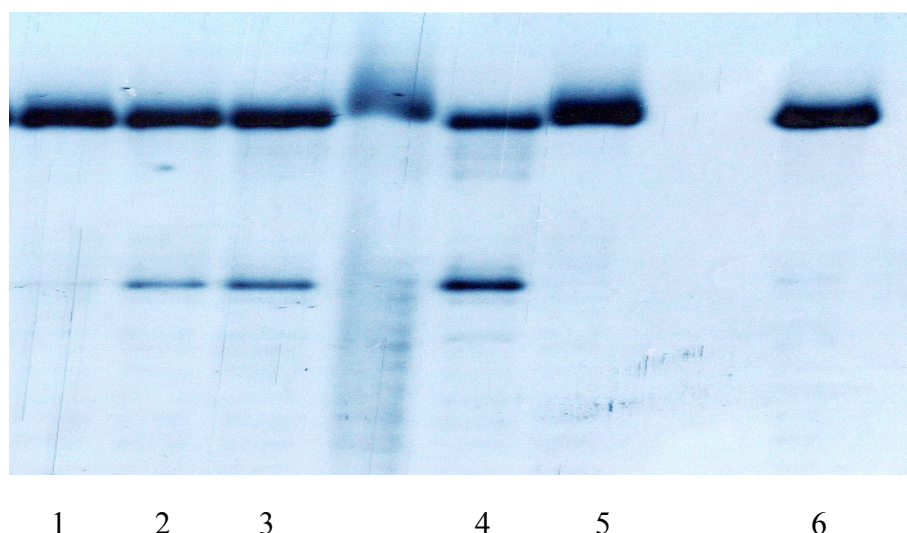
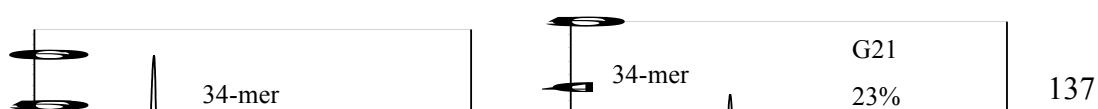


Figure 5.2.a. Time course experiment for irradiation of 34-mer in the presence of 10-fold excess of the ruthenium-ODN. Unless stated, all lanes are piperidine treated. Lane 1., 7.5mins. irradiation, Lane 2., 15mins. irradiation, Lane 3., 30 mins. irradiation, Lane 4., 60 mins irradiation, Lane 5., 0mins irradiation, Lane 6., 7.5mins. irradiation, no piperidine.

The main results from the above gel are that:

1. No cleavage occurs without irradiation (lane 5).
2. No cleavage occurs in an irradiated sample if piperidine treatment is not carried out (lane 6).
3. Lanes 1–4 show that increasing irradiation followed by piperidine treatment results in specific cleavage at the target base G21.
4. Lanes 3 and 4 reveal that at longer irradiation times a small amount of cleavage occurs at other guanine bases (specifically G18 in the double stranded region and G29, G31 and G32 at the extreme 3' end of the target. This group of 3 bases will hereafter be called the 3`G bases.

In order to quantify the amounts of cleavage products produced the above gel was phosphorimaged and then densitometry was used to plot the intensities of cleavage bands versus their relative position on the gel. Radioactive gels can be exposed to phosphorimaging screens for long time periods without overexposure. In contrast, radioactive gels exposed to autoradiography films become saturated easily and thus quantifiable densitometry is best carried out on phosphorimages. The following plots represent densitometry carried out on lanes 3 and 4 of the gel in figure 5.2.a.



*Figure 5.2.b. Phosphorimager densitometry plots for 30 mins. (left) and 60 mins. (right) irradiation of 34-mer target in the presence of a 10 fold excess of ruthenium-ODN.*

The above plots show that after 30 mins. irradiation, cleavage products at the target G21 represent 13% of the total plot, which increases to 23% after 60 mins. irradiation. Densitometry of lane 5 in the previous gel showed that the 34-mer represents 75% of the plot area after 0 mins irradiation. Thus, the percentage cleavage values. could be more accurately expressed relative to this 0 minutes. percentage value of the 34-mer. This would give values of 17.3% G21 damage after 30 minutes and 30.6% G21 damage after 60 minutes. In future all percentages will be expressed relative to 0 mins. irradiation unless stated.

Irradiation for 60 mins. produces a small percentage (3%) of cleavage products at G18 in the double stranded region of the system and some unresolved cleavage products are produced at G29, G31 and G32. It is difficult to say how accurate small percentage values are, as the background could contribute significantly.

With the knowledge that G21 cleavage of target 1 could be achieved specifically with a 10-fold excess of the conjugate, it was decided to lower the sensitiser : target ratio to 1:1 to compare the efficiency of cleavage (figure 5.1.c.). This experiment is necessary to show that cleavage is caused by hybridised conjugate and not by free sensitiser molecules, which could be present with an excess of the conjugate. Note that it is not valid to directly compare the percentages of peaks in densitometer plots between different gels. This is because gels are exposed for different amounts of time producing different levels of background contamination.

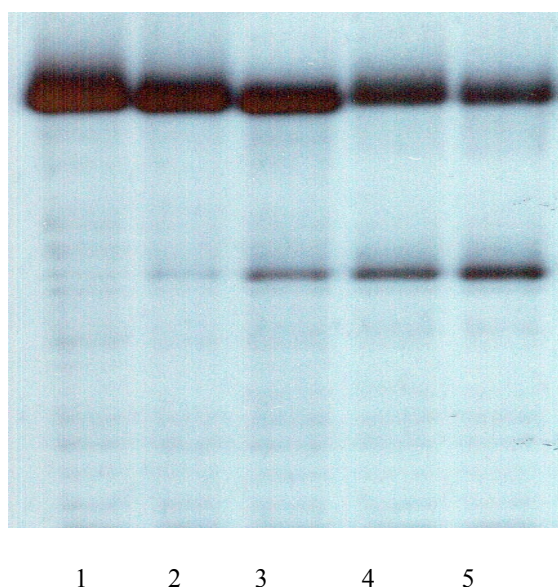


*Figure 5.2.c. Time course experiment for irradiation of 34-mer in presence of equivalent amount of the ruthenium-ODN. Unless stated, all lanes are piperidine treated. Lane 1. 0 mins. irradiation, Lane 2. 7.5mins. irradiation, Lane 3. 15mins. irradiation, Lane 4. 30 mins. irradiation, Lane 5. 60 mins irradiation.*

The above gel scan shows that G21 specific cleavage can be achieved with a 1:1 sensitiser:target ratio. The cleavage increases with irradiation time and seems to be more specific than using the excess of the conjugate as no real cleavage is seen at G18 or at G29, G31 and G32. The following table shows the percentages of cleavage products produced for the time course experiment.

Lane	Irradiation time (mins)	% 34-mer	% G21	% other G bases
1	0	100		
2	7.5	80.7	10.1	
3	15	61.2	21.7	
4	30	52.5	30.6	
5	60	42.5	41.8	3.3(G18)

*Figure 5.2.d. Table showing percentages of cleavage products obtained from time course experiment for irradiation of target 1 in presence of an equivalent amount of the ruthenium*

ODN. All percentages are expressed relative % 34-mer area at 0 mins. irradiation (i.e. background is neglected at 0 mins).

The table shows that almost equal amounts of the 34-mer and the G21 cleavage product are present after 60 mins. irradiation and that contributions from other cleavage products are minimal (3.3 % after 60 mins. irradiation).

### 5.2.1. Discussion of photocleavage results with the ruthenium-ODN.

Concerning the time course experiments, the previous results have shown that the ruthenium-ODN can photo-induce specific damage to the target oligonucleotide at guanine 21 (figure 5.2.c). It should firstly be noted that no damage occurs without irradiation of the system. This shows that we have a light activated reaction and that whatever ground state interactions occur between the conjugate photosensitiser and the target bases, they do not lead to base damage. Also of note is the fact that irradiated samples require piperidine treatment to reveal the sites of base damage. The fact that no direct strand or Frank breaks occur testifies that the photochemical processes involved do not generate radical species that can migrate and react indiscriminately with various sites in the oligonucleotide. This necessity to use piperidine can be explained by a photooxidation reaction occurring at G21, which renders the modified base susceptible to strand scission upon piperidine treatment. In general this can occur when the modified base is a better leaving group than guanine

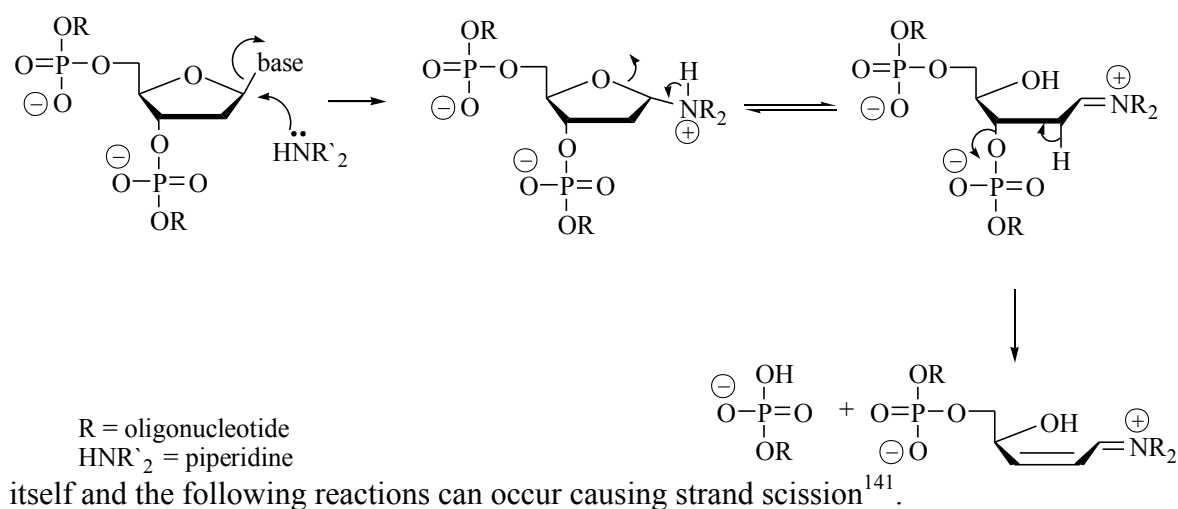


*Figure 5.2.e. Piperidine cleavage of base modified oligonucleotides.*

The results show that G21 is specifically damaged. This implies the design of the oligonucleotide conjugate is such that the sensitiser is located in close proximity to the target base to allow an efficient photochemical reaction to occur. With a 10-fold excess of the conjugate, approximately 23% of the cleavage products are generated at G21 after 60 minutes irradiation, although the excess of the conjugate causes some non-specific damage at other guanine bases in the target. Using an equal amount of the conjugate and the target decreases this non-specific damage. In this case, 41.8% of the cleavage products are produced at the target base after 60 minutes irradiation.

To understand the nature of the photochemical process involved we can look at the results for the model system of  $\text{Ru}(\text{phen})_3\text{Cl}_2$  and its photooxidation of 2'-deoxyguanosine. The HPLC data discussed earlier showed that the ruthenium complex photooxidises the nucleoside predominantly by a type II mechanism involving the transfer of energy from the excited complex to molecular oxygen generating the reactive species  $^1\text{O}_2$ . This species then reacts with 2'-deoxyguanosine via a cycloaddition reaction to lead to the formation of diastereomeric 4-hydroxy-8-oxo-2'-deoxyguanosine. Is it possible to apply this evidence to the case with the hybridised conjugate and target and say that a type II reaction operates as well?. Obviously, the molecular environment of  $\text{Ru}(\text{phen})_3\text{Cl}_2$  and 2'-deoxyguanosine in solution is considerably different from the hybridised conjugate and its target. In the latter case the ordered nature of the double stranded region in close proximity to the floppy single stranded portion of the system leads to a more complex reaction environment. It has been shown that the photooxidation products of free 2'-deoxyguanosine are different from those of guanine in single stranded and indeed double stranded DNA (section 1.6.3.). However, it is reasonable to assume that the photosensitiser will still operate by a type II mechanism if there is sufficient access to molecular oxygen and that it is the reaction products at guanine which will be different than those identified using the HPLC model assay.

Another possible mechanism for the photo-reaction could involve  $\text{Ru}^{3+}$  chemistry. It has been shown<sup>242</sup> that  $\text{Ru}^{2+}$  species can be oxidised in the presence of DNA with electron transfer quenchers such as  $\text{Ru}(\text{NH}_3)_6^{3+}$ . The  $\text{Ru}^{3+}$  produced is a more powerful oxidant than  $\text{Ru}^{2+}$  and can then undergo electron transfer with guanine very efficiently. In our case, the presence of trace amounts of quenchers such as  $\text{Fe}^{2+}$  could generate the more reactive  $\text{Ru}^{3+}$  species and contribute to the photodamage observed.

In any case, the effects of using additives such as a D<sub>2</sub>O based buffer reinforced the evidence of the operation of a type II mechanism in the case of Ru(phen)<sub>3</sub>Cl<sub>2</sub> and 2'-deoxyguanosine. It is possible that similar experiments using the oligonucleotide conjugate will show that a type II mechanism also applies in the this case.

### 5.3. Effects of additives on photocleavage by ruthenium ODN.

The results from chapter 4 showed that Ru(phen)<sub>3</sub>Cl<sub>2</sub> photooxidises 2'-deoxyguanosine by a combination of type I and type II mechanisms. The type II mechanism involving <sup>1</sup>O<sub>2</sub> was shown to predominate and carrying out irradiation experiments in D<sub>2</sub>O led to increased levels of type II products. This HPLC assay was used to model the photooxidation properties of such ruthenium polypyridyl complexes and the use of additives reinforced the evidence for a type II mechanism.

Experiments were then carried out using the ODN conjugates to examine how the use of additives would affect the specificity and extent of G21 cleavage. The following gel scan represents an experiment using:

1. A D<sub>2</sub>O based buffer (increases the lifetime of <sup>1</sup>O<sub>2</sub>).
2. Presence of 0.01M NaN<sub>3</sub> (known to quench <sup>1</sup>O<sub>2</sub>).
3. A blanket of argon covering the reaction (partial removal of molecular O<sub>2</sub>).

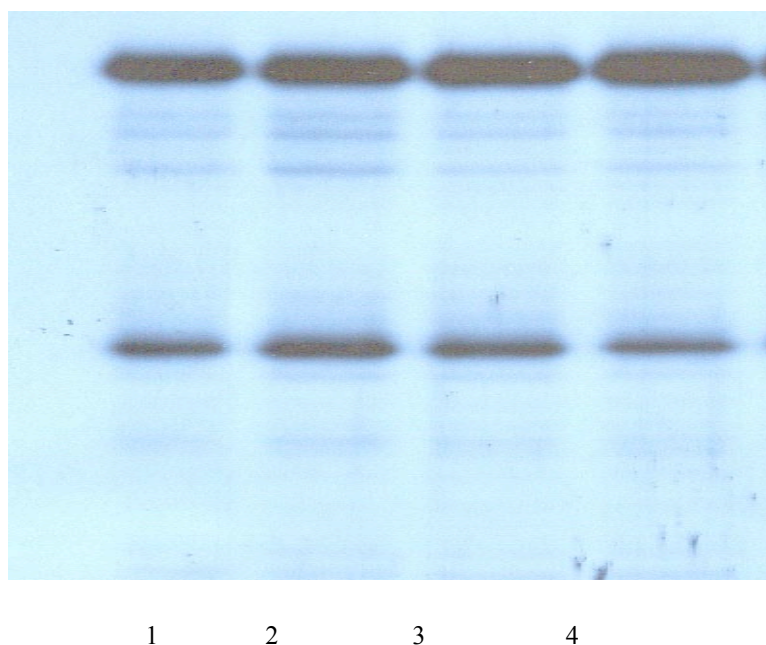


*Figure 5.3.a. Experiment for irradiation of 34-mer and ruthenium-ODN. in the presence of additives. All lanes are piperidine treated and represent 10 minute irradiations. Lane 1., H<sub>2</sub>O, Lane 2., D<sub>2</sub>O, Lane 3., NaN<sub>3</sub> Lane 4., Argon.*

The intensity of the bands representing cleavage at G 21 for lanes 1-4 seem to show slight increases in the extent of cleavage at G21 in D<sub>2</sub>O and decreases in the presence of NaN<sub>3</sub> and Argon. The Following table more clearly shows the effects of the additions on the percentage of G21 damaged.

Lane	Experiment.	% 34-mer.	G21	3`G damage
1	H <sub>2</sub> O	52.6	20.4	6
2	D <sub>2</sub> O	48.9	22.7	6.9
3	NaN <sub>3</sub>	58.9	17.8	4.8
4	Argon	65.8	12.8	4.6

*Figure 5.3.b. Table showing the percentage cleavage products for additives experiment. All percentages are expressed relative to the total densitometer plot area (i.e.background is included).*

The table shows that there is a 9% increase in cleavage at G21 upon changing from a H<sub>2</sub>O buffer to a D<sub>2</sub>O buffer. This effect is also seen in increased levels of damage at other guanine bases and decreased amounts of the 34-mer remaining. The results also show that the presence of NaN<sub>3</sub> decreases the amount of cleavage as does carrying out the experiment under an argon atmosphere.

### **5.3.1. Discussion of Ru-ODN photocleavage results in the presence of additives.**

The trends observed for the ruthenium-ODN and the 34-mer in the presence of additives can be summarised as follows: All results are relative to H<sub>2</sub>O (20.4% G21 damage and 6% non-specific G cleavage).

A decrease in G21 cleavage was observed in the presence of Argon (12.8% at G21 and 4.6% non-specific G cleavage).

An increase in G21 cleavage was observed using a D<sub>2</sub>O based buffer (22.7%).

An increase in non-specific G cleavage was also observed using a D<sub>2</sub>O based buffer (6.9%).

A decrease in all G cleavage was observed in the presence of 0.1M NaN<sub>3</sub>; 17.8% at G21 and 4.8% non-specific G cleavage.

With regard to point 1, the removal of molecular oxygen does not provide direct evidence for the involvement of a type II mechanism as O<sub>2</sub> is also involved in some intermediary reactions in type I mechanisms (figure 1.6.e.).

On face value the evidence from points 2, 3 and 4 suggest a definite role for <sup>1</sup>O<sub>2</sub> in the photodamage mechanism by the ruthenium-ODN. The HPLC results in chapter 4 showed that NaN<sub>3</sub> seemed to suppress both type I and type II mechanisms with 2'-deoxyguanosine and Ru(phen)<sub>3</sub>Cl<sub>2</sub> and thus the effect of D<sub>2</sub>O is the most reliable result to use. It is difficult to say that a type II mechanism operates exclusively. The actual mechanism is likely to be a competition between type I and type II mechanisms. There are a number of factors that will determine which mechanism predominates. The energy of the excited state ruthenium complex relative to the energy of the HOMO of the target guanine will determine the ability of an electron transfer reaction to occur. If the levels are sufficiently close in energy to allow an electron transfer, the sensitiser and substrate must also be in close proximity to each other to facilitate this. Competing with this will be the efficiency of energy transfer from the excited state ruthenium complex to molecular oxygen generating <sup>1</sup>O<sub>2</sub>.

There have been conflicting reports in the literature regarding using the evidence of free sensitiser photochemical behaviour to predict the properties of a sensitiser conjugate and using the effects of D<sub>2</sub>O and NaN<sub>3</sub> to explain the mechanism of a sensitiser conjugate. C<sub>60</sub> was shown to sensitise <sup>1</sup>O<sub>2</sub> formation in free solution with high efficiency<sup>133</sup>. A derivative of C<sub>60</sub> was conjugated to an oligonucleotide and targeted to its complementary strand in similar experiments to those presented in this research. The yield of target guanine damage with the conjugate was neither enhanced in D<sub>2</sub>O nor diminished in NaN<sub>3</sub> producing results contrary to the predictions of the free sensitiser. The results were explained by saying that the sensitiser was in such close proximity to electron rich guanines in the target that electron transfer occurred more rapidly than formation of <sup>1</sup>O<sub>2</sub>. Boutorine *et al.*<sup>85</sup> also found unusual results with a chlorin oligonucleotide conjugate targeted to damage guanines in a triple helix. In their case O<sub>2</sub> exclusion totally removed



target guanine damage,  $\text{NaN}_3$  decreased cleavage but no enhancement was found in  $\text{D}_2\text{O}$ . This was attributed to  $\text{D}_2\text{O}$  only increasing the lifetime of  $^1\text{O}_2$  in bulk solution and not that generated in the solvent cage around the sensitiser, which is also in a protected environment within the triple helix.

It can be concluded that the evidence from the HPLC assay and the gel results suggest that the ruthenium-ODN operates predominantly by a type II mechanism, although it is not possible to exclude contributions from a type I mechanism possibly from a  $\text{Ru}^{3+}$  species. The results using the pteridinone-ODN conjugate should help to clarify the issue as the free pteridinone was shown by HPLC results to have a greater contribution from a type I mechanism in the photooxidation of 2'-deoxyguanosine.

#### **5.4. Photocleavage results for variant target strands using ruthenium-ODN.**

A series of variant target strands were synthesised in which that target G21 base was either removed or shifted towards the 3' end of the 34-mer. The following 34-mer targets were used and are mentioned hereafter by the names adjacent to the base sequence. The bases are numbered as their distance from the 5'-end.

##### **Target 1.**

$5'\text{TGACCATCAATAAGGAAGAA}\mathbf{G}^{21}\text{CCCTTCAGCGGCC}3'$

##### **Variant 1.**

$5'\text{TGACCATCAATAAGGAAGAAATCCCTTCAGCGGCC}3'$

##### **Variant 2.**

$5'\text{TGACCATCAATAAGGAAGAAC}\mathbf{G}^{22}\text{CCTTCAGCGGCC}3'$

##### **Variant 3.**

$5'\text{TGACCATCAATAAGGAAGAAC}\mathbf{C}\mathbf{G}^{23}\text{CTTCAGCGGCC}3'$

##### **Non-hairpinning variant 3.**

$5'\text{TGACCATCAATAAGGAAGAA}\mathbf{T}\mathbf{A}\mathbf{G}^{23}\text{TTTCAGCGGCC}3'$

##### **Variant 4.**

$5^{\prime}$ TGACCATCAATAAGGAAGAACCC**G**<sup>24</sup>TTCAGCGGCC $3^{\prime}$

**Variant 5.**

$5^{\prime}$ TGACCATCAATAAGGAAGAACCCT**G**<sup>25</sup>TCAGCGGCC $3^{\prime}$

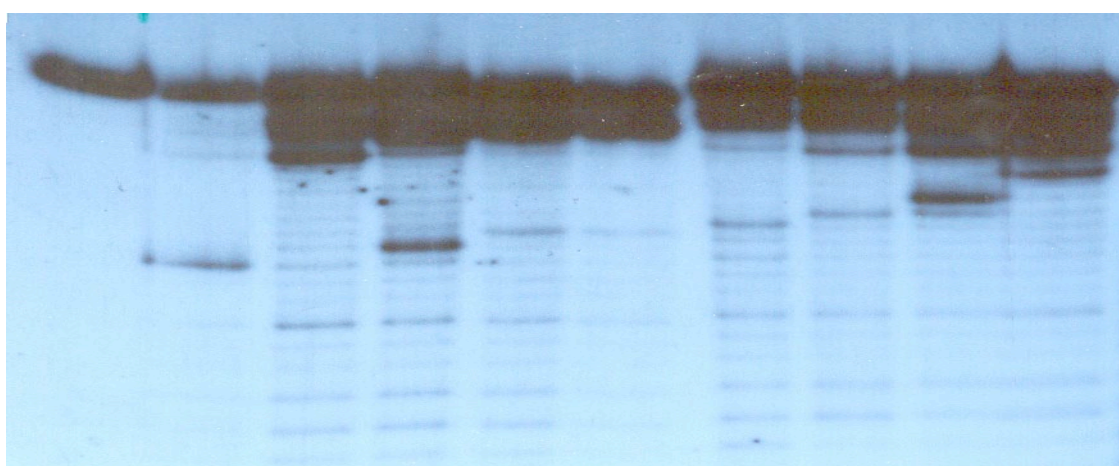
**Variant 6.**

$5^{\prime}$ TGACCATCAATAAGGAAGAACCCTTT**G**<sup>27</sup>AGCGGCC $3^{\prime}$

Examining the ability of the oligonucleotide conjugates to damage these variants should give useful information about the following:

1. The location of the photosensitising molecule relative to the target base and how this affects reactivity.
2. The nature of the reactive species, i.e. is close proximity to the target base necessary for efficient reaction or can the reactive species migrate and still give an efficient reaction.
3. As a side effect of using variant strands, one can look at the effect of secondary structures intrinsic to some of the variant targets and how this affects the photochemical reaction.

The following figure represents a gel scan for an experiment with the variant strand targets using the ruthenium-ODN and a table showing the percentages of products obtained at the various bases.



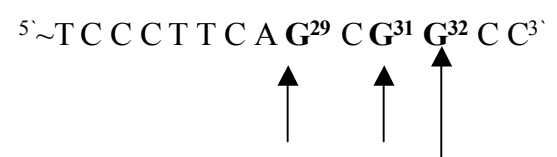
1	2	3	4	5	6	7	8	9
Lane	34-mer	% 34-mer.			Movable G	G29	G31	G32

2	Target 1	76.1	7.3			
3	Variant 1	32	-	8	6.3	12.8
4	Variant 2	32.7	2.8	0.9	22	14
5	Variant 3	29	1.2	-	-	25.4
6	Non-hairpinning variant 3	48	1.6	-	-	9.5
7	Variant 4	41.2	1.7	2.8	-	17.8
8	Variant 5	35.7	5.0	6	5.9	11.8
9	Variant 6	43.3	4.2	8	7.4	12.6

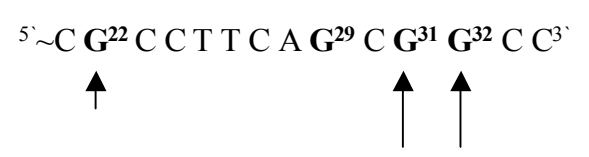
*Figure 5.4a. Gel scan of variant strand experiments. All experiments were irradiated for 10 mins. and piperidine treated unless stated. Lane 1, 0 mins irradiation 34-mer target 1. Lane 2, 34-mer target 1. Lane 3, Variant 1(No G). Lane 4, Variant 2 (G22). Lane 5, Variant 3 (G23). Lane 6, Non-hairpinning variant 3. Lane 7, Variant 4 (G24). Lane 8, Variant 5 (G25). Lane 9, Variant 6 (G27). In table, all percentages are expressed relative to total phosphorimager densitometry plot area for each gel lane including background (densitometry plots are shown in figure 5.4.b.).*

It should firstly be noted that direct visual comparison of cleavage bands between different variant targets is not entirely accurate. This is because the efficiency of the labelling reaction can be different for each oligonucleotide. Thus, the gel scan is generally a visual aid to explain trends and the table gives a more accurate reflection of the amount of each cleavage product produced. If we first concentrate on the area in each oligonucleotide where the target base is we can note the following points. Removing the target G (variant 1, lane 3) results in no base damage in the region of the photosensitiser. If the target guanine base is moved from G21 to G22, the reaction still occurs but is less efficient with a 62% decrease in the specific cleavage yield. Further movement of the target base to positions 23 and 24 (variants 3 and 4) decreases the percentage damage even further almost to a background level. However, when the guanine base is located in positions 25 and 27 (variants 5 and 6), the percentage damage at these bases increases to 5% and 4.2% respectively relative to the other variants.

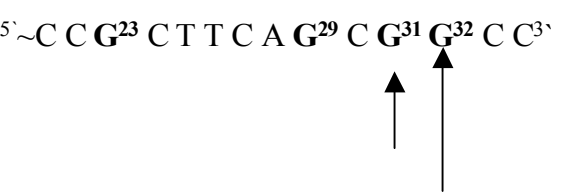
The more obvious results from the variant experiments are the damaged bases at the extreme 3' end of the targets. In the variant strands, some or all of the bases G29, G31 and G31 are damaged to a much greater extent than the movable guanine base. This result can be seen more effectively in the densitometry plots for all the variant strands.



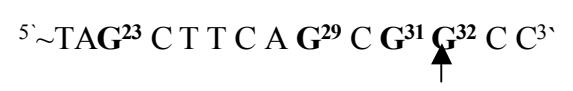
G29



34-mer.



G22



34-mer.



34-mer.



34-mer.

*Figure 5.4.b. Densitometer plots of variants 1 to 6. In the base sequences, the arrows show the site and approximate extent of cleavage in each variant.*

Firstly, It should be noted that there is not always clear resolution of the bands for G29, G31 and G32 and this makes it difficult to get accurate percentage values for the amounts of cleavage at each base, but the fact that the bases are damaged is clear. It is also notable that not all of the 3' guanine bases are equally damaged in each variant. The large amount of cleavage at G31, G32 in variant 3 is greatly reduced in non-hairpinning variant 3. This oligonucleotide was designed to investigate the reasons for the unusual cleavage pattern in the variant targets. The cause of this damage will be discussed later and is thought to be due to secondary structures within the variant strands, which by nature of short double stranded sequences or hairpins locates these 3' bases in close proximity to the photosensitiser.

#### **5.4.1. Discussion of photocleavage of variant target strands with ruthenium-ODN.**

With reference to figure 5.4.a., the results for the ruthenium-ODN showed that moving the target G from position 21 to 22 reduces the cleavage at the guanine from 7.3% to 2.8% respectively. Further movement of the target guanine to positions 23 and 24 decreases the cleavage even further to 1.2% and 1.7% respectively (almost to background levels of



Clearly, either of these hairpin structures, if stable would position G31, G32 close to the photosensitiser and explain the amount of cleavage seen. To investigate this further, non-hairpinning variant 3 was designed. The following structure shows that in comparison to variant 3, the possibility to form a stable hairpin is removed.

**Variant 3.**

5' TG ACC AT CA ATA AG GA AG AA CCG<sup>23</sup>CTTCAGCGGCC 3'

**non-hairpinning variant 3.**

5' TG ACC AT CA ATA AG GA AG AA TAG<sup>23</sup>TTTCAGCGGCC 3'

The underlined bases in non-hairpinning variant 3 cannot form a hairpin and the densitometer plot in figure 5.4.b. reveals that the cleavage at the 3'-end guanines is considerably reduced. If we look at each of the other target strands the following figure shows the possible bases that could be involved in hairpin formation.

**Target 1.**

5' TG ACC AT CA ATA AG GA AG AA G<sup>21</sup>CCCTTCAGCGGCC 3'

**Variant 1.**

5' TG ACC AT CA ATA AG GA AG AA TCCCTTCAGCGGCC 3'

**Variant 2.**

5' TG ACC AT CA ATA AG GA AG AA C<sup>22</sup>CCCTTCAGCGGCC 3'

**Variant 4.**

5' TG ACC AT CA ATA AG GA AG AA CCG<sup>24</sup>TTTCAGCGGCC 3'

**Variant 5.**

5' TG ACC AT CA ATA AG GA AG AA CCCTG<sup>25</sup>TCAGCGGCC 3'

**Variant 6.**

5' TG ACC AT CA ATA AG GA AG AA CCCTTTG<sup>27</sup>AGCGGCC 3'

*Figure 5.4.d. Regions of the target oligodeoxynucleotides that could form hairpins.*

This figure shows that all the variants could form at least two base hairpins and although not necessarily of equal stability their formation explains to some extent the 3'- guanine damage in the gel experiments. It is possible to calculate the free energy of formation

( $\Delta G_F$ ) of the possible hairpins within the variant strands. Perhaps the trend in  $\Delta G_F$  will correlate somewhat with the cleavage seen in the densitometry plots in Fig. 5.4.b. and aid explanation of the cleavage observed. This free energy of hairpin formation will have contributions from the energy released as a result of hydrogen bond formation and base stacking and the energy required to maintain non-bonded bases close together in the loop region. Using  $\Delta G_F$  values for G-C, A-T base pairs and different loop sizes from the literature<sup>9</sup>, the following values of  $\Delta G_F$  were calculated for the target strands examined.

Target	Loop size (bases)	$\Delta G_F$ (Kcal/mol)
34-mer	7	-1.9
Variant 1	7	+1.5
Variant 2	6	-1.9
Variant 3	2	-2.6
Variant 3	4	-0.9
Variant 4	5	-0.5
Variant 5	8 or 9	+1.5
Variant 6	8 or 9	+1.5

*Figure 5.4.e. Free energies of formation of possible hairpins within target 34-mer oligodeoxynucleotides.*

Comparing the values above with the densitometry plots in figure 5.4.b. it can be seen that variants 2 and 3 form the most stable hairpins and also give the most extensive 3`G damage. However, the values above show that formation of hairpins in variants 1, 5 and 6 is not energetically favourable and this conflicts with the densitometry plots, which show considerable 3`G damage for these variants. This suggests that some of the damage in variants 1, 5, and 6 is due to the floppy nature of the single stranded region, which locates

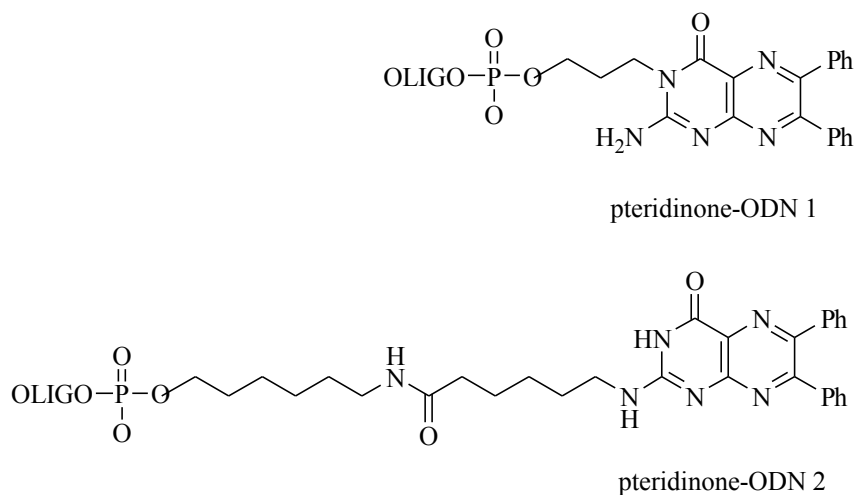


the 3`G bases close in space to the sensitiser. But the densitometry plots for variant 3 and non-hairpinning variant 3 show that hairpin formation does contribute to some of the cleavage observed. It is notable that target 1 has the ability to form a 3 base hairpin and yet no significant 3`-guanine damage is seen with this target. This could be explained by saying that the sensitiser is located in such close proximity to G21 in this target that the photochemical reaction occurs preferentially at this base rather than at the 3`-guanines or perhaps the damaged G21 prevents hairpin formation.

#### **5.5. Results with pteridinone-ODN conjugates.**

The two pteridinone-ODN conjugates synthesised in this research differ in a number of ways:

1. The site on the pteridinone used to attach the oligonucleotide.
  2. The different coupling chemistries employed.
  3. The size of the linking group between the chromophore and the oligonucleotide strand.
- These differences should allow for useful comparisons between the two conjugates and in particular should give information on how the efficiency of photoinduced cleavage depends on the length of the linker group. Pteridinone-ODN 1 has a 3 carbon linker chain to the 5`-phosphate, while pteridinone-ODN 2 has an 11 carbon chain plus an amide bond linking to the 5`phosphate of the 17-mer as shown below.



Initial time course experiments were carried out using a 10-fold excess of the pteridinone-ODN 1 relative to the target 34-mer as represented by the following gel scan.

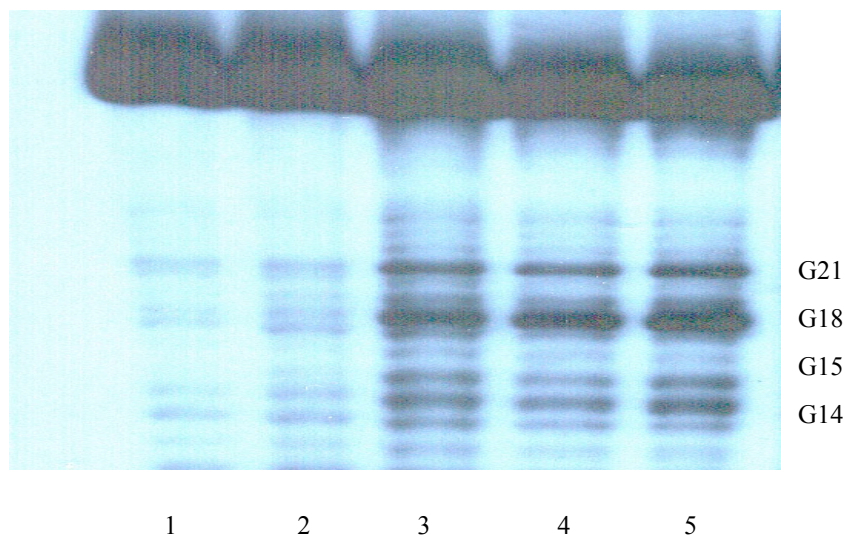


*Figure 5.5.a. Scan of gel of time course experiment with pteridinone-ODN 1 and target 34-mer 1. All lanes are piperidine treated unless stated. Lane 1. 0 mins irradi., Lane 2. 15 mins irradi. no piperidine, Lane 3. 15 mins irradi., Lane 4. 30 mins irradi., Lane 5. 60 mins irradi.*

The first results of note in the above gel scan are that no cleavage occurs without irradiation (lane 1) and also that with irradiation, piperidine treatment is required to reveal any cleavage that occurs (lane 2). Lanes 3, 4 and 5 show that in contrast to the ruthenium ODN, the pteridinone ODN 1 results in cleavage bands that occur at G21 and at guanines in the double stranded region of the duplex particularly G18 and to a lesser extent G14 and G15. The following densitometry plot represents lane 5 from fig. 5.5.a.

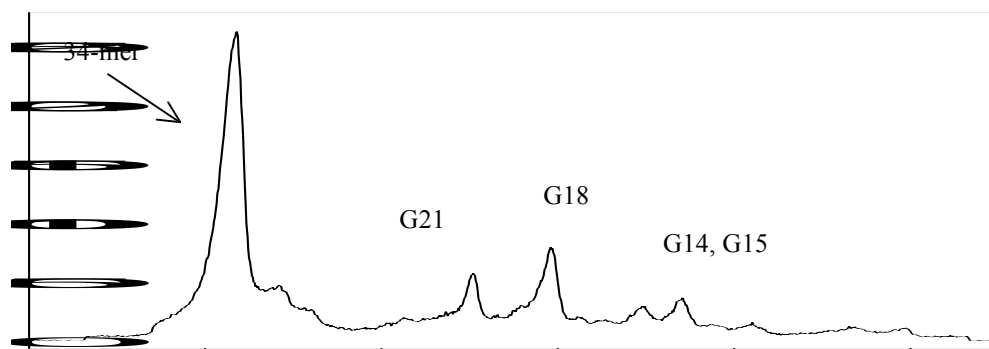


Figure 5.5.b. Densitometry plot of phosphorimage of 30 mins. experiment with 10:1 pteridinone-ODN 1 : target 34-mer 1.

The 2 dimensional plot more clearly shows the spread of the cleavage products and also reveals that a small amount of damage occurs at the G14, G15 doublet. The following table shows the percentages of products formed from the time course experiment.

Irradiation time. Mins.	% (of total plot area)				
	34-mer.	G21	G18	G15	G14
0	75 = 100				
15	80	4	5.3	3.2	3.1
30	81.3	4.4	8.1	3.1	4
60	70.3	5.2	10	3.9	4.5

Figure 5.5.c. Table of percentages of cleavage products produced from 10:1 ratio of pteridinone-ODN 1 to target 34-mer 1. All percentages are expressed relative % 34-mer area at 0 mins. irradiation.

The table confirms that the target G21 is indeed damaged by the pteridinone-ODN 1, but that guanine bases in the double stranded region contribute considerably to the overall percentage of cleaved products. At longer irradiation times the damage increases at G18 more than at G21. Also, within the G14, G15 doublet it is the 5' G that is damaged more. An experiment was then carried out using equivalent amounts of the pteridinone-ODN and target 1. The following gel scan represents a time course experiment using a 1:1 ratio of pteridinone-ODN 1 and 34-mer target 1.

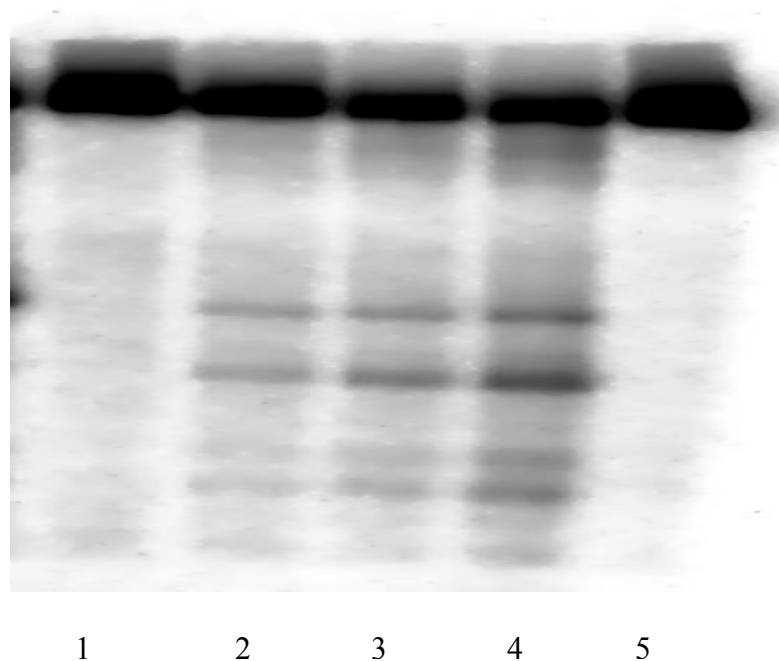


*Figure 5.5.d. Phosphorimage of time course experiment with 1:1 ratio of pteridinone-ODN 1 and target 34-mer 1. All lanes are piperidine treated unless stated. Lane 1. 0 mins irradi., Lane 2. 15 mins irradi., Lane 3. 30 mins irradi., Lane 4. 60 mins irradi., Lane 5 15 mins irradi. no piperidine.*

The above gel scan shows that pteridinone-ODN 1 is capable of photoinducing guanine specific cleavage at the reduced sensitiser : target ratio, which increases with increasing irradiation. Lane 4 reveals that a small amount of damage occurs at the guanine bases close to the 3'-end of the target oligonucleotide. The following table represents the percentages of cleavage products obtained from the above gel experiments

<b>Irradiation time. Mins.</b>	<b>% (of total plot area) 34-mer.</b>	<b>G21</b>	<b>G18</b>	<b>G15</b>	<b>G14</b>	<b>3`G</b>
0	72.4 = 100					
15	79.9	5.9	6.2			
30	62.4	7.3	8.5			
60	51.4	7.9	14.6	5.2	5.9	11.2

*Figure 5.5.e. Table of percentages of cleavage products produced from 1:1 ratio of pteridinone-ODN 1 to target 34-mer 1.*

The most notable result from this table is that going from 30 to 60 minutes irradiation increases the damage at the double stranded guanines much more than at G21. There is also significant damage at the 3' guanines at longer irradiation times.

When time course experiments were carried out using pteridinone-ODN 2, the results showed that this conjugate was not efficient at photoinducing damage to the target oligonucleotide. The conjugate with the longer linker group between the sensitiser and the oligonucleotide produced very little cleavage at the target guanine base. The following gel scan shows the damage produced after 3 hours irradiation of the system with a 10 fold excess of the sensitiser conjugate.



*Figure 5.5.f. Scan of gel of time course experiment with 10:1 ratio of pteridinone-ODN 2 and target 34-mer 1. All lanes are piperidine treated unless stated. Lane 1. 180 mins irradi., Lane 2. 0 mins irradi..*

The main bases damaged using pteridinone-ODN 2 were the 3'-guanines and G21. Interestingly, of the bases in the double stranded region G14 is the most damaged. This is what would be expected if electron transfer was occurring through the double strand with the 5' G of the GG doublet being most affected. However, a number of experiments with this conjugate showed it to be very inefficient at photoinducing damage to the target strands. This seemingly negative result could be important as it could give useful information about how the size of the linker group between the sensitiser and the ODN strand affects the photoactivity of the ODN conjugate.

### 5.5.1. Discussion of photocleavage results with pteridinone-ODN conjugates.

Concerning the time course photodamage of target 1 by pteridinone-ODN's 1 and 2, the obvious points for discussion are:

1. The comparison of the guanine cleavage pattern between the two pteridinone-ODN's and the ruthenium-ODN.
2. The efficiency of guanine cleavage between all three conjugates.

In contrast to the G21 specific cleavage obtained by the ruthenium-ODN, the pteridinone-ODN1 while damaging G21 causes greater damage at the guanine bases in the double stranded region of the model duplex as shown below.



The different cleavage patterns can be explained by the operation of different photo-mechanisms for the pteridinone and the ruthenium complex. The results presented in chapter 4 showed that the free pteridinone photooxidises 2'-deoxyguanosine by a combination of type I and type II mechanisms, but in contrast to Ru(phen)<sub>3</sub>Cl<sub>2</sub>, the pteridinone has a much greater contribution from a type I mechanism. This fact can be used to rationalise the cleavage pattern observed. One reason to favour a type I mechanism over a type II mechanism to explain the cleavage pattern is that <sup>1</sup>O<sub>2</sub> would not be expected to be able to react with the guanine bases in the protected environment of the double helix and thus a more likely explanation makes use of the following points. It is known that electron transfer from guanine in nucleosides or DNA to a photoexcited molecule can generate a guanine radical cation (section 1.6.3.). Also, it has been shown that guanine radical cations generated in double stranded DNA can migrate through the double helix to other nearby guanine sites by a hole jumping mechanism (section 1.6.1.). Using these two points it can be proposed that with pteridinone-ODN1 there is an electron transfer reaction from G21 to the photoexcited pteridinone generating a radical cation. This cation then migrates to G18 and to a lesser extent to G14 and G15. These cations then undergo further reaction to form piperidine sensitive lesions, which are revealed by electrophoresis. This might explain the cleavage pattern observed for pteridinone-ODN 1 if we assume that the pteridinone is in close enough proximity to G21 to allow an efficient electron transfer

process to occur. It also assumes that a radical cation generated at G21 in the single stranded region of the target can migrate to G18. This might be difficult as it is thought that it is the nature of the double helix itself, with the bases stacked on each other that allow the hole migration to occur.

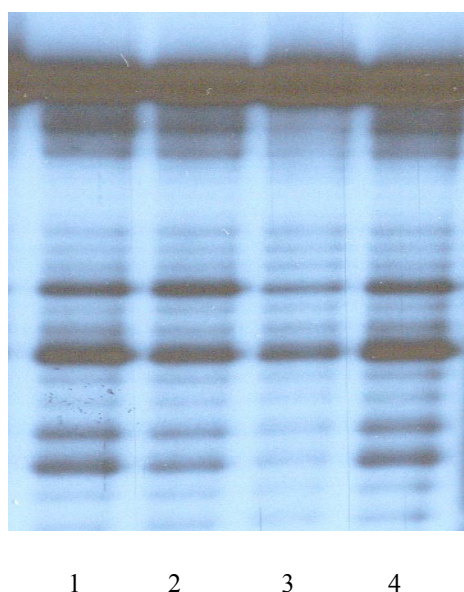
An alternative would be if the pteridinone were situated closer to G18 possibly by the linker group bending back and allowing the pteridinone to partially intercalate. Then, the guanine radical cation produced at G18 could migrate to G14, G15 and possibly in the other direction to G21. This second scenario might explain why G18 is the most damaged base and why its damage increases more rapidly with increasing irradiation than the damage at G21 (see table 5.5.c).

The photocleavage results obtained for pteridinone-ODN 2 showed that this conjugate was much less efficient than the other pteridinone conjugate. In time course experiments, three hours irradiation were required to achieve any observable cleavage. This result while seeming negative can be thought of in a positive light. The inefficiency of this conjugate can be explained in terms of the length of its linker group. It has an 11-carbon chain between the sensitiser and the oligodeoxynucleotide chain whereas pteridinone-ODN 1 has a 3-carbon linker group. It is possible that with the longer linker group the sensitiser is not positioned near the target base but could be imagined to be “flopping” about in space or intercalating. Therefore, any  $^1\text{O}_2$  might be quenched before it could migrate to any target sites or not be produced at all. Also, the sensitiser might not be close enough to the target guanine to allow an efficient electron transfer reaction to occur. We can conclude from this that a 3 carbon chain positions the sensitiser close enough to the target strand to allow reaction to occur and that an 11 carbon chain is too long a linker group to use. It could be imagined that the length of the linker group is crucial in optimising specific photocleavage. Other workers<sup>115</sup> have found dramatic dependence of cleavage efficiency on the length and type of linker group and perhaps a series of conjugates with linker groups of different lengths could be synthesised in the future to more fully investigate these effects.

## 5.6. Effects of additives on photocleavage by pteridinone-ODN 1.

The results from chapter 4 revealed that pteridinone (105) (as a model for pteridinones ) photooxidises 2'-deoxyguanosine by both type I and type II mechanisms. In contrast to Ru(phen)<sub>3</sub>Cl<sub>2</sub>, which operates mainly by a type II mechanism, the pteridinone was shown to have a much greater contribution from a type I mechanism. The effects of additives with the pteridinone-ODN 1 were investigated to see if results consistent with the HPLC assay could be obtained. This would provide supporting evidence for the use of the HPLC assay to predict the photochemical behaviour of ODN conjugates. The following gel scan and table represent the results of 30 minute irradiations using a 10:1 sensitiser : target ratio in the presence of H<sub>2</sub>O, D<sub>2</sub>O, NaN<sub>3</sub> and argon.





Lane	Experiment.	% (of total plot area)					
		34-mer.	G21	G18	G15	G14	Other 3' G
1	H <sub>2</sub> O	51.7	5.4	8.5	2.9	4	9
2	D <sub>2</sub> O	62.2	5.1	5.4	2.0	2.4	6.5
3	NaN <sub>3</sub>	74.4	2.4	3.7			
4	Argon	57.5	4.4	8.4	2.6	3.2	5.9

*Figure 5.6.a. Experiment for irradiation of 34-mer and pteridinone-ODN 1 in the presence of additives. All lanes are piperidine treated and represent 30 minute irradiations. Lane 1. H<sub>2</sub>O, Lane 2. D<sub>2</sub>O, Lane 3., NaN<sub>3</sub>, Lane 4., Argon. Table of percentages of cleavage products. All percentages are expressed relative to total plot area including background.*

The gel scan and the percentage values in the table show that D<sub>2</sub>O does not have an enhancing effect on the levels of cleavage products at G21 and seems to have an inhibitory effect on the levels of guanine damage at double stranded guanines. It is clear from the table that NaN<sub>3</sub> and to a lesser extent argon have an inhibitory effect on the amount of cleavage produced.

### **5.6.1. Discussion of the effects of additives using pteridinone-ODN 1.**

The discussion of the photocleavage results with pteridinone-ODN 1 can be rationalised in terms of a predominating type I mechanism as discussed in section 5.6.1. Do the effects of additives on the photocleavage reinforce this rationalisation ?. Figure 5.6.a shows the gel and densitometry results for the effects of additives with pteridinone-ODN 1. Comparisons between the H<sub>2</sub>O experiment and the other experiments show that:

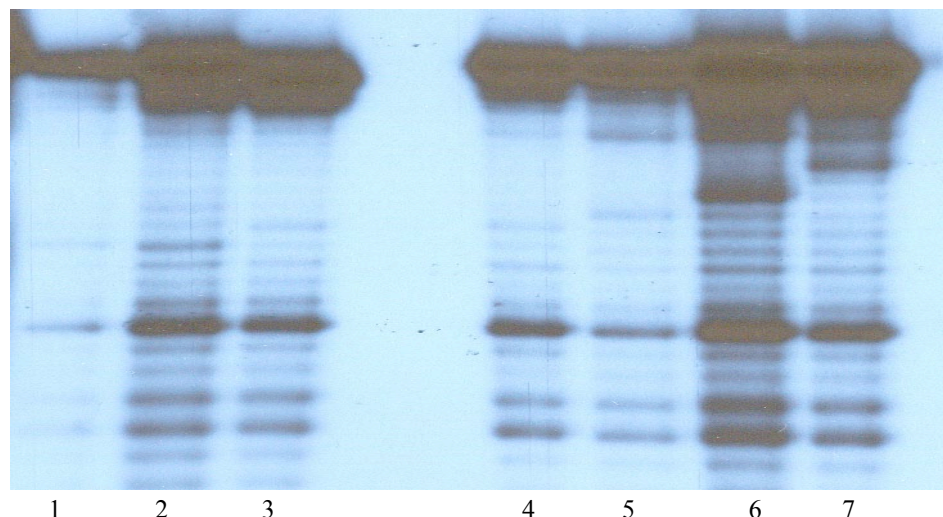
1. There is no enhancement in cleavage efficiency at all damaged guanines when the experiment is carried out in D<sub>2</sub>O. This supports the operation of a type I mechanism. In fact there is a slight decrease in the amount of cleavage and although this effect has been reported elsewhere<sup>125</sup> no explanation was given. This is an unusual result, as D<sub>2</sub>O should have no inhibitory effect on an electron transfer reaction.
2. There is a slight decrease in cleavage efficiency (19% for G21) when the experiment is carried out under a blanket of argon. This decrease is not as dramatic as was observed for the ruthenium-ODN (39% at G21). This could indicate the greater involvement of molecular oxygen in a type II mechanism than in a type I mechanism, although it could also indicate the difficulty in completely removing molecular oxygen by using a blanket of argon.
3. There is decreased cleavage for pteridinone-ODN 1 in the presence of NaN<sub>3</sub>, which in theory is not expected for a type I mechanism, but as was mentioned previously, the HPLC assay seemed to show inhibition of both type I and type II products in NaN<sub>3</sub> so this effect is difficult to qualify.

In summary, it seems that the use of additives to investigate the mechanisms of action of the sensitiser conjugates is contradictory but if taken on face value the results using D<sub>2</sub>O for both conjugates confirm the proposal that a type II mechanism predominates for the ruthenium-ODN and a type I mechanism predominates for pteridinone-ODN 1.

The best way to determine the relative contribution of the two possible photomechanisms would be by mass spec analysis of the G damage bands in the gel experiments prior to piperidine treatment to see what the modification is at guanine. Imidazolone or oxazolone would indicate a type I mechanism and 4-hydroxy-8-oxoguanine or oxaluric acid would indicate a type II mechanism.

## **5.7. Results for variant target strands using pteridinone-ODN 1.**

As was mentioned in section 5.3, the variant strands were designed to try and give more information about the effectiveness of design of the oligodeoxynucleotide conjugates and their mechanism of photodynamic action. The following figure represents a gel scan for an experiment with pteridinone-ODN 1 and the variant target strands. Also presented is a table of the percentage cleavage products produced at the various guanine sites.



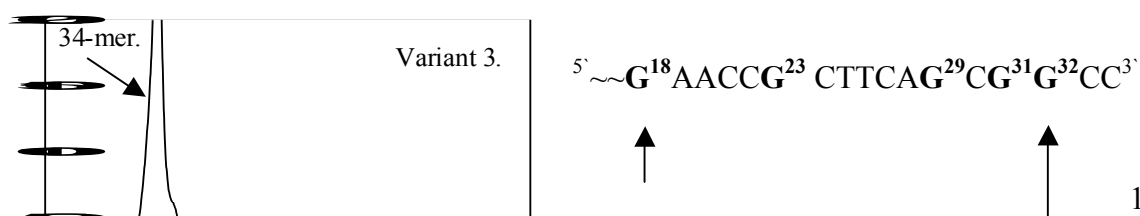
Lane	34-mer	% (of total plot area) 34-mer.	Movable G	G18	G15	G14	3'G
Not shown	Target 1	51.7	5.4	8.5	2.9	4	5.4
1	Variant 1	63.3	-	4.9	2.3	2.4	4.9
2	Variant 2	65.1	1	5.2	1.9	1.9	6.5
3	Variant 3	64.6	0.7	4.5	1.7	2.1	9.5
4	Non-hairpinning variant 3	68.8	0.9	6	1.8	2.6	4.9
5	Variant 4	69.6	1	3.2	1.9	2.1	6.6
6	Variant 5	65.9	1.9	4.2	2.2	2.3	6.2
7	Variant 6	67.4	1.7	3.5	1.5	1.5	7.4

*Figure 5.7.a. Gel scan of variant strand experiment with pteridinone-ODN 1. All experiments were irradiated for 30 mins. and piperidine treated unless stated. Lane 1, Variant 1 (No G). Lane 2, Variant 2 (G22). Lane 3, Variant 3 (G23). Lane 4, Non-hairpinning variant 3. Lane 5, Variant 4 (G24). Lane 6, Variant 5 (G25). Lane 7, Variant 6 (G27). In table, all percentages are expressed relative to total densitometry plot area including background.*

Firstly, the difference in the radiolabelling efficiency of variants can be seen by comparing the band intensities for variants 1 and 2. This difference takes away from the visual effect of the gel scan but does not affect the percentages obtained from the phosphorimaged gel.

Looking at the region of the gel lanes where the target G21 is shifted to the 3' end it can be seen that the amount of cleavage decreases as the G is moved away from the site of the photosensitiser. The column for movable G's in the table more clearly shows that as the G is moved the percentage cleavage decreases from 5.4% in the 34-mer to approximately 1% in variants 2-4. There is a slight relative increase in the percentage cleavage when the guanine is in positions 25 and 27 in variants 5 and 6 respectively. This trend was also observed for the ruthenium-ODN. The gel and table more clearly show that damage at the guanines in the double stranded region is not as greatly affected by the movement of G21. This gives information about the location of the pteridinone molecule in the hybridised duplex and some details about a possible mechanism for the photodamage. As was the case with the ruthenium-ODN, the variant target strands are damaged at some or all of the 3' end guanines in positions 29, 31 and 32. This effect is less pronounced for pteridinone-ODN 1 and reflects its general lower reactivity than the ruthenium-ODN.

As an example of this 3'-guanine damage, the following figure represents densitometry plots of variant 3 and non-hairpinning variant 3.



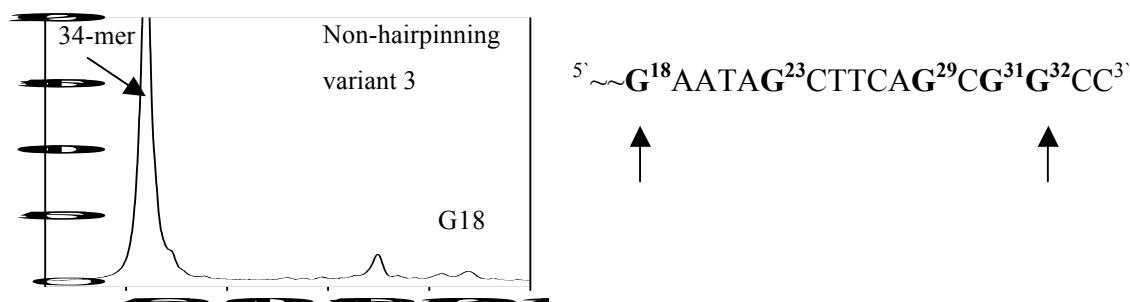


*Figure 5.7.b. Densitometer plots for variant 3 and non-hairpinning variant 3. The base sequences and arrows show the sites and approximate extent of cleavage*

From the above plots it can be seen that the resolution of the bands for cleavage at the 3'-end guanines is poor relative to that for the ruthenium-ODN shown in figure 5.3.b. It is possible to see that the level of cleavage is reduced in non-hairpinning variant 3 relative to variant 3 and thus the reasons for the 3'-end cleavage are likely to be the same as for the ruthenium-ODN.

### **5.7.1. Discussion of photocleavage results of variant target strands with Pteridinone-ODN 1.**

By firstly looking at the damage that occurs at the 3'-guanines in the variant targets in figure 5.6.a, and the densitometry plots in 5.6.b., it seems that similar trends are seen for pteridinone-ODN 1 as were seen with the ruthenium-ODN. A general comparison of the amount of damage that occur in the variants with each conjugate reveals that less damage occurs with the pteridinone-ODN. This could be due to the fact that with the pteridinone a type I electron transfer reaction would require closer contact between the sensitiser and the substrate and that the hairpins, if formed would locate the 3'-guanines close to the pteridinone but not close enough to get a very efficient electron transfer process.

If we concentrate on the region of G21 and its shifted position in the variant strands we can see that the trend with pteridinone-ODN 1 is the same as with the ruthenium-ODN, i.e.

moving the G further away from the location of the sensitiser decreases the percentage cleavage at this “movable” guanine. The exception is also seen with variants 5 and 6. With pteridinone-ODN 1 the decrease in cleavage when the guanine is in position 22 relative to position 21 is more dramatic than for the ruthenium-ODN. This suggests the reaction dies off more quickly with the pteridinone, a fact that is consistent with a type I reaction.

The most important result from the variant strand experiments with pteridinone-ODN 1 is that damage at the guanines 14, 15 and 18 is maintained in all the variant strands even though it is decreased slightly relative to target 1. This gives more information about the location of the sensitiser. The result supports the proposal that the guanine is closer to G18 than G21. If electron transfer occurred from G21 and subsequent radical cation migration occurred to the double stranded guanines from this site, then the double stranded damage would decrease as the target G is moved to the 3'-end. As this is not the case, the result suggests that the pteridinone is closer to G18 and that the extent of cleavage in the double stranded region is not really dependent on the location of the other guanines.

## **5.8. Conclusions and future work.**

The research presented in this thesis has shown that it is possible to synthesise, purify and characterise ODN conjugates with site specific incorporation of pteridinone and ruthenium polypyridyl complex derivatives. Comparisons between phosphoramidite and succinimide ester methodologies have shown that phosphoramidites are more difficult to synthesise and purify than succinimide esters but can lead to higher coupling yields and easier purification.

The HPLC assay showed that  $\text{Ru}(\text{phen})_3\text{Cl}_2$  photooxidises 2'-deoxyguanosine by a combination of type I and type II mechanisms with the type II mechanism predominating. The pteridinone (105) also operates by both mechanisms but seems to favour predominance by a type I mechanism. Both sensitisers were shown to photoinduce piperidine sensitive lesions specifically to guanines in the target 34-mer. The results also showed a slight preference for the 5'G of a GG doublet within the target suggesting the important role of secondary structures in natural DNA sequences.

The main conclusions from this research are concerning the ability of the ODN conjugates to damage specific guanines in the complementary 34-mer target. The Ru-

ODN was shown capable of inducing 42% target damage at G21 upon irradiation for 60 minutes. The use of additives showed evidence for the involvement of  $^1\text{O}_2$  in the photodamage mechanism but the effects of  $\text{D}_2\text{O}$  were not as dramatic as with the free sensitiser and 2'-deoxyguanosine. This suggests a significant difference between the reaction environments of the conjugate and the free sensitiser with regard to the access the sensitiser has to molecular oxygen within the conjugate : target hybrid. The pteridinone-ODN 1 was shown to produce specific damage to the target at G21 but also at guanines in the double stranded region. This was rationalised in terms of a type I mechanism where an intermediate mobile reactive species was generated in the double strand. The difference in reactivity between the two conjugates was judged to be due to the differing extents with which type I and type II mechanisms operate in each case. Pteridinone-ODN 2 was shown to be inefficient at damaging the target 34-mer and this was thought to be due to it having too long a linker group between the sensitiser and the 17-mer. Variant strand results indicated that the damage with both conjugates occurred over a short range with damage decreasing to background levels when the target G21 was moved to position 23. Some variants produced a significant amount of damage at guanines distant from the location of the sensitiser and this was shown to be due to the formation of stable hairpins within some of the variant targets.

There are a number of directions which future research in this area could take. The HPLC assay could be further used as a screening process for potential photosensitiser molecules and could help divide them into type I and type II sensitisers. This would allow for more effective comparison between photoactive ODN conjugates. This research has shown the importance of linker length on the efficiency of damage. Perhaps molecular modeling studies would help optimise the design of future ODN conjugates by deciding what size linker would place the sensitiser in closest proximity to the target base.

The characterisation of the ODN conjugates by mass spectrometry showed the power of this tool and it could have a big influence in more biological applications in the future. For example, it might be possible to use mass spectrometry instead of electrophoresis to assay the amounts and extent of damage to an oligonucleotide using a photoactive ODN conjugate. This would replace the need for radioactive labelling and could make the assay procedure more efficient.

The introduction to this thesis showed the difficulties involved in achieving actual antisense effects in cells. Experiments in this area with the ODN conjugates already synthesised could now be carried out to see firstly, if the conjugates could effectively enter

cells and specifically hybridise to the target region within a bcr/abl mRNA. Also, experiments need to be developed to see if photolysis of cells with the conjugates present could produce an antisense effect greater than normal oligonucleotides. Important considerations in this area include knowledge if the modifications induced would inhibit translation or be repaired by cellular enzymes.

Obviously, there is a lot of research that needs to be carried out before photoactive ODN conjugates can be considered as potential therapeutic agents in CML and other diseases. This research has highlighted approaches that can be used to tackle some of the problems faced when targeting cancer causing genes. The topics covered in this thesis have shown how necessary it is for chemists to study biological approaches and perhaps for biologists to do likewise, in order for future collaborative research to be as effective as possible.

## **6.0. MATERIALS AND METHODS.**

### **6.1. Apparatus and Instruments.**

Savant speed vac concentrator (Stratech Scientific, London).

Electrophoresis sequencing system (Life technology inc. USA.).

Combs and spacers (Gibco BRL apparatus Life technology inc. USA).

Power supply unit, Chandos E36, Joe Walsh scientific, Dublin.



Bench centrifuge, MSE micro-centaur.

Heating block, Lab line Instruments inc.

X-ray films, (Curix 100NIF, 35 x 43cm) Agfa Ltd.

Developer, Fuji photofilm Co. Ltd.

Fujifilm FLA-3000 phosphorimager

#### Light sources.

A. PTI 150W xenon lamp.

B. 500W mercury lamp

C. 100W fibreoptic lamp.

Electroelution apparatus, Biotrap, Schleicher & Schuell.

#### DNA Synthesisers.

A. Applied Biosystems 391 DNA synthesiser.

B. Beckman Oligo 1000m DNA synthesiser.

#### HPLC

Perkin Elmer series 2000LC pump.

Perkin Elmer 235C diode array detector.

Perkin Elmer Turbochrom 4.1 software.

Hypersil APS 5 $\mu$ m 150 x 4.6mm column, Supelco inc., Sigma Aldrich.

Supelcosil LC-NH<sub>2</sub> 5 $\mu$ m 250 x 4.6mm column, Supelco inc., Sigma Aldrich.

#### Spectroscopic measurements.

Nmr Spectrometers, Bruker 300 MHz. and Bruker 400 MHz. Instruments.

UV spectrometers, Shimadzu UV-2401 and Unicam UV-4 spectrometers.

IR spectrometers, Genesis II FTIR and Perkin Elmer paragon 1000 spectrometers.

#### Mass spectrometry.

Micromass LCT electrospray TOF spectrometer.

Shimadzu LC-10AD solvent delivery module.

Micromass, Mass Lynx software.

## **6.2. Syntheses.**

### *2,4-Diamino-6-pyrimidinethiol (126)*

Sodium hydrosulfide hydrate (80g, 0.727mols) was added to ethylene glycol (130 cm<sup>3</sup>) and heated to 60°C. 2,4-Diamino-6-chloropyrimidine (30g, 0.209 mols) was added and the

mixture was heated to reflux at 120°C for 3 hours. The solution was cooled to 60°C and H<sub>2</sub>O (400 cm<sup>3</sup>) was added. The solution was then acidified to pH 1 with conc. H<sub>2</sub>SO<sub>4</sub> and the sulphate salt isolated by filtration. To remove colloidal sulphur the salt was suspended in H<sub>2</sub>O (400 cm<sup>3</sup>) and heated to 60°C whereupon conc. NH<sub>3</sub> was added until the pH was 10. Following addition of activated charcoal and filtration through celite the sulphur was removed. The filtrate was acidified to pH 1 with conc. H<sub>2</sub>SO<sub>4</sub> and 17.25 g (58%) of 2,4-diamino-6-pyrimidinethiol was isolated by filtration as a yellow solid.

*2,4-Diamino-6-methylthiopyrimidine (127).*

The sulphate salt of 2,6-diamino-4-pyrimidinethiol (9.0 g, 37.5 mmol) was dissolved in distilled water (90 cm<sup>3</sup>) containing KOH (5.35 g, 0.095 mols). Iodomethane (9.79 g, 0.069 mols) was added dropwise over 15 mins and the reaction was stirred for 2 hours at room temperature. TLC (CH<sub>2</sub>Cl<sub>2</sub> : CH<sub>3</sub>OH, 9:1 ) showed that the reaction was complete. 8.3g (84%) of 2,4-diamino-6-methylthiopyrimidine was isolated by filtration as a white solid.

NMR  $\delta_{\text{H}}$  (400.13 MHz; d6-DMSO; Me<sub>4</sub>Si) 2.33 (3H, s, CH<sub>3</sub> ), 5.59 (1H, s, CH ), 5.88 (2H,s, NH<sub>2</sub> ), 6.15 ( 2H, s, NH<sub>2</sub>).

$\delta_{\text{C}}$  (100.6 MHz; d6-DMSO; Me<sub>4</sub>Si) 11.75 (CH<sub>3</sub>), 89.26 (CH), 162.37, 163.72, 167.33 quaternary carbons.

*2,4-Diamino-6-methylthio-5-nitrosopyrimidine (128).*

2,4-Diamino-6-methylthiopyrimidine (9.0 g, 0.057 mols) was added to H<sub>2</sub>O (79 cm<sup>3</sup>) and glacial acetic acid (18 cm<sup>3</sup>). Sodium nitrite (5.89 g, 0.085 mols) dissolved in H<sub>2</sub>O (13 cm<sup>3</sup>) was added dropwise to the flask over 10 mins. The brown suspension turned purple immediately and was stirred overnight at room temperature. The product was filtered off and washed with water, ethanol and dried to give 10.23g (95%) of 2,4-diamino-6-methylthio-5-nitrosopyrimidine as a purple solid .

*5-Amino-7-(methylthio)furazano[3,4-d]pyrimidine (129).*

2,4-Diamino-6-methylthio-5-nitrosopyrimidine (9.0 g, 0.048 mol) was suspended in glacial acetic acid (135 cm<sup>3</sup>). With the flask wrapped in tin foil, lead tetraacetate (22.65 g, 0.051 mols) was added in portions over a 60 min period against a flow of N<sub>2</sub> gas. The purple

suspension turned orange after this time period and was stirred for a further 2 hours at room temperature. 8.89 g (89%) of 5-amino-7-(methylthio) furazano[3,4-d]pyrimidine was isolated by filtration as an orange solid, washed with H<sub>2</sub>O and dried.

NMR  $\delta_{\text{H}}$  ( 400.13 MHz; d<sub>6</sub>-DMSO; Me<sub>4</sub>Si). 2.70 ( 3H, s, CH<sub>3</sub>), 7.92(1H, s, NH<sub>2</sub>).

$\delta_{\text{C}}$  (100.6 MHz; d<sub>6</sub>-DMSO; Me<sub>4</sub>Si) and DEPT spectrum. 11.7 ( SCH<sub>3</sub>), 138.3, 159.9, 160.7, 166.5 quaternary carbons.

*5-Amino-7-propoxyfurazano[3,4-d]pyrimidine (130).*

5-Amino-7-(methylthio)furazano[3,4-d]pyrimidine (2.0 g, 0.0109 mols) was suspended in 3-chloropropanol (30 cm<sup>3</sup>) and heated to 55°C in a flask with a drying tube and a dropping funnel attached. Bromine (2.0 g, 0.0125 mols) in 3-chloropropanol (8 cm<sup>3</sup>) was added dropwise to the flask. Each addition was made such that the bromine colour from the previous addition had disappeared. Additions were made until no decolourisation occurred. The reaction was then cooled to room temperature and poured with vigorous stirring onto ethyl acetate (600 cm<sup>3</sup>) containing sodium hydrogen carbonate (10 g). With a drying tube attached, the mixture was stirred for 10 mins. Saturated NaCl (aq) (40 cm<sup>3</sup>) was added with further stirring for 10 mins. The organic layer was extracted, washed with saturated NaCl, dried over MgSO<sub>4</sub> and evaporated *in vacuo* to give a yellow oil. Diethyl ether (20 cm<sup>3</sup>) was added and the solution placed in a freezer overnight. 1.18 g (48%) of 5-amino-7-propoxyfurazano[3,4-d]pyrimidine was isolated by filtration as a yellow solid, washed with cold diethyl ether and dried.

NMR  $\delta_{\text{H}}$  ( 400.13 MHz; d<sub>6</sub>-DMSO; Me<sub>4</sub>Si). 2.32 (2H, m, CH<sub>2</sub>CH<sub>2</sub>), 3.82 (2H, t, CH<sub>2</sub>Cl), 4.67 (2H, t, OCH<sub>2</sub>), 7.84 (2H, d, NH<sub>2</sub>).

$\delta_{\text{C}}$  (100.6 MHz; d<sub>6</sub>-DMSO; Me<sub>4</sub>Si) and DEPT spectrum. 30.74, 41.64, 65.3 (CH<sub>2</sub> carbons), 134.9, 160.2, 162.5 (aromatic carbons).

*2-Amino-3-(3-hydroxypropyl)-6,7-diphenyl-4(3H)-pteridinone (104).*

A suspension of 5-amino-7-propoxyfurazano[3,4-d]pyrimidine (200 mgs, 0.87 mmol) in deaerated water (18.5 cm<sup>3</sup>) containing 10% palladised carbon (50 mgs) was stirred vigorously during hydrogenolysis at atmospheric pressure until hydrogen uptake ceased. The catalyst was removed by vacuum filtration under an argon atmosphere. A solution of potassium hydroxide (123 mgs, 0.22 mol) and benzil (387 mgs, 1.92 mmol) in deaerated

ethanol (18.5 cm<sup>3</sup>) was added and the resulting suspension was stirred at 35-40 °C for 1.5 hours. The suspension was neutralised with dilute HCl and the solvent evaporated to give a yellow residue which was extracted with methanol. After removal of the methanol the solid obtained was chromatographed on a flash silica column and gave 216mgs (67%) of 2-amino-3-(3-hydroxypropyl)-6,7-diphenyl-4(3*H*)-pteridinone as a yellow solid by elution with chloroform : ethanol as solvents.

NMR  $\delta_H$  (400.13 MHz; d6-DMSO; Me<sub>4</sub>Si) 1.83 (2H, m, CH<sub>2</sub>CH<sub>2</sub>OH), 3.52 (2H, t, CH<sub>2</sub>OH), 4.09 (2H, t, NCH<sub>2</sub>), 4.71 (1H, s, OH), 7.57 (2H, s, NH<sub>2</sub>), 7.31-7.42 (10H, m, phenyl C-H).

$\delta_C$  (100.6 MHz; d6-DMSO; Me<sub>4</sub>Si) and DEPT spectrum. 30.16 (CH<sub>2</sub>CH<sub>2</sub>OH), 39.9 (NH<sub>2</sub>), 58.15 (CH<sub>2</sub>OH).

*2-(N,N-Dimethylaminomethyleneamino)-3-(3-hydroxypropyl)-6,7-diphenyl-4(3H)-pteridinone (134).*

2-Amino-3-(3-hydroxypropyl)-6,7-diphenyl-4(3*H*)-pteridinone (102 mgs, 0.278 mmol) was suspended in dry tetrahydrofuran (36 cm<sup>3</sup>) under an N<sub>2</sub> atmosphere. N,N-Dimethylformamidedimethylacetal (39  $\mu$ l, 0.295 mmol) was added *via* a syringe and the reaction was stirred overnight. TLC (CHCl<sub>3</sub> : EtOH; 15:2) showed no starting material remained. The solvent was evaporated to give a yellow oil which was purified by chromatography on a flash silica column using (CH<sub>2</sub>Cl<sub>2</sub> : EtOH ) 150 : 3 to 150 : 4. 73 mgs (62%) of 2-(N,N-dimethylaminomethyleneamino)-3-(3-hydroxy-propyl)-6,7-diphenyl-4(3*H*)-pteridinone was isolated as a yellow solid.

NMR  $\delta_H$  (400.13 MHz; d6-DMSO; Me<sub>4</sub>Si) 3.79 (1H, t, OH), 3.59 (2H, t, CH<sub>2</sub>OH), 4.55 (2H, t, NCH<sub>2</sub>), 2.07 (2H, m, CH<sub>2</sub>CH<sub>2</sub>OH), 3.22 (3H, s, NCH<sub>3</sub>), 3.27 (3H, s, NCH<sub>3</sub>), 7.26 – 7.57 (10H, m, phenyl C-H), 9.03 (1H, s, NCHN).

$\delta_C$  (100.6 MHz; d6-DMSO; Me<sub>4</sub>Si) and DEPT spectrum. 159.5(NCHN), 30.9, 39.9, 58.24 (3 x CH<sub>2</sub>), 35.6, 41.68 (2 x NCH<sub>3</sub>).

*(3-(2-N,N-Dimethylaminomethyleneamino-3,4-dihydro-4-oxo-6,7diphenyl-3-pteridinyl)-propoxy) (2-cyanoethoxy) (N,N-diisopropylamino)phosphoramidite (134).*

#### **Method A.**

2-(N,N-Dimethylaminomethyleneamino)-3-(3-hydroxypropyl)-6,7-diphenyl-4(3*H*)-pteridinone (30 mgs, 0.07 mmol) was dried by performing 3 coevaporations with dry dichloromethane (1 cm<sup>3</sup>). 1(*H*) tetrazole (2.5 mgs, 0.036 mmol) dissolved in dry acetonitrile (1 cm<sup>3</sup>) was added and the solvent was removed by vacuum pump. Dry dichloromethane (1 cm<sup>3</sup>) was added and the solution was stirred for 30 mins under an N<sub>2</sub> atmosphere. 2-Cyanoethyl N, N, N', N'-tetraisopropylphosphorodiamidite (46.7 μl; 0.14 mmol) was added by micropipette and the reaction was stirred in an icebath in the dark for 30 mins. TLC (alumina plates): CH<sub>2</sub>Cl<sub>2</sub> : DIPEA 25 : 1, showed no starting material remained. The solvent was removed by vacuum pump with the flask wrapped in tin foil. Ethyl acetate (5 cm<sup>3</sup>) and dichloromethane (5 cm<sup>3</sup>) were added. To the solution was added 5% (aq) NaHCO<sub>3</sub> (10 cm<sup>3</sup>). The organic layer was extracted and dried with Na<sub>2</sub>SO<sub>4</sub>. The solvent was then removed by a vacuum pump and the crude yellow solid was stored in the freezer in the dark.

NMR δ<sub>p</sub> (161.9 MHz, CDCl<sub>3</sub>) peaks at 15, 32, 124.1, 148.4 and 149.7.

δ<sub>H</sub> (400.13 MHz, CDCl<sub>3</sub>, Me<sub>4</sub>Si) 1.18 (12H, m, 2 x CH(CH<sub>3</sub>)<sub>2</sub>), 2.06 (2H, m, CH<sub>2</sub>CH<sub>2</sub>CH<sub>2</sub>), 2.75 (2H, t, CH<sub>2</sub>CN), 3.28 (3H, s, NCH<sub>3</sub>), 3.39 (3H, s, NCH<sub>3</sub>), 3.55 - 3.70 (4H, m, 2 x POCH<sub>2</sub>), 3.75 - 3.9 (2H, m, 2 x CH(CH<sub>3</sub>)<sub>2</sub>), 4.68 (2H, t, NCH<sub>2</sub>), 7.3 - 7.7 (10H, m, phenyl C-H), 8.93 (1H, s, NCHN).

#### **Method B.**

2-(N,N-Dimethylaminomethyleneamino)-3-(3-hydroxypropyl)-6,7-diphenyl-4(3*H*)-pteridinone (25 mgs, 0.058 mmol) was dissolved in dry dichloromethane (2 cm<sup>3</sup>) in a two necked flask with a septum and a gas tap attached under an N<sub>2</sub> atmosphere. Diisopropylethylamine (225 μl, 1.25 mmol) was added to the flask. 2-Cyanoethyl N,N-diisopropyl-chlorophosphoramidite (37.5 μl, 0.167 mmol) was then added via a micropipette. The reaction was stirred at room temperature in the dark for 30 mins and the solvent was removed by vacuum pump. Ethyl acetate (5 cm<sup>3</sup>) and dichloromethane (5 cm<sup>3</sup>) were added. To the solution was added 5%(aq) NaHCO<sub>3</sub> (10 cm<sup>3</sup>). The organic layer was extracted and dried with Na<sub>2</sub>SO<sub>4</sub>. The solvent was then removed by vacuum pump and the crude product was stored in the freezer in the dark. The product was purified by chromatography using neutral alumina with CH<sub>2</sub>Cl<sub>2</sub> : DIPEA, 25 : 1 as the solvent system. 17.2 mgs (46.6%) of (3-(2-N,N-dimethylaminomethyleneamino-3,4-dihydro-4-oxo-

6,7diphenyl-3-pteridinyl)-propoxy) (2-cyanoethoxy) (N,N-diisopropylamino) phosphine was isolated as a yellow solid.

NMR  $\delta_P$  (161.97 MHz, d6-acetone) Peaks at 9.2 and 148.4.

$\delta_H$  (400.13 MHz, d6-acetone, Me<sub>4</sub>Si) 1.18 (12H, d, 2 x NCH(CH<sub>3</sub>)<sub>2</sub>), 2.12 (2H, m, CH<sub>2</sub>CH<sub>2</sub>N), 2.76 (2H, t, CH<sub>2</sub>CN), 3.29 (3H, s, NCH<sub>3</sub>), 3.40 (3H, s, NCH<sub>3</sub>), 3.65 (2H, m, 2 x CH(CH<sub>3</sub>)<sub>2</sub>), 3.85 (4H, m, 2 x POCH<sub>2</sub>), 4.48 (2H, t, NCH<sub>2</sub>), 7.34 – 7.54 (10H, m, phenyl C-H), 8.94 (1H, s, NCHN).

*6-Amino-2-methylthio-4-(3H) pyrimidinone (143).*

6-Amino-2-mercapto-4-(3H) pyrimidinone (7.5 g, 46 mmol) was suspended in H<sub>2</sub>O (50 cm<sup>3</sup>) and heated to 60°C. NaOH (5M) was added dropwise until a solution formed. Dimethylsulphate (5.87 g, 4.4 cm<sup>3</sup>, 46 mmol) was added by syringe and the solution was refluxed for 60 mins. Upon cooling 5.05g (70%) of 6-amino-2-methylthio-4-(3H)pyrimidinone as a white solid was isolated by filtration.

NMR  $\delta_H$  (400.13 MHz; d6-DMSO; Me<sub>4</sub>Si) 2.4 (3H, s, SCH<sub>3</sub>), 4.9 (1H, s, CH), 6.4 (2H, s, NH<sub>2</sub>).

$\delta_C$  (100.6 MHz; d6-DMSO; Me<sub>4</sub>Si) 12.9 (CH<sub>3</sub>), 81.6 (CH), 154.2, 161.6, 163.2, 174.5 (quaternary carbons).

*6-Amino-2-methylthio-5-nitroso-4-(3H) pyrimidinone (138).*

6-Amino-2-methylthio-4-(3H) pyrimidinone (5.0g, 32mmol) was suspended in 10% (aq) glacial acetic acid (50 cm<sup>3</sup>) and cooled to 0°C in an ice bath. NaNO<sub>2</sub> (3.3 g, 48 mmol) was dissolved in H<sub>2</sub>O (10 cm<sup>3</sup>) and added dropwise to the suspension. The reaction was stirred at room temperature overnight. TLC (CH<sub>2</sub>Cl<sub>2</sub> : MeOH; 8 : 2) showed no starting material remained. 5.1 g (86%) of 6-amino-2-methylthio-5-nitroso-4-(3H) pyrimidinone as a blue solid was isolated by filtration.

*2-(6-Carboxyhexylamino)-6-amino-5-nitroso-4-(3H) pyrimidinone (140).*

6-Amino-2-methylthio-5-nitroso-4-(3H) pyrimidinone (500 mgs, 2.7 mmol) and 6-aminohexanoic acid (1.0 g, 7.6 mmol) were suspended in H<sub>2</sub>O (20 cm<sup>3</sup>). The suspension was refluxed for 1 hour (with a H<sub>2</sub>S scrubber attached to the condenser). After this time the blue suspension changed to a red solution. The reaction was cooled down in an ice bath

and 300mgs (45%) of 2-(6-carboxyhexylamino)-6-amino-5-nitroso-4-(3*H*) pyrimidinone was isolated by filtration as an orange solid.

NMR  $\delta_{\text{H}}$  (400.13 MHz; d<sub>6</sub>-DMSO; Me<sub>4</sub>Si) 1.3 (2H, m, CH<sub>2</sub>), 1.52 (4H, m, 2 x CH<sub>2</sub>), 2.21 (2H, t, CH<sub>2</sub>), 7.53-8.4 (2H,s, NH<sub>2</sub>).

$\delta_{\text{H}}$  (400.13 MHz; NaOD; Me<sub>4</sub>Si) 1.31 (2H, brs, CH<sub>2</sub>), 1.52 (4H, brs, 2 x CH<sub>2</sub>), 2.14 (2H, t, CH<sub>2</sub>), 3.31 (2H, t, CH<sub>2</sub>).

$\delta_{\text{C}}$  (100.6 MHz; d<sub>6</sub>-DMSO; Me<sub>4</sub>Si) + DEPT spectrum. 24.5, 26.2, 28.8, 34.0, 40.7 (5 x CH<sub>2</sub>), 141.7, 152.3, 154.5, 161.6 (4 x pyrimidine carbons), 175 (C=O).

*2-(6-Carboxyhexylamino)-6,7-diphenyl-4-(-3H) pteridinone (105).*

2-(6-Carboxyhexylamino)-6-amino-5-nitroso-4-(3*H*) pyrimidinone (100mgs, 3.17 x 10<sup>-4</sup> mol) was dissolved in 2M NaOH (10 cm<sup>3</sup>) and was stirred vigorously during hydrogenolysis at atmospheric pressure until hydrogen uptake ceased using 10% palladised carbon (60 mgs) as a catalyst. After H<sub>2</sub> uptake ceased the mixture was filtered under vacuum into a solution of benzil, (78 mgs, 3.2 x 10<sup>-4</sup> mol) in ethanol (10 cm<sup>3</sup>). The solution was refluxed until TLC (CH<sub>2</sub>Cl<sub>2</sub> : MeOH; 15 : 2) showed that no benzil remained. The solution was cooled to room temperature, neutralised to pH 7 with dilute HCl and evaporated to dryness. The solid was extracted twice with methanol (2 x 15 cm<sup>3</sup>) and the product was purified by column chromatography (100% CHCl<sub>2</sub> followed by an increasing gradient of methanol. Pure fractions were pooled and the solvent evaporated to give 115 mgs (73%) of 2-(6-carboxyhexylamino)-6,7-diphenyl-4-(-3*H*) pteridinone as a yellow solid.

NMR  $\delta_{\text{H}}$  ( 400.13 MHz; d<sub>6</sub>-DMSO; Me<sub>4</sub>Si) 1.3 (2H, m, CH<sub>2</sub>), 1.52 (4H, m, 2 x CH<sub>2</sub>), 2.21 (2H, t, CH<sub>2</sub>) 3.37 (2H, s, CH<sub>2</sub>),4.5 (2H, brs, 2 x NH) 7.29-7.4 (10H, m, phenyl C-H).

$\delta_{\text{C}}$  (100.6 MHz; d<sub>6</sub>-DMSO; Me<sub>4</sub>Si) + DEPT spectrum. 25.1, 26.5, 29.0, 35.3, 40.7 (5 x CH<sub>2</sub>), 128-130 ( 5 x CH), 174.1 (C=O),

Mass spec., ESMS ( ES<sup>-</sup>) ( M<sup>+</sup>, 428).

*2-(6-Succinimido-carboxyhexylamino)-6,7-diphenyl-4-(-3H) pteridinone (141).*

2-(6-carboxyhexylamino)-6,7-diphenyl-4-(-3*H*) pteridinone (86mgs, 2 x 10<sup>-4</sup>m) was suspended in anhydrous DMF (2.5cm<sup>3</sup>) and diisopropylethylamine (61 $\mu$ l). TSU (72mgs,

$2.2 \times 10^{-4}$ m) was added and the yellow suspension was stirred in the dark overnight under an  $N_2$  atmosphere. TLC the next morning ( $CH_2Cl_2$  : MeOH) 15 : 2 showed no starting material remained. The brown reaction mixture was evaporated to dryness under vacuum and purified by flash chromatography using  $CH_2Cl_2$  with increasing amounts of ethanol as solvents. Pure fractions were pooled and the solvent evaporated to give 2-(6-N-hydroxysuccinimido-carboxyhexylamino)-6,7-diphenyl-4-(-3*H*) pteridinone (58mgs, 55%) as a yellow solid.

NMR  $\delta_H$  ( 400.13 MHz;  $CDCl_3$ ;  $Me_4Si$ ), 1.4 (2H, m,  $CH_2$ ), 1.6 (4h, M, 2 x  $CH_2$ ), 2.6 (2H, t,  $CH_2$ ), 2.81 (4H, brs, 2 x  $CH_2$ ) 3.4 (2H, t,  $CH_2$ ), 17.3-7.4 (10H, m, 10 x phenyl CH).

$\delta_C$  (100.6 MHz;  $CDCl_3$ ;  $Me_4Si$ ) + DEPT spectrum, 24.4, 25.8, 28.6, 29.3, 30.5, 40.4 ( $CH_2$  carbons), 128.4-129.9 (5 x CH), 168.9, 170.2 (carbonyl carbons).

Mass spec. ESMS. ( $ES^+$ )  $M^+$ , 527.4.

*4'-Methyl-2,2'-bipyridine-4-carboxaldehyde (119).*

$SeO_2$  (132mgs, 1.18mmol) was added to a solution of 4,4'-dimethyl-2,2'-bipyridine (200 mgs, 1.08 mmol) in dry dioxane ( $50\text{ cm}^3$ ) and refluxed under a  $N_2$  atmosphere for 24 hours. The solution was then filtered hot and the dioxane was removed in *vacuo*. The pink residue was dissolved in ethyl acetate and extracted with 1M  $Na_2CO_3$  (2 x  $20\text{ cm}^3$ ) and 0.3M  $Na_2S_2O_5$  (3 x  $20\text{ cm}^3$ ) to form the aldehyde bisulfite. The aqueous extracts were combined and adjusted to pH 10 with 1M  $Na_2CO_3$ , then extracted with dichloromethane (3 x  $30\text{ cm}^3$ ). Evaporation of solvent gave 80 mgs, (37 %) of 4'-methyl-2,2'-bipyridine-4-carboxaldehyde as a white solid.

NMR.  $\delta_H$  (400.13MHz;  $CDCl_3$ ;  $Me_4Si$ ) 2.47 (3H, s,  $CH_3$ ), 7.18-7.19 (1H, d, H5), 7.71-7.72 (1H, d, H5'), 8.28 (1H, s, H3), 8.57-8.58 (1H, d, H6), 8.83 (1H, s, H3'), 8.88-8.9 (1H, d, H6'), 10.19 (1H, s, CHO).

$\delta_C$  (100.6 MHz;  $CDCl_3$ ;  $Me_4Si$ ) + DEPT spectrum. 20.73 ( $CH_3$ ), 120.5, 121.3, 122.0, 125.3, 149.1, 150.2, (6 x CH), 142.2, 147.9, 154.3, 157.8, (quaternary carbons), 191.2 (CHO).



*4'-Methyl-2, 2'-bipyridine-4-carboxylic acid (46).*

A solution of AgNO<sub>3</sub> (315 mgs) in H<sub>2</sub>O (8 cm<sup>3</sup>) was added to a suspension of 4'-methyl-2,2'-bipyridine-4-carboxaldehyde, (100 mgs, 5.02 x 10<sup>-4</sup>mol) in 95% ethanol (10 cm<sup>3</sup>). The suspension was stirred rapidly and 1M NaOH (8 cm<sup>3</sup>) was added dropwise over 20 mins. to form Ag<sub>2</sub>O. The black suspension was stirred for 16 hours at room temperature. The ethanol was then removed in *vacuo* and the Ag<sub>2</sub>O filtered off. The residue was washed with 1.3M NaOH (2 x 3 cm<sup>3</sup>) and H<sub>2</sub>O (1 x 3 cm<sup>3</sup>). The combined filtrates were extracted with dichloromethane (2 x 5 cm<sup>3</sup>). The aqueous layer was adjusted to pH 3.5 with 1 : 1, 4N HCl : Acetic acid and placed in a fridge overnight. 4'-Methyl-2, 2'-bipyridine-4-carboxylic acid, 80 mgs (74 %) was isolated as a white solid by filtration.

NMR. δ<sub>H</sub> (400.13MHz; d6-DMSO; Me<sub>4</sub>Si) 2.42 (3H, s, CH<sub>3</sub>), 7.31-7.32 (1H, d, H5), 7.84-7.85 (1H, d, H5'), 8.25 (1H, s, H3), 8.56-8.57 (1H, d, H6), 8.81 (1H, s, H3'), 8.82-8.83 (1H, D, H6').

δ<sub>C</sub> (100.6 MHz; d6-DMSO; Me<sub>4</sub>Si) + DEPT spectrum. 20.7 (CH<sub>3</sub>), 120.1, 121.6, 123.4, 125.5, 149.5, 150.3 (6 x CH), 141.8, 146.0, 154.6, 156.1 (quaternary carbons), 166.7 (COOH).

*Ru [(1,10-phenanthroline)<sub>2</sub> (4'-methyl-2, 2'-bipyridine-4-carboxylic acid)]<sup>2+</sup> (PF<sub>6</sub>)<sub>2</sub> (114).*

4'-Methyl-2, 2'-bipyridine-4-carboxylic acid (100mgs, 4.66 x 10<sup>-4</sup>m) dissolved in hot degassed ethanol (20cm<sup>3</sup>) was added to a solution of Ru [(1,10-phenanthroline)<sub>2</sub> Cl<sub>2</sub> (225mgs, 4.23 x 10<sup>-4</sup>m) in hot degassed H<sub>2</sub>O (30cm<sup>3</sup>). The solution was refluxed under N<sub>2</sub> for 3 hours. TLC, (H<sub>2</sub>O : DMF : 2M NH<sub>4</sub>Cl), 1 : 1 : 2. Showed that no Ru [(1,10-phenanthroline)<sub>2</sub> Cl<sub>2</sub> remained. The ethanol was removed by rotary evaporation and NH<sub>4</sub>PF<sub>6</sub> (345mgs, 2.1 x 10<sup>-3</sup>m) dissolved in H<sub>2</sub>O (20cm<sup>3</sup>) was added to precipitate the product as its hexafluorophosphate salt. Ru [(1,10-phenanthroline)<sub>2</sub> (4'-methyl-2, 2'-bipyridine-4-carboxylic acid)]<sup>2+</sup> (PF<sub>6</sub>)<sub>2</sub> (316 mgs, 3.3 x 10<sup>-4</sup>m) was isolated as a dark orange solid by filtration and dried under vacuum.

NMR see section 3.3.2.

*Ru[(1,10-phenanthroline)<sub>2</sub> (4'-methyl-2, 2'-bipyridine-4-carboxysuccinimide)]<sup>2+</sup>(PF<sub>6</sub>)<sup>-</sup><sub>2</sub>(145).*

Ru [(1,10-phenanthroline)<sub>2</sub> (4'-methyl-2, 2'-bipyridine-4-carboxylic acid)]<sup>2+</sup> (PF<sub>6</sub>)<sup>-</sup><sub>2</sub> (114) (75 mgs, 7.76 x 10<sup>-4</sup>m) was dissolved in anhydrous DMF (2 cm<sup>3</sup>) and diisopropylethylamine (28 μl). TSU (35 mgs, 1.16 x 10<sup>-4</sup>m) was added and the solution was stirred in the dark under an N<sub>2</sub> atmosphere, The reaction was monitored by TLC (H<sub>2</sub>O : DMF : 2M NH<sub>4</sub>Cl), 1 : 1 : 2 which showed the appearance of a second species after 1 hour. The amount of this species relative to the starting material did not increase after further stirring or after addition of another 0.5 equivalents of TSU. The two species were identified by mass spec. to be the starting material and the desired product. The reaction mixture was then used in subsequent reactions.

Mass spec.

Starting material. M/Z<sup>+</sup> = 338.02.

Product. M/Z<sup>+</sup> = 387.2.

*4-(6-bromohexyl-4'-methyl-2,2'-bipyridine (113))<sup>199</sup>.*

*4-(6-hydroxyhexyl-4'-methyl-2,2'-bipyridine (114))<sup>199</sup>.*

*Ru[(1,10-phenanthroline)<sub>2</sub> 4-(6-hydroxyhexyl-4'-methyl-2,2'-bipyridine)] (PF<sub>6</sub>)<sub>2</sub> (114).*

Ru (phen)<sub>2</sub>Cl<sub>2</sub>, (158mgs, 2.96 x 10<sup>-4</sup>M) was dissolved in methanol : water, (1:1), (40cm<sup>3</sup>) and refluxed for 30mins. at 80<sup>0</sup>C. 4-(6-hydroxyhexyl-4'-methyl-2,2'-bipyridine (80mgs, 2.96 x 10<sup>-4</sup>M) dissolved in in methanol : water, (1:1), (20cm<sup>3</sup>) was added and the reaction mixture was refluxed and monitored by TLC (H<sub>2</sub>O : DMF : 2M NH<sub>4</sub>Cl), 1 : 1 : 2. After 2.5 hours no free ligand was visible on TLC and the methanol was removed by rotary evaporation and ammonium hexafluorophosphate (48.3mgs, 2.96 x 10<sup>-4</sup>M) dissolved in water (2cm<sup>3</sup>) was added. The product was isolated by filtration and purified using sephadex SP-C25 ion exchange resin using an increasing gradient of NaCl.

*Ru[(1,10-phenanthroline)<sub>2</sub>4-(6-(2-cyanoethoxy) (N,N-diisopropylamino) phosphoramidite) hexyl-4'-methyl-2,2'-bipyridine] (PF<sub>6</sub>)<sub>2</sub> (116).*

The ruthenium complex, (15mgs,  $1.75 \times 10^{-5}$ M) was dried by two coevaporations from CH<sub>2</sub>Cl<sub>2</sub> (2cm<sup>3</sup>). To this were added CH<sub>2</sub>Cl<sub>2</sub> (2cm<sup>3</sup>) and di-isopropylethylamine (64  $\mu$ l,  $3.68 \times 10^{-4}$ M) and the mixture was stirred in the dark for 20mins. under an N<sub>2</sub> atmosphere. 2-Cyanoethyl N,N-diisopropylchlorophosphoramidite (12  $\mu$ l,  $4.9 \times 10^{-5}$ M) was added by micropipette and the reaction was stirred in the dark for 30 mins. The solvent was then removed under vacuum and CH<sub>2</sub>Cl<sub>2</sub> (10cm<sup>3</sup>) was added and the solution was washed with 5% NaHCO<sub>3</sub> solution. The organic layer was extracted, dried with anhydrous MgSO<sub>4</sub> and the solvent removed under vacuum at room temperature. The crude product was analysed by <sup>31</sup>P NMR spectroscopy. Purification of the product was then attempted using silica and alumina chromatography with (CH<sub>2</sub>Cl<sub>2</sub> : DIPEA) (25 : 1) as mobile phase. Collected fractions were analysed by <sup>31</sup>P NMR spectroscopy

NMR  $\delta_p$  (161.97 MHz, d<sub>3</sub>-CH<sub>3</sub>CN) Peaks at 5 - 25 ppm and 148.6ppm.

*Pteridinone-ODN (1).*

The pteridinone phosphoramidite (134) (17mgs,  $2.7 \times 10^{-3}$ M) dissolved in dry acetonitrile (365 $\mu$ l) was added to the automated DNA synthesiser following removal of the 5'-OH protecting dimethoxytrityl group. The coupling reaction was allowed proceed for 120 secs. and the synthetic cycle was completed as per scheme 1.3.e.. Deprotection of base sensitive protecting groups was effected by treatment of the conjugate solution with conc. NH<sub>3</sub> at 55<sup>o</sup>C for 3 hours. The solvent was then removed by vacuum centrifuge and the conjugate pellet was precipitated from *n*-butanol. The pellet was then divided into 3 samples one of which was used in attempted purification by 12% PAGE.

After the gel had run for ~2 hours it was removed from the glass plates by a sheet of clingfilm, placed on a fluorescently backed TLC plate and the conjugate bands were visualised under a UV lamp. Comparison of the fluorescence intensities between the conjugate and unreacted 17-mer bands led to an estimation of a coupling yield of 60%. The bands representing the pteridinone ODN were excised from the gel and injected into an electroelution apparatus, which was run for 2 hours at 2-3 watts. The purified conjugate was extracted from the appropriate well in the electroelution apparatus, precipitated from 95% ethanol and analysed by UV spectroscopy.

### *Pteridinone-ODN (2).*

The pteridinone succinimide ester (141), (15mgs,  $2.85 \times 10^{-5}$ M) dissolved in anhydrous DMF (150 $\mu$ l) was added to an eppendorf containing 16 odus of the amino 17-mer dissolved in tris borate buffer (pH = 8.8), (100 $\mu$ l). The mixture was vortexed and heated at 40<sup>0</sup>C for 1 hour. The reaction mixture was then passed through a NAP<sup>TM</sup>10 column (sephadex G-25 DNA grade resin) and eluted with 2 x 1cm<sup>3</sup> of water. The fractions were pooled, dried down and purified by 12% PAGE. After the gel had run for ~2 hours it was removed from the glass plates by a sheet of clingfilm, placed on a fluorescently backed TLC plate and the conjugate bands were visualised under a UV lamp. Comparison of the fluorescence intensities between the conjugate and unreacted 17-mer bands led to an estimation of a coupling yield of 30%. The bands representing the pteridinone-ODN (2) were excised from the gel and injected into an electroelution apparatus, which was run for 2 hours at 2-3 watts. The purified conjugate was extracted from the appropriate well in the electroelution apparatus, precipitated from 95% ethanol and analysed by UV spectroscopy.

### *Ruthenium-ODN.*

The succinimido ruthenium complex (145) (250 $\mu$ l of reaction solution estimated to contain 50% active ester ~2.65  $\mu$ M) was added to an eppendorf containing 16 odus of the amino 17-mer dissolved in tris borate buffer (pH = 8.8), (100 $\mu$ l). The mixture was vortexed and heated at 40<sup>0</sup>C for 1 hour. The soluble material in the eppendorf was then prepurified by electroelution to remove free ruthenium species. The apparatus was run until the central well was a clear solution (indicating all orange ruthenium species had passed through). The Ru-ODN was extracted from the cathodic well, dried down and purified by 12% PAGE to give very small amounts of a species containing ruthenium and some ODN.

The reaction eppendorf was then re-examined and found to contain a dark orange pellet, which was redissolved in loading dye and run on a 12% PAGE gel producing Gel C in figure 3.4.c. The major and minor bands were excised, electroeluted and precipitated to give orange Ru-ODN pellets.

### *Radiolabelling experiment.*

The 34 base ODNs were synthesised without a phosphate group at their 5' termini and were labelled by the transfer of the  $\gamma^{32}$ P from  $\gamma^{32}$ P[ATP] using the enzyme bacteriophage T4 polynucleotide kinase (PNK). The procedure followed was that described by O'Keefe<sup>137</sup>.

The ODN (5 $\mu$ l of 5 $\mu$ M stock  $\Rightarrow$  25pmol), radioactive isotope ( $\gamma^{32}$ P[ATP], 2 $\mu$ l (specific activity 5000ci/mmol  $\Rightarrow$  4pmol)), PNK buffer (10 x PNK buffer, 2 $\mu$ l) and the water (9 $\mu$ l) were placed in a sterile eppendorf tube and vortexed. The enzyme (PNK enzyme, 2 $\mu$ l (20 units)) was then added and the tube was tapped rather than vortexed to mix the contents since vortexing is known to denature the enzyme. The reaction was incubated at 37 $^{\circ}$ C for 40 mins, followed by 10 mins at 68 $^{\circ}$ C (which inactivates the enzyme). 3M ammonium acetate (100 $\mu$ l) and cold 98% ethanol (400 $\mu$ l) were added to the reaction mixture which was then vortexed and placed at -20 $^{\circ}$ C for 20 mins. The reaction tube was then centrifuged at 12000 g for 20 mins. and the supernatant was removed. Cold 98% ethanol (1cm $^3$ ) was added and the mixture was vortexed and stored at -20 $^{\circ}$ C for 20 mins. The reaction tube was then centrifuged at 12000 g for 20 mins. Following removal of the supernatant the pellet was dried at room temperature and stored in sterile water.

#### *General procedure for Irradiation experiments.*

To an eppendorf were added, 1 $\mu$ l of the photoactive conjugate, 1 $\mu$ l of the radiolabelled target and 8 $\mu$ l of 12.5mM phosphate buffer / 125mM NaCl. The eppendorf was vortexed to equilibrate the contents and centrifuged at 5000 rpm. The eppendorf was then heated to 90 $^{\circ}$ C for 5 mins. and cooled slowly to room temperature to allow hybridisation to occur. The eppendorf was then placed in an ice water bath and irradiated with light of wavelength >330nm (isoing pyrex glass filter). After irradiation, the sample was dried down by vacuum centrifuge and 1M piperidine (15 $\mu$ l) was added. After vortexing and centrifuging the sample was heated at 90 $^{\circ}$ C for 30 mins. and dried down by vacuum centrifuge. The sample was washed by adding water (10 $\mu$ l) then vortexing and centrifuging. The sample was then dried by vacuum centrifuge. 5 $\mu$ l of the loading dye (1% bromophenol blue, 1% xylene cyanol in an 80% aqueous formamide solution) was then added to the sample prior to electrophoresis.

#### *Experiments with NaN $_3$ .*

The procedure was as described above except that to an eppendorf were added, 1 $\mu$ l of the photoactive conjugate, 1 $\mu$ l of the radiolabelled target, 2 $\mu$ l of NaN $_3$  (0.05M) and 6 $\mu$ l of 16.67mM phosphate buffer / 166.7mM NaCl.

### *Experiments with D<sub>2</sub>O.*

The procedure was as described above except that the water in the buffer was removed by vacuum centrifuge and replaced with D<sub>2</sub>O.

### *Electrophoresis experiments.*

#### *Solutions.*

##### *10 x TBE buffer.*

Boric acid (27.5g), 0.5M EDTA (20cm<sup>3</sup>), tris (hydroxymethyl) aminomethane (54g) in sterile water (500cm<sup>3</sup>).

##### *30% acrylamide stock.*

Acrylamide (190g), N,N-methylenebisacrylamide (10g) and sterile water to 500mls.

##### *Procedure for 19% polyacrylamide electrophoresis gel.*

Urea (31g) was added to water (7.5cm<sup>3</sup>), 10 x TBE buffer (7.5cm<sup>3</sup>) and 30% acrylamide stock (37.5cm<sup>3</sup>). When the solution had formed, the polymerisation triggers (10% (w / v) ammonium (450µl) persulphate and N,N,N,N,tetramethylethylenediamine (35µl)). were added and the solution was poured between the taped glass plates which were placed at an angle of  $\approx 10^\circ$ . The comb was clamped in position and the gel was left for 2 hours to set. The comb was then removed and the plates were placed in the electrophoresis apparatus. The upper and lower reservoirs were filled with 1 x TBE buffer. The gel lanes were then rinsed with buffer to remove residual urea from the polymerisation. 5µl of loading dye was added to some lanes in the gel, which was then pre-electrophoresed for 45mins. 5 µl of the loading dye was then added to each of the eppendorfs, which were vortexed and centrifuged at 5000 rpm. The contents of the eppendorfs were then loaded in the lanes and the gel was allowed run for 2 – 3 hours using 50 – 60 watts of power. After this time had elapsed the gel was removed from between the glass plates, covered in clingfilm and placed in a gel container. In a dark room a photographic film was placed in the gel container which was stored at  $-70^\circ\text{C}$  for an appropriate period of time depending on the age of the radiolabelled material.

### *HPLC assay for oxidative damage to 2`deoxyguanosine.*

#### ***General procedure.***

To a cuvette (3 cm<sup>3</sup>) were added 2'-deoxyguanosine (750µl of 2mM solution) and the relevant photosensitiser (750µl of a 1mM solution). The cuvette was placed 20 cm from the beam of the lamp with a filter appropriate to the sensitiser in a cuvette between the beam and the sensitiser. The solution was irradiated and 50 µl aliquots were taken at time intervals and dried down by speedy vac. The samples were then dissolved in 100 µl of mobile phase (75 : 25 acetonitrile : 25mM ammonium formate) and analysed by normal phase HPLC using an amino propyl silica column.

*HPLC experiments with D<sub>2</sub>O.*

The procedure was as described above except that samples of the photosensitiser (750 µl of 1mM) and 2'-deoxyguanosine (750 µl of 2 mM solution) were dried down and then dissolved in equivalent amounts of D<sub>2</sub>O.

*HPLC experiments with NaN<sub>3</sub>.*

The procedure was as described above except that samples of the photosensitiser (750 µl of 1mM solution) and 2'-deoxyguanosine (750 µl of 2 mM solution) were dried down and then dissolved in equivalent amounts of NaN<sub>3</sub> (10mM).

## References.

1. *Nucleic acids in Chemistry and Biology*, 2<sup>nd</sup> edition, Ed. G.M. Blackburn and M.J. Gait, Oxford university press, 1996.
2. D.M. Brown and A.R. Todd, *J. Chem. Soc.*, 1952, **1**, 44.
3. D.M. Brown and A.R. Todd, *J. Chem. Soc.*, 1952, **1**, 52.
4. W.T. Astbury, *Symp. Soc. Exp. Biol. (Nucleic Acids)*, 1947, **1**, 66.
5. J.M. Gulland, *Cold spring harbor symp. Quant. Biol.*, 1947, **12**, 95.
6. L. Pauling and R.B. Corey, *Proc. Natl. Acad. Sci. U.S.A.*, 1953, **39**, 84.
7. S. Zamenhot, G. Brawermann and E. Chargaff, *Biochim. Biophys. Acta*, 1952, **9**, 402.
8. J.D. Watson and F.H.C. Crick, *Nature*, 1953, **171**, 737.
9. *Genes VI*, 1997, B. Lewin, Oxford University Press.
10. Diagram taken from *Genes VI*, 1997, B. Lewin, Oxford University Press.
11. P.B. Dervan and R. Beal, *Science*, 1991, **251**, 1360.
12. J.C. Barrett, L.T. Braiterman and P.O.P. Ts`O, *Biochemistry*, 1974, **16**, 1988.
13. C.C. Smith, L. Aurelian, M.P. Reddy, P.S. Miller and P.O.P. Ts`O, *Proc. Natl. Acad. Sci. U.S.A.*, 1986, **83**, 2787.
14. T. Taniguchi and C. Weissman, *Nature*, 1979, **275**, 770.
15. C. Hélène and J-J. Toulmé, *Biochim. Biophys. Acta.*, 1990, **1049**, 99.
16. J. Goodchild, E. Carroll III and J.R. Greenberg, *Arch. Biochem. and Biophys.*, 1988, **236**, 401.



- 
17. B.M. Patterson, B.E. Roberts and E.L. Kuff, *Proc. Natl. Acad. Sci. U.S.A.*, 1977, **74**, 4370.
  18. J. Minshull and T. Hunt, *Nucleic Acids Res.*, 1986, **14**, 6433.
  19. A.M. Michelson and A.R. Todd, *J. Chem. Soc.*, 1955, 2632.
  20. S.L. Beaucage and R.P. Iyer, *Tetrahedron*, 1992, **48**, 2223.
  21. K.L. Agrawal, A. Yamazaki, P.J. Cashion and H.G. Khorana, *Angew. Chem. Int. Ed.*, 1972, **11**, 451.
  22. G. Weimann and H.G. Khorana, *J. Amer. Chem. Soc.*, 1962, **84**, 4329.
  23. R.L. Letsinger and K.K. Ogilvie, *J. Amer. Chem. Soc.*, 1967, **89**, 4801.
  24. R.L. Letsinger and K.K. Ogilvie, *J. Amer. Chem. Soc.*, 1969, **91**, 3350.
  25. M.D. Mateucci and M.H. Caruthers, *Tetrahedron Lett.*, 1980, **21**, 719.
  26. M.D. Mateucci and M.H. Caruthers, *J. Amer. Chem. Soc.*, 1981, **103**, 3185.
  27. S.L. Beaucage and M.H. Caruthers, *Tetrahedron Lett.*, 1981, **22**, 1859.
  28. L.J. McBride and M.H. Caruthers, *Tetrahedron Lett.*, 1983, **24**, 245.
  29. S.P. Adams, K.S. Kavka, E.J. Wykes, S.B. Holder and G.R. Galluppi, *J. Amer. Chem. Soc.*, 1983, **105**, 661.
  30. N.D. Sinha, J. Biernat and H. Koster, *Tetrahedron Lett.*, 1983, **24**, 5843.
  31. S. Hamamoto and H. Takaku, *Chem. Lett.*, 1986, 1401.
  32. *New trends in Synthetic medicinal chemistry*, Wiley-Chichester, 2000, Ed. F. Gualtieri, 273.
  33. R. Iyengar, F. Eckstein, P.A. Frey, *J. Amer. Chem. Soc.*, 1984, **106**, 8309.
  34. E. Uhlmann and A. Peymann, *Chem. Rev.*, 1990, **90**, 544.
  35. P.M.J. Burgers and F. Eckstein, *Tetrahedron Lett.*, 1978, **40**, 3835.
  36. B. Uznanski, W. Niewiarowski and W.J. Stec, *Tetrahedron Lett.*, 1982, **23**, 4289.
  37. W. J. Stec, G. Zon, W. Egan and B. Stec, *J. Amer. Chem. Soc.*, 1984, **106**, 6077.
  38. R.P. Iyer, W. Egan, J.B. Regan and S.L. Beaucage, *J. Amer. Chem. Soc.*, 1990, **112**, 1253.
  39. H. Vu and B.L. Hirschbein, *Tetrahedron Lett.*, 1991, **32**, 3005.
  40. M.V. Rao, C.B. Reese and Z. Zhengyun, *Tetrahedron Lett.*, 1992, **33**, 4839.
  41. P. Guga, M. Koziolkiewicz, A. Okruszek and W.J. Stec in *Applied Antisense Oligonucleotide Technology*, Wiley-Liss, 1998, Ed. C.A. Stein and A.M. King.
  42. Y. Hayakawa, M. Hirose and R. Noyori, *Nucleosides and Nucleotides*, 1994, **13**, 1337.
  43. Y. Jin, G. Biancotto and G. Just, *Tetrahedron Lett.*, 1996, **37**, 973.

- 
44. A. Jaeger and J. Engels, *Tetrahedron Lett.*, 1984, **25**, 1437.
  45. M.A. Dorman, S.A. Noble, L.J. Mc Bride and M.H. Caruthers, *Tetrahedron*, 1984, **40**, 95.
  46. Z.J. Lesnikowski, P.J. Wolkanin and W.J. Stec, *Tetrahedron Lett.*, 1987, **28**, 5535.
  47. Z.J. Lesnikowski, M. Jaworska and W.J. Stec, *Nuc. Acids Res.*, 1988, **16**, 11675.
  48. Y Hayakawa, *Tetrahedron Lett.*, 1984, **25**, 4003.
  49. C. Le Bec and E. Wickstrom, *J. Org. Chem.*, 1996, **61**, 50.
  50. M.J. Nemer and K.K. Ogilvie, *Tetrahedron Lett.*, 1980, **21**, 4149.
  51. W. Bannwarth, *Helv. Chim. Acta.*, 1988, **71**, 1517.
  52. J.S. Nelson, K.L. Fearon, M.Q. Nguyen, S.N. Mc. Curdy, J.E. Frediani, M.F. Foy and B.L. Hirschbein, *J. Org. Chem.*, 1997, **62**, 7278.
  53. F. Morvan, B. Rayner, J-P. Lleonetti and J-L. Imbach, *Nucleic Acids Res.*, 1988, **16**, 833.
  54. P.D. Cook, *Anticancer Drug Design*, 1991, **6**, 585.
  55. P. Guga, M. Koziolkiewicz, A. Okruszek and W.J. Stec, *Applied Antisense Oligonucleotide Technology*, Wiley-Liss, 1998, Ed. C.A. Stein and A.M. Krieg, 23 - 50.
  56. C. Gagnor, J.-J. Bertrand, S. Thenet, M. Lemaitre, F. Morvan, B. Rayner, C. Malvy, B. Lebleu, J.-L. Imbach and C. Paoletti, *Nucleic Acids Res.*, 1987, 10419.
  57. H. Inoue, Y. Hayase, A. Imura, S. Iwai, K. Miura and E. Ohtsuka, *Nucleic Acids Res.*, 1987, **15**, 6131.
  58. J.M. Kean, S.A. Kipp, P.S. Miller, M. Kulka and L. Aurelian, *Biochem.*, 1995, **34**, 14617.
  59. W.J. Stec, G. Zon, W. Egan and D. Stec, *J. Amer. Chem. Soc.*, 1984, **106**, 6077.
  60. S. Agrawal, S.H. Mayrand, P.C. Zamecnik and T. Pederson, *Proc. Natl. Acad. Sci. U.S.A.*, 1990, **87**, 1401.
  61. M.H. Carruthers, G. Beaton, L. Cummins and seven others, *Nucleosides and Nucleotides*, 1991, **10**, 47.
  62. C. Boizau, R. Kurfurst, C. Cazenave, V. Roig, N.T. Thuong and J.-J. Toulmé, *Nucleic Acids Res.*, 1991, **19**, 1113.
  63. R. Kole, *Applied Antisense Oligonucleotide Technology*, Wiley-Liss 1998, Ed. C.A. Stein and A.M. Krieg, 451 - 469.

- 
64. H. Inoue, Y. Hayase, S. Iwai and E. Ohtsuka, *FEBS Lett.*, 1987, **215**, 327.
  65. D.M. Tidd, *Applied Antisense Oligonucleotide Technology*, Wiley-Liss 1998, Ed. C.A. Stein and A.M. Krieg, 161 – 169.
  66. D.M. Tidd and R.V. Giles, *Pharmaceutical Aspects of Oligonucleotides*, Taylor and Francis, 2000, Ed. P. Couvreur and C. Malvy, 1-22.
  67. C. Cazenave, N. Loreau, N.T. Thuong, J.-J. Toulmé and C. Helene, *Nucleic Acids Res.*, 1987, **15**, 4717.
  68. L.M. Neckers and K. Iyer, *Applied Antisense Oligonucleotide Technology*, Wiley-Liss 1998, Ed. C.A. Stein and A.M. Krieg, 147.
  69. R. Bergan, Y. Connell, B. Fahmy, E. Kyle and L. Neckers, *Nucleic Acids Res.*, 1994, **22**, 2150.
  70. S. Agrawal, *Mol. Med. Today*, 2000, **6**, 72.
  71. L. Benimetskaya, M. Berton, A. Kolbanovsky, S. Benimetsky and C.A. Stein, *Nucleic Acids Res.*, 1997, **25**, 2648.
  72. S.G. O'Brien and T.F.C.M. Snetters, *Applied Antisense Oligonucleotide Technology*, Wiley-Liss, 1998, Ed. C.A. Stein and A.M. Krieg, 207.
  73. C. Szczylik, T. Skorski, N.C. Nicolaides, L. Manzella, L. Malaguarnera, D. Venturelli, A.M. Gewirtz and B. Calabretta, *Science*, 1991, **253**, 562.
  74. X. Gao, F.K. Brown, P. Jeffs, N. Bischofberger, K.Y. Lin, A.J. Pipe and S.A. Noble, *Biochem.*, 1992, **31**, 6228.
  75. D.M. Tidd and S.A. Noble, *Brit. J. Cancer*, 1989, **60**, 343
  76. S.L. Beaucage and R.P. Iyer, *Tetrahedron*, 1993, **49**, 1925.
  77. W. Bannwarth and D. Schmidt, *Tetrahedron Lett.*, 1989, **30**, 1513.
  78. W. Bannwarth, W. Pfliederer and F. Muller, *Helv. Chim. Acta*, 1991, **74**, 1991.
  79. W. Bannwarth and F. Muller, *Helv. Chim. Acta*, 1991, **74**, 2000.
  80. E. Meggers, D. Kusch and B. Giese, *Helv. Chim. Acta*, 1997, **80**, 640.
  81. D. Ossipov, E. Zamaratski and J. Chattopadhyaya, *Helv. Chim. Acta*, 1999, **82**, 2180.
  82. D.G. Knorre, V.V. Vlasov, V.F. Zarykova, A.V. Lebedev and O.S. Federova, *Design and targetted reactions of oligonucleotide derivatives*, CRC press, 1993.
  83. M. Pitie, C. Casas, C.J. Lacey, G. Pratviel, J. Bernadou and B. Meunier, *Angew. Chem. Int. Ed.*, 1993, **32**, 557.
  84. B. Mestre, A. Jakobs, G. Pratviel and B. Meunier, *Biochem.*, 1996, **35**, 9140.

- 
85. A.S. Boutorine, D. Brault, M. Takasugi, O. Delgado and C. Helene, *J. Amer. Chem. Soc.*, 1996, **118**, 9469.
  86. J. Telser, K.A. Cruichshank, K.S. Schanze and T.L. Netzel, *J. Amer. Chem. Soc.*, 1989, **111**, 7221.
  87. P.J. Dandliker, M.E. Nunez and J.K. Barton, *Biochem.*, 1998, **37**, 6491.
  88. I. Ortmans, S. Content, N. Boutonnet, A. Kirsch-De Mesmaeker, W. Bannwarth, J-F. Constant, E. Defrancq and J. Lhomme, *Chem. Eur. J.*, 1999, **5**, 2712.
  89. C.B. Shen and D. Sigman, *Proc. Natl. Acad. Sci. U.S.A.*, 1986, **63**, 7147.
  90. B.C.F. Chu and L.E. Orgel, *Proc. Natl. Acad. Sci. U.S.A.*, 1985, **82**, 963.
  91. B.L. Lee, A. Murakami, K.R. Blake, S.B. Lin and P.S. Miller, *Biochem.*, 1988, **27**, 3197.
  92. J.M. Kean, A. Murakami, K.R. Blake, C.B. Cushman and P.S. Miller, *Biochem.*, 1988, **27**, 9113.
  93. G.C. Silver, J.S. Sun, C.H. Nguyen, A.S. Boutorine, E. Bisagni and C. Helene, *J. Amer. Chem. Soc.*, 1997, **119**, 263.
  94. P.B. Arimondo, P. Moreau, A. Boutorine, C. Bailly, M. Prudhomme, J.S. Sun, T. Garestier and C. Helene, *Biorg. Med. Chem.*, 2000, **8**, 727.
  95. E. Uhlmann and J. Engels, *Tetrahedron Lett.*, 1986, **27**, 1023.
  96. T. Le Doan, L. Perroualt, D. Praseuth, N. Habhoub, J-L. Decout, N.T. Thuong, J. Lhomme and C. Helene, *Nucleic Acids Res.* 1987, 7749.
  97. D. Praseuth, T. Le Doan, M. Chassignol, J-L. Decout, N. Habhoub, J. Lhomme, N.T. Thuong and C. Helene, *Biochem.*, 1988, **27**, 3031
  98. C. Giovannangeli, M. Rougee, T. Garestier, N.T. Thuong and C. Helene, *Proc. Natl. Acad. Sci. U.S.A.*, 1992, **89**, 8631.
  99. G.N. Grimm, A.S. Boutorine and C. Helene, *Nucleos. Nucleot. Nucleic Acids*, 2000, **19**, 1943.
  100. N.T. Thuong and C. Helene, *Angew. Chem. Int. Ed.*, 1993, **32**, 666.
  101. A. De Mesmaeker, R. Haner, P. Martin and H.E. Moser, *Acc. Chem. Res.*, 1995, **28**, 366.
  102. J.J. Toulme, H.M. Krisch, N. Loreau, N.T. Thuong and C. Helene, *Proc. Natl. Acad. Sci. U.S.A.*, 1986, **83**, 1227.
  103. P. Verspieren, A.W.C.A. Cornelissen, N.T. Thuong, C. Helene and J.J. Toulme, *Gene*, 1987, **61**, 307.

- 
104. J.S. Sun, J-C. Francois, T. Montenay-Garestier, T. Saison-Behmoaras, V. Roig, N.T. Thuong and C. Helene, *Proc. Natl. Acad. Sci. U.S.A.*, 1989, **86**, 9198.
  105. S. A. Cassidy, L. Strekowski, W.D. Wilson and K.R. Fox, *Biochem.*, 1994, **33**, 15338
  106. D.G. Knorre, V.V. Vlasov and V.F. Zaryhova, in *Oligodeoxynucleotides, Antisense inhibitors of gene expression*, MacMillan press, Ed. J.S. Cohen, 1989, 173.
  107. A.S. Boutorine, V.V. Vlasov, S.A. Kazakov, I.V. Kutiavin and M.A. Podyminogin, *FEBS, Lett.*, 1984, **172**, 43.
  108. G.B. Dreyer and P.B. Dervan, *Proc. Natl. Acad. Sci. U.S.A.*, 1985, **82**, 968.
  109. M. Boidot-Forget, M. Chassignol, M. Takasugi, N.T. Thuong and C. Helene, *Gene*, 1988, **72**, 361.
  110. T. Le Doan, L. Perrouault and C. Helene, *Biochem.*, 1986, **25**, 6376.
  111. T. Le Doan, L. Perrouault, M. Chassignol, N.T. Thuong and C. Helene, *Nucleic Acids Res.*, 1987, **15**, 8643.
  112. S.A. Strobel, H.E. Moser, and P.B. Dervan, *J. Am. Chem. Soc.*, 1988, **110**, 7927.
  113. C.B. Shen, and D.B. Sigman, *J. Amer. Chem. Soc.*, 1988, **110**, 6570.
  114. D. Magda, R.A. Miller, J.L. Sessler and B.L. Iverson, *J. Amer. Chem. Soc.*, 1994, **116**, 7439.
  115. P. Bigey, G. Pratviel and B. Meunier, *Nucleic Acids Res.*, 1995, **23**, 3894.
  116. B. Mestre, A. Jakobs, G. Pratviel and B. Meunier, *Biochem.*, 1996, **35**, 9140
  117. S. Steenken, *Chem Rev.*, 1989, **89**, 503.
  118. I. Dubey, G. Pratviel and B. Meunier, *J. Chem. Soc., Perkin Trans., I*, 2000 3088.
  119. D. Praseuth, M. Chassignol, M. Takasugi, T. Le Doan, N.T. Thuong and C. Helene, *J. Mol. Biol.*, 1987, **196**, 939.
  120. O.S. Federova, A.P. Savitski, K.G. Shoikhet and G.V. Ponomarev, *FEBS. Lett.*, 1990, **259**, 335.
  121. L. Perrouault, U. Asseline, C. Rivalle, N.T.Thuong, E. Bisagni, C. Giovannangeli, T. Le Doan and C. Helene, *Nature*, 1990, **334**, 358.
  122. J. Woo and P.B. Hopkins, *J. Amer. Chem. Soc.*, 1991, **113**, 5457.
  123. A.S. Levina, M.V. Berezovskii, A.G. Venjaminova, M.I. Dobrikov, M.N. Repkova and V.F. Zarytova, *Biochimie*, 1993, **75**, 25.
  124. D. Magda, M. Wright, R. A. Miller, J.L. Sessler and P.I. Sansom, *J. Amer. Chem. Soc.*, 1995, **117**, 3629.

- 
125. J. L. Sessler, P.I. Sansom, V. Kral, D. O'Connor and B. L. Iverson, *J. Amer. Chem. Soc.*, 1996, **118**, 12322.
126. H. Ikeda, K. Fuli and K. Tanaka, *Bioorg. Med. Chem. Lett.*, 1996, **6**, 101.
127. B. Armitage, T. Koch, H. Frydenlund, H. Orum, H-G. Batz and G.B. Schuster, *Nucleic Acids Res.*, 1997, **25**, 4675.
128. K. Nakatani, J. Shirai, S. Sando and I. Saito, *J. Amer. Chem. Soc.*, 1997, **119**, 7626.
129. J. Piette, C.M. Calberg-Bacq and A.V. De Vorst, *Photochem. Photobiol.*, 1977, **26**, 377.
130. A. Graslund, A. Ruprecht and G. Strom, *Photochem. Photobiol.*, 1975, **21**, 153
131. L. Jacquet, R.J. Davies, A. Kirsch-De Mesmaeker and J.M. Kelly, *J. Amer. Chem. Soc.*, 1997, **119**, 11763.
132. B. Armitage, *Chem. Rev.*, 1998, **98**, 1171
133. Y.Z. An, C.B. Shen, J.L. anderson, C.S. Foote and Y. Rubin, *Tetrahedron*, 1996, **52**, 5179
134. C. Vever-Bizet, A.S. Boutorine, O. Delgado, D. Brault and C. Helene, *FEBS. Lett.*, 1999, **462**, 467.
135. P.J. Dandliker, R.E. Holmlin and J.K. Barton, *Science*, 1997, **275**, 1465.
136. D.B. Hall, R.E. Holmlin and J.K. Barton, *Nature*, 1996, **382**, 731.
137. C. O'Keeffe, Ph.D. thesis, University of Dublin, 1998.
138. Y. Kavanagh, Ph.D. thesis to be published 2001.
139. J. Cadet and P. Vigny in *Biorganic Photochemistry, Photochemistry and the Nucleic Acids*, Ed. H. Morrison, Wiley Interscience, New York, 1990, **1**, 1.
140. G.J. Fisher and H.E. Johns in *Photochemistry and Photobiology of Nucleic Acids*, Academic Press, New York, **1**, 225.
141. C.J. Burrows and J.G. Muller, *Chem. Rev.*, 1998, **98**, 1109.
142. H. Gorner, C. Stradowski, and D. Schulte-Frolinde, *Photochem. Photobiol.*, 1998, **47**, 15.
143. O.S. Feederova, and L.M. Podust, *J. Inorg. Biochem.*, 1988, **34**, 149.
144. D. Ly, Y. Kan, B. Armitage and G.B. Schuster, *J. Amer. Chem. Soc.*, 1996, **118**, 8747.
145. K. Ito, S. Inoue, K. Yamamoto and S. Kawanishi, *J. Biol. Chem.*, 1993, **268**, 13221.
146. K. Ito and S. Kawanishi, *Biochem.*, 1997, **36**, 1774.

- 
147. I. Saito, M. Takayama, H. Sugiyama and K. Nakatani, *J. Amer. Chem. Soc.*, 1995, **117**, 6406.
148. H. Sugiyama and I. Saito, *J. Amer. Chem. Soc.*, 1996, **118**, 7063.
149. T. Melvin, S. Botchway, A.W. Parker and P.O'Neill, *J. Chem. Soc., Chem. Commun.*, 1995, 653.
150. D.B. Hall and J.K. Barton, *J. Amer. Chem. Soc.*, 1997, **119**, 5045.
151. E. Meggers, M.E. Michel-Beyerle and B. Giese, *J. Amer. Chem. Soc.*, 1998, **120**, 12950.
152. B. Giese, S. Wessely, M. Sporman, U. Lindeman, E. Meggers and M.E. Michel-Beyerle, *Angew. Chem. Int. Ed.*, 1999, **38**, 996.
153. E. Meggers, A. Dussy, T. Sachafter and B. Giese, *Chem. Eur. J.*, 2000, **6**, 485.
154. B. Giese, *Chemistry in Britain*, July 2000, 44.
155. P. O'Neill, *Radiat. Res.*, 1983, **96**, 198.
156. P. O'Neill, and S.E. Davies, *Int. J. Radiat. Biol.*, 1986, **49**, 937.
157. S. Steenken, *Chem. Rev.*, 1989, **89**, 503.
158. A.P. Breen and J.A. Murphy, *Free Rad. Biol. & Med.*, 1995, **18**, 6, 1033.
159. M. Dizdaroglu, *Biochem.*, 1985, **24**, 4477.
160. J.E. Schneider, S. Price, L. Maitt, J.M.C. Gutteridge, and R.A. Floyd, *Nucleic Acids Res.*, 1990, **18**, 631.
161. M. Berger and J. Cadet, *J. Amer. Chem. Soc.*, 1992, **114**, 9692.
162. D. Angelov, M. Spassky, M. Berger and J. Cadet, *J. Amer. Chem. Soc.*, 1997, **119**, 11373.
163. J. Cadet, M. Berger, G.W. Buchko, P.C. Joshi, S. Raoul and J-L. Ravanat, *J. Amer. Chem. Soc.*, 1994, **116**, 7403.
164. J-L. Ravanat, M. Berger, F. Benard, R. Langlois, J.E. Van Lier and J. Cadet, *Photochem. Photobiol.*, 1992, **114**, 809.
165. G.W. Buchko, J. Cadet, B. Morin, and M. Weinfeld, *Nucleic Acids Res.*, 1995, **23**, 3954.
166. W. Adam, C.R. Saha-Moller, and A. Schonberger, *J. Amer. Chem. Soc.*, 1997, **119**, 719.
167. S. Raoul, M. Berger, G.W. Buchko, P.C. Joshi, B. Morin, M. Weinfeld and J. Cadet, *J. Chem. Soc., Perkin 2*, 1996, 371.
168. A. Spassky, and D. Angelov, *Biochem.*, 1997, **36**, 6574.
169. J-L. Ravanat, and J. Cadet, *Chem. Res. In Toxicology*, 1995, **8**, 379.

- 
170. C. Sheu, and C.S. Foote, *J. Amer. Chem. Soc.*, 1995, **117**, 474.
171. M.L. Wood, M. Dizdaroglu, E. Gajewski, and J.M. Essigmann, *Biochem.*, 1990, **29**, 7024.
172. T.J. Mc. Bride, J.E. Schneider, R.A. Floyd, and L.A. Loeb, *Proc. Natl. Acad. Sci. USA*, 1992, **89**, 6866.
173. G.W. Buchko, J.R. Wagner, J. Cadet, S. Raoul and M. Weinfeld, *Biochim. Biophys. Acta*, 1995, **17**, 1263.
174. S. Raoul and J. Cadet, *J. Am. Chem. Soc.*, 1996, **118**, 1892.
175. V. Duarte, D. Gasparutto, L.F. Yamaguchi, J-L. Ravanat, G.R. Martinez, M.H.G. Medeiros, P.D. Mascio and J. Cadet, *J. Am. Chem. Soc.*, 2000, **51**, 12622.
176. V. Duarte, D. Gasparutto, M. Jaquinod, J-L. Ravanat, and J. Cadet, *Chem. Res. Toxicol.*, 2001, *1*, 46.
177. R.A. Floyd, J.J. Watson, P.K. Wong, D.H. Altmiller, and C.R. Richard, *Free Rad. Res. Comm.*, 1986, **1**, 163.
178. M. Berger, C. Anselmino, J-F. Mouret and J. Cadet, *J. Liq. Chrom.*, 1990, **13**, 5, 929.
179. J-L. Ravanat, T. Douki, M-F. Incardona and J. Cadet, *J. Liq. Chrom.*, 1993, **16**, 3185.
180. M. Berger, J. Cadet, R. Berube, R. Langlois, and J-E. Van Lier, *J. Chrom.*, 1992, **593**, 133.
181. J-L. Ravanat, T. Douki, R. Turesky and J. Cadet, *J. Chim. Phys.*, 1997, 306.
182. A. Collins, J. Cadet, B. Epe, and C. Gedik, *Carcinogenesis*, 1997, **18**, 9, 1833.
183. T. Douki, R. Martini, J-L. Ravanat, R. Turesky, and J. Cadet, *Carcinogenesis*, 1997, **18**, 12, 2385.
184. J-L. Ravanat, B. Duret, A. Guiller, T. Douki, and J. Cadet, *J. Chrom. B*, 1998, **715**, 349.
185. V. Duarte, D. Gasparutto, and J. Cadet, *Reported at European society of photo biology meeting*, Granada, Spain, Sept. 1999.
186. M. Pflaum, I. Schulz, S. Boiteux, and B. Epe, *Reported at European society of photobiology meeting*, Granada, Spain, Sept. 1999.
187. Photochemistry of polypyridine and porphyrin complexes, K. Kaylyanasundaram, Academic press, 1992.
188. A.J. Yeh, C.V. Shank and J.K. Mc Cusker, *Science*, 2000, **289**, 935.



- 
189. J.M. Kelly, D.J. Mc Connell, C. OhUigin, A.B. Tossi, A. Kirsch-De Mesmaeker, A. Masschlein and J. Nassielski, *J. Chem. Soc., Chem. Commun.*, 1987, 1821.
190. J-P. Lecomte, A. Kirsch-De Mesmaeker, M.M. Feeney and J.M. Kelly, *Inorg. Chem.*, 1995, **34**, 6481.
191. A. Kirsch-De Mesmaeker, C. Moucheron and N. Boutonnet, *J. Phys. Org. Chem.*, 1998, **11**, 556.
192. J.N. Demas, E.W. Harris and R.P. Mc Bride, *J. Amer. Chem. Soc.*, 1977, **99**, 3547.
193. J.M. Kelly, A.B. Tossi, D.J. Mc Connell and C. OhUigin, *Nucleic Acids Res.*, 1985, **13**, 6017.
194. M.B. Fleisher, K.C. Waterman, N.J. Turro and J.K. Barton, *Inorg. Chem.*, 1986, **25**, 3549.
195. J.M. Kelly, A.B. Tossi, D.J. Mc Connell, C. OhUigin, C. Helene and T. Le Doan, *Free Radicals, Metal Ions and Biopolymers*, 1989, 143.
196. C.J. Murphy, M.R. Arkin, Y. Jenkins, N.D. Ghatlia, S.H. Bossman, N.J. Turro and J.K. Barton, *Science*, 1993, **262**, 1025
197. W. Bannwarth, D. Schmidt, R.L. Stallard, C. Hornung, R. Knorr and F. Muller, *Helv. Chim. Acta*, 1988, **71**, 2085.
198. W. Bannwarth and D. Schmidt, *Tetrahedron Lett.*, 1989, **30**, 1515.
199. S. Leturgie, M.Sc., University of Dublin, 1998.
200. D.K. Ellison and R.T. Iwamoto, *Tetrahedron Lett.*, 1983, **24**, 31.
201. C.D. Ellis, L.D. Margerum, R.W. Murray and T.J. Meyer, *Inorg. Chem.*, 1983, **22**, 1283.
202. A.S. Modak, J.K. Gard, M.C. Merriman, K.A. Winkeler, J.K. Bashkin and M.K. Stern, *J. Amer. Chem. Soc.*, 1991, **113**, 283.
203. W. Bannwarth and R. Knorr, *Tetrahedron Lett.*, 1991, **32**, 1157.
204. S.I. Khan, A.E. Beilstein, G.D. Smith, M. Sykora and M.W. Grinstaff, *Inorg. Chem.*, 1999, **38**, 2411.
205. S.I. Khan, A.E. Beilstein, and M.W. Grinstaff, *Inorg. Chem.*, 1999, **38**, 418.
206. S.I. Khan, A.E. Beilstein, M. Sykora, X. Hiu and M.W. Grinstaff, *Inorg. Chem.*, 1999, **38**, 3992.
207. S.I. Khan, A.E. Beilstein, M.T. Tierney, M. Sykora and M.W. Grinstaff, *Inorg. Chem.*, 1999, **38**, 5999.

- 
208. X. Hiu, G.D. Smith, M. Sykora, S.J. Lee and M.W. Grinstaff, *Inorg. Chem.*, 2000, **39**, 2500.
209. D.J. Brown, *The Chemistry of Heterocyclic Molecules, Part III*, Wiley Interscience, 1988.
210. G. Suarez, F.M. Cabrerizo, C. Lorente, A.H. Thomas, A.L. Caparelli, *J. Photochem. Photobiol. A. Chem.*, 2000, **132**, 53.
211. J.L. Johnson, S. Hamm-Alvarez, G. Payne, G.B. Sancar, K.V. Rayagopalan and A. Sancar, *Proc. Natl. Acad. Sci. U.S.A.*, 1988, **85**, 2046.
212. C. Chahidi, M. Aubailly, A. Momzikoff, M. Bazin and R. Santus, *Photochem. and Photobiol.*, 1981, **33**, 641.
213. R. Mengel, W. Pfeleiderer and W.R. Knappe, *Tetrahedron, Lett*, 1977, **32**, 2817.
214. C. Chahidi, M. Giraud, M. Aubailly, A. Valla and R. Santus, *Photochem. and Photobiol.*, 1986, **44**, 231.
215. J. W. Ledbetter, W. Pfeleiderer and J. H. Freishman, *Photochem. and Photobiol.*, 1995, **62**, 71.
216. A.H. Thomas, G. Suarez, F.M. Cabrerizo, R. Martino and A.L. Caparelli, *J. Photochem. Photobiol. A. Chem.*, 2000, **135**, 147.
217. K. Ito and S. Kawanishi, *Biochem.*, 1997, **36**, 1774.
218. W. Bannwarth, W. Pfeleiderer and F. Muller, *Helv. Chim. Acta*, 1991, **74**, 1991.
219. W. Bannwarth and F. Muller *Helv. Chim. Acta*, 1991, **74**, 2000.
220. M.E. Hawkins, W. Pfeleiderer, F.M. Balis, D. Porter and J.R. Knutson, *Anal. Biochem.*, 1997, **244**, 86.
221. P.H. Boyle and R.J. Lockhart, *J. Org. Chem.*, 1985, **50**, 5127.
222. P.H. Boyle and R. Camier, *Chemistry and Biology of Pteridines and Folates*, Ed., J.E. Ayling, Plenum press, New York, 1993, 17.
223. G. Doyle Daves, C.W. Noell, R.K. Robins, H.C. Koppel and A. G. Beaman, *J. Amer. Chem. Soc.*, 1960, 2633.
224. G. Konrad and W. Pfeleiderer, *Chem. Ber.*, 1970 **103**, 722.
225. E.C. Taylor, G. P. Beardsley and Y. Maki, *J. Org. Chem.*, 1971, **34**, 3211.
226. R.J. Lockhart, Ph.D. thesis, *University of Dublin*, 1984.
227. M. Sako, S. O'Hara, K. Hirota, K. Kano, Y. Maki and E.C. Taylor, *J. Org. Chem.*, 1991, **56**, 6302.
228. R. Camier, Ph.D. thesis, *University of Dublin*, 1992.
229. P. Martin, MSc. thesis, *University of Dublin*, 1998.

- 
230. L.J. McBride, R. Kierzek, S.L. Beaucage and M.H. Caruthers, *J. Amer. Chem. Soc.*, 1986, **108**, 2040.
231. C. Frier, J-L. Decout and M. Fontecave, *J. Org. Chem.*, 1997, **62**, 3520.
232. T. Sugimoto, K. Shibata, S. Matsuura and T. Nagatsu, *Bull. Chem. Soc. Japan*, 1979, **52**, 2933
233. A.D. Ward and B.R. Baker, *J. Med. Chem.*, 1977, **20**, 88.
234. B.R. Baker, J.P. Joseph and R.E. Schaub. *J. Org. Chem.*, 1954, **19**, 631.
235. S. Berger, S. Braun and H.O. Kalinowski, *NMR spectroscopy of the non-metallic elements*, Wiley & Sons, Chichester, 1997.
236. R.M. Cresswell and T. Strauss, *J. Org. Chem.*, 1963, **28**, 2563.
237. *The Chemistry of Ruthenium*, E.A. Seddon and K.R. Seddon, Elsevier, 1984, 428.
238. D. Ossipov, P.I. Pradeepkumar, M. Holmer and J. Chattopadhyaya, *J. Amer. Chem. Soc.*, 2001, **123**, 3551.
239. M.A.J. Rodgers and P.T. Snowden, *J. Amer. Chem. Soc.*, 1982, **104**, 5541.
240. N. Hasty, P.B. Merkel and D.R. Kearns, *Photochem. Photobiol.*, 1972, **1**, 49.
241. *Molecular Cloning, A Laboratory Manual*, J. Sambrook, E.F. Fritsch and T. Maniatis, Cold Spring Harbour laboratory press, 1989.
242. E.D.A. Stemp, M.R. Arkin and J.K. Barton, *J. Amer. Chem. Soc.*, 1997, **119**, 2921.